UNIVERSITY
OF MICHIGAN
DEC 24 1958
PHYSICS
LIBRARY

Journal of Research

of the National Bureau of Standards

NOVEMBER 1958

VOLUME 61 NUMBER 5

DEPARTMENT OF COMMERCE
NATIONAL BUREAU OF STANDARDS
A. V. Astin, Director

NOVEMBER [illegible]
VOLUME [illegible]
NUMBER [illegible]

JOURNAL OF RESEARCH

of the

NATIONAL BUREAU OF STANDARDS

The National Bureau of Standards

Functions and Activities

The functions of the National Bureau of Standards are set forth in the Act of Congress, March 3, 1901, as amended by Congress in Public Law 619, 1950. These include the development and maintenance of the national standards of measurement and the provision of means and methods for making measurements consistent with these standards; the determination of physical constants and properties of materials; the development of methods and instruments for testing materials, devices, and structures; advisory services to Government agencies on scientific and technical problems; invention and development of devices to serve special needs of the Government; and the development of standard practices, codes, and specifications. The work includes basic and applied research, development, engineering, instrumentation, testing, evaluation, calibration services, and various consultation and information services. Research projects are also performed for other Government agencies when the work relates to and supplements the basic program of the Bureau or when the Bureau's unique competence is required. The scope of activities is suggested by the listing of divisions and sections on the inside of the back cover.

Publications

The results of the Bureau's work take the form of either actual equipment and devices or published papers. These papers appear either in the Bureau's own series of publications or in the journals of professional and scientific societies. The Bureau itself publishes three monthly periodicals, available from the Government Printing Office: The Journal of Research, which presents complete papers reporting technical investigations; the Technical News Bulletin, which presents summary and preliminary reports on work in progress; and Basic Radio Propagation Predictions, which provides data for determining the best frequencies to use for radio communications throughout the world. There are also five series of nonperiodical publications: The Applied Mathematics Series, Circulars, Handbooks, Building Materials and Structures Reports, and Miscellaneous Publications.

Information on the Bureau's publications can be found in NBS Circular 460, Publications of the National Bureau of Standards ($1.25) and its Supplement ($1.50), available from the Superintendent of Documents, Government Printing Office, Washington 25, D. C.

Order all publications from the Superintendent of Documents
U. S. Government Printing Office, Washington 25, D. C.

The use of funds for printing this publication approved by the Director of the Bureau of the Budget (June 29, 1953)

Journal of Research of the National Bureau of Standards Vol. 61, No. 5, November 1958 Research Paper 2906

On the Diffraction and Reflection of Waves and Pulses by Wedges and Corners

F. Oberhettinger [1]

Various problems arising in the theory of the excitation of a perfectly reflecting wedge or corner by a plane, cylindrical, or spherical wave, are dealt with. The incident wave is represented by a line source (acoustic or electromagnetic) parallel to the edge. The spherical wave is emitted by an acoustic point source or by a Hertz dipole with its axis parallel to the edge. The case of an incident plane wave field is obtained as the limiting case (for large distances of the source from the edge) of the cylindrical or spherical wave excitation.

1. Introduction

Sommerfeld's classical problem of the excitation of a perfectly reflecting half plane by a plane (acoustic or electromagnetic) wave field is based upon the theory of multivalued solutions of the wave equation [34].[2] Subsequently this method was extended to the problem of the diffraction of cylindrical or spherical waves by a half plane [3] or by a wedge [44] (in the latter case also for a plane incident wave). Here the incident cylindrical wave is emitted by a line source parallel to the edge (of the half plane or wedge) and the spherical wave is emitted by a point source (in the acoustic case) or by a Hertz dipole (in the electromagnetic case) parallel to the edge. The solutions for the half plane problem are given in the form of integral expressions involving a real variable, while the corresponding wedge problem solutions are given as contour integrals.

The problems described above have been treated ever since with the aid of various techniques. The wedge problem as treated by MacDonald [22] requires the conventional methods of nineteenth century mathematical physics only. Here the solution is given by an infinite series and this is transformed into Wiegrefe's complex integral. For the special case of a half plane (angle of the wedge equal to 2π), reductions to integrals involving a real variable are given. Another approach is a generalization of the method of the images [1, 16, 43].

At first the solution for a wedge of an angle π/m with positive integer m is established as the sum of the effects of the original source and its $2m$-1 images. This sum is replaced by a contour integral which is extended so as to obtain a formula valid for any positive m and henceforth for any angle α of the wedge. Again, the solution is given by a contour integral. In more recent times a number of attempts have been made to apply integral transform methods [20, 17] and integral equation methods [23, 7, 14, 13] to the half plane diffraction problem. Finally, the problem of the diffraction by a perfectly conducting half plane of electromagnetic waves emitted by an arbitrarily oriented electric or magnetic dipole has also been solved [32, 39, 15].

Sommerfeld's solution (plane waves incident on a half plane) is given in a form readily available for numerical computation inasmuch as it contains only the tabulated error function besides elementary functions. The solution of the other cases can either be given in the form of infinite series (usually suitable for the numerical evaluation of the near field) or in the form of integral expressions. A reduction of the latter to an asymptotic series has to be carried out if approximate expressions are desired for distances that are large compared to the wave length. Expressions of this form have been derived for the case of the diffraction of a plane wave by a wedge [44, 29]. (An asymptotic expansion which fails to give the proper behavior in the neighborhood of the boundaries of geometric optics is ignored here [36].) The main feature of these asymptotic series is that their terms are generalized error functions. The work referred to above is concerned only with time harmonic problems.

---

[1] Guest worker, National Bureau of Standards, from American University. Present address, Oregon State College, Corvallis, Ore. This research was carried out in part under Contract No. DA-11-022-ORD-2059 with the University of Wisconsin.

[2] Figures in brackets indicate the literature references at the end of this paper.

A second group of investigations centers around problems in which the dependence upon time is not periodic. This is the case of the diffraction of a pulse or a transient wave by a wedge or a half plane. This group of investigations was initiated by Sommerfeld [35]. The following contributions are listed here: Normal incidence of a plane pulse on a half plane [21,11]; two-dimensional pulse incident on a half plane [12]; plane pulse (unit step function) incident on a wedge or a corner [19,24, 25]; arbitrary pulse incident on a wedge or a corner [18]; cylindrical Dirac pulse incident on a half plane [38]; and spherical pulse (unit step function) incident on a half plane [40]. This paper will deal with various problems arising in the theory of the excitation of a perfectly reflecting wedge or corner by a plane, cylindrical, or spherical wave field.

The incident cylindrical wave is represented by an acoustic or electromagnetic line source parallel to the edge. The spherical wave is emitted by an acoustic point source or by a Hertz dipole with its axis parallel to the edge. The case of an incident plane wave field is obtained as the limiting case (for large distances of the source from the edge) of the cylindrical or spherical wave excitation.

In section 2 of this paper, various representations for the time harmonic solution of the problems outlined before are given with special emphasis to a representation upon which the investigations of sections 3 to 6 are based. A straightforward method is applied based upon the representation of the incident field in the form of a Kantorovich-Lebedev transform.

Section 3 contains a detailed discussion of the results obtained in section 2. Relations to geometric optics are discussed.

Section 4 contains an asymptotic expansion for the far field excited by the incidence of a plane wave on a wedge. This expansion is not of the Wiegrefe-Pauli type inasmuch as it consists of two error function terms and an asymptotic series with inverse powers of the variable. Remarkable is the fact, that this series represents asymptotically (for large distances from the edge) the deviation of the wedge field from the corresponding half-plane field.

Section 5 contains expressions for the energy radiated from a Hertz dipole in the presence of a perfectly reflecting wedge or corner (antenna and corner reflector).

Section 6 gives the pulse or transient solutions corresponding to the time harmonic problems investigated in section 2. It is shown that previously known results can be obtained as special cases of the expressions given here.

2. Time Harmonic Wedge Diffraction Problems

The case of the excitation of a perfectly reflecting wedge by a (acoustic or electromagnetic) line source parallel to the edge of the wedge is considered first. (The solution for the excitation by a point source can then be obtained by a further integration.) Cylindrical coordinates (ρ,ϕ,z) are introduced such that the z axis coincides with the edge of the wedge and the walls of the wedge are bounded by $\phi=0$ and $\phi=\alpha$. Let the locations of the line source and the point of observation be characterized by $Q(\rho',\phi')$ and $P(\rho,\phi)$, respectively (fig. 1). Let the field inside the wedge be periodic of the form

$$\Phi=U(\rho,\phi)\exp(i\omega t), \tag{1}$$

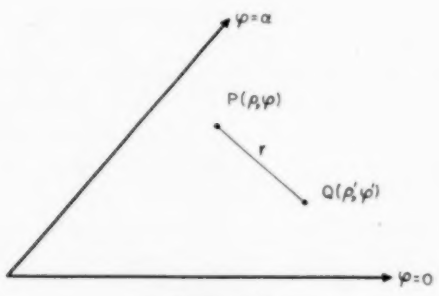

FIGURE 1.

where U satisfies the two-dimensional wave equation

$$\Delta U+k^2U=\frac{\partial^2U}{\partial\rho^2}+\frac{1}{\rho}\frac{\partial U}{\partial\rho}+\frac{1}{\rho^2}\frac{\partial^2U}{\partial\phi^2}+k^2U=0. \tag{2}$$

A solution of (2) representing divergent waves is of the form

$$U=\exp(\pm i\nu\phi)H_\nu^{(2)}(k\rho). \tag{3}$$

$H_\nu^{(2)}(k\rho)$ is the second Hankel function, and ν is an arbitrary parameter. Following a procedure used elsewhere [26], the substitution

$$k=2\pi/\lambda=\omega/c=-i\gamma \tag{4}$$

is introduced. This means that instead of (2) and (1)

$$\Delta U-\gamma^2U=0, \quad \Phi=U(\rho,\phi)\exp(\gamma ct) \tag{5}$$

is considered with a particular solution corresponding to (3)

$$U=\exp(\pm i\nu\phi)K_\nu(\gamma\rho), \tag{6}$$

where

$$K_\nu(z)=-\tfrac{1}{2}i\pi\exp(-i\tfrac{1}{2}\nu\pi)H_\nu^{(2)}(-iz) \tag{7}$$

denotes the modified Hankel function. The transition from k to γ amounts to the transition from a wave problem to an exponential decay problem. At first the exponential decay problem is solved, and the wave problem solution is established by returning from γ to k. This will not only simplify questions with respect to convergence but the investigations in sections 4 and 6 are based upon the exponential decay solution and not on the time harmonic solution. The incident field in $P(\rho,\phi)$ due to the line source $Q(\rho',\phi')$ is given by

$$U^i=H_0^{(2)}(kr)=\frac{2i}{\pi}K_0\{\gamma[\rho^2+\rho'^2-2\rho\rho'\cos(\phi-\phi')]^{1/2}\}. \tag{8}$$

Let the total field U be represented as a sum of the incident field U^i and a reflected field U^r, where U^r has no singularities within the wedge:

$$U=U^i+U^r. \tag{9}$$

In order to represent U^i in a form suitable for the problem considered here it is advisable to express the modified Hankel function on the r. h. s. of (8) not by means of its well-known addition theorem [9, p. 44] but by the equivalent expression ((3A) appendix):

$$\begin{aligned}U^i&=\frac{2i}{\pi}K_0\{\gamma[\rho^2+\rho'^2-2\rho\rho'\cos(\phi-\phi')]^{1/2}\}\\&=4i\pi^{-2}\int_0^\infty K_{i\nu}(\gamma\rho)K_{i\nu}(\gamma\rho')\cosh[\nu(\pi-|\phi-\phi'|)]d\nu,\end{aligned} \tag{10}$$

which is of the form (6). Let the reflected field be represented in the same form:

$$U^r=4i\pi^{-2}\int_0^\infty K_{i\nu}(\gamma\rho)K_{i\nu}(\gamma\rho')[f_1(\nu)\exp(\nu\phi)+f_2(\nu)\exp(-\nu\phi)]d\nu. \tag{11}$$

The so far unknown functions f_1 and f_2 are to be determined by the boundary conditions.

There are two cases of boundary conditions: (a) $U=0$ and (b) $\partial U/\partial\phi=0$ on the walls $\phi=0$ and $\phi=\alpha$ of the wedge. With electromagnetic waves on a perfect conducting wedge,

case (a) refers to the electric field, case (b) refers to the magnetic field. With acoustic waves, case (a) refers to free wall, and case (b) refers to rigid wall.

This leads to

$$f_1+f_2=-\cosh[\nu(\pi-\phi')]$$

$$f_1\exp(\nu\alpha)+f_2\exp(-\nu\alpha)=-\cosh[\nu(\pi-\alpha+\phi')] \tag{12}$$

and

$$f_1-f_2=-\sinh[\nu(\pi-\phi')]$$

$$f_1\exp(\nu\alpha)-f_2\exp(-\nu\alpha)=\sinh[\nu(\pi-\alpha+\phi')]. \tag{13}$$

for cases (a) and (b), respectively. It may be noted that the boundary conditions have been satisfied by putting the integrand equal to zero. This can be justified by verifying that the solution thus obtained satisfies all necessary conditions [31]. But it may also be remarked that U is represented as a Kontorovich-Lebedev transform [9, p. 75]. After f_1 and f_2 have been determined by (12) and (13) the solution is then, by (9), (10), and (11),

$$U=4i\pi^{-2}\int_0^\infty K_{i\nu}(\gamma\rho)K_{i\nu}(\gamma\rho')\frac{\sinh(\pi\nu)}{\sinh(\alpha\nu)}\{\cosh[\nu(\alpha-|\phi-\phi'|)]\mp\cosh[\nu(\alpha-\phi-\phi')]\}d\nu. \tag{14}$$

The upper and lower sign is valid for cases (a) and (b), respectively. The relation ((9A) appendix) shows that the convergence of the integral (14) at its upper limit for a real and positive γ is secured when

$$0\leqq|\phi\mp\phi'|\leqq 2\alpha,$$

and this region contains the whole region of the wedge. If one returns now to the wave problem replacing γ by ik according to (4) one arrives at the result

$$U=-i\int_0^\infty \exp(\pi\nu)H^{(2)}_{i\nu}(k\rho)H^{(2)}_{i\nu}(k\rho')\frac{\sinh(\pi\nu)}{\sinh(\alpha\nu)}\{\cosh[\nu(\alpha-|\phi-\phi'|)]\mp\cosh[\nu(\alpha-\phi-\phi')]\}d\nu. \tag{15}$$

The behavior of the integrand at its upper limit leads by [9, p. 88, form. 22] to the condition

$$\pi\leqq|\phi\mp\phi'|\leqq 2\alpha+\pi.$$

This restricts the validity of (15) to the case of a wedge of an angle α larger than π with the point of observation P in the geometric shadow of the source Q. The expression (14) shall now be transformed into an infinite series. For this purpose the elementary relation [2, p. 368]

$$\frac{\cosh[\nu(\alpha-\theta)]}{\sinh(\alpha\nu)}=\frac{\nu}{\alpha}\sum_{n=0}^{\infty}\frac{\epsilon_n\cos(n\pi\theta/\alpha)}{n^2+(n\pi/\alpha)^2},\quad \epsilon_0=1,\quad \epsilon_n=2\quad\text{for } n\geqq 1,$$

valid for $0\leqq\theta\leqq 2\alpha$ is used. Term by term integration yields

$$\int_0^\infty K_{i\nu}(\gamma\rho)K_{i\nu}(\gamma\rho')\frac{\cosh[\nu(\alpha-\theta)]}{\sinh(\nu\alpha)}\sinh(\pi\nu)d\nu=\frac{1}{\alpha}\sum_{n=0}^{\infty}\epsilon_n\cos(n\pi\theta/\alpha)\int_0^\infty\frac{\nu\sinh(\pi\nu)}{\nu^2+(n\pi/\alpha)^2}K_{i\nu}(\gamma\rho')K_{i\nu}(\gamma\rho)d\nu.$$

The integral is known [10, vol. 2, p. 176]. (Note that this formula is not only valid for positive integers but for Re $n>0$). Hence

$$\int_0^\infty\frac{\nu\sinh(\pi\nu)}{\nu^2+(n\pi/\alpha)^2}K_{i\nu}(\gamma\rho)K_{i\nu}(\gamma\rho')d\nu=\frac{1}{2}\pi^2 I_{n\pi/\alpha}(\gamma\rho)K_{n\pi/\alpha}(\gamma\rho')$$

for $\rho<\rho'$ and for $\rho>\rho'$ the same formula with ρ and ρ' interchanged. Therefore, the field U can be written as

$$U=\frac{2i}{\alpha}\sum_{n=0}^{\infty}\epsilon_n\left\{\cos\left[\frac{n\pi}{\alpha}(\phi-\phi)'\right]\mp\cos\left[\frac{n\pi}{\alpha}(\phi+\phi)'\right]\right\}I_{n\pi/\alpha}(\gamma\rho)K_{n\pi/\alpha}(\gamma\rho') \tag{16}$$

for $\rho<\rho'$ and for $\rho>\rho'$ the same formula with ρ and ρ' interchanged. The expression (16) is valid for arbitrarily complex γ and if γ is replaced by ik the solution for the corresponding wave problem becomes

$$U=\frac{\pi}{\alpha}\sum_{n=0}^{\infty}\epsilon_n\left\{\cos\left[n\frac{\pi}{\alpha}(\phi-\phi')\right]\mp\cos\left[n\frac{\pi}{\alpha}(\phi+\phi')\right]\right\}J_{n\pi/\alpha}(k\rho)H^{(2)}_{n\pi/\alpha}(k\rho') \tag{17}$$

for $\rho<\rho'$, and for $\rho>\rho'$ the same expression is used with ρ and ρ' interchanged. The preceding expressions (16) and (17) represent rapidly convergent series if the arguments of the Bessel functions are small. The expressions (16) and (17) shall now be transferred back into another integral expression which is the basis of the investigations in sections 3 and 6. For this purpose the product $I_{n\pi/\alpha}(\gamma\rho)K_{n\pi/\alpha}(\gamma\rho')$ in (16) is replaced by an integral representation ((1A) appendix). This leads to the following expressions.

$$\begin{aligned}s&=\sum_{n=0}^{\infty}\epsilon_n\cos(n\pi\theta/\alpha)I_{n\pi/\alpha}(\gamma\rho)K_{n\pi/\alpha}(\gamma\rho')\\&=\pi^{-1}\sum_{n=0}^{\infty}\epsilon_n\cos(n\pi\theta/\alpha)\int_0^{\pi}K_0[\gamma(\rho^2+\rho'^2-2\rho\rho'\cos x)^{1/2}]\cos(n\pi x/\alpha)dx\\&\quad-\pi^{-1}\sum_{n=0}^{\infty}\epsilon_n\cos(n\pi\theta/\alpha)\sin(n\pi^2/\alpha)\int_0^{\infty}\exp(-n\pi x/\alpha)K_0[\gamma(\rho^2+\rho'^2+2\rho\rho'\cosh x)^{1/2}]dx.\end{aligned} \tag{18}$$

The second sum vanishes when $\alpha=\pi/m$, $m=1, 2, 3, \ldots$. The two sums on the r. h. s. of (18) are denoted by s_1 and s_2.

Interchanging the order of summation and integration one finds

$$s_1=(2\pi)^{-1}\lim_{N\to\infty}\int_0^{\pi}K_0[\gamma(\rho^2+\rho'^2-2\rho\rho'\cos x)^{1/2}]\sum_{n=0}^{N}\epsilon_n\left\{\cos\left[n\frac{\pi}{\alpha}(x+\theta)\right]+\cos\left[n\frac{\pi}{\alpha}(x-\theta)\right]\right\}dx, \tag{19}$$

$$\begin{aligned}s_2=-\pi^{-1}\int_0^{\infty}&K_0[\gamma(\rho^2+\rho'^2+2\rho\rho'\cosh x)^{1/2}]\\&\cdot\sum_{n=1}^{\infty}\exp(-n\pi x/\alpha)\left\{\sin\left[n\frac{\pi}{\alpha}(\pi+\theta)\right]+\sin\left[n\frac{\pi}{\alpha}(\pi-\theta)\right]\right\}dx.\end{aligned} \tag{20}$$

The sum in the integrand of (20) can be summed [2, p. 203] and the result is

$$\begin{aligned}s_2=-(2\pi)^{-1}\int_0^{\infty}&K_0[\gamma(\rho^2+\rho'^2+2\rho\rho'\cosh x)^{1/2}]\\&\left\{\frac{\sin\left[\frac{\pi}{\alpha}(\pi-\theta)\right]}{\cosh(\pi x/\alpha)-\cos\left[\frac{\pi}{\alpha}(\pi-\theta)\right]}+\frac{\sin\left[\frac{\pi}{\alpha}(\pi+\theta)\right]}{\cosh(\pi x/\alpha)-\cos\left[\frac{\pi}{\alpha}(\pi+\theta)\right]}\right\}dx.\end{aligned} \tag{21}$$

s_1 as given by (19) can be expressed as a sum of a finite number of terms. The result is (appendix)

$$s_1=\alpha\pi^{-1}\sum_{r=r_1}^{r_2}K_0\left\{\gamma[\rho^2+\rho'^2-2\rho\rho'\cos(2\alpha r+\theta)]^{1/2}\right\}. \tag{22}$$

The limits of the summation in (22) are

$$r_1=-\left[\frac{\pi+\theta}{2\alpha}\right],\quad r_2=\left[\frac{\pi-\theta}{2\alpha}\right], \tag{23}$$

where the well-known symbol $\left[\frac{\pi\pm\theta}{2\alpha}\right]$ means the largest positive or negative number which

is smaller or equal to $\frac{\pi \pm \theta}{2\alpha}$. The sum (22) is zero when $r_1 > r_2$ and the first or last term of the sum has to be halved when r_1 or r_2 is an integer. With (18) to (23) the expression (16) for the field can also be written as

$$U = F(\phi - \phi') \mp F(\phi + \phi'), \tag{24}$$

with

$$F(\theta) = 2i\pi^{-1} \sum_{r=r_1}^{r_2} K_0\{\gamma[\rho^2 + \rho'^2 - \rho\rho' \cos(2\alpha r + \theta)]^{1/2}\} - i\alpha\pi^{-1} \int_0^\infty K_0[\gamma(\rho^2 + \rho'^2 + 2\rho\rho' \cosh x)^{1/2}]$$

$$\cdot \left\{ \frac{\sin\left[\frac{\pi}{\alpha}(\pi - \theta)\right]}{\cosh(\pi x/\alpha) - \cos\left[\frac{\pi}{\alpha}(\pi - \theta)\right]} + \frac{\sin\left[\frac{\pi}{\alpha}(\pi + \theta)\right]}{\cosh(\pi x/\alpha) - \cos\left[\frac{\pi}{\alpha}(\pi + \theta)\right]} \right\} dx, \tag{25}$$

and r_1 and r_2 defined by (23).

2.1. Spherical and Plane Field Excitation

The formula [9, p. 95, formula 53]

$$(r^2 + z^2)^{-1/2} \exp[-\gamma(r^2 + z^2)^{1/2}] = 2\pi^{-1} \int_0^\infty K_0[r(\gamma^2 + v^2)^{1/2}] \cos(zv)\, dv, \tag{26}$$

expresses the generation of a spherical wave function by means of a cylindrical wave function. To obtain the field U corresponding to an incident spherical field multiply the r. h. s. of (8) and (25) by $\cos(zr)$, replace γ by $(\gamma^2 + v^2)^{1/2}$ and integrate the resulting expression with respect to v from 0 to ∞. This operation performed on (8) gives, using (26),

$$2i\pi^{-1} \int_0^\infty K_0[r(\gamma^2 + v^2)^{1/2}] \cos(zv)\, dv = i(r^2 + z^2)^{-\frac{1}{2}} \exp[-\gamma(r^2 + z^2)^{1/2}] \tag{27}$$

i. e., an incident spherical field originating from a source point $Q(\rho', \phi', 0)$. The same operation performed on (25) gives similar expressions. (For similar procedures, see [42, 5]). It follows then that in the case of an incident plane, cylindrical or spherical field the field U within the wedge of an angle α can be written in the form

$$U = F(\phi - \phi') \mp F(\phi + \phi'). \tag{28}$$

$F(\theta)$ is expressed as the sum of two functions F_1 and F_2:

$$F(\theta) = F_1(\theta) + F_2(\theta), \tag{29}$$

where

$$F_1(\theta) = \sum_{r=r_1}^{r_2} f(\theta + 2\alpha r), \tag{30}$$

$$F_2(\theta) = -(2\alpha)^{-1} \int_0^\infty H(x) \left\{ \frac{\sin\left[\frac{\pi}{\alpha}(\pi - \theta)\right]}{\cosh(\pi x/\alpha) - \cos\left[\frac{\pi}{\alpha}(\pi - \theta)\right]} + \frac{\sin\left[\frac{\pi}{\alpha}(\pi + \theta)\right]}{\cosh(\pi x/\alpha) - \cos\left[\frac{\pi}{\alpha}(\pi + \theta)\right]} \right\} dx. \tag{31}$$

The representations (28) are also valid for complex values of γ with Re $\gamma \geqq 0$ and consequently for $\gamma = ik$ with Im $k \leqq 0$. The functions f and H in (30) and (31) depend on the character of the excitation and are listed below. (The incident plane field case is obtained as the limiting case of the incident spherical field case for $\rho' \to \infty$.)

Functions f and H for the exponential decay problem

$f(\phi-\phi')$ (incident field)	$H(x)$
$\exp[\gamma\rho\cos(\phi-\phi')]$ (plane field)	$\exp(-\gamma\rho\cosh x)$
$2i\pi^{-1}K_0(\gamma r)$ (cylindrical field)	$2i\pi^{-1}K_0[\gamma(\rho^2+\rho'^2+2\rho\rho'\cosh x)^{1/2}]$
$(r^2+z^2)^{-1/2}\exp[-\gamma(r^2+z^2)^{1/2}]$ (spherical field)	$(\rho^2+\rho'^2+z^2+2\rho\rho'\cosh x)^{-1/2}$ $\cdot\exp[-\gamma(\rho^2+\rho'^2+z^2+2\rho\rho'\cosh x)^{1/2}]$.

Functions f and H for the wave problem

$f(\phi-\phi')$ (incident field)	$H(x)$
$\exp[ik\rho\cos(\phi-\phi')]$ (plane wave)	$\exp(-ik\rho\cosh x)$
$H_0^{(2)}(kr)$ (cylindrical wave)	$H_0^{(2)}[k(\rho^2+\rho'^2+2\rho\rho'\cosh x)^{1/2}]$
$(r^2+z^2)^{-1/2}\exp[-ik(r^2+z^2)^{1/2}]$ (spherical wave)	$(\rho^2+\rho'^2+z^2+2\rho\rho'\cosh x)^{-1/2}$ $\cdot\exp[-ik(\rho^2+\rho'^2+2\rho\rho'\cosh x+z^2)^{1/2}]$.

$$r=[\rho^2+\rho'^2-2\rho\rho'\cos(\phi-\phi')]^{1/2}. \tag{32}$$

The function $f(\phi-\phi')$ represents the analytic character of the incident plane, cylindrical, or spherical field. The upper or lower sign in (28) has to be taken according as an incident electromagnetic or acoustic field is considered. The total field U is now represented in three different forms, (14), (16), (28) and (15), (17), (28) for the exponential decay and the wave problem, respectively. Since in the following, (28) will be dealt with exclusively, the expressions for U of the form (14), (16), (15), and (17) corresponding to an incident plane or spherical field are not listed here. They are obtained in the same manner. The field as represented by (28) consists of the sum of two functions F_1 and F_2. Each term $r=0$ of F_1 represents a field of the same character as the incident field ($r=0$) but originating from one of the images of the source Q with respect to the walls of the wedge. The number of the images and their location depend on r_1 and r_2 and henceforth on the configuration. F_2 is given by an integral expression which vanishes when the angle of the wedge is of the form π/m, $m=1, 2, 3, \ldots$. It is easily seen that in this case $U=F_1(\phi-\phi')\pm F_1(\phi\mp\phi')$ is composed of the effect of the original source and its $2m-1$ images. In case of an incident plane field and an angle 2π (half plane), F_2 can be reduced to the error integral (39).

3. Discussion of F_1 and F_2 for Particular Cases

It is obvious that the number of terms of the sum (30) can be made arbitrarily large if α is arbitrarily small. The case $0<\alpha<\pi$ shall from now on be referred to as a corner. It will be shown now that for a wedge ($\pi<\alpha<2\pi$) the sum (30) consists of at most one term. Two cases must be distinguished here: case a, $\alpha>\pi$, $0<\phi'<\alpha-\pi$, figure 2; and case b, $\alpha>\pi$, $\alpha-\pi<\phi'<\frac{1}{2}\alpha$, figure 3. The restriction $\phi<\frac{1}{2}\alpha$ means no loss of generality.

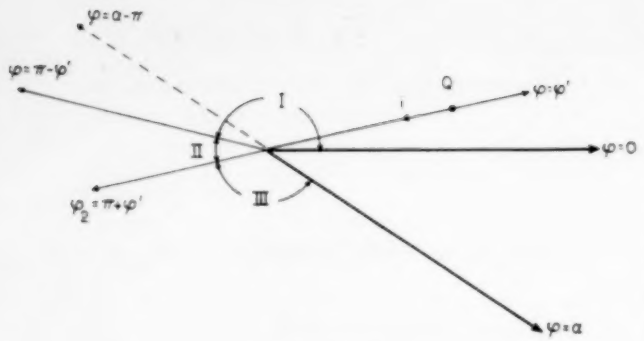

FIGURE 2.

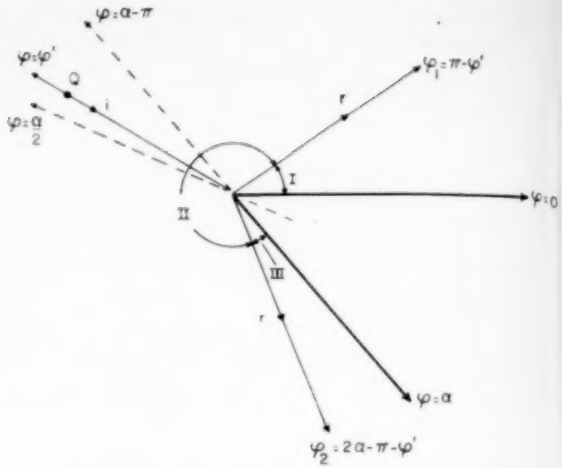

FIGURE 3.

These cases represent the two possible configurations.

Case a. The direction ϕ' of the source Q is such, that a geometric shadow region exists. The boundary of the geometric reflection is $\phi_1=\pi-\phi'$ and the boundary of the geometric shadow is $\phi_2=\pi+\phi'$.

Case b. The direction ϕ' of the source Q is such that no geometric shadow region exists. The boundaries of the geometric reflection with respect to the walls $\phi=0$ and $\phi=\alpha$ are $\phi_1=\pi-\phi'$ and $\phi_2=2\alpha-\pi-\alpha'$, respectively.

Let the region $0\leqq\phi\leqq\alpha$ be subdivided into three regions I, II, III bounded by the walls and the boundaries of geometric optics $\phi=\phi_1$ and $\phi=\phi_2$. They are defined by:

Region I. $0\leqq\phi\leqq\phi_1$
Region II. $\phi_1\leqq\phi\leqq\phi_2$
Region III. $\phi_2\leqq\phi\leqq\alpha$

and

$$\phi_1=\pi-\phi',\quad \phi_2=\pi+\phi' \qquad \text{case a,} \tag{33}$$

$$\phi_1=\pi-\phi',\quad \phi_2=2\alpha-\pi-\phi' \qquad \text{case b.} \tag{34}$$

In these cases the limits r_1, r_2 of (30) are easily found to be as listed below.

	Case a			Case b		
Region	I	II	III	I	II	III
r_1,r_2	0,0	0,0	0, −1	0,0	0,0	0,0
r_1,r_2	0,0	0, −1	0, −1	0,0	0, −1	−1, −1

The upper or lower line for (r_1,r_2) is valid according as $\theta=\phi-\phi'$ or $\theta=\phi+\phi'$. With these results one obtains by (30) for both cases a and b,

$$F_1(\phi-\phi')\mp F_1(\phi+\phi')=f(\phi-\phi')\mp f(\phi+\phi') \qquad \text{valid in I,} \tag{35}$$

$$F_1(\phi-\phi')\mp F_1(\phi+\phi')=f(\phi-\phi') \qquad \text{valid in II,} \tag{36}$$

while in region III

$$F_1(\phi-\phi')\mp F_1(\phi+\phi')=0 \qquad \text{case a} \tag{37}$$

$$F_1(\phi-\phi')\mp F_1(\phi+\phi')=f(\phi-\phi')\mp f(\phi+\phi'-2\alpha) \qquad \text{case b.} \tag{38}$$

Equations (35) to (38) together with (31) give the representation for the field U by (28) and (29) in agreement with the results obtained elsewhere [26]. The case of a source within a corner ($0<\alpha<\pi$) (fig. 4) and referred to as case c is treated the same way. At first r_1 and r_2 are determined by (23) and then F_1 by (30). Together with F_2 by (31), the field U is known by (28).

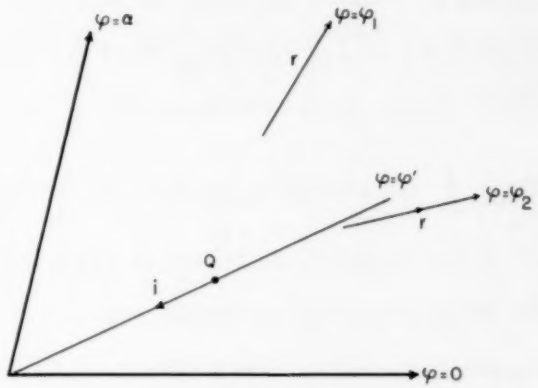

FIGURE 4.

Analogous to the cases a and b there exist two directions ϕ_1 and ϕ_2 in which a plane wave field incident on the corner emerges after multiple reflections on the walls. They are given in (50) and (51).

The second function $F_2(\theta)$ given by the integral (31) can be given explicitly when $\alpha=2\pi$ (half plane) and when the incident field is a plane field. Since this result will be needed later it is represented again although known [34]. Now, for a plane incident field, $f(\phi-\phi')=\exp[\gamma\rho\cos(\phi-\phi')]$ and $H(x)=\exp(-\gamma\rho\cosh x)$. For $\alpha=2\pi$,

$$F_2(\theta)=-\pi^{-1}\cos(\tfrac{1}{2}\theta)\int_0^\infty \cosh\left(\frac{1}{2}x\right)(\cosh x+\cos\theta)^{-1}\exp(-\gamma\rho\cosh x)dx,$$

by (31). The substitution $\cosh x=1+t$ gives

$$F_2(\theta)=-\pi^{-1}2^{-1/2}\cos\left(\frac{1}{2}\theta\right)\exp(-\gamma\rho)\int_0^\infty t^{-1/2}(1+\cos\theta+t)^{-1}\exp(-\gamma\rho t)dt.$$

This integral is known [10, vol. 1, p. 136]. Thus

$$F_2(\theta)=-\tfrac{1}{2}\cos(\tfrac{1}{2}\theta)\,|\sec(\tfrac{1}{2}\theta)|\operatorname{Erfc}[(2\gamma\rho)^{1/2}|\cos\tfrac{1}{2}\theta|]\exp(\gamma\rho\cos\theta), \tag{39}$$

where

$$\operatorname{Erfc}(z)=2\pi^{-1/2}\int_z^\infty \exp(-t^2)dt. \tag{40}$$

Since the half plane case is represented by case a, as described in figure 1, the matching expression for F_1 in the three regions is known by (35) to (37), and the field U (28) excited by an incident plane field on a perfectly reflecting half plane can be written down explicitly. It can easily be verified that U can be represented by an expression which is valid over the whole range of the half plane observing that by (40)

$$\operatorname{Erf}(-z)=2-\operatorname{Erfc}(z), \tag{41}$$

and so U becomes

$$U=\exp\,[\gamma\rho\,\cos\,(\phi-\phi')]\{1-\tfrac{1}{2}\,\mathrm{Erfc}\,[(2\gamma\rho)^{1/2}\,\cos\,(\tfrac{1}{2}\phi-\tfrac{1}{2}\phi')]\}$$

$$\mp\exp\,[\gamma\rho\,\cos\,(\phi+\phi')]\{1-\tfrac{1}{2}\,\mathrm{Erfc}\,[(2\gamma\rho)^{1/2}\,\cos(\tfrac{1}{2}\,\phi+\tfrac{1}{2}\phi')]\}, \quad (42)$$

for the exponential decay problem. The solution for the wave problem is obtained as

$$U=\exp\,[ik\rho\,\cos\,(\phi-\phi')]\{1-\tfrac{1}{2}\,\mathrm{Erfc}\,[(2ik\rho)^{1/2}\,\cos\,(\tfrac{1}{2}\,\phi-\tfrac{1}{2}\,\phi')]\}$$

$$\mp\exp\,[ik\rho\,\cos\,(\phi+\phi')]\{1-\tfrac{1}{2}\,\mathrm{Erfc}\,[(2ik\rho)^{1/2}\,\cos\,(\tfrac{1}{2}\,\phi+\tfrac{1}{2}\phi')]\}. \quad (43)$$

(For tables of the error function for complex argument see [6].)

In general case, F_2 consists of a sum of two integrals of the form

$$F_2(\theta)=I(\alpha,\pi-\theta)+I(\alpha,\pi+\theta), \quad (44)$$

with

$$I(\alpha,\psi)=-(2\alpha)^{-1}\int_0^{\infty}H(x)\,\sin\,(\pi\psi/\alpha)[(\cosh\,(\pi x/\alpha)-\cos\,(\pi\psi/\alpha)]^{-1}dx. \quad (45)$$

Obviously the denominator of the integrand (45) is zero at its lower limit $x=0$ when

$$\psi=\psi_n=\pi\pm(\phi\pm\phi')=2n\alpha, \quad n=0,\pm1,\pm2,\ldots. \quad (46)$$

But the numerator of the integrand vanishes likewise for the same value. It is easily shown [27] that

$$\lim_{\psi\to\pm0} I(\alpha,\psi)=\mp\tfrac{1}{2}H(0) \quad (47)$$

and the behavior of (45) is the same for $\psi\to\pm2n\alpha$. It may be noted that (47) does not depend on the angle of the wedge. For any configuration is always

$$0<\phi+\phi'<2\alpha, \quad 0<|\phi-\phi'|<\alpha. \quad (48)$$

This condition restricts (46) to only two possible directions ϕ_1 and ϕ_2 which define the boundaries of geometric optics as outlined before. They are defined by

$$\text{case a:}\quad \phi_1=\pi-\phi',(n=0);\quad \phi_2=\pi+\phi',(n=0),$$

$$\text{case b:}\quad \phi_1=\pi-\phi',\ (n=0);\quad \phi_2=2\alpha-\pi-\phi',\ (n=1),$$

in agreement with (36). A choice of values for the parameter n other than given above is incompatible with the configurations under consideration. In order to treat case c it is practical to subdivide this case according as the angle α of the corner can be described as

$$\begin{aligned}&\alpha=\pi/(2l+\epsilon), \quad l=1,\,2,\,3,\ldots \quad \text{case } c_1\\ &\alpha=\pi/(2l+1+\epsilon),\ l=0,\,1,\,2,\ldots \quad \text{case } c_2,\end{aligned} \quad (49)$$

where ϵ is a number between 0 and 1. Then the relation (46) leads to

$$\left.\begin{aligned}&\phi_1=|\epsilon\alpha-\phi'|\\ &\phi_2=\mathrm{Min}\,[\alpha(2-\epsilon)-\phi',\phi'+\epsilon\alpha]\end{aligned}\right\}\text{case } c_1 \quad (50)$$

and

$$\left.\begin{aligned}&\phi_1=|\alpha(1-\epsilon)-\phi'|\\ &\phi_2=\mathrm{Min}[\alpha(1+\epsilon)-\phi',\alpha(1-\epsilon)+\phi']\end{aligned}\right\}\text{case } c_2 \quad (51)$$

and ϵ is connected with α by (49). In case $\epsilon=0$, this leads to $\varphi_1=\varphi_2$ and particularly,

$$\phi_1=\phi_2=\phi' \qquad \text{when } \alpha=\pi/(2l)$$

$$\phi_1=\phi_2=\alpha-\phi' \quad \text{when } \alpha=\pi/(2l+1).$$

An elementary expression for the upper limit of $I(\alpha,\psi)$ can be given. Integration of (45) by parts gives

$$-\pi I(\alpha_1\psi)=H(x)\ \arctan\left[\operatorname{cotan}\left(\tfrac{1}{2}\pi\psi/\alpha\right)\tanh\left(\tfrac{1}{2}\pi x/\alpha\right)\right]\Big|_0^\infty$$

$$-\int_0^\infty H'(x)\ \arctan\left[\operatorname{cotan}\left(\tfrac{1}{2}\pi\psi/\alpha\right)\tanh\left(\tfrac{1}{2}\pi x/\alpha\right)\right]dx.$$

Since, with the exception of the plane wave case, $H(x)\to 0$ when $x\to\infty$ it becomes

$$I(\alpha_1\psi)=\pi^{-1}\int_0^\infty H'(x)\ \arctan\left[\operatorname{cotan}\left(\frac{1}{2}\pi\psi/\alpha\right)\tanh\left(\frac{1}{2}\pi x/\alpha\right)\right]dx, \tag{52}$$

and hence

$$|I(\alpha_1\psi)|\leqq\pi^{-1}\int_0^\infty|H'(x)|\,|\arctan\left[\operatorname{cotan}\left(\frac{1}{2}\pi\psi/\alpha\right)\tanh\left(\frac{1}{2}\pi x/\alpha\right)\right]|dx,$$

and, after replacing $\tanh(\frac{1}{2}\pi x/\alpha)$ by its upper limit 1,

$$|I(\alpha_1\psi)|\leqq|H(0)|\,|\arctan[\operatorname{cotan}(\tfrac{1}{2}\pi\psi/\alpha)]|\pi^{-1}. \tag{53}$$

The equal sign holds when ψ has one of the values defined by (46) and the accuracy of the inequality (53) increases with decreasing α. Since, in general $\frac{1}{2}\pi\psi/\alpha$ will not lie between 0 and π the "reduced" property

$$\tfrac{1}{2}\pi\bar{\psi}/\alpha=\tfrac{1}{2}\pi\psi/\alpha\pm\pi l_n,\quad l_n=0,\ 1,\ 2,\ \ldots, \tag{54}$$

is introduced and l_n is such that $\frac{1}{2}\pi\bar{\psi}/\alpha$ is between 0 and π. Thus

$$|I(\alpha_1\psi)|\leqq\pi^{-1}|H(0)|\,|\arctan[\operatorname{cotan}(\tfrac{1}{2}\pi\bar{\psi}/\alpha)]|,$$

and finally

$$|I(\alpha_1\psi)|\leqq\tfrac{1}{2}|H(0)|\,|1-\bar{\psi}/\alpha|. \tag{55}$$

4. Asymptotic Expansions

The derivation of an asymptotic expansion of the field U for large distances from the edge of the wedge is equivalent with the reduction of the integral (31) to an asymptotic series. Comparatively simple is the case of a plane field incidence (fig. 5). Then for the exponential decay problem

$$H(x)=\exp(-\gamma\rho\cosh x). \tag{56}$$

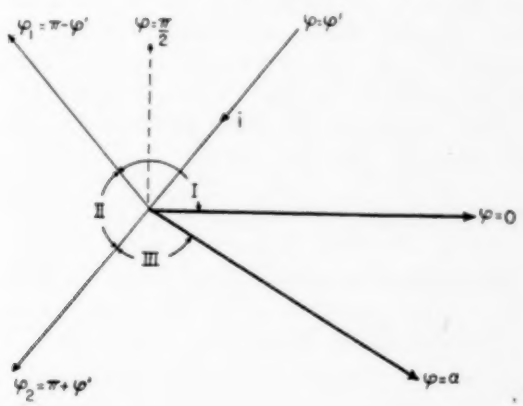

FIGURE 5.

In this case $F_2(\theta)$ is represented as a Laplace transform with $\gamma\rho$ as parameter. Methods for the asymptotic development of integrals of this type are known [8, p. 45]. Since by (44) $F_2(\theta)$ is composed of two integrals of the form (45) it is sufficient to investigate

$$I(\alpha,\psi)=-(2\alpha)^{-1}\sin(\pi\psi/\alpha)\int_0^\infty[\cosh(\pi x/\alpha)-\cos(\pi\psi/\alpha)]^{-1}\exp(-\gamma\rho\cosh x)dx, \tag{57}$$

and ψ has one of the values $\pi\pm(\phi\pm\phi')$. The substitution

$$\cosh x=1+t \tag{58}$$

transforms (57) into

$$I(\alpha,\psi)=-\exp(-\gamma\rho)\int_0^\infty t^{-1/2}K(t)\exp(-\gamma\rho t)dt, \tag{59}$$

with

$$K(t)=(2\alpha)^{-1}\sin(\pi\psi/\alpha)(2+t)^{-1/2}\{\cosh[\pi/\alpha\log(1+t+(t^2+2t)^{\frac{1}{2}}]-\cos(\pi\psi/\alpha)\}^{-1}. \tag{60}$$

Thus (59) is represented as a Laplace transform. For the following, the discussion shall be restricted to case a, as described in section 3 and fig. 2. Cases b and c, as described in section 3, can be treated in the same manner. Now, $K(t)$ as given by (60) represents a regular function in the vicinity of $t=0$ provided that $\phi\pm\phi'\neq\pi$ (corresponding to $\psi\neq 0$ by (46)). The singularities of $K(t)$ lie on the negative axis and the smallest of their moduli is equal to Min $[1+\cos(\phi\pm\phi')]$.

The Taylor expansion of $K(t)$ near the origin is

$$K(t)=\sum_{n=0}^{\infty}A_n(\alpha,\psi)t^n,\quad |t|<\mathrm{Min}[1+\cos(\phi\pm\phi')], \tag{61}$$

with

$$A_n(\alpha,\psi)=(n!)^{-1}[d^nK(t)/(dt^n)]_{t=0}. \tag{62}$$

The first two coefficients are

$$A_0(\alpha,\psi)=(2\alpha)^{-1}2^{-1/2}\mathrm{cotan}(\tfrac{1}{2}\pi\psi/\alpha),$$

$$A_1(\alpha,\psi)=-(8\alpha)^{-1}2^{-1/2}\mathrm{cotan}(\tfrac{1}{2}\pi\psi/\alpha)\{1+2(\pi/\alpha)^2[\sin(\tfrac{1}{2}\pi\psi/\alpha)]^{-2}\}. \tag{63}$$

The asymptotic expansion of $I(\alpha,\psi)$ for large $\gamma\rho$ is obtained by inserting the series (61) into (59) and integrating term by term [8, p. 48, theorem 6]. The result is

$$I(\alpha,\psi)\sim-\exp(-\gamma\rho)\sum_{n=0}^{\infty}A_n(\alpha,\psi)\,\Gamma(n+\tfrac{1}{2})(\gamma\rho)^{-n-1/2},\quad -3\pi/2<\arg\gamma<3\pi/2. \tag{64}$$

The coefficients A_n tend to infinity when $\phi\pm\phi'$ tends to π (and hence ψ to 0) and the expansion (64) becomes useless. This is the case when the configuration is such that one of the boundaries of geometric optics is approached. In this case the point $t=0$ becomes a singular point of $K(t)$ and no expansion of the type (61) exists. In order to obtain an asymptotic expansion which is valid over the whole region one proceeds as follows. The integrand of (57) at $x=0$ is equal to $-(2\alpha)^{-1}\cot(\tfrac{1}{2}\pi\psi/\alpha)$. In the vicinity of $\psi=0$ (the boundaries of geometric optics)

$$-(2\alpha)^{-1}\mathrm{cotan}(\tfrac{1}{2}\pi\psi/\alpha)=-(\pi\psi)^{-1}+O(\psi) \tag{65}$$

and the singular part of (65) is independent of the angle α. Let the field U be now written in the form

$$U=(U)_{\alpha=2\pi}+[U-(U)_{\alpha=2\pi}] \tag{66}$$

and by (28), (29), and (35) to (37)

$$U=(U)_{\alpha=2\pi}+F_2(\phi-\phi')-[F_2(\phi-\phi')]_{\alpha=2\pi}\mp\{F_2(\phi+\phi')-[F_2(\phi+\phi')]_{\alpha=2\pi}\}. \tag{67}$$

Now, $(U)_{\alpha=2\pi}$ is given by (42), and by (44)

$$F_2(\phi\pm\phi')-[F_2(\phi\pm\phi')]_{\alpha=2\pi}=I(\alpha,\pi-\phi\mp\phi')-I(2\pi,\pi-\phi\mp\phi')+I(\alpha,\pi+\phi\pm\phi')-(I(2\pi,\pi+\phi\pm\phi').$$

The difference

$$I(\alpha,\pi-\phi\mp\phi')-I(2\pi,\pi-\phi\mp\phi')$$

$$=-\int_0^\infty\left[\frac{(2\alpha)^{-1}\sin\left[\frac{\pi}{\alpha}(\pi-\phi\mp\phi')\right]}{\cosh(\pi x/\alpha)-\cos\left[\frac{\pi}{\alpha}(\pi-\phi\mp\phi')\right]}-\frac{(4\pi)^{-1}\cos(\frac{1}{2}\phi\pm\frac{1}{2}\phi')}{\cosh(\frac{1}{2}x)-\sin(\frac{1}{2}\phi\pm\frac{1}{2}\phi')}\right]\exp(-\gamma\rho\cosh x)\,dx \tag{68}$$

is by (65) such that the integrand of (68) vanishes identically when $\phi\pm\phi'=\pi$, and the asymptotic expansion of (68) is given as the difference of two series of the type (64) whose coefficients $A_n(\alpha,\pi-\phi\mp\phi')-A_n(2\pi,\pi-\phi\mp\phi')$ tend to zero when $\phi\mp\phi'$ tends to π. Using (64) one arrives at the asymptotic expansion

$$F_2(\phi-\phi')-[F_2(\phi-\phi')]_{\alpha=2\pi}\pm\{F_2(\phi+\phi')-[F_2(\phi+\phi')]_{\alpha=2\pi}\}=S(\gamma\rho)$$

$$\sim-\exp(-\gamma\rho)\sum_{n=0}^{\infty}B_n(\gamma\rho)^{-n-\frac{1}{2}},\quad -3\pi/2<\arg\gamma<3\pi/2. \tag{69}$$

The coefficients B_n are defined by

$$B_n=\Gamma(n+\tfrac{1}{2})\{A_n(\alpha,\pi-\phi+\phi')-A_n(2\pi,\pi-\phi+\phi')+A_n(\alpha,\pi+\phi-\phi')-A_n(2\pi,\pi+\phi-\phi')$$

$$\mp[A_n(\alpha,\pi-\phi-\phi')-A_n(2\pi,\pi-\phi-\phi')+A_n(\alpha,\pi+\phi+\phi')-A_n(2\pi,\pi+\phi+\phi')]\} \tag{70}$$

With the A_n given by (62), (63). It follows then from (67), (42), and (69) for the field excited by an incident plane field on a perfectly reflecting wedge of an angle α for case a (fig. 5)

$$U=\exp[\gamma\rho\cos(\phi-\phi')]\{1-\tfrac{1}{2}\mathrm{Erfc}[(2\gamma\rho)^{1/2}\cos(\tfrac{1}{2}\phi-\tfrac{1}{2}\phi')]\}$$

$$\mp\exp[\gamma\rho\cos(\phi+\phi)]\{1-\tfrac{1}{2}\mathrm{Erfc}[(2\gamma\rho)^{1/2}\cos(\tfrac{1}{2}\phi+\tfrac{1}{2}\phi')]\}+S(\gamma\rho),$$

where $S(\gamma\rho)$ is asymptotically given by (69). It follows then for the wave problem

$$U=\exp[ik\rho\cos(\phi-\phi')]\{1-\tfrac{1}{2}\mathrm{Erfc}[(2ik\rho)^{1/2}\cos(\tfrac{1}{2}\phi-\tfrac{1}{2}\phi')]\}$$

$$\mp\exp[ik\rho\cos(\phi+\phi')]\{1-\tfrac{1}{2}\mathrm{Erfc}[(2ik\rho)^{1/2}\cos(\tfrac{1}{2}\phi+\tfrac{1}{2}\phi')]\}+S(ik\rho), \tag{71}$$

where for large $k\rho$

$$S(ik\rho)\sim-\exp(-ik\rho-i\pi/4)\sum_{n=0}^{\infty}B_n i^n(k\rho)^{-n-\frac{1}{2}} \tag{72}$$

and these expressions are valid over the whole region of the wedge. The plus or minus sign has to be taken according as the acoustic or the electromagnetic case is considered. Obviously S represents the deviation of the wedge field from the half-plane field and the expansions (69) and (72) represent asymptotic expansions for this deviation term. If $(\gamma\rho)^{1/2}\cos(\frac{1}{2}\phi\pm\frac{1}{2}\phi')$ and $(k\rho)^{1/2}\cos(\frac{1}{2}\varphi\pm\frac{1}{2}\phi')$ are large, i. e., for the far field at large distances from the boundaries of geometric optics one can replace the error function by its asymptotic expansion [9, p. 147],

$$\mathrm{Erfc}\,(z)\sim\pi^{-1}\exp(-z^2)\sum_{n=0}^{\infty}(-1)^n\Gamma(n+\tfrac{1}{2})z^{-2n-1},\quad -3\pi/4<\arg z<3\pi/4, \tag{73}$$

and the asymptotic expansion of U is of the same type as the one for S. On the boundary of the geometric reflection ($\phi+\phi'=\pi$), (71) becomes

$$U=\exp\,[ik\rho\,\cos\,(\phi-\phi')]\{1-\tfrac{1}{2}\,\mathrm{Erfc}\,[(2ik\rho)^{1/2}\cos\,(\tfrac{1}{2}\phi-\tfrac{1}{2}\phi')]\}\mp\tfrac{1}{2}\exp\,(-ik\rho)+S(ik\rho). \quad (74)$$

On the boundary of the geometric shadow ($\phi-\phi'=\pi$),

$$U=\tfrac{1}{2}\exp\,(-ik\rho)\mp\exp\,[(ik\rho\,\cos\,(\phi+\phi')]\cdot\{1-\tfrac{1}{2}\,\mathrm{Erfc}\,[(2ik\rho)^{1/2}\cos\,(\tfrac{1}{2}\phi+\tfrac{1}{2}\phi')]\}+S(ik\rho). \quad (75)$$

Using (73) these results can be written as

$$U=\exp\,[ik\rho\,\cos\,(\phi-\phi')]\mp\tfrac{1}{2}\exp\,(-ik\rho)+O[(k\rho)^{-1/2}], \quad (74a)$$

$$U=\tfrac{1}{2}\exp\,(-ik\rho)+O[(k\rho)^{-\frac{1}{2}}]. \quad (75a)$$

These equations express the fact that the far field on the boundaries of geometric optics is independent of the angle of the wedge.

5. Energy Radiated From a Hertz Dipole and From an Acoustic Point Source in the Presence of a Perfectly Reflecting Wedge or Corner

Let the source $Q(\rho',\,\phi',\,0)$ be a Hertz dipole with its axis parallel to the edge. The functions $f(\theta)$ and $H(x)$ are then

$$f(\theta)=(r^2+z^2)^{-1/2}\exp[-ik(r^2+z^2)^{1/2}], \quad (76)$$

$$r=(\rho^2+\rho'^2-2\rho\rho'\,\cos\,\theta)^{1/2},$$

$$H(x)=(\rho^2+\rho'^2+2\rho\rho'\,\cosh\,x+z^2)^{-1/2}\exp[-ik(\rho^2+\rho'^2+2\rho\rho'\,\cosh\,x+z^2)^{1/2}]. \quad (77)$$

The function U given by (28) (taken with the minus sign) represents the vector potential A of the electromagnetic field. Its components are

$$A_x=A_y=0,\quad A_z=U. \quad (78)$$

With this relation the components E_x, E_y, E_z of the electric field vector E are known and the radiated energy can be determined by Poyntings method. The application of this method is very difficult in view of the complexity of the expression for U. It is therefore advisable to use the so called E. M. F. method for the determination of the radiation resistance R of the dipole [37, p. 457] and [33, p. 134]. R is given by

$$R=-(L/J)\mathrm{Re}(E_z)_D. \quad (79)$$

Here L and J are the length and the current of the dipole respectively. $\mathrm{Re}(E_z)_D$ is the real part of the z component of the electric field at the location of the dipole $Q(\rho',\,\phi',\,0)$. It follows from (78) for the field,

$$E_z=-iC\left(\frac{\partial^2 U}{\partial z^2}+k^2U\right). \quad (80)$$

C is a constant (real >0) and is of no importance here since the "reduced" radiation resistance R/R_0 will be determined. This is the quotient of the radiation resistance R for the complete system (dipole plus reflector) and the radiation resistance R_0 of the dipole in free space (without the presence of the reflector). At first the contribution of F_1 (which represents a set of dipoles consisting of the original source and a number of images) to E_z is considered. From (30) and (76)

$$U_1=F_1(\phi-\phi')-F_1(\phi+\phi')$$

$$=\sum_{p=p_1}^{p_2}(r_p^2+z^2)^{-1/2}\exp\,[(-ik(r_p^2+z^2)^{1/2}]-\sum_{q=q_1}^{q_2}(r_q^2+z^2)^{-1/2}\exp\,[-ik(r_q^2+z^2)^{1/2}], \quad (81)$$

$$r_p^2=\rho^2+\rho'^2-2\rho\rho'\,\cos\,(\phi-\phi'+2\alpha p)$$

$$r_q^2=\rho^2+\rho'^2-2\rho\rho'\cos(\phi+\phi'+2\alpha q) \tag{82}$$

$$p_1=-\left[\frac{\pi+\phi-\phi'}{2\alpha}\right],\quad p_2=\left[\frac{\pi-\phi+\phi'}{2\alpha}\right]$$

$$q_1=-\left[\frac{\pi+\phi+\phi'}{2\alpha}\right],\quad q_2=\left[\frac{\pi-\phi-\phi'}{2\alpha}\right].$$

It is then easily found that

$$\mathrm{Re}\left[-iC\left(\frac{\partial^2 U_1}{\partial z^2}+k^2U_1\right)_D\right]=-Ck^3\left[\sum_{n=n_1}^{n_2} g(kd_n)-\sum_{m=m_1}^{m_2} g(kd_m)\right] \tag{83}$$

with

$$d_n=2\rho'\sin(\alpha n),\quad d_m=2\rho'\sin(\phi'+\alpha m)$$

$$n_1=-[\tfrac{1}{2}\pi/\alpha],\qquad n_2=[\tfrac{1}{2}\pi/\alpha],$$

$$m_1=-\left[\frac{\pi+2\phi'}{2\alpha}\right],\quad m_2=\left[\frac{\pi-2\phi'}{2\alpha}\right], \tag{84}$$

$$g(\zeta)=\zeta^{-1}\sin\zeta+\zeta^{-2}\cos\zeta-\zeta^{-3}\sin\zeta,\quad g(0)=2/3.$$

The term $n=0$ in the sum (83) represents the contribution of the original dipole source. It follows then for the radiation resistance of the Hertz dipole in free space by (83) and (79)

$$R_0=2L/(3J)Ck^3. \tag{85}$$

The contribution of F_2 to U is

$$U_2=F_2(\phi-\phi')-F_2(\phi+\phi') \tag{86}$$

and it follows by (31) and (77)

$$\mathrm{Re}\left[-iC\left(\frac{\partial^2 U_2}{\partial z^2}+k^2U_2\right)_D\right]=(2\alpha)^{-1}Ck^3\left\{2\sin(\pi^2/\alpha)\int_0^\infty \frac{g(2k\rho'\cosh x/2)}{\cosh(\pi x/\alpha)-\cos(\pi^2/\alpha)}\,dx\right.$$

$$\left.-\int_0^\infty g\left(2k\rho'\cosh\frac{x}{2}\right)\left[\frac{\sin\left[\frac{\pi}{\alpha}(\pi-2\phi')\right]}{\cosh(\pi x/\alpha)-\cos\left[\frac{\pi}{\alpha}(\pi-2\phi')\right]}+\frac{\sin\left[\frac{\pi}{\alpha}(\pi+2\phi')\right]}{\cosh(\pi x/\alpha)-\cos\left[\frac{\pi}{\alpha}(\pi+2\phi')\right]}\right]dx\right\}. \tag{87}$$

It follows, then, for the quotient of the radiation resistance R of the dipole in the presence of the reflector and the radiation resistance R_0 of the dipole in free space by eq (79), (83), (87), and (85).

$$R/R_0=3/2\left[\sum_{n=n_1}^{n_2} g(kd_n)-\sum_{m=m_1}^{m_2} g(kd_m)\right]-\frac{3}{4\alpha}\left\{2\sin(\pi^2/\alpha)\int_0^\infty \frac{g\left(2k\rho'\cosh\frac{x}{2}\right)}{\cosh(\pi x/\alpha)-\cos(\pi^2/\alpha)}\,dx\right.$$

$$\left.-\int_0^\infty g\left(2k\rho'\cosh\frac{x}{2}\right)\left[\frac{\sin\left[\frac{\pi}{\alpha}(\pi-2\phi')\right]}{\cosh(\pi x/\alpha)-\cos\left[\frac{\pi}{\alpha}(\pi-2\phi')\right]}+\frac{\sin\left[\frac{\pi}{\alpha}(\pi+2\phi')\right]}{\cosh(\pi x/\alpha)-\cos\left[\frac{\pi}{\alpha}(\pi+2\phi')\right]}\right]dx\right\}. \tag{88}$$

The occurring parameters and $g(\zeta)$ are given in (84). Since $g(\zeta)$ vanishes for large ζ it is clear that if the distance of the dipole from the walls is large ($\rho'\to\infty$) only the term $n=0$ in the sum gives a contribution, and then

$$\lim R/R_0=3/2g(0)=1.$$

The formula (88) is valid for an arbitrary α. But if $\alpha>\pi$, i. e., in the case of a wedge reflector (figs. 2 and 3), the two sums on the r. h. s. of (88) can be given explicitly. By (84) the limits n_1, n_2, m_1, m_2, of the sums in case $\alpha>\pi$ are

$$n_1=n_2=m_1=m_2=0 \qquad \text{for } 0<\phi'<\tfrac{1}{2}\pi,$$

$$n_1=n_2=m_1=0, \quad m_2=-1 \qquad \text{for } \tfrac{1}{2}\pi<\phi'<\tfrac{1}{2}\alpha.$$

Thus

$$\sum_{n=n_1}^{n_2} g(kd_n)-\sum_{m=m_1}^{m_2} g(kd_m)=2/3-g(2k\rho' \sin \phi'), \qquad \text{if } 0<\phi'<\tfrac{1}{2}\pi,$$

$$=2/3, \qquad \text{if } \tfrac{1}{2}\pi<\phi'<\tfrac{1}{2}\alpha.$$

The analysis is exactly the same when the source $Q(\rho',\phi,0)$ is an acoustic point source. In this case the plus sign in (28) has to be taken. The function $g(\zeta)$ in (84) which characterizes the coupling term between two Hertz dipoles (parallel to each other and the line connecting their centers perpendicular to their axis) has to be replaced by the corresponding coupling term $g_1(\zeta)$ for two acoustic point sources [30].

$$g_1(\zeta)=\zeta^{-1}\sin \zeta. \tag{89}$$

In this case the corresponding formula for the relative radiation resistance as defined before is

$$R/R_0=\sum_{n=n_1}^{n_2} g_1(kd_n)+\sum_{m=m_1}^{m_2} g_1(kd_m)-(2\alpha)^{-1}\left\{2 \sin (\pi^2/\alpha)\int_0^\infty \frac{g_1\left(2k\rho' \cosh \frac{x}{2}\right)}{\cosh (\pi x/\alpha)-\cos (\pi^2/\alpha)}dx\right.$$

$$\left.+\int_0^\infty g_1\left(2k\rho' \cosh \frac{x}{2}\right)\left[\frac{\sin\left[\frac{\pi}{\alpha}(\pi-2\phi')\right]}{\cosh (\pi x/\alpha)-\cos\left[\frac{\pi}{\alpha}(\pi-2\rho')\right]}+\frac{\sin\left[\frac{\pi}{\alpha}(\pi+2\phi')\right]}{\cosh (\pi x/\alpha)-\cos\left[\frac{\pi}{\alpha}(\pi+2\phi')\right]}\right]dx\right\}. \tag{90}$$

The definition of the n_1, n_2, m_1, m_2, d_n, d_m is the same as in (84), while $g_1(\zeta)$ is given by (89). If $\alpha>\pi$, then as before

$$n_1=n_2=m_1=m_2=0 \qquad \text{for } 0<\phi'<\tfrac{1}{2}\pi,$$

$$n_1=n_2=m_1=0, \quad m_2=-1 \qquad \text{for } \tfrac{1}{2}\pi<\phi'<\tfrac{1}{2}\alpha.$$

and

$$\sum_{n=n_1}^{n_2} g_1(kd_n)+\sum_{m=m_1}^{m_2} g_1(kd_m)=1+g_1(2k\rho' \sin \phi'), \qquad 0<\phi'<\tfrac{1}{2}\pi,$$

$$=1, \qquad \tfrac{1}{2}\pi'<\phi'<\tfrac{1}{2}\alpha.$$

6. Transient Solutions

The results obtained in section 2 shall now be used to investigate the corresponding pulse problems. The majority of the contributions quoted at the beginning of this paper are based upon a direct attack on the time dependent wave equation. Integral transform methods were used in [38] (Kontorovich-Lebedev transform) and [40] (Fourier transform). In the cases considered here the application of Laplace's transform leads rapidly to the desired results. Let the excitation of the source be represented by a pulse starting at the time $t=0$. Let the pulse function be $g(t)$, and $g(t)=0$ for $t<0$. Let the pulse function be such that it admits its representation by Laplace's integral formula:

$$g(t)=(2\pi i)^{-1}\int_{c-i\infty}^{c+i\infty}\left[\int_0^\infty g(\tau)\exp(-\gamma\tau)d\tau\right]\exp(\gamma t)d\gamma. \tag{91}$$

In section 2, various expressions U for the exponential decay problem were given. This case corresponded according to (5) to the time dependency $\exp(\gamma t)$, (put $c=1$). It can then be concluded that for a pulse excitation $g(t)$ as represented by (91) the expression for the field is represented by

$$\Phi(t)=(2\pi i)^{-1}\int_{c-i\infty}^{c+i\infty}\left[\int_0^\infty g(\tau)\exp(-\gamma\tau)\,d\tau\right]U\exp(\gamma t)d\gamma. \tag{92}$$

The solution of the pulse problem is therefore given as the inverse Laplace transformation of

$$U\int_0^\infty g(\tau)\exp(-\gamma\tau)d\tau, \tag{93}$$

with respect to γ.

6.1. Special Cases for $g(t)$

For a unit step function $g(t)=1$, the field (92) becomes

$$\Phi(t)=(2\pi i)^{-1}\int_{c-i\infty}^{c+i\infty}U\gamma^{-1}\exp(\gamma t)d\gamma. \tag{94}$$

For a "Dirac" pulse excitation imposed at the time $t=t_1>0$: $g(t)=\delta(t-t_1)$, one finds first

$$\int_0^\infty g(\tau)\exp(-\gamma\tau)d\tau=\int_0^\infty\delta(\tau-t_1)\exp(-\gamma\tau)d\tau=\exp(-\gamma t_1). \tag{95}$$

The field due to a "Dirac" pulse excitation becomes then

$$\Phi_D(t-t_1)=(2\pi i)^{-1}\int_{c-i\infty}^{c+i\infty}U\exp[\gamma(t-t_1)]\,d\gamma. \tag{96}$$

If the order of integration in (92) can be interchanged, it results in

$$\Phi(t)=\int_0^\infty g(\tau)\left\{(2\pi i)^{-1}\int_{c-i\infty}^{c+i\infty}U\exp[\gamma(t-\tau)]\,d\gamma\right\}d\tau. \tag{97}$$

Since by (96) the inner integral is the effect of a "Dirac" pulse, excitation (97) can be written as

$$\Phi(t)=\int_0^\infty g(\tau)\Phi_D(t-\tau)d\tau, \tag{98}$$

i. e., the field due to an excitation $g(t)$ of the source Q can be obtained by an integration process involving the field due to a "Dirac" pulse excitation. The general equations (96), (98) shall now be applied to the problem of the diffraction of arbitrary pulses (plane, cylindrical, and spherical) incident on a perfectly reflecting wedge or corner. The case of "Dirac" pulse excitation imposed at the time $t=0$ shall be considered first. The Laplace inversion of a function $h(\gamma)$ with respect to γ shall be denoted by $\bar{h}(t)$, i. e.,

$$\bar{h}(t)=(2\pi i)^{-1}\int_{c-i\infty}^{c+i\infty}h\exp(\gamma t)d\gamma. \tag{99}$$

It follows from (96) and (28) for the field Φ_D due to a plane, cylindrical or spherical "Dirac" pulse:

$$\Phi_D(t)=\bar{F}(\phi-\phi')\mp\bar{F}(\phi+\phi')$$

$$=\sum_{n=n_1}^{n_2}\bar{f}(\phi-\phi'+2\alpha n)\mp\sum_{m=m_1}^{m_2}\bar{f}(\phi+\phi'+2\alpha m)+\int_0^\infty \overline{H}(x)[G(\phi-\phi')\mp G(\phi+\phi')]dx, \tag{100}$$

where

$$n_1=-\left[\frac{\pi+\phi-\phi'}{2\alpha}\right],\quad n_2=\left[\frac{\pi-\phi-\phi'}{2\alpha}\right],\quad m_1=-\left[\frac{\pi+\phi+\phi'}{2\alpha}\right],\quad m_2=\left[\frac{\pi-\phi-\phi'}{2\alpha}\right],$$

$$G(\theta)\equiv-(2\alpha)^{-1}\left\{\frac{\sin\left[\frac{\pi}{\alpha}(\pi-\theta)\right]}{\cosh(\pi x/\alpha)-\cos\left[\frac{\pi}{\alpha}(\pi-\theta)\right]}+\frac{\sin\left[\frac{\pi}{\alpha}(\pi+\theta)\right]}{\cosh(\pi x/\alpha)-\cos\left[\frac{\pi}{\alpha}(\pi+\theta)\right]}\right\}. \tag{101}$$

The respective Laplace inversions $\bar{f}(\theta)$ and $\overline{H}(x)$ are for a plane pulse:

$$\bar{f}(\theta)=\delta(t+\rho\cos\theta) \tag{102}$$

$$\overline{H}(x)=\delta(t-\rho\cosh x). \tag{103}$$

For a cylindrical pulse one has

$$\bar{f}(\theta)=2i\pi^{-1}(t^2-\rho^2-\rho'^2+2\rho\rho'\cos\theta)^{-1/2},\quad \text{for } t>(\rho^2+\rho'^2-2\rho\rho'\cos\theta)^{1/2},$$
$$=0,\quad \text{otherwise.} \tag{104}$$

$$\overline{H}(x)=2i\pi^{-1}(t^2-\rho^2-\rho'^2-2\rho\rho'\cosh x)^{-1/2},\quad \text{for } 2\rho\rho'\cosh x<t^2-\rho^2-\rho'^2,$$
$$=0,\quad \text{otherwise.} \tag{105}$$

Finally, for a spherical pulse

$$\bar{f}(\theta)=(r^2+z^2)^{-1/2}\,\delta[t-(r^2+z^2)^{1/2}] \tag{106}$$

$$\overline{H}(x)=(\rho^2+\rho'^2+z^2+2\rho\rho'\cosh x)^{-1/2}\delta[t-(\rho^2+\rho'^2+z^2+2\rho\rho'\cosh x)^{1/2}]. \tag{107}$$

The Laplace inversions for $f(\theta)$ and $H(x)$ are obtained from (95) for the plane and for the spherical pulse, while [10, vol. 1, p. 277, formula 8] gives the inversion for the cylindrical pulse. It does not seem possible to express the integral $\int_0^\infty \overline{H}(x)G(\theta)dx$ in a closed form in the case of a cylindrical pulse. To obtain the field due to a pulse excitation $g(t)$, the equations (98) and (100) have to be used. For a plane and a spherical pulse the integration process in (98) can be performed immediately. The results are

$$\Phi(t)=\sum_{n=n_1}^{n_2} g[t+\rho\cos(\phi-\phi'+2\alpha n)]\mp\sum_{m=m_1}^{m_2} g[t+\rho\cos(\phi+\phi'+2\alpha m)]$$
$$+\int_0^{\cosh x=t/\rho} g(t-\rho\cosh x)[G(\phi-\phi')\mp G(\phi+\phi')]dx, \tag{108}$$

for the plane pulse.

$$\Phi(t)=\sum_{n=n_1}^{n_2} R_n^{-1}g(t-R_n)\mp\sum_{m=m_1}^{m_2} R_m^{-1}g(t-R_m)$$
$$+\int_0^{x_1}(\rho^2+\rho'^2+z^2+2\rho\rho'\cosh x)^{-1/2}\,g[t-(\rho^2+\rho'^2+z^2+2\rho\rho'\cosh x)^{1/2}]\{G(\phi-\phi')\mp G(\phi+\phi')\}dx, \tag{109}$$

for the spherical pulse.

The upper limit x_1 of the integral is given by

$$2\rho\rho'\cosh x_1=t^2-\rho^2-\rho'^2-z^2 \text{ for (109), and } \cosh x_1=t/\rho \text{ for (108).} \tag{110}$$

$$R_n=[\rho^2+\rho'^2+z^2-2\rho\rho'\cos(\phi-\phi'+2\alpha n)]^{1/2}$$
$$R_m=[\rho^2+\rho'^2+z^2-2\rho\rho'\cos(\phi+\phi'+2\alpha m)]^{1/2}. \tag{111}$$

The other properties are given in (101). Again in the case of a wedge ($\alpha>\pi$), the properties n_1, n_2, m_1, m_2 are given in section 3. The representation of the cylindrical pulse field leads to a double integral. For the special case of a half plane, however, the integral occurring in (100) can be solved. In the following some special cases are considered in which the solution for the transient field become elementary.

6.2. Special Cases

a. Cylindrical Pulse and Half Plane

The case of a line source Q parallel to the edge of a perfectly reflecting half plane is considered. The regions I, II, III as described in section 3 are indicated in figure 6. For a half plane ($\alpha=2\pi$), one obtains from (101),

$$G(\theta)=-\pi^{-1}\cos(\tfrac{1}{2}\theta)\cosh(\tfrac{1}{2}x)(\cosh x+\cos\theta)^{-1}. \tag{112}$$

It follows then for a cylindrical "Dirac" pulse by (105),

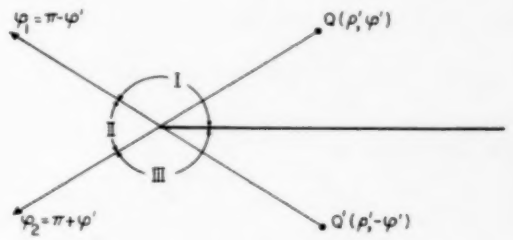

FIGURE 6.

$$\int_0^\infty \overline{H}(x)\,G(\theta)dx=-2i\pi^{-2}\cos(\tfrac{1}{2}\theta)\int_0^{x_1}\cosh(\tfrac{1}{2}x)\,\frac{(t^2-\rho^2-\rho'^2-\rho\rho'\cosh x)^{-1/2}}{\cosh x+\cos\theta}\,dx.$$

The upper limit x_1 of the integral is given by $2\rho\rho'\cosh x_1=t^2-\rho^2-\rho'^2$, and from (105) it is obvious that the integral is only different from zero when $t>\rho+\rho'$. The substitution $\cosh x=1+v^2$, $\cosh(\tfrac{1}{2}x)dx=2^{1/2}dv$ gives for the integral

$$\int_0^\infty \overline{H}(x)\,G(\theta)dx=-i\pi^{-1}\cos(\tfrac{1}{2}\theta)|\sec(\tfrac{1}{2}\theta)|(t^2-\rho^2-\rho'^2+2\rho\rho'\cos\theta)^{-1/2},\ \text{if } t>\rho+\rho',$$
$$=0, \qquad \text{otherwise.} \tag{113}$$

It follows then from (100) by means of (35), (36), (37), (104), and (113) for the field due to a cylindrical "Dirac" pulse incident on a half plane

$$\Phi_D(t)=2i\pi^{-1}\{(t^2-R_1^2)^{-1/2}\mp(t^2-R_2^2)^{-1/2}-\tfrac{1}{2}[(t^2-R_1^2)^{-1/2}\mp(t^2-R_2^2)^{-1/2}]\} \quad \text{for region I,}$$
$$=2i\pi^{-1}\{(t^2-R_1^2)^{-1/2}-\tfrac{1}{2}[(t^2-R_1^2)^{-1/2}\pm(t^2-R_2^2)^{-1/2}]\}, \quad \text{for region II,}$$
$$=i\pi^{-1}[(t^2-R_1^2)^{-1/2}\mp(t^2-R_2^2)^{-1/2}], \quad \text{for region III,} \tag{114}$$

where

$$R_1^2=\rho^2+\rho'^2-2\rho\rho'\cos(\phi-\phi'), \quad R_2^2=\rho^2+\rho'^2-2\rho\rho'\cos(\phi+\phi'). \tag{115}$$

In (114), $(t^2-R_{1,2}^2)^{-1/2}=0$ for $t<\rho+\rho'$ when this expression is within the brackets; otherwise zero for $t<R_{1,2}$. The expression (114) is elementary in all the three regions. Former investigations [38] established $\Phi_D(t)$ as an infinite series involving Legendre functions. (It

can be shown that this series can be summed and leads to the expressions in (114).) From (114) and (98) it follows for the field Φ due to an excitation $g(t)$,

$$\Phi(t)=2i\pi^{-1}\left\{\int_0^{t-R_1}[(t-\tau)^2-R_1^2]^{-1/2}g(\tau)d\tau\mp\int_0^{t-R_2}[(t-\tau)^2-R_2^2]^{-1/2}g(\tau)d\tau\right.$$

$$\left.-\tfrac{1}{2}\int_0^{t-\rho-\rho'}[((t-\tau)^2-R_1^2)^{-1/2}\mp((t-\tau)^2-R_2^2)^{-1/2}]g(\tau)d\tau\right\},\quad\text{region I.}$$

$$\Phi(t)=2i\pi^{-1}\left\{\int_0^{t-R_1}[(t-\tau)^2-R_1^2]^{-1/2}g(\tau)d\tau\right.$$

$$\left.-\tfrac{1}{2}\int_0^{t-\rho-\rho'}[((t-\tau)^2-R_1^2)^{-1/2}\pm((t-\tau)^2-R_2^2)^{-1/2}]g(\tau)d\tau\right\},\quad\text{region II.}$$

$$\Phi)t)=i\pi^{-1}\int_0^{t-\rho-\rho'}[((t-\tau)^2-R_1^2)^{-1/2}\mp((t-\tau)^2-R_2^2)^{-1/2}]g(\tau)d\tau,\qquad\text{region III.}\qquad(116)$$

b. Plane Unit Step Function Pulse and Wedge or Corner

Now, $g(t)=1$ for $t>0$, and $g(t)=0$ for $t<0$. Then the terms of the sums on the r. h. s. of (108) are either zero or one according as the argument of g is negative or positive. The well-known formula

$$\int[\cosh(bx)-a]^{-1}dx=2b^{-1}(1-a^2)^{-1/2}\arctan\left[\left(\frac{1+a}{1-a}\right)^{1/2}\tanh(\tfrac{1}{2}bx)\right]$$

gives for the integral in (108) by (101)

$$\int_0^{\cosh x=t/\rho}G(\theta)dx=-\pi^{-1}\arctan\left\{\frac{[t+(t^2-\rho^2)^{1/2}]^{\pi/\alpha}-\rho^{\pi/\alpha}}{[t+(t^2-\rho^2)^{1/2}]^{\pi/\alpha}+\rho^{\pi/\alpha}}\operatorname{cotan}\left[\frac{\pi}{2\alpha}(\pi-\theta)\right]\right\}$$

$$-\pi^{-1}\arctan\left\{\frac{[t+(t^2-\rho^2)^{1/2}]^{\pi/\alpha}-\rho^{\pi/\alpha}}{[t+(t^2-\rho^2)^{1/2}]^{\pi/\alpha}+\rho^{\pi/\alpha}}\operatorname{cotan}\left[\frac{\pi}{2\alpha}(\pi+\theta)\right]\right\}$$

for $t>\rho$ and equal to zero for $t<\rho$. Thus the field (108) for a unit step function excitation [19, 24] is elementary.

c. Spherical Unit Step Function Pulse and Half Plane

The center of the spherical pulse is Q (fig. 6). Again, $g(t)=1$. The excited field is given by (109) and $G(\theta)$ is given by (112). The integral occuring in 109) is of the form

$$\int_0^{x_1}(\rho^2+\rho'^2+2\rho\rho\cosh x)^{-1/2}G(\theta)\,dx$$

$$=-\pi^{-1}\cos(\tfrac{1}{2}\theta)\int_0^{x_1}\cosh(\tfrac{1}{2}x)(\cosh x+\cos\theta)^{-1}(\rho^2+\rho'^2+z^2+2\rho\rho'\cosh x)^{-1/2}dx$$

$$=-2^{1/2}\pi^{-1}\cos(\tfrac{1}{2}\theta)\int_0^{v_1}(1+\cos\theta+v^2)^{-1}[(\rho+\rho')^2+z^2+2\rho\rho'v^2]^{-1/2}dv,$$

using the substitution $\cosh x=1+v^2$, $\cosh(\tfrac{1}{2}x)dx=2^{1/2}\,dv$. The upper limit v_1 is given by $v_1=[t^2-(\rho+\rho')^2-z^2]^{\frac{1}{2}}$. Again this integral is elementary. Each sum in (109) reduces to at most one elementary term (see the tables in section 3), and the resulting field [40] is elementary.

It should be remembered that the previous investigations were based on the assumption that the velocity of the field is unity. The time parameter t has therefore to be replaced by ct when the velocity of the field is equal to c. The expression U for the time harmonic field as given in section 2 can easily be regained as the limiting case of a transient field Φ due to an excitation $g(t)=\exp(i\omega t)$.

7. References

[1] T. J. Bromwich, Diffraction of waves by a wedge, Proc. London Math. Soc. **14,** 450–463 (1915).

[2] T. J. Bromwich, An introduction to the theory of infinite series (MacMillan & Co., Ltd., London, 1931)

[3] H. S. Carslaw, Some multiform solutions of the partial differential equations of physics and mathematics and their applications, Proc. London Math. Soc. **30,** 121–163 (1899).

[4] H. S. Carslaw, Diffraction of waves by a wedge of any angle, Proc. London Math. Soc. **18,** 291–306 (1920).

[5] P. C. Clemmow, A note on the diffraction of a cylindrical wave by a perfectly conducting half plane, Quart. J. Mech. Appl. Math. **3,** 377–384 (1950).

[6] P. C. Clemmow and C. M. Munford, A table of $\sqrt{\frac{1}{2}}\,\pi \exp\left(\frac{1}{2} i\pi\rho^2\right)\int_\rho^\infty \exp\left(-\frac{1}{2} i\pi\lambda^2\right) d\lambda$ for complex values of ρ. Philos. Trans. Roy. Soc. London [A]**245,** 189–211 (1953).

[7] E. T. Copson, On an integral equation arising in the theory of diffraction, Quart. J. Math. Oxford Ser. **17,** 19–34 (1946).

[8] G. Doetsch, Handbuch der Laplace Transformation, Vol. 2 (Birkhauser Verlag, Basel, 1955).

[9] A. Erdelyi, Higher transcendental functions, Vol. 2 (McGraw-Hill Book Co., Inc., New York, N. Y., 1953).

[10] A. Erdelyi, Tables of integral transforms, 2 vols. (McGraw-Hill Book Co., Inc., New York, N. Y., 1954).

[11] F. G. Friedlander, The diffraction of sound pulses, Proc. Roy. Soc. London, [A]**186,** 322–351 (1946).

[12] F. G. Friedlander, On the half plane diffraction problem, Quart. J. Mech. Appl. Math. **4,** 344–357 (1951).

[13] R. C. Gast, Half plane diffraction with line source excitation, Tech. Report No. 24, Carnegie Institute of Technology (1956).

[14] R. F. Harrington, Current element near the edge of a conducting half plane, J. Appl. Phys. **24,** 547–550 (1953).

[15] A. E. Heins, The excitation of a perfectly conducting half plane by a dipole field. Tech. Report No. 17, Carnegie Institute of Technology (1955).

[16] G. Herglotz, Die Greensche Funktion der Wellengleichung für eine keilformige Begrenzung, Math. Ann. **124,** 219–234 (1952).

[17] S. Karp, Separation of variables and Wiener-Hopf techniques, New York Univ. Math. Research Group, Research Rept. No. EM 25 (1950).

[18] I. Kay, The diffraction of an arbitrary pulse by a wedge, Comm. Pure Appl. Math. **6,** 419–434 (1953).

[19] J. B. Keller and A. Blank, Diffraction and reflection of pulses by wedges and corners, Comm. Pure Appl. Math. **4,** 75–94 (1951).

[20] M. J. Kontorovich and N. N. Lebedev, On a method of solution of some problems in the diffraction theory, J. Phys. Moscow, **1,** 229–241 (1939).

[21] H. Lamb, On the diffraction of a solitary wave, Proc. London Math. Soc. **8,** 422–437 (1910).

[22] H. M. MacDonald, A class of diffraction problems, Proc. London Math. Soc. **14,** 410–427 (1915).

[23] W. Magnus, Über die Beugung elektromagnetischer Wellen an einer Halbebene, A. Phys. **177,** 168–179 (1941).

[24] J. W. Miles, On the diffraction of an acoustic pulse by a wedge, Proc. Roy. Soc. London [A]**212,** 543 (1952).

[25] J. W. Miles, On the diffraction of an electromagnetic pulse by a wedge, Proc. Roy. Soc. London [A]**212,** 547–551 (1952).

[26] F. Oberhettinger, Diffraction of waves by a wedge, Comm. Pure Appl. Math. **7,** 551–563 (1954).

[27] F. Oberhettinger, On asymptotic series for functions occurring in the theory of diffraction of waves by wedges, J. Math. Physics, **34,** 245–255 (1956).

[28] F. Oberhettinger, On the propagation of pulses, Z. Physik **146,** 423–435 (1956).

[29] W. Pauli, On asymptotic series for functions in the theory of diffraction of light, Phys. Rev. **54,** 924–931 (1938).

[30] Rayleigh, Lord, On the production and distribution of sound, Phil. Mag. **6,** 289–305 (1903).

[31] F. Rellich, Über das asymptotische Verhalten der Lösungen von $\Delta u + \lambda u = 0$ in unendlichen Gebieten, Jber. Deutsch. Math. Verein **53,** 57–65 (1943).

[32] T. B. A, Senior, The diffraction of a dipole field by a perfectly conducting half plane, Quart. J. Mech. Appl. Math. **6,** 101–114 (1953).

[33] S. A. Schelkunoff, Electromagnetic waves (D. Van Nostrand Co., Inc., New York, N. Y., 1943).

[34] A. Sommerfeld, Mathematische Theorie der Diffraktion, Math. Ann. **47,** 317–341 (1896).

[35] A. Sommerfeld, Theoretisches uber die Beugung der Roentgenstrahlen, Z. Math. Phys. **46,** 11–97 (1901).

[36] A. Sommerfeld, Asymptotische Darstellung von Formeln aus der Beugungstheorie des Lichtes, J. reine angew. Math. **158,** 199–208 (1928).

[37] J. A. Stratton, Electromagnetic theory (McGraw-Hill Book Co., Inc., New York, N. Y., 1941).

[38] R. D. Turner, The diffraction of a cylindrical pulse by a half plane, Quart. Appl. Math. **14,** 63–73 (1956).

[39] Y. V. Vandakurov, Diffraction by a perfectly conducting half plane of electromagnetic waves emitted by an arbitrarily oriented electric and magnetic dipole, Zh. Eks. Teor. Fiz. **26,** 3–18 (1954).

[40] J. Wait, Diffraction of a spherical wave pulse by a half screen, Canadian J. Phys. **35,** 693–696 (1957).
[41] J. Wait, On the theory of an antenna with infinite corner reflector, Canadian J. Phys. **32,** 365–371 (1954).
[42] H. Weyl, Ausbreitung elektromagnetischer Wellen über einem ebenen Leiter, Ann. Phys. **60,** 481–500 (1919).
[43] F. J. Whipple, Diffraction by a wedge and kindred problems, Proc. London Math. Soc. **16,** 94–111 (1917).
[44] A. Wiegrefe, Über einige mehrwertige Lösungen der Wellengleichung $\Delta u + k^2 u = 0$ und ihre Anwendungen in der Beugungstheorie, Ann. Phys. **39,** 449–484 (1912).

8. Appendix

To prove

$$\pi I_\nu(a) K_\nu(b) = \int_0^\pi K_0[(a^2+b^2-2ab\cos t)^{1/2}] \cos(\nu t)\, dt - \sin(\pi\nu) \cdot \int_0^\infty \exp(-\nu t) K_0[(a^2+b^2+2ab\cosh t)^{1/2}]\, dt, \quad a<b, \tag{A1}$$

$$K_\nu(a) K_\nu(b) = \int_0^\infty K_0[(a^2+b^2+2ab\cosh t)^{1/2}] \cosh(\nu t)\, dt, \tag{A2}$$

$$K_0[(a^2+b^2-2ab\cos\phi)^{1/2}] = 2\pi^{-1}\int_0^\infty K_{i\nu}(a) K_{i\nu}(b) \cosh[\nu(\pi-|\phi|)]\, d\nu, \quad 0 \leqq \mathrm{Re}\,\phi \leqq 2\pi, \tag{A3}$$

one uses the formulas

$$\pi I_\nu(z) = \int_0^\pi \exp(z\cos t)\cos(\nu t)\, dt - \sin(\pi\nu)\int_0^\infty \exp(-z\cosh t - \nu t)\, dt \quad [9, \text{p. } 21], \tag{A4}$$

$$K_\nu(z) = \frac{1}{2}\int_0^\infty x^{-\nu-1}\exp\left(-x-\frac{1}{4}z^2/x\right)dx, \quad [9, \text{p. } 82], \tag{A5}$$

$$I_\nu(a) K_\nu(b) = \frac{1}{2}\int_0^\infty x^{-1}\exp\left(-x-\frac{a^2+b^2}{4x}\right) I_\nu\left(\frac{1}{2}ab/x\right)dx, \quad [9, \text{p. } 53]. \tag{A6}$$

8.1. Proof of (A1)

Starting with (A6) and replacing the modified Bessel function in the integrand by (4), one obtains, interchanging the order of integration,

$$\pi I_\nu(a) K_\nu(b) = \frac{1}{2}\int_0^\pi \cos(\nu t)\left[\int_0^\infty x^{-1}\exp\left(-x-\frac{a^2+b^2-2ab\cos t}{4x}\right)dx\right]dt - \frac{1}{2}\sin(\pi\nu)\int_0^\infty \exp(-\nu t)\left[\int_0^\infty x^{-1}\exp\left(-x-\frac{a^2+b^2+2ab\cosh t}{4x}\right)dx\right]dt.$$

The inner integrals on the r. h. s. are known by (A5). This proves (A1).

8.2. Proof of (A2)

The relation

$$K_\nu(z) = \tfrac{1}{2}\pi\sec(\pi\nu)[I_{-\nu}(z) - I_\nu(z)], \tag{A7}$$

together with (A1) gives (A2).

8.3. Proof of (A3)

Replace in (A2) ν by $i\nu$ and obtain by Fourier's inversion theorem

$$K_0[(a^2+b^2+ab\cosh t)^{1/2}] = 2\pi^{-1}\int_0^\infty K_{i\nu}(a) K_{i\nu}(b)\cos(\nu t)\, d\nu. \tag{A8}$$

Replace here t by $i(\pi-\phi)$ and obtain (A3). The restriction $0 \leq \mathrm{Re}\ \phi \leq 2\pi$ is necessary to ensure convergence of the integral in (A3) at its upper limit, since for fixed real x and large positive $\nu \gg x$ [9, p. 88, formula 19],

$$K_{i\nu}(x) = (2\pi)^{1/2}(\nu^2-x^2)^{-1/4} \exp\left(-\frac{1}{2}\pi\nu\right)\left\{\sin\left[[\nu \cosh^{-1}(\nu/x) - (\nu^2-x^2)^{1/2} + \frac{\pi}{4}\right] + O(\nu^{-1})\right\}. \quad \text{(A9)}$$

8.4. Evaluation of s_1 Defined in (19)

Using the formula

$$\sum_{n=0}^{N} \epsilon_n \cos(ny) = \frac{\sin[(2N+1)y/2]}{\sin(y/2)},$$

one obtains instead of (19)

$$s_1 = (2\pi)^{-1} \lim_{N\to\infty} \int_0^{\pi} K_0[\gamma(\rho^2+\rho'^2-2\rho\rho' \cos x)^{1/2}] \cdot \left\{\frac{\sin\left[\frac{\pi}{2\alpha}(2N+1)(x+\theta)\right]}{\sin\left[\frac{\pi}{2\alpha}(x+\theta)\right]} + \frac{\sin\left[\frac{\pi}{2\alpha}(2N+1)(x-\theta)\right]}{\sin\left[\frac{\pi}{2\alpha}(x-\theta)\right]}\right\} dx.$$

Substitute in the first integral $\pi(x+\theta) = -2\alpha t$ and in the second $\pi(x-\theta) = 2\alpha t$. It follows then that

$$s_1 = \alpha\pi^{-2} \lim_{N\to\infty} \int_{t_1}^{t_2} K_0\{\gamma[\rho^2+\rho'^2-2\rho\rho' \cos(\theta+2\alpha t/\pi)]\}^{1/2} \frac{\sin(2N+1)t}{\sin t}\, dt,$$

where $t_1 = -\frac{\pi}{2\alpha}(\pi+\theta)$ and $t_2 = \frac{\pi}{2\alpha}(\pi-\theta)$. Now s_1 is a Dirichlet integral and its value follows immediately [2, p. 492] as represented in (22).

WASHINGTON, D. C., January 14, 1958.

Journal of Research of the National Bureau of Standards Vol. 61, No. 5, November 1958 Research Paper 2907

A Liquid-Helium Cold Cell for Use With an X-ray Diffractometer

Igor A. Black,[1] Leonard H. Bolz, Frank P. Brooks,[1] Floyd A. Mauer, and H. Steffen Peiser

A liquid-helium cold cell for use with the General Electric X-ray goniometer has been designed and constructed. It is used to obtain X-ray diffraction patterns of polycrystalline solids deposited from the gaseous phase on a helium-cooled surface. This work is part of the program for studying the stabilization of free radicals.

1. Introduction

A 3-yr program of basic research has been undertaken at the National Bureau of Standards to study the preparation of free radicals and the preservation of these unstable molecular fragments by freezing. The usual technique involves dissociating a gas in a furnace, an rf field, or a spark discharge, and depositing the products on a surface cooled by liquid helium.

The freezing technique is widely used to store molecular fragments for study by spectroscopy, calorimetry, paramagnetic resonance, and other techniques. A knowledge of the structures of the solids deposited and the transformations they undergo during warmup is important in interpreting the results of these experiments. In calorimetry, for example, it may be difficult to determine whether an observed heat effect should be attributed to recombination of free radicals or crystallization of an amorphous deposit. To aid in settling such questions, a study of the structures and transformations of solids encountered in free-radical research was initiated. Special equipment was used for freezing gaseous samples at liquid-helium temperature and obtaining X-ray powder diffraction patterns. This paper describes the construction and use of the liquid-helium cold cell or cryostat developed for this work.

2. Selection of Techniques and Equipment

Reviews of the literature on low-temperature X-ray diffraction by Ruhemann [1][2] and by Steward [2] as well as the additional references at the end of this paper [3 to 8] show that a considerable number of X-ray cryostats have been described. Most of these, however, are for use with film cameras and are not well adapted to observing transient effects that occur on warmup of samples containing trapped free radicals. Of the diffractometer cryostats described, only the one by Barrett [7] can be used at liquid-helium temperature, and it is designed to fit X-ray equipment that is no longer available.

In order to take advantage of the rapid-recording feature of modern electronic-counter diffractometers, design of a cryostat that could be substituted for the room-temperature specimen mount on one of these instruments was undertaken. The X-ray equipment selected for modification was the General Electric diffractometer, the advantage of this instrument being that it has a vertical goniometer axis. The cryostat can be made to turn on this axis as required without causing liquid refrigerants to shift position.

3. Design and Construction

Once the X-ray technique and equipment had been selected, design of the cryostat followed along fairly conventional lines. It may be considered to have evolved from the optical cold cell described by Duerig and Mador [9]. X–ray windows and other special fittings had to be provided, and many changes were made to take advantage of modern manufacturing techniques, but the basic design is quite similar.

In constructing the cryostat, stainless steel was used wherever possible. Joints that do not have to be demountable were "heli-arc" welded and leak tested before assembly. This type of construction complicates modification or repair of the apparatus but almost completely eliminates troubles from vacuum leaks. Of the demountable joints, only two gasket seals and one soft-solder joint have to be vacuum tight.

The X-ray specimen cryostat is shown (in section) in figure 1. It is made up of two concentric Dewar vessels. Liquid helium is contained in the inner vessel (8) which has a hemicylindrical copper block (17) at the bottom. The specimen deposited on the plane, vertical surface of this block replaces the usual room temperature specimen. Beryllium windows (19) in the outer wall permit the X-ray beam to enter and leave the cryostat so that diffraction patterns of the material deposited on the surface can be obtained.

The helium vessel is surrounded by a liquid-nitrogen tank in the shape of a hollow cylinder (9) with copper radiation shields, (7) and (15), attached to it. The X-ray window in the radiation shield is covered with 0.00035-in.-thick nickel foil (18) which shields the specimen from room-temperature surfaces and filters the X-ray beam to eliminate copper Kβ radiation. Except for small openings for the specimen tube and optical windows, the helium vessel is entirely surrounded by surfaces which are at or near liquid-nitrogen temperature.

Vacuum spaces around the helium-cooled specimen

[1] Arthur D. Little, Inc.
[2] Figures in brackets indicate the literature reference at the end of this paper.

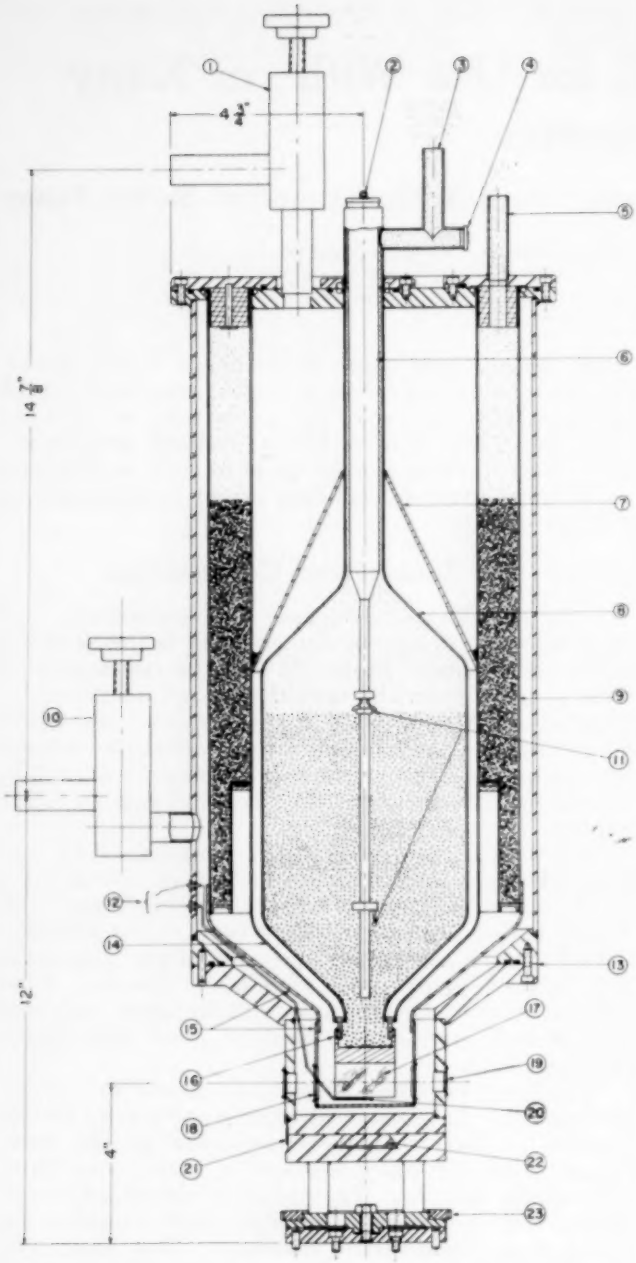

FIGURE 1. *Section through the X-ray-diffraction cryostat.*

1, Valve for evacuating helium Dewar; 2, helium fill-tube stopper; 3, helium vent; 4, electrical connector for helium-level indicator; 5, nitrogen vent or fill tube (one not shown); 6, helium fill tube; 7, upper radiation shield; 8, helium vessel; 9, nitrogen vessel; 10, valve for evacuating specimen chamber and nitrogen Dewar; 11, resistors for helium-level indicator (2); 12, thermocouple leads; 13, demountable flange; 14, inner-vacuum wall; 15, lower radiation shield; 16, brass ring and soft-solder joint; 17, copper block; 18, nickel foil X-ray windows 0.0005 in. thick; 19, beryllium X-ray windows; 20, thermocouple junction; 21, translational-adjustment vernier; 22, translational-adjustment slide; 23, rotational-adjustment worm gear.

block and around the outside of the nitrogen container are connected and are evacuated through a single valve (10) at the back of the apparatus. Another valve (1) is used to evacuate the space around the helium container. This space is separated from the specimen chamber by a wall (14) and seldom requires pumping. The wall probably accounts for as much as 75 percent of the heat transferred to the helium vessel once the specimen has been deposited, and reduces the operating time available on one filling to about 2 hr. However, separating the vacuum space around the helium vessel from that around the specimen prevents the sudden loss of helium and specimen that would result if the pressure in the specimen chamber should rise excessively during deposition or warmup of the sample.

X-ray windows (19) in the outer wall of the cryostat are covered with beryllium strips 0.025 in. thick. The two windows cover 85° of arc each and permit measurements to be made in the angular range from $-2°$ to $+168°$ 2θ. The beryllium strips are held in place with wire bands tightened by screws and are sealed to the stainless steel walls with Glyptal. The windows have not leaked during 6 months of use and have even survived a small azide explosion inside the cryostat.

A thermocouple (20) is used to measure the temperature of the copper block. For the alloys used (Ag plus 0.37 atomic percent Au versus Au plus 2.1 atomic percent Co) the sensitivity is approximately 10 μv/°K at 4.2 °K. The junction is inserted in a well at the bottom edge of the specimen surface and the leads are cemented to the copper block to keep them at the temperature of the junction. The presence of gas in the specimen chamber affects heat-transfer conditions, and if this precaution is not taken, temperature readings are pressure dependent.

The resistance of two carbon resistors (11) mounted in the helium vessel is recorded to indicate when liquid helium reaches the ¼-liter and the 2-liter levels. A current of about 50 ma flows through the two 15-ohm resistors and the rate at which heat is carried away (by the gas in one case or the liquid in the other) determines the temperature and, hence, the resistance.

The outputs of the thermocouple and the liquid-level gage are recorded continuously on a chart that is synchronized with the diffractometer chart.

Pressure measurements are made with a Philips cold-cathode ionization gage. Although the modification is not shown in the figures in this paper, the gage tube has recently been mounted on the cryostat itself so that pressure measurements can be made after the pumping manifold has been detached.

A slide (22) is provided for moving the cryostat on its base in a direction normal to the specimen surface in order to aline that surface with the axis of the goniometer. A worm gear (23) on the base is used to rotate the cryostat around a vertical axis to make the normal to the specimen surface bisect the angle between the incident and diffracted beams.

The dimensions have been chosen so that the slide can be removed from the base shown in figure 1 and inserted in another base that fits the North American Philips high-angle goniometer. However, that instrument has to be modified to operate with its axis vertical.

The lower chamber can be detached at the flange (13) to make the specimen block, thermocouple and lower radiation shield accessible for cleaning and

repairs. The flange is also intended to permit the lower chamber to be replaced with a film cassette. If modification of the copper block is required, it can be removed by unsoldering the soft-solder joint (16). These provisions are intended to make it possible to modify the cryostat (e. g., for single-crystal work) if necessary.

The cryostat is shown mounted on the X-ray-diffraction unit in figure 2. X-rays from the source slit (1) enter the cryostat through the beryllium windows (2). The diffracted beam enters the detector slit system (3). Its intensity is plotted by the recorder (4) against the diffraction angle, indicated on the protractor (5). Gaseous samples are introduced through the silica tube (6). The specimen surface can be viewed through a glass window (7) in the outer wall. A system of pulleys and a counterweight balance the weight of the cryostat (68 lb) while leaving it free to rotate with the goniometer table. The supporting cables can be seen at the top of the cryostat.

FIGURE 2. *The cryostat mounted on the X-ray goniometer.*

1, X-ray source slit; 2, beryllium window; 3, detector slit; 4, X-ray recorder; 5, protractor; 6, specimen discharge tube; 7, window for viewing specimen surface (2).

4. Operation

The system used to evacuate the cryostat and deposit gaseous samples is shown schematically in figure 3. In preparing for a run at liquid-helium temperature, the specimen chamber is pumped down to 10^{-4} mm of Hg and liquid nitrogen is added to the cold trap. Within 15 min the pressure drops below 3×10^{-5} mm of Hg and the cryostat is ready to be filled.

Before refrigerants are introduced, the gas to be deposited is usually pumped through the specimen chamber to simulate actual deposition of a sample on the helium-cooled surface. This aids in flushing the specimen manifold to remove contaminants, and permits the flow rate to be adjusted. After this adjustment the stopcock (fig. 3) between the capillary and the sample-gas input tube is closed so that the

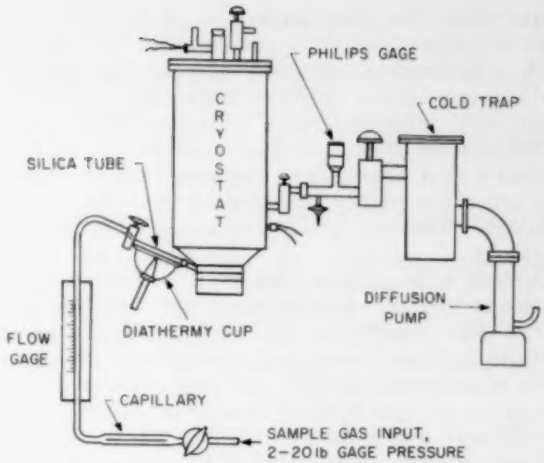

FIGURE 3. *Gas train and pumping system used with the cryostat.*

train up to that point is evacuated and gas does not collect in the tubing. The cryostat is then isolated from the pumping manifold by closing the valve and liquid nitrogen is introduced. Because of the cost of liquid helium, care must be taken to cool the apparatus to the temperature of liquid nitrogen before the helium is transferred. We prefer to fill the inner vessel to overflowing with liquid nitrogen and then syphon the liquid into the outer vessel. This method brings liquid nitrogen into contact with all the surfaces that must later be cooled by helium. After thorough precooling of the apparatus, approximately half a liter of helium is required to cool the inner Dewar to liquid helium temperature.

The procedure for producing free radicals and depositing them on a helium-cooled surface has been described by Broida and Pellam [10]. The system shown in figure 3 is suitable for most gases, but different equipment is sometimes used to deposit a liquid (through the vapor phase) or the gaseous products of a chemical reaction.

When the gas being deposited is to be dissociated to produce free radicals, it is passed through a silica tube in the rf field of a waveguide or diathermy cup. Power is provided by a 125-w microwave-diathermy unit operating in the 2,400- to 2,500-mc band. With the power on, the gas flow is increased relative to the rate of condensation on the helium-cooled surface. When the flow is sufficient to give a pressure of 0.01 to 0.1 mm of Hg in the silica tube, a Tesla coil can be used to initiate the discharge. The gas (or free radicals) is allowed to deposit until the surface of the copper block loses its metallic appearance. Fifteen or twenty minutes is required to deposit the 0.001- to 0.005-in. layer ordinarily used.

5. Performance

Once the sample has been deposited, obtaining X-ray patterns is routine. Although 25 percent of the X-ray beam is lost in passing through the beryllium windows, this loss is partly compensated when the path inside the cryostat is evacuated. For

copper radiation, the net loss is 15 percent. Intensities are adequate when the samples are crystalline. With the widest slits (3° beam-divergence slit, medium-resolution detector Soller slit, and 0.2° detector slit) counting rates considerably in excess of 10,000 cps are often attained. However, we do have evidence that crystallites deposited on the cold surface are often highly oriented so that the intensities of certain lines are greatly enhanced at the expense of others.

Helium is transferred from a 25-liter storage flask by means of a vacuum-insulated transfer syphon with a ⅛-in. inner tube that extends 12 in. below the vacuum wall and reaches the bottom of the cryostat. With a pressure of 0.75 psi, less than 5 min is required to fill the helium Dewar to the 2-liter level. The Dewar will hold as much as 2½ liters of liquid helium, enough to last for 3 hr under ideal conditions. Depositing samples always increases the boil-off rate and reduces the time at liquid-helium temperature to about 2 hr. This is sufficient for the measurements required. Much of the data is taken during normal warmup of the Dewar and additional helium capacity would only delay this important phase of the experiments.

If care is taken in alining the cryostat to allow for the thickness of the film deposited, there is no loss in the accuracy of interplanar spacings. Expansion curves are easily obtained by measuring the lattice constant of the specimen during warmup.

Resolving power of the diffractometer is not appreciably affected by the cryostat. The diffraction peak reproduced in figure 4 shows partial resolution of the Cu $K\alpha_1$–$K\alpha_2$ doublet at 43.46° 2θ where the separation is about 0.1° 2θ. Complete resolution of lines only 1.2° 2θ apart is shown in figure 5.

The apparatus has been useful not only in determining the nature of the deposits originally frozen out at liquid-helium temperature, but in following the changes during warmup as well. The sudden crystallization of amorphous deposits with the evolution of considerable heat has been observed in several cases. Phase changes inferred from other types of measurements have been confirmed, and additional phases have been discovered. For example, X-ray patterns of the three phases of oxygen are shown in figure 6 along with a pattern of ozone

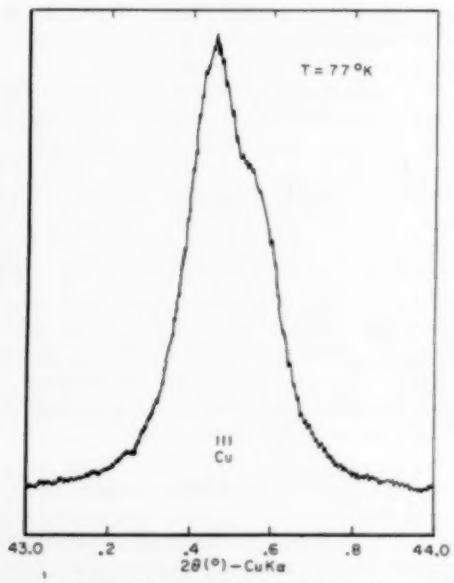

FIGURE 4. *Diffraction peak showing partial resolution of the* Cu$K\alpha_1$–$K\alpha_2$ *doublet.*

The specimen was the copper block on which gaseous specimens are deposited.

FIGURE 5. *A portion of the diffraction pattern of annealed solid* CO_2 *showing one peak due to the gold plating on the copper specimen block.*

The pattern indicates the amount of instrumental line broadening to be expected.

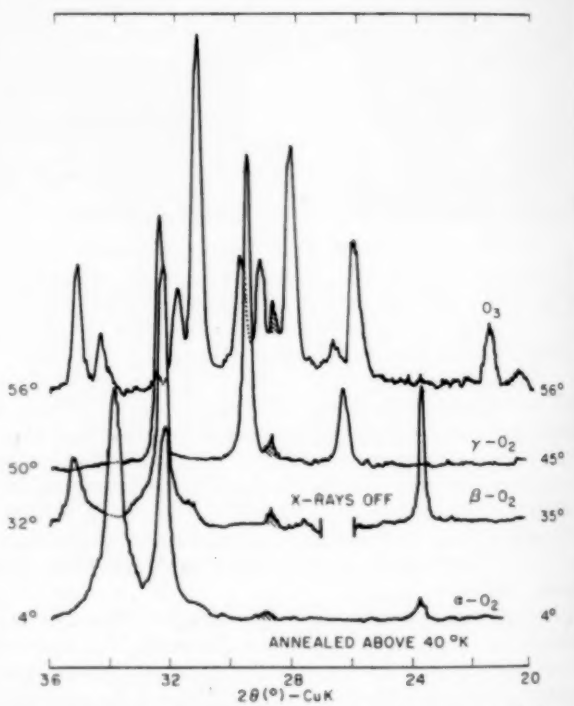

FIGURE 6. *Diffraction patterns of solid ozone and the three phases of solid oxygen.*

Numbers given in the margin are the approximate temperature in °K at the beginning and end of each diffractometer trace.
The line at 28.8° (2θ) is due to contamination of the gold surface.

prepared in a separate experiment by dissociating oxygen in a rf field. The dissociation products were deposited at 4.2° K and allowed to warm up until the residual oxygen sublimed at about 50° K. A temperature of 56° K was maintained by pumping on nitrogen in the inner Dewar. These results will be reported in more detail in later papers dealing with specific materials.

The performance of the X-ray cryostat during 6 months of use has been entirely satisfactory. However, the natural warmup characteristics sometimes do not give enough time in a given temperature range to make the measurements required. Swenson and Stahl [8] have described a Dewar for maintaining temperatures between 4° and 80° K by circulating helium gas cooled by liquid helium. Plans are being considered for adapting their technique or providing an auxiliary Dewar from which very small quantities of helium can be transferred at frequent intervals to arrest the warmup. Other modifications may become necessary if emphasis changes to the investigation of single crystals or orientation textures.

6. References

[1] M. and B. Ruhemann, Low temperature physics (Cambridge University Press, 1937)

[2] H. S. Peiser, H. P. Rooksby, and A. J. C. Wilson, X-ray diffraction by polycrystalline materials (The Institute of Physics, London, 1955); (see chapter 10, Low temperature methods by E. G. Steward).

[3] A. G. Tweet, Phys. Rev. **93,** 15 (1954).

[4] W. L. Gordon, C. H. Shaw, and J. G. Daunt, Phys. Rev. **96,** 1444 (1954).

[5] Arthur Stephen Pavlovic, The design and application of a Weissenberg X-ray camera for studies near liquid helium temperature, The Pennsylvania State University, Doctoral Dissertation Series, 1956, Publication No. 16725.

[6] L. K. Jetter, C. J. McHargue, R. O. Williams, and H. L. Yakel, Jr., Rev. Sci. Instr. **28,** 1087 (1957).

[7] C. S. Barrett, Acta Cryst. **9,** 671 (1956).

[8] C. A. Swenson and R. H. Stahl, Rev. Sci. Instr. **25,** 608 (1954).

[9] W. H. Duerig and I. L. Mador, Rev. Sci. Instr. **23,** 421 (1952).

[10] H. P. Broida and J. R. Pellam, Phys. Rev. **95,** 845 (1954).

WASHINGTON, June 23, 1958.

Journal of Research of the National Bureau of Standards Vol. 61, No. 5, November 1958 Research Paper 2908

The Second Spectrum of Ruthenium (Ru II)

Allen G. Shenstone[1] and William F. Meggers

Wavelengths and estimated intensities of 2,227 spectral lines characteristic of singly ionized ruthenium atoms are presented. The wavelengths range from 1054.684 to 6371.29 A. The Zeeman effect has been investigated for 488 lines ranging from 2323 to 4010 A. Analysis of these basic data of Ru II has resulted in the classification of 1,633 lines as transitions between 68-even, and 140-odd energy levels. All but three of these levels have been grouped into designated spectral terms and assigned to electron configurations. The low-even terms arise from $4d^7$, $4d^6\,5s$, and $4d^5\,5s^2$. All the terms from the $4d^7$ configuration have been found, and $4d^7\,a^4$F represents the ground state of Ru II. From two members of the $4d^6\,ns^6$D series a limit, 135200 cm^{-1}, has been calculated which indicates a principal ionization potential (I. P.) of 16.76 electron volts for Ru^+ ions.

As far back as 1930 [1][2] an analysis was undertaken of the first spark spectrum of ruthenium, element number 44. Although the fundamental multiplets were easily found, the complexity of the spectrum made further work unrewarding until more complete and accurate measurements could be made. In 1955 [2] Kessler and Meggers published new measurements, and in 1952 Meggers measured Zeeman effects on plates taken at the Massachusetts Institute of Technology with their large-field magnet and high-dispersion spectrographs. In addition, the spectrum was photographed on the Princeton vacuum instrument to provide wavelengths from 500 A to 2200 A. This instrument uses a 30,000 line per inch grating of 2m radius of curvature in a normal incidence mounting. All of the measurements of wavelength were made from spectrograms of the spark, a source which is not altogether satisfactory for first-spark spectra. For instance, Dobbie's [3] excellent analysis of Fe II was made entirely from the polar lines in an arc. Therefore, some further observations were made with such a source, and a considerable number of lines were found in the longer wavelength region which were not observed in the spark. All of the arc and spark photographs were made with buttons of pure compressed ruthenium powder. The metallic impurities were very faint and easily eliminated. In the vacuum region the gas and carbon lines, which are always present, were used as standards. In that region the differentiation of stages of ionization was made from an examination of the polarity of the lines on a number of plates. In some cases, it was even possible to distinguish lines due to the lowest levels from those due to levels only 20000 cm^{-1} higher. As usual, lines due to transitions from high even levels to intermediate odd levels are very wide and displaced from the position they occupy in an arc source.

Although the Zeeman effect on ruthenium lines was photographed and machine-measured at the Massachusetts Institute of Technology in 1940 only the results for Ru I were exploited and published [4]. In 1949 new Zeeman spectrograms of ruthenium were made at the Massachusetts Institute of Technology but the magnetic field intensity did not exceed 80,000 oersteds. Because some of the earlier spectrograms were made with higher field intensities which greatly enhanced Ru II, the best of these (Z-74) were loaned to the National Bureau of Standards where they were hand-measured and computed. A field intensity of 88,200 oersteds was derived from the magnetic splitting of impurity lines (Mg II 2795.53 and 2802.60 A, Cu I 3247.54 and 3273.96 A, Ag I 3280.68 and 3382.89 A, and Ca II 3933.66 and 3968.47 A).

The Ru II lines were easily distinguished from Ru I by comparing the total intensities of the Zeeman patterns with the intensities in the central comparison spectrum produced without the magnetic field; the Ru II lines were greatly enhanced by the magnetic field. In addition, the fully recorded and resolved patterns of Ru II lines were recognized by their types 4, 5, and 6 characteristic of even multiplicities according to Back and Landé [5]. Type 4 exhibits two symmetrically least-displaced p-components of equal intensity, and the two strongest n-components are also least displaced, when the level with the larger J has the smaller g. Type 5 occurs when the larger J has the larger g, in which case the two strongest n-components exhibit the maximum displacement. Type 6 is produced by levels with equal J but unequal g, in which case the strongest p-components show the largest displacement, and the strongest n-components an average displacement. The observed g-factors given to 3 decimals in tables 1, 2, and 5 are the average of all calculations from resolved patterns, indicated in table 6 by Δg. Only the displacements of maximum intensities of unresolved patterns on the MIT spectrograms were measured, and the types noted. Then after such a line was classified it was often possible to calculate a g-factor for one level if the other one is known. In many type 6 patterns the over-all width (w) of the unresolved p-components was measured so that g-values could be calculated for both energy levels when their J-values were fixed by the classification; in these cases the Δg (in table 6) is inclosed in parentheses and the g-factors are given to two deci-

[1] Present address: Palmer Physical Laboratory, Princeton University, Princeton, N. J.

[2] Figures in brackets indicate the literature references on page 378.

mals. For a few levels, the g-values were calculated to two decimals from unresolved patterns on plates taken 30 years ago at Princeton, according to a procedure described by Shenstone and Blair [6].

As remarked above, the lowest multiplets were found many years ago; but even after the new wavelength measurements were made and Zeeman effects observed, it still proved very difficult to break into the higher groups of terms. This was surprising since in a spectrum of this kind, one expects many intersystem and interfamily lines. There are many such combinations but few of them are with the sextet system. In point of fact, the strongest interfamily combinations with that system are in the long wavelength region where the lines can be observed only at the poles of the arc. This was unfortunately discovered after the analysis was practically complete.

The break into the higher quartet terms was made through a search in the Schumann region for the differences occurring in the low ^4F term. From such differences the usual square array was built up, though the work was not made any easier by the fact that great reliance was placed on a comparison with Fe II. Only after a very arduous numerical analysis was it possible to assign term designations to the even levels and a reasonable identification of odd levels was impossible until the analysis was nearly complete. A warning must be given against too great reliance on the names chosen. The levels are so mixed in character that the most that can be hoped is that designations have been selected which correspond to the particular Russell-Saunders type that is the chief contributor to each level. The terms of $4d^7$ and $4d^6(^5D)5s$ are the most reliably named because they are reasonably pure. The remaining even levels are in general less pure the higher they are.

The names of the odd levels are considerably less reliable than those of the even levels. The levels were found chiefly by the numerical analysis mentioned above, assisted by rough predictions of position and intensity of combinations. Because the spectrum Tc I, isoelectronic with Ru II, is only partially analyzed [7], the chief reliance had to be on the homologous spectrum Fe II [8] for predictions of position. Unfortunately, the correspondence is much rougher than was expected. For instance, the terms $a\ ^4H$ and

TABLE 1. *Even levels of* Ru II

Configuration	Designation	J	Level	g(obs)	g(Landé)	Configuration	Designation	J	Level	g(obs)	g(Landé)
$4d^7$	$a\ ^4F$	$4\frac{1}{2}$	0.0	.....	1.333	$4d^6(^3G)5s$	$a\ ^4G$	$5\frac{1}{2}$	29018.6	1.232	1.273
$4d^7$	$a\ ^4F$	$3\frac{1}{2}$	1523.1	.....	1.238	$4d^6(^3P)5s$	$b\ ^4P$	$1\frac{1}{2}$	29091.0	1.646	1.733
$4d^7$	$a\ ^4F$	$2\frac{1}{2}$	2493.9	.....	1.029	$4d^6(^3G)5s$	$a\ ^4G$	$4\frac{1}{2}$	30099.6	1.167	1.172
$4d^7$	$a\ ^4F$	$1\frac{1}{2}$	3104.2	.....	0.419	$4d^6(^3G)5s$	$a\ ^4G$	$2\frac{1}{2}$	30293.3	0.651	0.571
$4d^7$	$a\ ^4P$	$2\frac{1}{2}$	8256.7	1.57	1.600	$4d^6(^3G)5s$	$a\ ^4G$	$3\frac{1}{2}$	30439.5	1.021	0.984
$4d^7$	$a\ ^4P$	$1\frac{1}{2}$	8477.7	1.68	1.733	$4d^6(^3P)5s$	$b\ ^4P$	$0\frac{1}{2}$	30489.3	2.541	2.667
$4d^6(^5D)5s$	$a\ ^6D$	$4\frac{1}{2}$	9151.4	1.53	1.556	$4d^6(^3H)5s$	$b\ ^2H$	$5\frac{1}{2}$	32623.0	1.065	1.091
$4d^7$	$a\ ^4P$	$0\frac{1}{2}$	9373.9	2.60	2.667	$4d^6(^3H)5s$	$b\ ^2H$	$4\frac{1}{2}$	32686.7	0.955	0.909
$4d^6(^5D)5s$	$a\ ^6D$	$3\frac{1}{2}$	10150.4	1.576	1.587	$4d^6(^3D)5s$	$b\ ^4D$	$1\frac{1}{2}$	32888.4	1.200	1.200
$4d^6(^5D)5s$	$a\ ^6D$	$2\frac{1}{2}$	10851.7	1.641	1.657	$4d^6(^3D)5s$	$b\ ^4D$	$0\frac{1}{2}$	32960.8	0.138	0.00
$4d^7$	$a\ ^2G$	$4\frac{1}{2}$	10860.9	.....	1.111	$4d^6(^3D)5s$	$b\ ^4D$	$2\frac{1}{2}$	33018.8	1.338	1.371
$4d^6(^5D)5s$	$a\ ^6D$	$1\frac{1}{2}$	11303.8	1.843	1.867	$4d^6(^3D)5s$	$b\ ^4D$	$3\frac{1}{2}$	33332.7	1.397	1.429
$4d^6(^5D)5s$	$a\ ^6D$	$0\frac{1}{2}$	11604.0	3.271	3.333	$4d^6(^3P)5s$	$b\ ^2P$	$1\frac{1}{2}$	33734.8	1.185	1.333
$4d^7$	$a\ ^2G$	$3\frac{1}{2}$	12293.4	.....	0.889	$4d^6(^3F)5s$	$b\ ^2F$	$3\frac{1}{2}$	34038.3	1.083	1.143
$4d^7$	$a\ ^2P$	$1\frac{1}{2}$	12956.6	.....	1.333	$4d^7$	$b\ ^2D$	$1\frac{1}{2}$	34793.1	0.965	0.800
$4d^7$	$a\ ^2D$	$2\frac{1}{2}$	14581.2	.....	1.200	$4d^7$	$b\ ^2D$	$2\frac{1}{2}$	34829.3	1.102	1.200
$4d^7$	$a\ ^2H$	$5\frac{1}{2}$	14663.4	.....	1.091	$4d^6(^3F)5s$	$b\ ^2F$	$2\frac{1}{2}$	35298.4	0.945	0.857
$4d^7$	$a\ ^2P$	$0\frac{1}{2}$	14799.5	.....	0.667	$4d^5\ 5s^2$	$a\ ^6S$	$2\frac{1}{2}$	35857.6	.....	2.000
$4d^7$	$a\ ^2H$	$4\frac{1}{2}$	16125.0	.....	0.909	$4d^6(^1I)5s$	$a\ ^2I$	$6\frac{1}{2}$	35939.6	1.06	1.077
$4d^7$	$a\ ^2D$	$1\frac{1}{2}$	17017.6	.....	0.800	$4d^6(^3G)5s$	$b\ ^2G$	$4\frac{1}{2}$	36016.0	1.067	1.111
$4d^6(^5D)5s$	$a\ ^4D$	$3\frac{1}{2}$	19378.7	1.402	1.429	$4d^6(^3P)5s$	$b\ ^2P$	$0\frac{1}{2}$	36095.0	0.875	0.667
$4d^6(^5D)5s$	$a\ ^4D$	$2\frac{1}{2}$	20515.0	1.337	1.371	$4d^6(^1I)5s$	$a\ ^2I$	$5\frac{1}{2}$	36229.7	0.93	0.923
$4d^6(^5D)5s$	$a\ ^4D$	$1\frac{1}{2}$	21246.4	1.188	1.200	$4d^6(^3G)5s$	$b\ ^2G$	$3\frac{1}{2}$	36515.8	0.885	0.889
$4d^7$	$a\ ^2F$	$2\frac{1}{2}$	21557.8	0.863	0.857	$4d^6(^1G)5s$	$c\ ^2G$	$4\frac{1}{2}$	37433.0	1.078	1.111
$4d^6(^5D)5s$	$a\ ^4D$	$0\frac{1}{2}$	21645.6	0.015	0.000	$4d^6(^1G)5s$	$c\ ^2G$	$3\frac{1}{2}$	37981.5	0.942	0.889
$4d^7$	$a\ ^2F$	$3\frac{1}{2}$	22289.0	1.138	1.143	$4d^6(^3D)5s$	$c\ ^2D$	$2\frac{1}{2}$	38981.8	1.18	1.200
$4d^6(^3H)5s$	$a\ ^4H$	$6\frac{1}{2}$	25952.2	1.235	1.231	$4d^6(^3D)5s$	$c\ ^2D$	$1\frac{1}{2}$	39711.9	0.797	0.800
$4d^6(^3H)5s$	$a\ ^4H$	$5\frac{1}{2}$	26109.4	1.16	1.133	$4d^6(^1S)5s$	$a\ ^2S$	$0\frac{1}{2}$	40226.2	1.800	2.000
$4d^6(^3H)5s$	$a\ ^4H$	$4\frac{1}{2}$	26118.4	1.08	0.970	$4d^6(^1D)5s$	$d\ ^2D$	$1\frac{1}{2}$	42750.1	0.803	0.800
$4d^6(^3H)5s$	$a\ ^4H$	$3\frac{1}{2}$	26468.0	0.759	0.667	$4d^6(^1D)5s$	$d\ ^2D$	$2\frac{1}{2}$	43609.9	1.216	1.200
$4d^6(^3P)5s$	$b\ ^4P$	$2\frac{1}{2}$	26911.4	1.578	1.600	$4d^6(^5D)6s$	$e\ ^6D$	$4\frac{1}{2}$	84510.9	.....	1.556
$4d^6(^3F)5s$	$b\ ^4F$	$4\frac{1}{2}$	27544.6	1.200	1.333	$4d^6(^5D)6s$	$e\ ^4D$	$3\frac{1}{2}$	86440.4	.....	1.429
$4d^6(^3F)5s$	$b\ ^4F$	$3\frac{1}{2}$	27948.8	1.091	1.238	$4d^6(^5D)6s$	$e\ ^4D$	$2\frac{1}{2}$	87523.4	.....	1.371
$4d^6(^3F)5s$	$b\ ^4F$	$2\frac{1}{2}$	28138.8	0.941	1.029						
$4d^6(^3F)5s$	$b\ ^4F$	$1\frac{1}{2}$	28495.3	0.420	0.419	$4d^6\ ^5D_4$ (Ru III)	Limit	...	135200	.....	.....

TABLE 2. *Odd levels of* Ru II

Configuration	Designation	J	Level	g(obs)	g(Landé)	Configuration	Designation	J	Level	g(obs)	g(Landé)
$4d^6(^5D)5p$	$z\ ^6D°$	$4\frac{1}{2}$	*46471.0*	1.530	1.556	$4d^6(^3G)5p$	$x\ ^4F°$	$4\frac{1}{2}$	*67900.9*	1.19	1.333
$4d^6(^5D)5p$	$z\ ^6D°$	$3\frac{1}{2}$	*46711.5*	1.569	1.587	$4d^6(^3F)5p$	$y\ ^4G°$	$2\frac{1}{2}$	*67946.6*	0.689	0.571
$4d^6(^5D)5p$	$z\ ^6D°$	$2\frac{1}{2}$	*47285.1*	1.634	1.657	$4d^6(^3F)5p$	$x\ ^4D°$	$0\frac{1}{2}$	*68096.9*	0.385	0.000
$4d^6(^5D)5p$	$z\ ^6D°$	$1\frac{1}{2}$	*47708.6*	1.840	1.867	$4d^6(^3H)5p$	$z\ ^2H°$	$4\frac{1}{2}$	*68120.3*	1.015	0.909
$4d^6(^5D)5p$	$z\ ^6D°$	$0\frac{1}{2}$	*47983.8*	3.280	3.333	$4d^6(^3F)5p$	$x\ ^4D°$	$3\frac{1}{2}$	*68229.3*	0.955	1.429
$4d^6(^5D)5p$	$z\ ^6F°$	$5\frac{1}{2}$	*50758.3*	1.44	1.455	$4d^6(^3F)5p$	$y\ ^2G°$	$3\frac{1}{2}$	*68265.6*	1.028	0.889
$4d^6(^5D)5p$	$z\ ^6F°$	$4\frac{1}{2}$	*50845.3*	1.42	1.434	$4d^6(^3G)5p$	$x\ ^4G°$	$5\frac{1}{2}$	*68328.3*	1.152	1.273
$4d^6(^5D)5p$	$z\ ^6F°$	$3\frac{1}{2}$	*50862.5*	1.457	1.397	$4d^6(^3P)5p$	$z\ ^2P°$	$1\frac{1}{2}$	*68445.8*	1.160	1.333
$4d^6(^5D)5p$	$z\ ^6F°$	$2\frac{1}{2}$	*51179.7*	1.312	1.314	$4d^6(^3P)5p$	$y\ ^4D°$	$2\frac{1}{2}$	*68773.9*	1.308	1.371
$4d^6(^5D)5p$	$z\ ^6F°$	$1\frac{1}{2}$	*51317.0*	1.058	1.067	$4d^6(^3G)5p$	$x\ ^4G°$	$4\frac{1}{2}$	*68906.5*	1.17	1.172
$4d^6(^5D)5p$	$z\ ^6F°$	$0\frac{1}{2}$	*51380.1*	−0.62	−0.667	$4d^6(^3G)5p$	$x\ ^4G°$	$2\frac{1}{2}$	*69054.8*	0.706	0.571
$4d^6(^5D)5p$	$z\ ^6P°$	$3\frac{1}{2}$	*51548.8*	1.580	1.714	$4d^6(^3F)5p$	$y\ ^2G°$	$4\frac{1}{2}$	*69180.8*	1.058	1.111
$4d^6(^5D)5p$	$z\ ^6P°$	$2\frac{1}{2}$	*52820.3*	1.835	1.886	$4d^6(^3G)5p$	$y\ ^4H°$	$6\frac{1}{2}$	*69311.1*	1.180	1.231
$4d^6(^5D)5p$	$z\ ^4F°$	$4\frac{1}{2}$	*52964.4*	1.346	1.333	$4d^6(^3G)5p$	$x\ ^4F°$	$3\frac{1}{2}$	*69404.1*	1.059	1.238
$4d^6(^5D)5p$	$z\ ^4D°$	$3\frac{1}{2}$	*53317.1*	1.391	1.429	$4d^6(^3P)5p$	$z\ ^2P°$	$0\frac{1}{2}$	*69439.5*	0.829	0.667
$4d^6(^5D)5p$	$z\ ^6P°$	$1\frac{1}{2}$	*53685.2*	2.365	2.400	$4d^6(^3G)5p$	$x\ ^4G°$	$3\frac{1}{2}$	*69552.5*	1.00	0.984
$4d^6(^5D)5p$	$z\ ^4D°$	$2\frac{1}{2}$	*54065.4*	1.348	1.371	$4d^6(^3G)5p$	$y\ ^4H°$	$4\frac{1}{2}$	*69612.9*	0.99	0.970
$4d^6(^5D)5p$	$z\ ^4F°$	$3\frac{1}{2}$	*54225.5*	1.274	1.238	$4d^6(^3G)5p$	$x\ ^4F°$	$1\frac{1}{2}$	*69619.9*	0.648	0.400
$4d^6(^5D)5p$	$z\ ^4D°$	$1\frac{1}{2}$	*54663.4*	1.145	1.200	$4d^6(^3G)5p$	$x\ ^4F°$	$2\frac{1}{2}$	*69646.4*	0.99	1.029
$4d^6(^5D)5p$	$z\ ^4F°$	$2\frac{1}{2}$	*54794.3*	1.077	1.029	$4d^6(^3G)5p$	$y\ ^4H°$	$5\frac{1}{2}$	*69646.9*	1.108	1.133
$4d^6(^5D)5p$	$z\ ^4D°$	$0\frac{1}{2}$	*54981.5*	0.011	0.000	$4d^6(^3G)5p$	$y\ ^4H°$	$3\frac{1}{2}$	*69655.5*	0.797	0.667
$4d^6(^5D)5p$	$z\ ^4F°$	$1\frac{1}{2}$	*55224.2*	0.468	0.400	----------	$1°$	$1\frac{1}{2}$	*70150.7*	1.209	-----
$4d^6(^5D)5p$	$z\ ^4P°$	$2\frac{1}{2}$	*55695.2*	1.570	1.600	$4d^6(^3F)5p$	$y\ ^2D°$	$2\frac{1}{2}$	*70571.9*	1.157	1.200
$4d^6(^5D)5p$	$z\ ^4P°$	$1\frac{1}{2}$	*56664.9*	1.708	1.733	$4d^6(^3F)5p$	$y\ ^2D°$	$1\frac{1}{2}$	*70779.6*	0.744	0.800
$4d^6(^5D)5p$	$z\ ^4P°$	$0\frac{1}{2}$	*57263.8*	2.648	2.667	$4d^6(^3P)4p$	$z\ ^2S°$	$0\frac{1}{2}$	*71036.3*	2.046	2.00
$4d^6(^3P)5p$	$z\ ^4S°$	$1\frac{1}{2}$	*62446.1*	1.798	2.000	$4d^6(^3D)5p$	$z\ ^4P°$	$2\frac{1}{2}$	*71114.8*	1.247	1.600
$4d^6(^3H)5p$	$z\ ^4H°$	$3\frac{1}{2}$	*62526.6*	0.961	0.667	$4d^6(^3G)5p$	$y\ ^2H°$	$5\frac{1}{2}$	*71202.9*	1.32	1.091
$4d^6(^3H)5p$	$z\ ^4H°$	$4\frac{1}{2}$	*62906.8*	1.024	0.970	$4d^6(^3G)5p$	$y\ ^2F°$	$2\frac{1}{2}$	*71598.7*	1.193	0.857
$4d^6(^3H)5p$	$z\ ^4H°$	$5\frac{1}{2}$	*63307.7*	1.068	1.133	$4d^6(^1I)5p$	$z\ ^2K°$	$6\frac{1}{2}$	*71798.3*	0.91	0.933
$4d^6(^3H)5p$	$z\ ^4G°$	$5\frac{1}{2}$	*63518.5*	1.24	1.273	$4d^6(^3D)5p$	$x\ ^4P°$	$1\frac{1}{2}$	*71866.1*	1.567	1.733
$4d^6(^3H)5p$	$z\ ^4H°$	$6\frac{1}{2}$	*63588.2*	1.14	1.231	$4d^6(^3G)5p$	$y\ ^2H°$	$4\frac{1}{2}$	*71926.4*	0.96	0.909
$4d^6(^3P)5p$	$y\ ^4P°$	$2\frac{1}{2}$	*63797.6*	1.295	1.600	$4d^6(^3G)5p$	$y\ ^2F°$	$3\frac{1}{2}$	*72010.3*	1.121	1.143
$4d^6(^3H)5p$	$z\ ^4G°$	$4\frac{1}{2}$	*63851.3*	1.136	1.172	$4d^6(^3D)5p$	$x\ ^2F°$	$3\frac{1}{2}$	*72248.6*	1.14	1.143
$4d^6(^3H)5p$	$z\ ^4G°$	$3\frac{1}{2}$	*63941.2*	0.978	0.984	$4d^6(^3D)5p$	$w\ ^4F°$	$1\frac{1}{2}$	*72523.5*	0.490	0.400
$4d^6(^3H)5p$	$z\ ^4G°$	$2\frac{1}{2}$	*64025.3*	0.646	0.571	$4d^5\ 5s(^7S)5p$	$y\ ^6P°$	$1\frac{1}{2}$	*72760.7*	2.49	2.400
$4d^6(^3H)5p$	$z\ ^4I°$	$4\frac{1}{2}$	*64385.3*	.959	.727	----------	$2°$	$1\frac{1}{2}$	*72786.0?*	1.34	-----
$4d^6(^3F)5p$	$y\ ^4F°$	$2\frac{1}{2}$	*64463.8*	1.022	1.029	$4d^6(^1I)5p$	$z\ ^2K°$	$7\frac{1}{2}$	*72903.0*	1.07	1.067
$4d^6(^3F)5p$	$y\ ^4F°$	$3\frac{1}{2}$	*64748.8*	1.045	1.238	$4d^5\ 5s(^7S)5p$	$y\ ^6P°$	$2\frac{1}{2}$	*72908.8*	1.712	1.886
$4d^6(^3F)5p$	$y\ ^4F°$	$1\frac{1}{2}$	*64921.6*	0.428	0.400	$4d^5(^3D)5p$	$w\ ^4F°$	$2\frac{1}{2}$	*72970.1*	0.984	1.029
$4d^6(^3H)5p$	$z\ ^2G°$	$3\frac{1}{2}$	*65212.9*	1.032	0.889	$4d^5(^3D)5p$	$w\ ^4F°$	$3\frac{1}{2}$	*73142.1*	1.32	1.238
$4d^6(^3P)5p$	$z\ ^2D°$	$2\frac{1}{2}$	*65244.7*	1.324	1.200	$4d^5(^3D)5p$	$x\ ^4P°$	$0\frac{1}{2}$	*73195.4*	1.749	2.667
$4d^6(^3H)5p$	$z\ ^4I°$	$7\frac{1}{2}$	*65259.8*	1.205	1.200	$4d^5\ 5s(^7S)5p$	$y\ ^6P°$	$3\frac{1}{2}$	*73213.2*	1.57	1.714
$4d^6(^3F)5p$	$y\ ^4F°$	$4\frac{1}{2}$	*65326.7*	1.152	1.333	$4d^6(^3D)5p$	$w\ ^4F°$	$4\frac{1}{2}$	*73218.3*	1.28	1.333
$4d^6(^3H)5p$	$z\ ^4I°$	$5\frac{1}{2}$	*65472.1*	1.046	0.965	$4d^6(^3D)5p$	$w\ ^4D°$	$2\frac{1}{2}$	*73284.0*	1.301	1.371
$4d^6(^2P)5p$	$y\ ^4P°$	$1\frac{1}{2}$	*65508.1*	1.85?	1.733	$4d^6(^3D)5p$	$w\ ^4D°$	$1\frac{1}{2}$	*73315.7*	1.214	1.200
$4d^6(^3H)5p$	$z\ ^2I°$	$6\frac{1}{2}$	*65546.5*	1.14	1.077	$4d^6(^1I)5p$	$x\ ^2H°$	$4\frac{1}{2}$	*73363.4*	0.96	0.909
$4d^6(^3H)5p$	$z\ ^2G°$	$4\frac{1}{2}$	*65776.1*	0.991	1.111	$4d^6(^3D)5p$	$w\ ^4D°$	$0\frac{1}{2}$	*73750.0*	0.552	0.000
$4d^6(^3F)5p$	$z\ ^2F°$	$3\frac{1}{2}$	*66012.4*	1.199	1.143	$4d^6(^3D)5p$	$x\ ^2G°$	$3\frac{1}{2}$	*73810.0*	1.114	0.889
$4d^6(^3H)5p$	$z\ ^4I°$	$6\frac{1}{2}$	*66198.6*	1.09	1.108	$4d^6(^1I)5p$	$x\ ^2H°$	$5\frac{1}{2}$	*73950.6*	1.07	1.091
$4d^6(^3H)5p$	$z\ ^2I°$	$5\frac{1}{2}$	*66249.3*	1.04	0.923	$4d^6(^3G)5p$	$x\ ^2G°$	$4\frac{1}{2}$	*74045.7*	0.809	1.111
$4d^6(^3P)5p$	$y\ ^4D°$	$3\frac{1}{2}$	*66338.0*	1.343	1.429	$4d^6(^3D)5p$	$x\ ^2D°$	$1\frac{1}{2}$	*74592.2*	0.87	0.800
$4d^6(^3P)5p$	$y\ ^4D°$	$0\frac{1}{2}$	*66633.3*	0.789	0.000	$4d^6(^3D)5p$	$w\ ^4D°$	$3\frac{1}{2}$	*74594.0*	1.134	1.429
$4d^6(^3F)5p$	$x\ ^4D°$	$2\frac{1}{2}$	*66651.0*	1.279	1.371	$4d^6(^3D)5p$	$x\ ^2D°$	$2\frac{1}{2}$	*75117.4*	1.20	1.200
$4d^6(^3F)5p$	$z\ ^2F°$	$2\frac{1}{2}$	*67099.3*	0.855	0.857	$4d^6(^1G)5p$	$w\ ^2G°$	$4\frac{1}{2}$	*75346.3*	1.03	1.111
$4d^6(^3F)5p$	$x\ ^4D°$	$1\frac{1}{2}$	*67103.0*	1.187	1.200	$4d^6(^1G)5p$	$w\ ^2G°$	$3\frac{1}{2}$	*75431.7*	0.913	0.889
$4d^6(^3F)5p$	$y\ ^4G°$	$4\frac{1}{2}$	*67165.3*	1.158	1.172	$4d^6(^1G)5p$	$w\ ^2H°$	$5\frac{1}{2}$	*75662.1*	1.08	1.091
$4d^6(^3H)5p$	$z\ ^2H°$	$5\frac{1}{2}$	*67501.4*	1.13	1.091	$4d^6(^1I)5p$	$y\ ^2I°$	$6\frac{1}{2}$	*75789.5*	1.08	1.077
$4d^6(^3F)5p$	$y\ ^4G°$	$5\frac{1}{2}$	*67601.7*	1.166	1.273	$4d^6(^1I)5p$	$y\ ^2I°$	$5\frac{1}{2}$	*75925.4*	0.98	0.923
$4d^6(^3F)5p$	$y\ ^4G°$	$3\frac{1}{2}$	*67646.1*	1.02	0.984	$4d^6(^1G)5p$	$w\ ^2H°$	$4\frac{1}{2}$	*76389.0*	0.93	0.909
$4d^6(^3P)5p$	$y\ ^4D°$	$1\frac{1}{2}$	*67900.1*	1.234	1.200	$4d^6(^1G)5p$	$w\ ^2F°$	$3\frac{1}{2}$	*76977.5*	1.14	1.143

TABLE 2. *Odd levels of* Ru II—Continued

Configuration	Designation	J	Level	g(obs)	g(Landé)	Configuration	Designation	J	Level	g(obs)	g(Landé)
$4d^6(^1D)5p$	$y\ ^2P^\circ$	$1\frac{1}{2}$	*77292.7*	1.291	1.333	$4d^5\ 5s(^5S)5p$	$x\ ^6P^\circ$	$2\frac{1}{2}$	*90829.9*	-----	-----
$4d^6(^1D)5p$	$w\ ^2D^\circ$	$2\frac{1}{2}$	*77819.1*	1.068	1.200	$4d^5\ 5s(^5S)5p$	$x\ ^6P^\circ$	$1\frac{1}{2}$	*91503.7*	-----	-----
$4d^6(^1D)5p$	$w\ ^2D^\circ$	$1\frac{1}{2}$	*78617.3*	0.87	0.800	$4d^5\ (b^3F)5p?$	$v\ ^4D^\circ$	$3\frac{1}{2}$	*95324.8*	-----	-----
$4d^6(^1D)5p$	$v\ ^2F^\circ$	$2\frac{1}{2}$	*79114.8*	0.96	0.857	$4d^6(b^3F)5p?$	$w\ ^4G^\circ$	$2\frac{1}{2}$	*95713.4*	-----	-----
----------	3°	$3\frac{1}{2}$	*79503.7*	1.033	-----	$4d^6(b^3F)5p?$	$w\ ^4G^\circ$	$3\frac{1}{2}$	*96109.3*	-----	-----
$4d^6(^1D)5p$	$v\ ^2F^\circ$	$3\frac{1}{2}$	*79804.0*	1.046	1.143	$4d^5(b^3F)5p?$	$v\ ^4D^\circ$	$1\frac{1}{2}$	*96349.7*	-----	-----
$4d^5\ 5s(^5S)5p$	$w\ ^4P^\circ$	$2\frac{1}{2}$	*81721.7*	-----	-----	$4d^6(b^3F)5p?$	$w\ ^4G^\circ$	$4\frac{1}{2}$	*96501.7*	-----	-----
$4d^5\ 5s(^5S)5p$	$w\ ^4P^\circ$	$1\frac{1}{2}$	*82239.5*	-----	-----	$4d^6(b^3F)5p?$	$w\ ^4G^\circ$	$5\frac{1}{2}$	*96722.4*	-----	-----
$4d^5\ 5s(^5S)5p$	$w\ ^4P^\circ$	$0\frac{1}{2}$	*82650.8*	-----	-----	$4d^6(b^3F)5p?$	$v\ ^2G^\circ$	$3\frac{1}{2}$	*102865.4*	-----	-----
$4d^5\ 5s(^5S)5p$	$x\ ^6P^\circ$	$3\frac{1}{2}$	*90165.8*	-----	-----	$4d^6(b^3F)5p?$	$v\ ^2G^\circ$	$4\frac{1}{2}$	*103434.2*	-----	-----
						$4d^6\ ^5D_4$(Ru III) Limit ---- ~135200					

TABLE 3. Ru II

Configuration $1s^2\ 2s^2\ 2p^6\ 3s^2\ 3p^6\ 3d^{10}\ 4s^2\ 4p^6+$	Observed Terms														
$4d^7$	$a\ ^4P$	$a\ ^2P$	$a\ ^2D$	$b\ ^2D$	$a\ ^4F$	$a\ ^2F$	$a\ ^2G$	$a\ ^2H$							
$4d^5\ 5s^2$	$a\ ^6S$														
	$ns\ (n \geq 5)$								$np\ (n \geq 5)$						
$4d^6(^5D)nx$	$a, e\ ^6D$	$a, e\ ^4D$							$z\ ^6P^\circ$	$z\ ^4P^\circ$	$z\ ^6D^\circ$	$z\ ^4D^\circ$	$z\ ^6F^\circ$	$z\ ^4F^\circ$	
$4d^6(^3H)nx$	$a\ ^4H$	$b\ ^2H$							$z\ ^4G^\circ$	$z\ ^2G^\circ$	$z\ ^4H^\circ$	$z\ ^2H^\circ$	$z\ ^4I^\circ$	$z\ ^2I^\circ$	
$4d^6(^3P)nx$	$b\ ^4P$	$b\ ^2P$							$z\ ^4S^\circ$	$z\ ^2S^\circ$	$y\ ^4P^\circ$	$z\ ^2P^\circ$	$y\ ^4D^\circ$	$z\ ^2D^\circ$	
$4d^6(^3F)nx$	$b\ ^4F$	$b\ ^2F$							$x\ ^4D^\circ$	$y\ ^2D^\circ$	$y\ ^4F^\circ$	$z\ ^2F^\circ$	$y\ ^4G^\circ$	$y\ ^2G^\circ$	
$4d^6(^3G)nx$	$a\ ^4G$	$b\ ^2G$							$x\ ^4F^\circ$	$y\ ^2F^\circ$	$x\ ^4G^\circ$	$x\ ^2G^\circ$	$y\ ^4H^\circ$	$y\ ^2H^\circ$	
$4d^6(^3D)nx$	$b\ ^4D$	$c\ ^2D$							$x\ ^4P^\circ$	$x\ ^2D^\circ$	$w\ ^4D^\circ$	$x\ ^2F^\circ$	$w\ ^4F^\circ$		
$4d^6(^1I)nx$	$a\ ^2I$								$x\ ^2H^\circ$	$y\ ^2I^\circ$	$z\ ^2K^\circ$				
$4d^6(^1G)nx$	$c\ ^2G$								$w\ ^2F^\circ$	$w\ ^2G^\circ$	$w\ ^2H^\circ$				
$4d^6(^1S)nx$	$a\ ^2S$														
$4d^6(^1D)nx$	$d\ ^2D$								$y\ ^2P^\circ$	$w\ ^2D^\circ$	$v\ ^2F^\circ$				
$4d^6(b\ ^3F)5p$									$v\ ^4D^\circ$		$w\ ^4G^\circ$	$v\ ^2G^\circ$			
$4d^5\ 5s(^7S)nx$									$y\ ^6P^\circ$						
$4d^5\ 5s(^5S)nx$									$x\ ^6P^\circ$	$^4P^\circ$					

TABLE 4. *Numbers of levels of each J-value of the structure $4d^6\,5p$ below 80000 cm^{-1}*

No. of levels $J=$	7½	6½	5½	4½	3½	2½	1½	0½
Predicted	2	6	13	20	25	26	23	14
Identified	2	6	13	20	25	24	20	10
Observed (not identified)	---	---	---	---	1	---	2	---

$b\,^4$F have quite regular intervals in Fe II but in Ru II they are so irregular that parts of the terms at first eluded discovery. Figure 1 shows these unusual intervals in the terms $a\,^4$H, $b\,^4$F, $b\,^4$P and $a\,^4$G. Of considerable assistance, however, was the fact that the positions of the sextet and quartet terms of $d^6\,s$ in Fe II when multiplied by ¾ give a rather close correspondence with the same terms in Ru II. The differences between the higher and lower multiplicities based on the same ion term is greater by an average factor of about 1.30 in Ru II.

The naming of the levels was based on relative intensities of combination, on the Zeeman effect, and on the comparison with Fe II. The various criteria were frequently at variance and compromises were therefore necessary. It will be noticed that hardly any of the g-values are in close agreement with the Landé values, and that the values tend to have less variation from the mean than do the Landé values. The worst disagreements are for the levels $x\,^4D^\circ_{3½}$ and $y\,^4D^\circ_{0½}$, and it is quite probable that these levels are either misnamed or unaccountably perturbed.

In Fe II there are known a number of even levels based on the high terms ^{3}F, ^{3}P, ^{1}F, ^{1}G from d^6 in Fe III. A thorough search has been made for the equivalent levels in Ru II without success, although there remain unidentified a number of lines which could be combinations of such levels with known terms. This failure is all the stranger when it is noticed that some odd terms of this same group have apparently been discovered. It is possible that the observations are not sufficiently exhaustive. Some plates taken at Princeton definitely show a considerably increased number of lines.

Tables 1 and 2, respectively, list all of the known even and odd levels in order of magnitude, and Table 3 relates them to the atomic structure. The levels are all given Russell-Saunders names except three odd levels which are numbered. Table 4 lists the numbers of $4d^6\,5p$ levels to be expected with each J-value in the region below 80000 cm^{-1}. It is satisfactory that the numbers discovered are so nearly those predicted, but two discrepancies must be noted. The most striking is the presence of an extra level of $J=3½$. A quite thorough examination of all the $J=3½$ levels has been made and no one of them appears in any way spurious or to have been given an incorrect J-value. The two unidentified levels of $J=1½$ do not present such a serious problem since there is room for them numerically even if they do not fit the names and positions of any of the missing levels. The $J=2½$ column lacks two levels, and the $J=0½$ four levels, but the latter fact is not surprising because such levels are always difficult to find.

It was satisfactory to find the $4d^5\,5s^2\,^6$S level and three of its associated P° terms, $y,x\,^6$P° and $w\,^4$P°. The odd terms are confirmed by strong multiplets in combination with $a\,^6$D, and the ^{6}S itself combines with $z\,^6$P°. The ^{4}P° term of the odd structure was found from its combinations with a^4D in the Schumann region. An unsuccessful search was made for $4d^5\,5s(^7\text{S})5p\,^8$P°.

Most of the data in tables 1 and 2 were supplied in October 1957 for inclusion in Volume III of *Atomic Energy Levels* [9], where all the levels are grouped in spectral terms and the terms themselves are arranged in order of magnitude of the lowest level of each. This style of presentation has been used consistently in *Atomic Energy Levels;* it has the advantage of displaying directly the intervals between levels of terms and thus showing the actual splitting as well as whether any complex term is normal, inverted, or partially inverted. Since some slight revisions of level values, intervals, and g-factors for Ru II have been made during the past year our final results are shown in table 5 in the same style as in *Atomic Energy Levels* [9]. A large majority of the Ru II terms are inverted as expected, because they arise from configurations containing six or seven type-d electrons, that is, the d-shell is more than half filled. However, some terms produced by configurations containing six d-electrons are normal or only partially inverted, and even d^7, expected to give inverted terms, yields two terms, $a\,^2$F and $b\,^2$D, that are erect instead of inverted.

For pure LS coupling the intervals in complex terms are proportional to the larger J-values defining an interval. Thus, for $4d^7\,a\,^4$F the intervals should be proportional to 4.5:3.5:2.5 whereas they are actually in ratio 4.5:2.9:1.8. Similarly, the intervals between levels of $4d^6\,(^5\text{D})5s\,a\,^6$D should be proportional to 4.50:3.50:2.50:1.50, but their ratios are observed to be 4.50:3.16:2.04:1.36. The irregular distribution of levels in four $4d^6\,5s$ terms is illustrated in figure 1. The remaining Ru II terms with three or more levels all flagrantly violate the interval rule. These violations, as well as the departures of g-factors from the Landé values, indicate that LS coupling is far from perfect in the ruthenium ion but nevertheless strong enough to permit plausible designations of the spectral terms.

The line list (table 6) is given complete although a considerable number of lines remain unidentified. The majority of these are in the Schumann region and many are of large intensity. They probably have their origin in terms of the $4d^5\,5s\,5p$ structure, a few of which have been found. At 1937 A there is a pair of very strong lines which have been worked over very completely, but unsuccessfully. In the longer wavelength region there is a scattering of unidentified lines of some intensity and even two with resolved Zeeman patterns. They may be due to terms built on high levels of $3d^6$ or to terms of $3d^5\,4s^2$. A few lines have been remeasured on plates taken in Princeton on high dispersion and have been separated into pairs or threes.

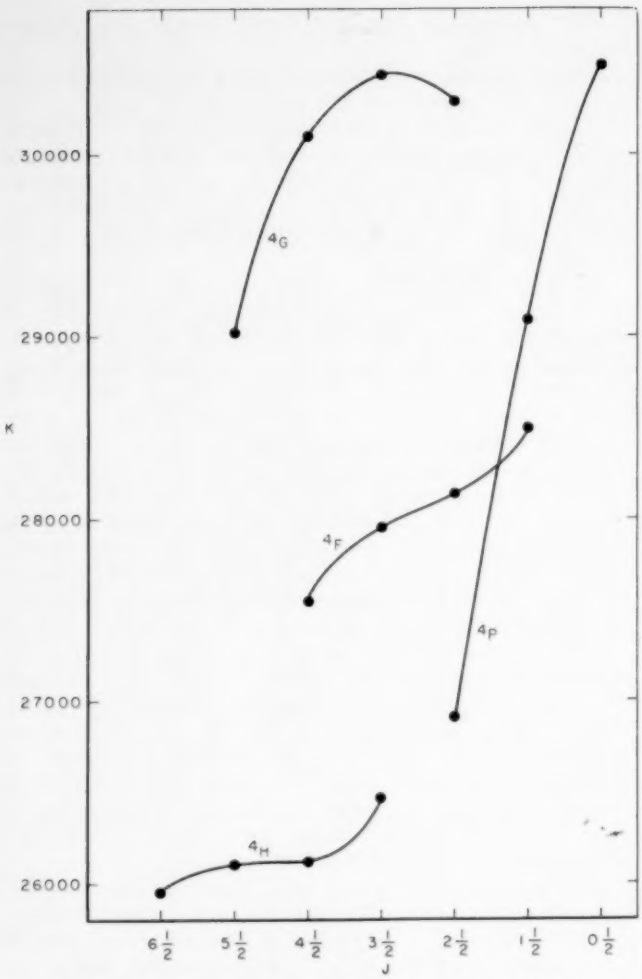

FIGURE 1. *A plot of four* Ru II *terms from* $4d^6\,5s$.

Table 6 contains the measured wavelengths and estimated relative intensities of 2,227 spectral lines ascribed to Ru II in the wavelength range 1054.684 to 6371.29 A. The wavelengths shorter than 2000 A are valid for vacuum, but the longer ones are proper for standard air. For purposes of analysis and interpretation all wavelengths have been converted to vacuum wavenumbers, σ, in K ($=\mathrm{cm}^{-1}$) units in column 3. The 4th column contains the designations of two energy levels (tables 1, 2, 5) which differ in value by the amount shown in column 3.

For wavelengths greater than 2322 A six additional columns are required in table 6 to report the Zeeman data for 488 Ru II lines. Instead of giving all the observed components of each Zeeman pattern, only the strongest p- and n-components are reported in columns 9 and 10, respectively. This information together with the Zeeman-type numbers [5] in column 5, and the g-factors in columns 7 and 8 corresponding to the J-values in column 4, permits the reconstruction of the complete Zeeman pattern. Actually the absolute values of J and g were first derived from fully observed and resolved Zeeman patterns indicated by Δg in column 6. Later, when many more lines were connected by the usual methods of interval analysis, most of the unresolved Zeeman patterns could be interpreted as confirming the analysis and extending the system of g-factors. Only a few Zeeman patterns were too unsymmetrical (*us*) to be useful. There are only two resolved and four unresolved Zeeman patterns that appear to disagree with the classification indicated in column 4. These are marked with asterisks accompanying the type number; they may be ascribed to errors of observation in a rich mixture of Zeeman patterns belonging to Ru I, Ru II, and to impurities.

The total number of Ru II lines classified in table 6 is 1,633, and, excepting the spectral range 1054 to 1400 A, there remain relatively few lines of any importance to explain.

Series Limit. Because only two members of the $4d^6\,ns\ ^6\mathrm{D}$ series are known, an accurate limit cannot be calculated directly because such series usually obey the Ritz formula

$$\frac{T}{4}=\frac{R}{\left(n+\mu+\alpha\frac{T}{4}\right)^2},$$

and the constant α is by no means negligible. An estimate of the value of α is, therefore, necessary and this can be obtained only by a general comparison of spectra of both the first and second long periods. Catalán and Rico [10] have made such a comparison and they deduce a value of $\alpha=4.09\times10^{-6}$. With this value and the correct value of the separation between $a\ ^6\mathrm{D}$ and $e\ ^6\mathrm{D}$, the limit is at 135200 cm^{-1} to the nearest 100 cm^{-1}, giving an I. P. of 16.76 v.

In a private communication the late Professor Catalán furnished a term table of Rh III, a spectrum isoelectronic with Ru II and Tc I. The agreement is excellent in the parts based on the $^5\mathrm{D}$ ion, but some of the $4d^7$ terms and many of the high odd and even terms show a considerable deviation from the positions which would be predicted from our analysis of Ru II.

References

[1] W. F. Meggers and A. G. Shenstone, Phys. Rev. **35,** 868 (1930).

[2] K. G. Kessler and W. F. Meggers, J. Research NBS **55,** 97 (1955) RP 2609.

[3] J. C. Dobbie, Ann. Solar Phys. Obs., Cambridge, Engl. 5, Part 1, 1 (1938).

[4] G. R. Harrison and J. R. McNally, Jr., Phys. Rev. **58,** 703 (1940)).

[5] E. Back and A. Landé, Zeemaneffekt und Multiplettstruktur der Spektrallinien, 168, (Julius Springer, Berlin, Germany (1925)).

[6] A. G. Shenstone and H. A. Blair, Phil. Mag. [VIII], 765 (1929).

[7] C. E. Moore, Atomic Energy Levels, NBS Circ. 467, III, 19 (1958).

[8] C. E. Moore, Atomic Energy Levels, NBS Circ. 467, II, 55 1952).

[9] C. E. Moore, Atomic Energy Levels, NBS Circ. 467, III, 25 (1958).

[10] M. A. Catalán and F. R. Rico, Anales real soc. espan. fis. y quim. (Madrid) [A] **48,** 328 (1952).

TABLE 5. *Terms and intervals of* Ru II

Configuration	Designation	J	Level	Interval	Obs. g	Configuration	Designation	J	Level	Interval	Obs. g
$4d^7$	$a\ ^4F$	4½	0. 0	−1523. 1		$4d^6(^3G)5s$	$b\ ^2G$	4½	36016. 0	−499. 8	1. 067
		3½	1523. 1	−970. 8				3½	36515. 8		0. 885
		2½	2493. 9	−610. 3							
		1½	3104. 2			$4d^6(^1G)5s$	$c\ ^2G$	4½	37433. 0	−548. 5	1. 078
								3½	37981. 5		0. 942
$4d^7$	$a\ ^4P$	2½	8256. 7	−221. 0	1. 57						
		1½	8477. 7	−896. 2	1. 68	$4d^6(^3D)5s$	$c\ ^2D$	2½	38981. 8	−730. 1	1. 18
		½	9373. 9		2. 60			1½	39711. 9		0. 797
$4d^6(^3D)5s$	$a\ ^6D$	4½	9151. 4	−999. 0	1. 53	$4d^6(^1S)5s$	$a\ ^2S$	½	40226. 2		1. 800
		3½	10150. 4	−701. 3	1. 576						
		2½	10851. 7	−452. 1	1. 641	$4d^6(^1D)5s$	$d\ ^2D$	1½	42750. 1	859. 8	0. 803
		1½	11303 8	−300. 2	1 849			2½	43609. 9		1. 216
		½	11604. 0		3. 271						
						$4d^6(^5D)5p$	$z\ ^6D°$	4½	*46471. 0*	−240. 5	1. 530
$4d^7$	$a\ ^2G$	4½	10860. 9	−1432. 5				3½	*46711. 5*	−573. 6	1. 569
		3½	12293. 4					2½	*47285. 1*	−423. 5	1. 634
								1½	*47708. 6*	−275. 2	1. 840
$4d^7$	$a\ ^2P$	1½	12956. 6	−1842. 9				½	*47983. 8*		3. 280
		½	14799. 5								
						$4d^6(^5D)5p$	$z\ ^6F°$	5½	*50758. 3*	−87. 0	1. 44
$4d^7$	$a\ ^2D$	2½	14581. 2	−2436. 4				4½	*50845. 3*	−17. 2	1. 42
		1½	17017. 6					3½	*50862. 5*	−317. 2	1. 457
								2½	*51179. 7*	−137. 3	1. 312
$4d^7$	$a\ ^2H$	5½	14663. 4	−1461. 6				1½	*51317. 0*	−63. 1	1. 058
		4½	16125. 0					½	*51380. 1*		0. 62
$4d^6(^5D)5s$	$a\ ^4D$	3½	19378. 7	−1136. 3	1. 402	$4d^6(^3D)5p$	$z\ ^6P°$	3½	*51548. 8*	−1271. 5	1. 580
		2½	20515. 0	−713. 4	1. 337			2½	*52820. 3*	−864. 9	1. 835
		1½	21246. 4	−399. 2	1. 188			1½	*53685. 2*		2. 365
		½	21645. 6		−0. 015						
						$4d^6(^5D)5p$	$z\ ^4F°$	4½	*52964. 4*	−1261. 1	1. 346
$4d^7$	$a\ ^2F$	2½	21557. 8	731. 2	0. 863			3½	*54225. 5*	−568. 8	1. 274
		3½	22289. 0		1. 138			2½	*54794. 3*	−429. 9	1. 077
								1½	*55224. 2*		0. 468
$4d^6(^3H)5s$	$a\ ^4H$	6½	25952. 2	−157. 2	1. 235						
		5½	26109. 4	−9. 0	1. 16	$4d^6(^5D)5p$	$z\ ^4D°$	3½	*53317. 1*	−748. 3	1. 391
		4½	26118. 4	−349. 6	1. 08			2½	*54065. 4*	−598. 0	1. 348
		3½	26468. 0		0. 759			1½	*54663. 4*	−318. 1	1. 145
								½	*54981. 5*		0. 011
$4d^6(^3P)5s$	$b\ ^4P$	2½	26911. 4	−2179. 6	1. 578						
		1½	29091. 0	−1398. 3	1. 646	$4d^6(^5D)5p$	$z\ ^4P°$	2½	*55695. 2*	−969. 7	1. 570
		½	30489. 3		2. 541			1½	*56664. 9*	−598. 9	1. 708
								½	*57263. 8*		2. 648
$4d^6(^3F)5s$	$b\ ^4F$	4½	27544. 6	−404. 2	1. 200						
		3½	27948. 8	−190. 0	1. 091	$4d^6(^3P)5p$	$z\ ^4S°$	1½	*62446. 1*		1. 798
		2½	28138. 8	−356. 5	0. 941						
		1½	28495. 3		0. 420	$4d^6(^3H)5p$	$z\ ^4H°$	3½	*62526. 6*	380. 2	0. 961
								4½	*62906. 8*	400. 9	1. 024
$4d^6(^3G)5s$	$a\ ^4G$	5½	29018. 6	−1081. 0	1. 232			5½	*63307. 7*	280. 5	1. 068
		4½	30099. 6	−339. 9	1. 167			6½	*63588. 2*		1. 14
		3½	30439. 5	146. 2	1. 021						
		2½	30293. 3		0. 651	$4d^6(^3H)5p$	$z\ ^4G°$	5½	*63518. 5*	−332. 8	1. 24
								4½	*63851. 3*	−89. 9	1. 136
$4d^6(^3H)5s$	$b\ ^2H$	5½	32623. 0	−63. 7	1. 065			3½	*63941. 2*	−84. 1	0. 978
		4½	32686. 7		0. 955			2½	*64025. 3*		0. 646
$4d^6(^3D)5s$	$b\ ^4D$	½	32960. 8	−72. 4	0. 138						
		1½	32888. 4	130. 4	1. 200	$4d^6(^3P)5p$	$y\ ^4P°$	2½	*63797. 6*	−1710. 5	1. 295
		2½	33018. 8	313. 9	1. 338			1½	*65508. 1*		1. 85?
		3½	33332. 7		1. 396			½			
$4d^6(^3P)5s$	$b\ ^2P$	1½	33734. 8	−2360. 2	1. 185	$4d^6(^3H)5p$	$z\ ^4I°$	4½	*64385. 3*	1086. 8	0. 959
		½	36095. 0		0. 875			5½	*65472. 1*	726. 5	1. 046
								6½	*66198. 6*	−938. 8	1. 09
$4d^6(^3F)5s$	$b\ ^2F$	3½	34038. 3	−1260. 1	1. 083			7½	*65259. 8*		1. 205
		2½	35298. 4		0. 945						
$4d^7$	$b\ ^2D$	1½	34793. 1	36. 2	0. 965	$4d^6(^3F)5p$	$y\ ^4F°$	1½	*64921. 6*	−457. 8	0. 428
		2½	34829. 3		1. 102			2½	*64463. 8*	285. 0	1. 022
								3½	*64748. 8*	577. 9	1. 045
$4d^5\ 5s^2$	$a\ ^6S$	2½	35857. 6					4½	*65326. 7*		1. 152
$4d^6(^1I)5s$	$a\ ^2I$	6½	35939. 6	−290. 1	1. 06	$4d^6(^3H)5p$	$z\ ^2G°$	3½	*65212. 9*	563. 2	1. 032
		5½	36229. 7		0. 93			4½	*65776. 1*		0. 991

TABLE 5. *Terms and intervals of* Ru II—Continued

Configuration	Designation	J	Level	Interval	Obs. g
$4d^6(^3P)5p$	$z\ ^2D°$	$2\frac{1}{2}$	*65244. 7*		1. 324
		$1\frac{1}{2}$			
$4d^6(^3H)5p$	$z\ ^2I°$	$6\frac{1}{2}$	*65546. 5*	−702. 8	1. 14
		$5\frac{1}{2}$	*66249. 3*		1. 04
$4d^6(^3F)5p$	$z\ ^2F°$	$3\frac{1}{2}$	*66012. 4*	−1086. 9	1. 199
		$2\frac{1}{2}$	*67099. 3*		0. 855
$4d^6(^3P)5p$	$y\ ^4D°$	$3\frac{1}{2}$	*66338. 0*	−2435. 9	1. 343
		$2\frac{1}{2}$	*68773. 9*	873. 8	1. 308
		$1\frac{1}{2}$	*67900. 1*	1266. 8	1. 234
		$0\frac{1}{2}$	*66633. 3*		0. 789
$4d^6(^3F)5p$	$x\ ^4D°$	$0\frac{1}{2}$	*68096. 9*	−993. 9	0. 385
		$1\frac{1}{2}$	*67103. 0*	−452. 0	1. 187
		$2\frac{1}{2}$	*66651. 0*	1578. 3	1. 279
		$3\frac{1}{2}$	*68229. 3*		0. 955
$4d^6(^3F)5p$	$y\ ^4G°$	$5\frac{1}{2}$	*67601. 7*	436. 4	1. 166
		$4\frac{1}{2}$	*67165. 3*	−480. 8	1. 158
		$3\frac{1}{2}$	*67646. 1*	−500. 5	1. 02
		$2\frac{1}{2}$	*67946. 6*		0. 689
$4d^6(^3H)5p$	$z\ ^2H°$	$5\frac{1}{2}$	*67501. 4*	−618. 9	1. 130
		$4\frac{1}{2}$	*68120. 3*		1. 015
$4d^6(^3G)5p$	$x\ ^4F°$	$4\frac{1}{2}$	*67900. 9*	−1503. 2	1. 19
		$3\frac{1}{2}$	*69404. 1*	−242. 3	1. 059
		$2\frac{1}{2}$	*69646. 4*	26. 5	0. 99
		$1\frac{1}{2}$	*69619. 9*		0. 648
$4d^6(^3F)5p$	$y\ ^2G°$	$3\frac{1}{2}$	*68265. 6*	915. 2	1. 028
		$4\frac{1}{2}$	*69180. 8*		1. 058
$4d^6(^3G)5p$	$x\ ^4G°$	$5\frac{1}{2}$	*68328. 3*	−578. 2	1. 152
		$4\frac{1}{2}$	*68906. 5*	−646. 0	1. 17
		$3\frac{1}{2}$	*69552. 5*	497. 7	1. 00
		$2\frac{1}{2}$	*69054. 8*		0. 706
$4d^6(^3P)5p$	$z\ ^2P°$	$1\frac{1}{2}$	*68445. 8*	−993. 7	1. 160
		$0\frac{1}{2}$	*69439. 5*		0. 829
$4d^6(^3G)5p$	$y\ ^4H°$	$6\frac{1}{2}$	*69311. 1*	−335. 8	1. 180
		$5\frac{1}{2}$	*69646. 9*	34. 0	1. 108
		$4\frac{1}{2}$	*69612. 9*	−42. 6	0. 99
		$3\frac{1}{2}$	*69655. 5*		0. 797
	$I°$	$1\frac{1}{2}$	*70150. 7*		1. 209
$4d^6(^3F)5p$	$y\ ^2D°$	$2\frac{1}{2}$	*70571. 9*	−207. 7	1. 157
		$1\frac{1}{2}$	*70779. 6*		0. 744
$4d^6(^3P)5p$	$z\ ^2S°$	$0\frac{1}{2}$	*71036. 3*		2. 046
$4d^6(^3D)5p$	$x\ ^4P°$	$2\frac{1}{2}$	*71114. 8*	−751. 3	1. 247
		$1\frac{1}{2}$	*71866. 1*	−1329. 3	1. 567
		$0\frac{1}{2}$	*73195. 4*		1. 749
$4d^6(^3G)5p$	$y\ ^2H°$	$5\frac{1}{2}$	*71202. 9*	−723. 5	1. 32
		$4\frac{1}{2}$	*71926. 4*		0. 96
$4d^6(^3G)5p$	$y\ ^2F°$	$2\frac{1}{2}$	*71598. 7*	411. 6	1. 193
		$3\frac{1}{2}$	*72010. 3*		1. 121
$4d^6(^1I)5p$	$z\ ^2K°$	$6\frac{1}{2}$	*71798. 3*	1104. 7	0. 91
		$7\frac{1}{2}$	*72903. 0*		1. 07
$4d^6(^3D)5p$	$x\ ^2F°$	$2\frac{1}{2}$			
		$3\frac{1}{2}$	*72248. 6*		1. 14
$4d^6(^3D)5p$	$w\ ^4F°$	$1\frac{1}{2}$	*72523. 5*	446. 6	0. 490
		$2\frac{1}{2}$	*72970. 1*	172. 0	0. 984
		$3\frac{1}{2}$	*73142. 1*	76. 2	1. 32
		$4\frac{1}{2}$	*73218. 3*		1. 28
$4d^5\ 5s(^7S)5p$	$y\ ^6P°$	$1\frac{1}{2}$	*72760. 7*	148. 1	2. 49
		$2\frac{1}{2}$	*72908. 8*	304. 4	1. 712
		$3\frac{1}{2}$	*73213. 2*		1. 57
	$2°$	$1\frac{1}{2}$	*72786. 0*		1. 34
$4d^6(^3D)5p$	$w\ ^4D°$	$0\frac{1}{2}$	*73750. 0*	−434. 3	0. 552
		$1\frac{1}{2}$	*73315. 7*	−31. 7	1. 214
		$2\frac{1}{2}$	*73284. 0*	1310. 0	1. 301
		$3\frac{1}{2}$	*74594. 0*		1. 134
$4d^6(^1I)5p$	$x\ ^2H°$	$4\frac{1}{2}$	*73363. 4*	587. 2	0. 96
		$5\frac{1}{2}$	*73950. 6*		1. 07
$4d^6(^3G)5p$	$x\ ^2G°$	$3\frac{1}{2}$	*73810. 0*	235. 7	1. 114
		$4\frac{1}{2}$	*74045. 7*		0. 809
$4d^6(^3D)5p$	$x\ ^2D°$	$1\frac{1}{2}$	*74592. 2*	525. 2	0. 87
		$2\frac{1}{2}$	*75117. 4*		1. 20
$4d^6(^1G)5p$	$w\ ^2G°$	$4\frac{1}{2}$	*75346. 3*	−85. 4	1. 03
		$3\frac{1}{2}$	*75431. 7*		0. 913
$4d^6(^1G)5p$	$w\ ^2H°$	$5\frac{1}{2}$	*75662. 1*	−726. 9	1. 08
		$4\frac{1}{2}$	*76389. 0*		0 93
$4d^6(^1I)5p$	$y\ ^2I°$	$6\frac{1}{2}$	*75789. 5*	−135. 9	1. 08
		$5\frac{1}{2}$	*75925. 4*		0. 98
$4d^6(^1G)5p$	$w\ ^2F°$	$3\frac{1}{2}$	*76977. 5*		1. 14
		$2\frac{1}{2}$			
$4d^6(^1D)5p$	$y\ ^2P°$	$1\frac{1}{2}$	*77292. 7*		1. 291
		$0\frac{1}{2}$			
$4d^6(^1D)5p$	$w\ ^2D°$	$2\frac{1}{2}$	*77819. 1*	−798. 2	1. 068
		$1\frac{1}{2}$	*78617. 3*		0. 87
$4d^6(^1D)5p$	$v\ ^2F°$	$2\frac{1}{2}$	*79114. 8*	689. 2	0. 96
		$3\frac{1}{2}$	*79804. 0*		1. 046
	$3°$	$3\frac{1}{2}$	*79503. 7*		1. 033
$4d^5\ 5s(^5S)5p$	$w\ ^4P°$	$2\frac{1}{2}$	*81721. 7*	−517. 8	
		$1\frac{1}{2}$	*82239. 5*	−411. 3	
		$0\frac{1}{2}$	*82650. 8*		
$4d^6(^5D)6s$	$e\ ^6D$	$4\frac{1}{2}$	84510. 9		
		$3\frac{1}{2}$			
		$2\frac{1}{2}$			
		$1\frac{1}{2}$			
		$0\frac{1}{2}$			
$4d^6(^5D)6s$	$e\ ^4D$	$3\frac{1}{2}$	86440. 4	−1083. 0	
		$2\frac{1}{2}$	87523. 4		
		$1\frac{1}{2}$			
		$0\frac{1}{2}$			
$4d^5\ 5s(^5S)6p$	$x\ ^6P°$	$3\frac{1}{2}$	*90165. 8*	−664. 1	
		$2\frac{1}{2}$	*90829. 9*	−673. 8	
		$1\frac{1}{2}$	*91503. 7*		
$4d^6(b^3F)5p$	$v\ ^4D°$	$3\frac{1}{2}$	*95324. 8*		
		$2\frac{1}{2}$			
		$1\frac{1}{2}$	*96349. 7*		
		$0\frac{1}{2}$			
$4d^6(b^3F)5p$	$v\ ^4G°$	$2\frac{1}{2}$	*95713. 4*	395. 9	
		$3\frac{1}{2}$	*96109. 3*	392. 4	
		$4\frac{1}{2}$	*96501. 7*	220. 7	
		$5\frac{1}{2}$	*96722. 4*		
$4d^6(b^3F)5p$	$v\ ^2G°$	$3\frac{1}{2}$	*102865. 4*	568. 8	
		$4\frac{1}{2}$	*103434. 2*		

1 Intensity	2 λ (vacuum)	3 σ	4 Term combination	1 Intensity	2 λ (vacuum)	3 σ	4 Term combination
	A	*K*			*A*	*K*	
10	1054.684	94815.1	.....	2	1242.580	80477.7	.....
0	1066.361	93776.9	.....	5	1243.176	80439.1	.....
10	1069.266	93522.1	.....	50	1245.657	80278.9	.....
1	1074.380	93076.9	.....	50	1246.887	80199.7	$a\ ^4F_{3\frac{1}{2}}$—$w\ ^6P^\circ_{3\frac{1}{2}}$
1	1080.243	92571.8	$a\ ^2G_{4\frac{1}{2}}$—$v\ ^2G^\circ_{4\frac{1}{2}}$	15	1249.774	80014.5	$a\ ^6D_{3\frac{1}{2}}$—$x\ ^6P^\circ_{3\frac{1}{2}}$
0	1080.945	92511.6	.....	3	1250.171	79989.1	.....
2	1081.684	92448.4	.....	20	1250.340	79978.2	$a\ ^6D_{2\frac{1}{2}}$—$x\ ^6P^\circ_{2\frac{1}{2}}$
2	1083.701	92276.4	.....	5	1251.174	79924.9	.....
15	1093.505	91449.1	.....	15	1251.582	79898.9	$a\ ^6D_{0\frac{1}{2}}$—$x\ ^6P^\circ_{1\frac{1}{2}}$
1	1101.132	90815.6	.....	50	1252.789	79821.9	.....
10	1103.223	90643.5	.....	50	1253.419	79781.8	.....
15	1105.125	90487.5	.....	50	1253.622	79768.9	.....
10	1109.227	90152.9	.....	20	1254.717	79699.2	.....
5	1117.906	89453.0	.....	30	1255.329	79660.4	.....
2	1139.255	87776.7	.....	10	1255.430	79654.0	.....
1	1144.504	87374.1	.....	2	1256.082	79612.6	.....
1	1147.835	87120.5	.....	2	1256.898	79561.0	.....
1	1153.309	86707.0	.....	40	1257.443	79526.5	$a\ ^6D_{1\frac{1}{2}}$—$x\ ^6P^\circ_{2\frac{1}{2}}$
5	1162.357	86032.1	.....	15	1258.127	79483.2	.....
2	1163.330	85900.1	.....	20	1258.351	79469.1	.....
2	1163.537	85944.8	.....	10	1259.038	79425.7	.....
1	1169.846	85481.3	.....	15	1259.539	79394.1	.....
1	1176.783	84977.4	.....	50	1260.502	79333.5	.....
1	1182.233	84585.7	.....	20	1260.817	79313.7	$a\ ^6D_{2\frac{1}{2}}$—$x\ ^6P^\circ_{3\frac{1}{2}}$
1	1186.583	84275.6	.....	20	1261.418	79275.9	.....
100	1190.243	84016.5	.....	10	1262.688	79196.1	.....
10	1190.302	84012.3	.....	5	1263.172	79165.8	.....
10	1195.261	83663.7	.....	10	1263.396	79151.7	.....
10	1196.983	83543.4	.....	30	1263.537	79142.9	.....
2	1197.511	83506.5	.....	3	1263.848	79123.4	.....
5	1199.341	83379.1	.....	100	1264.726	79068.5	.....
5	1202.726	83144.5	.....	15	1265.944	78992.4	.....
50	1204.564	83017.6	.....	10	1266.010	78987.8	.....
30	1204.636	83012.6	.....	15?	1266.099	78982.8	.....
30	1204.995	82987.9	.....	20	1267.348	78904.9	.....
15	1205.200	82973.8	.....	10	1267.674	78884.6	.....
10	1206.195	82905.3	.....	2	1268.046	78861.5	.....
50	1207.811	82794.4	.....	3	1268.497	78833.5	.....
5	1208.863	82722.4	.....	2	1268.776	78816.1	.....
10	1213.028	82438.3	.....	50	1269.324	78782.1	.....
5	1213.644	82396.5	.....	15	1270.911	78683.7	.....
10	1213.863	82381.6	.....	5	1271.528	78645.5	.....
5	1222.201	81819.6	.....	3	1271.653	78637.8	.....
3	1223.684	81720.4	.....	30	1271.775	78630.3	.....
10	1226.736	81517.1	.....	15	1271.921	78621.2	.....
5	1226.867	81508.4	.....	5	1273.192	78542.7	.....
50	1227.101	81492.9	.....	200	1273.344	78533.4	.....
20	1228.255	81416.3	.....	300	1278.543	78214.0	.....
2	1232.670	81124.7	.....	30	1280.736	78080.1	.....
10	1232.809	81115.6	.....	3	1281.079	78059.2	.....
100	1234.347	81014.5	$a\ ^6D_{4\frac{1}{2}}$—$x\ ^6P^\circ_{3\frac{1}{2}}$	5	1281.183	78052.9	.....
3	1234.834	80982.5	.....	20	1281.419	78038.5	.....
10	1235.247	80955.5	.....	5	1282.159	77993.4	.....
10	1239.289	80691.4	.....	5	1283.769	77895.6	.....
100	1239.467	80679.8	$a\ ^6D_{3\frac{1}{2}}$—$x\ ^6P^\circ_{2\frac{1}{2}}$	5	1283.981	77882.8	.....
50	1239.879	80653.0	$a\ ^6D_{2\frac{1}{2}}$—$x\ ^6P^\circ_{1\frac{1}{2}}$	1	1284.292	77863.9	.....
20	1240.647	80603.1	.....	5	1285.006	77820.6	.....
3	1241.920	80520.5	.....	50	1285.528	77789.0	.....
5	1242.056	80511.7	.....	2	1285.811	77771.9	.....
3	1242.356	80492.2	.....	5	1285.923	77765.2	.....

TABLE 6. *The second spectrum of ruthenium* (Ru II)—Continued

1 Intensity	2 λ (vacuum)	3 σ	4 Term combination	1 Intensity	2 λ (vacuum)	3 σ	4 Term combination
	A	*K*			*A*	*K*	
10	1286.574	77725.8	.....	5	1360.634	73495.2	.....
20	1287.965	77641.9	.....	2	1360.888	73481.6	.....
15	1288.658	77600.1	.....	2	1362.346	73402.8	.....
5	1288.884	77586.5	.....	3	1364.284	73298.5	.....
15	1290.177	77508.7	.....	20	1365.465	73235.1	.....
50	1290.780	77472.5	.....	5	1366.434	73183.2	.....
5	1291.757	77413.9	.....	5	1368.503	73072.5	$a\ ^4F_{3½}$—$w\ ^4D^\circ_{3½}$
15	1293.009	77339.0	.....	50	1369.106	73040.4	.....
10	1295.920	77165.3	.....	30	1369.852	73001.3	.....
10	1296.239	77146.3	.....	1	1376.344	72657.8	.....
50	1296.425	77135.2	.....	2	1381.703	72374.8	.....
5	1306.874	76518.5	.....	2	1382.354	72340.4	.....
5	1307.325	76492.1	.....	3	1384.134	72242.3	.....
5	1307.494	76482.2	.....	10	1385.133	72195.2	.....
10	1307.662	76472.4	.....	3	1386.015	72149.3	.....
10	1308.162	76443.1	.....	5	1388.640	72012.9	$a\ ^4F_{4½}$—$y\ ^2F^\circ_{3½}$ $a\ ^4F_{1½}$—$x\ ^2D^\circ_{2½}$
5	1308.656	76414.3	.....	5	1392.145	71831.6	.....
2	1311.302	76260.1	.....	20	1393.535	71759.9	$a\ ^4F_{3½}$—$w\ ^4D^\circ_{2½}$
20	1312.099	76213.8	.....	1h	1396.162	71624.9	.....
10	1312.557	76187.2	.....	2	1398.472	71506.6	.....
50	1313.384	76139.2	.....	5	1399.427	71457.8	.....
0	1314.306	76085.8	.....	50	1405.338	71157.3	.....
5	1314.886	76052.2	.....	10	1411.991	70822.0	$a\ ^4F_{2½}$—$w\ ^4D^\circ_{1½}$
2	1315.624	76009.6	$a\ ^4F_{1½}$—$v\ ^2F^\circ_{2½}$	50	1412.206	70811.2	$b\ ^2H_{5½}$—$v\ ^2G^\circ_{4½}$
1	1315.949	75990.8	.....	100	1413.017	70770.6	$a\ ^4H_{6½}$—$w\ ^4G^\circ_{5½}$
50	1316.573	75954.8	$b\ ^4P_{2½}$—$v\ ^2G^\circ_{3½}$	5	1415.500	70646.4	$a\ ^4F_{2½}$—$w\ ^4F^\circ_{3½}$ $a\ ^4F_{1½}$—$w\ ^4D^\circ_{0½}$
20	1316.740	75945.1	$a\ ^4D_{3½}$—$v\ ^4D^\circ_{3½}$	5	1415.678	70637.5	$a\ ^4P_{1½}$—$v\ ^2F^\circ_{2½}$
1	1320.043	75755.1	.....	10	1416.358	70603.6	$a\ ^4H_{4½}$—$w\ ^4G^\circ_{3½}$
2	1321.495	75671.9	.....	1	1418.299	70507.0	.....
10	1324.275	75513.0	$a\ ^4F_{1½}$—$w\ ^2D^\circ_{1½}$	2	1418.909	70476.7	$a\ ^4F_{2½}$—$w\ ^4F^\circ_{2½}$
1	1324.654	75491.4	.....	100	1420.606	70392.5	$a\ ^4H_{5½}$—$w\ ^4G^\circ_{4½}$
3	1326.118	75408.1	.....	1	1420.793	70383.2	$a\ ^4H_{4½}$—$w\ ^4G^\circ_{4½}$
10	1326.318	75396.7	.....	5	1421.828	70332.0	.....
5	1327.776	75313.9	.....	3	1422.661	70290.8	$a\ ^4F_{2½}$—$2i^\circ_{1½}$
1	1329.403	75221.7	.....	2	1423.056	70271.3	.....
2	1329.583	75211.6	.....	5	1424.272	70211.3	$a\ ^4F_{1½}$—$w\ ^4D^\circ_{1½}$
1	1329.836	75197.2	$a\ ^4D_{2½}$—$w\ ^4G^\circ_{2½}$	50	1424.934	70178.7	$b\ ^2H_{4½}$—$v\ ^2G^\circ_{3½}$
1	1333.018	75017.7	.....	10	1424.039	70173.5	.....
1	1334.830	74915.9	$b\ ^4F_{3½}$—$v\ ^2G^\circ_{3½}$	2	1426.391	70107.0	.....
3	1335.008	74905.9	.....	5	1426.503	70101.5	$b\ ^4D_{3½}$—$v\ ^2G^\circ_{4½}$
5*h*	1336.023	74849.0	.....	3	1426.706	70091.5	$a\ ^4F_{1½}$—$x\ ^4P^\circ_{0½}$
20	1338.388	74716.7	.....	3	1427.890	70033.4	$a\ ^4H_{3½}$—$w\ ^4G^\circ_{4½}$
10?	1339.517	74653.8	.....	5	1427.964	70029.8	$a\ ^4F_{2½}$—$w\ ^4F^\circ_{1½}$
8	1340.165	74617.7	.....	100	1428.751	69991.2	$a\ ^4H_{4½}$—$w\ ^4G^\circ_{3½}$
15	1340.590	74594.0	$a\ ^4F_{4½}$—$w\ ^4D^\circ_{3½}$	30	1429.002	69978.9	.....
50	1340.754	74584.9	.....	0	1429.348	69962.0	.....
10	1341.649	74535.1	.....	2	1431.278	69867.6	$a\ ^4F_{1½}$—$w\ ^4F^\circ_{2½}$
50	1342.358	74495.8	.....	1	1431.606	69851.6	.....
10	1342.798	74471.4	.....	1	1431.705	69846.8	$b\ ^4D_{2½}$—$v\ ^2G^\circ_{3½}$
3	1346.839	74247.9	.....	1	1431.819	69841.2	.....
200	1348.385	74162.8	.....	2	1433.294	69769.4	.....
15	1350.856	74027.1	.....	30	1434.330	69719.0	.....
3	1351.857	73972.3	.....	20	1435.085	69682.3	$a\ ^4F_{1½}$—$2i^\circ_{1½}$
15	1353.907	73860.3	.....	20	1435.286	69672.5	.....
10	1354.835	73807.7	.....	50	1437.460	69567.2	.....
2	1357.221	73680.0	.....	50	1437.839	69548.8	.....
2	1357.524	73663.5	.....	1	1439.001	69492.7	.....
				30	1440.514	69419.7	$a\ ^4F_{1½}$—$w\ ^4F^\circ_{1½}$

1 Intensity	2 λ (vacuum)	3 σ	4 Term combination	1 Intensity	2 λ (vacuum)	3 σ	4 Term combination
	A	*K*			*A*	*K*	
5	1440.820	69404.9	*a* $^4F_{4\frac{1}{2}}$—*x* $^4F^{\circ}_{3\frac{1}{2}}$	1	1471.057	67978.3	
5	1441.012	69395.7	*b* $^2F_{3\frac{1}{2}}$—*v* $^2G^{\circ}_{4\frac{1}{2}}$	10	1471.220	67970.8	*b* $^4F_{2\frac{1}{2}}$—*w* $^4G^{\circ}_{3\frac{1}{2}}$
5	1441.268	69383.3		10	1471.328	67965.8	
5	1441.344	69379.7		2	1471.632	67951.8	
30	1442.147	69341.1	*a* $^4P_{1\frac{1}{2}}$—*w* $^2D^{\circ}_{2\frac{1}{2}}$	1	1471.735	67947.0	
3	1442.373	69330.2		1	1471.828	67942.7	
50	1444.144	69245.2	*a* $^4H_{3\frac{1}{2}}$—*w* $^4G^{\circ}_{2\frac{1}{2}}$	3	1472.234	67924.0	
15	1444.645	69221.2		500	1472.717	67901.7	*a* $^4F_{4\frac{1}{2}}$—*x* $^4F^{\circ}_{4\frac{1}{2}}$
15	1445.491	69180.6	*a* $^4F_{4\frac{1}{2}}$—*y* $^2G^{\circ}_{4\frac{1}{2}}$				
30	1445.552	69177.7	*b* $^4F_{4\frac{1}{2}}$—*w* $^4G^{\circ}_{5\frac{1}{2}}$	400	1473.151	67881.7	*a* $^4F_{3\frac{1}{2}}$—*x* $^4F^{\circ}_{3\frac{1}{2}}$
				3	1473.739	67854.6	*b* $^4F_{1\frac{1}{2}}$—*v* $^4D^{\circ}_{1\frac{1}{2}}$
3	1446.144	69149.4		2	1473.860	67849.0	
2	1447.084	69104.5	*a* $^4F_{2\frac{1}{2}}$—*y* $^2F^{\circ}_{2\frac{1}{2}}$	3	1473.999	67842.7	
2	1447.292	69094.6		50	1475.361	67780.0	*b* $^4F_{4\frac{1}{2}}$—*v* $^4D^{\circ}_{3\frac{1}{2}}$
10	1447.776	69071.5					
15	1449.323	68997.7		50	1477.025	67703.7	*a* $^4G_{3\frac{1}{2}}$—*w* $^4G^{\circ}_{3\frac{1}{2}}$
				1	1477.269	67692.5	
2	1449.705	68979.6		100	1477.632	67675.8	*a* $^4F_{1\frac{1}{2}}$—*y* $^2D^{\circ}_{1\frac{1}{2}}$
2	1449.955	68967.7		30	1478.021	67658.0	*a* $^4F_{3\frac{1}{2}}$—*y* $^2G^{\circ}_{4\frac{1}{2}}$
10	1450.177	68957.1	*b* $^4F_{4\frac{1}{2}}$—*w* $^4G^{\circ}_{4\frac{1}{2}}$	1	1478.960	67615.1	
10	1450.466	68943.4	*a* $^2G_{4\frac{1}{2}}$—*v* $^2F^{\circ}_{3\frac{1}{2}}$				
1	1450.623	68935.9		1	1479.089	67609.2	
				50	1479.242	67602.2	*a* $^4F_{4\frac{1}{2}}$—*y* $^4G^{\circ}_{3\frac{1}{2}}$
1	1451.033	68916.4		15	1479.732	67579.8	
100	1451.224	68907.3	*a* $^4F_{4\frac{1}{2}}$—*x* $^4G^{\circ}_{4\frac{1}{2}}$	2	1479.858	67574.1	*b* $^4F_{2\frac{1}{2}}$—*w* $^4G^{\circ}_{2\frac{1}{2}}$
5	1451.505	68894.0		5	1480.004	67567.4	*b* $^2F_{2\frac{1}{2}}$—*v* $^2G^{\circ}_{3\frac{1}{2}}$
3	1451.985	68871.2					
10	1452.288	68856.9	*a* $^4H_{3\frac{1}{2}}$—*v* $^4D^{\circ}_{3\frac{1}{2}}$	100	1481.435	67502.1	*a* $^4F_{4\frac{1}{2}}$—*z* $^2H^{\circ}_{3\frac{1}{2}}$
				10	1482.193	67467.6	*a* $^4F_{1\frac{1}{2}}$—*y* $^2D^{\circ}_{2\frac{1}{2}}$
2	1452.598	68842.2		1	1483.033	67429.4	
10	1452.860	68829.8		2	1483.276	67418.3	*b* $^2G_{4\frac{1}{2}}$—v $^2G^{\circ}_{4\frac{1}{2}}$
5	1453.443	68802.1	*b* $^4P_{2\frac{1}{2}}$—*w* $^4G^{\circ}_{2\frac{1}{2}}$	300	1484.035	67383.9	*a* $^4F_{3\frac{1}{2}}$—*x* $^4G^{\circ}_{4\frac{1}{2}}$
3	1453.633	68793.2					
15	1454.666	68744.3		1	1484.513	67362.2	
				2	1485.568	67314.3	*a* $^6D_{1\frac{1}{2}}$—*w* $^2D^{\circ}_{1\frac{1}{2}}$?
2	1455.950	68683.7		15	1486.006	67294.5	
3	1457.220	68623.8		1	1486.468	67273.6	
30	1458.491	68564.0	*b* $^4F_{4\frac{1}{2}}$—*w* $^4G^{\circ}_{3\frac{1}{2}}$?	500	1486.957	67251.4	*a* $^4F_{3\frac{1}{2}}$—*y* $^4D^{\circ}_{2\frac{1}{2}}$
20	1458.721	68553.2	*b* $^4F_{3\frac{1}{2}}$—*w* $^4G^{\circ}_{4\frac{1}{2}}$				
40	1459.028	68538.8	*a* $^2F_{3\frac{1}{2}}$—*x* $^6P^{\circ}_{2\frac{1}{2}}$?	1	1487.138	67243.3	
				10*h*	1487.417	67230.6	
5	1459.416	68520.6		5	1487.688	67218.4	*b* $^4F_{1\frac{1}{2}}$—*w* $^4G^{\circ}_{2\frac{1}{2}}$
5	1459.974	68494.4	*a* $^4F_{1\frac{1}{2}}$—*y* $^2F^{\circ}_{2\frac{1}{2}}$	2	1487.857	67210.8	*a* $^2G_{3\frac{1}{2}}$—$3^{\circ}_{3\frac{1}{2}}$
5	1461.222	68435.9		1	1487.992	67204.7	*a* $^2I_{3\frac{1}{2}}$—*v* $^2G^{\circ}_{4\frac{1}{2}}$
50	1461.699	68413.5	*b* $^4P_{2\frac{1}{2}}$—*v* $^4D^{\circ}_{3\frac{1}{2}}$				
30	1462.437	68379.0		2	1488.402	67186.1	*b* $^4F_{2\frac{1}{2}}$—*v* $^4D^{\circ}_{3\frac{1}{2}}$
				200	1488.618	67176.4	*a* $^4P_{2\frac{1}{2}}$—*w* $^2G^{\circ}_{3\frac{1}{2}}$?
2	1462.619	68370.5		1000	1488.855	67165.7	*a* $^4F_{4\frac{1}{2}}$—*y* $^4G^{\circ}_{4\frac{1}{2}}$
100	1463.215	68342.7		500	1489.136	67153.0	*a* $^4F_{2\frac{1}{2}}$—*x* $^4F^{\circ}_{2\frac{1}{2}}$
30	1463.515	68328.6	*a* $^4F_{4\frac{1}{2}}$—*x* $^4G^{\circ}_{5\frac{1}{2}}$	20	1489.734	67126.1	*a* $^4F_{2\frac{1}{2}}$—*x* $^4F^{\circ}_{1\frac{1}{2}}$
50	1464.022	68305.0					
0	1464.426	68286.1	*a* $^4F_{2\frac{1}{2}}$—*y* $^2D^{\circ}_{1\frac{1}{2}}$	100*h*	1490.707	67082.3	
				5	1491.224	67059.0	*a* $^4F_{2\frac{1}{2}}$—*x* $^4G^{\circ}_{3\frac{1}{2}}$
15	1464.855	68266.1	*a* $^4F_{4\frac{1}{2}}$—*y* $^2G^{\circ}_{3\frac{1}{2}}$	5	1491.497	67046.7	*a* $^4F_{1\frac{1}{2}}$—$1^{\circ}_{1\frac{1}{2}}$
1	1465.195	68250.3		30*h*	1492.355	67008.2	*a* $^6S_{2\frac{1}{2}}$—*v* $^2G^{\circ}_{3\frac{1}{2}}$?
50	1466.039	68211.0	*b* $^4F_{2\frac{1}{2}}$—*v* $^4D^{\circ}_{1\frac{1}{2}}$	10	1493.188	66970.8	
15	1467.127	68160.4	*b* $^4F_{3\frac{1}{2}}$—*w* $^4G^{\circ}_{3\frac{1}{2}}$				
30	1467.723	68132.7	*a* $^4F_{3\frac{1}{2}}$—*y* $^4H^{\circ}_{3\frac{1}{2}}$	2	1493.450	66959.1	
				500	1494.524	66910.9	*a* $^4F_{2\frac{1}{2}}$—*x* $^4F^{\circ}_{3\frac{1}{2}}$
30	1467.933	68123.0	*a* $^4F_{3\frac{1}{2}}$—*x* $^4F^{\circ}_{2\frac{1}{2}}$	5	1495.810	66853.4	
100	1467.977	68121.0	*a* $^4F_{4\frac{1}{2}}$—*z* $^2H^{\circ}_{4\frac{1}{2}}$	50	1498.289	66742.4	*a* $^4F_{3\frac{1}{2}}$—*y* $^2G^{\circ}_{3\frac{1}{2}}$
30	1468.158	68112.6		0	1498.841	66718.2	
10	1468.660	68089.3	*a* $^4F_{3\frac{1}{2}}$—*y* $^4H^{\circ}_{4\frac{1}{2}}$				
10	1468.725	68086.3		2	1499.104	66706.5	*a* $^4F_{3\frac{1}{2}}$—*x* $^4D^{\circ}_{3\frac{1}{2}}$
				0	1499.759	66677.4	
200	1468.909	68077.7	*a* $^4F_{2\frac{1}{2}}$—*y* $^2D^{\circ}_{2\frac{1}{2}}$	2	1501.216	66612.7	
2	1469.805	68036.2	*b* $^2D_{2\frac{1}{2}}$—*v* $^2G^{\circ}_{3\frac{1}{2}}$	2	1501.558	66597.5	*a* $^4F_{3\frac{1}{2}}$—*z* $^2H^{\circ}_{4\frac{1}{2}}$
100	1469.941	68029.9	*a* $^4F_{3\frac{1}{2}}$—*x* $^4G^{\circ}_{3\frac{1}{2}}$	2	1502.383	66560.9	*a* $^4F_{2\frac{1}{2}}$—*x* $^4G^{\circ}_{2\frac{1}{2}}$
1	1470.674	67996.0					
1	1470.854	67987.7					

TABLE 6. *The second spectrum of ruthenium* (Ru II)—Continued

1 Intensity	2 λ (vacuum)	3 σ	4 Term combination
	A	*K*	
1	1502. 596	66551. 5	----------
30	1502. 802	66542. 4	$a\ {}^4F_{1\frac{1}{2}}$—$x\ {}^4F^\circ_{2\frac{1}{2}}$
30	1503. 401	66515. 9	$a\ {}^4F_{1\frac{1}{2}}$—$x\ {}^4F^\circ_{1\frac{1}{2}}$
1	1504. 724	66457. 4	----------
0	1504. 855	66451. 6	----------
0	1505. 128	66439. 5	----------
20	1505. 610	66418. 3	----------
50	1506. 515	66378. 4	$a\ {}^4F_{3\frac{1}{2}}$—$x\ {}^4F^\circ_{4\frac{1}{2}}$
0	1507. 077	66353. 6	----------
100*d*?	1507. 429	66338. 1	$a\ {}^4F_{4\frac{1}{2}}$—$y\ {}^4D^\circ_{3\frac{1}{2}}$ $a\ {}^4P_{2\frac{1}{2}}$—$w\ {}^4D^\circ_{3\frac{1}{2}}$
0	1508. 001	66313. 0	----------
40	1509. 432	66250. 1	$a\ {}^4F_{4\frac{1}{2}}$—$z\ {}^2I^\circ_{5\frac{1}{2}}$
1	1511. 523	66158. 4	$a\ {}^2P_{1\frac{1}{2}}$—$v\ {}^2F^\circ_{2\frac{1}{2}}$
30	1512. 325	66123. 4	$a\ {}^4F_{3\frac{1}{2}}$—$y\ {}^4G^\circ_{3\frac{1}{2}}$
40	1512. 483	66116. 4	$a\ {}^2G_{4\frac{1}{2}}$—$w\ {}^2F^\circ_{3\frac{1}{2}}$
2	1513. 345	66078. 8	----------
0	1513. 495	66072. 2	----------
0	1514. 068	66047. 2	----------
30	1514. 564	66025. 6	----------
1	1514. 850	66013. 1	$a\ {}^4F_{4\frac{1}{2}}$—$z\ {}^2F^\circ_{3\frac{1}{2}}$
0	1515. 062	66003. 9	----------
0	1515. 459	65986. 6	----------
0	1515. 791	65972. 2	----------
30	1516. 256	65951. 9	$a\ {}^4F_{2\frac{1}{2}}$—$z\ {}^2P^\circ_{1\frac{1}{2}}$ $a\ {}^4F_{1\frac{1}{2}}$—$x\ {}^4G^\circ_{2\frac{1}{2}}$
2	1518. 374	65859. 9	$b\ {}^4P_{0\frac{1}{2}}$—$v\ {}^4D^\circ_{1\frac{1}{2}}$
0	1519. 486	65811. 7	----------
2	1520. 294	65776. 8	$a\ {}^4F_{4\frac{1}{2}}$—$z\ {}^2G^\circ_{4\frac{1}{2}}$
16	1520. 406	65771. 9	$a\ {}^4F_{2\frac{1}{2}}$—$y\ {}^2G^\circ_{3\frac{1}{2}}$
3	1520. 765	65756. 8	----------
10	1520. 961	65747. 9	----------
25	1521. 238	65735. 9	$a\ {}^4F_{2\frac{1}{2}}$—$x\ {}^4D^\circ_{3\frac{1}{2}}$
2	1522. 786	65669. 1	$a\ {}^4F_{1\frac{1}{2}}$—$y\ {}^4D^\circ_{2\frac{1}{2}}$
2	1522. 981	65660. 7	$a\ {}^2P_{1\frac{1}{2}}$—$w\ {}^2D^\circ_{1\frac{1}{2}}$
5	1523. 408	65642. 3	$a\ {}^4F_{3\frac{1}{2}}$—$y\ {}^4G^\circ_{4\frac{1}{2}}$
3	1524. 606	65590. 7	----------
15	1524. 937	65576. 5	$a\ {}^4F_{2\frac{1}{2}}$—$z\ {}^2F^\circ_{2\frac{1}{2}}$
10	1525. 464	65553. 8	$a\ {}^4P_{2\frac{1}{2}}$—$x\ {}^2G^\circ_{3\frac{1}{2}}$
10*h*	1526. 071	65527. 8	$a\ {}^2G_{4\frac{1}{2}}$—$w\ {}^2H^\circ_{5\frac{1}{2}}$
1	1526. 712	65500. 2	----------
1	1527. 350	65472. 9	$a\ {}^4F_{4\frac{1}{2}}$—$z\ {}^4I^\circ_{5\frac{1}{2}}$
30	1527. 813	65453. 0	$a\ {}^4F_{2\frac{1}{2}}$—$y\ {}^4G^\circ_{2\frac{1}{2}}$
5	1528. 903	65406. 4	$a\ {}^4F_{2\frac{1}{2}}$—$y\ {}^4D^\circ_{1\frac{1}{2}}$
3	1529. 395	65385. 3	----------
2	1529. 942	65362. 0	----------
10	1530. 415	65341. 8	$a\ {}^4F_{1\frac{1}{2}}$—$z\ {}^2P^\circ_{1\frac{1}{2}}$
5	1530. 762	65327. 9	$a\ {}^4F_{4\frac{1}{2}}$—$y\ {}^4F^\circ_{4\frac{1}{2}}$
0	1531. 113	65312. 0	----------
10	1533. 236	65221. 5	$a\ {}^2D_{2\frac{1}{2}}$—$v\ {}^2F^\circ_{3\frac{1}{2}}$
10	1533. 435	65213. 1	$a\ {}^4F_{4\frac{1}{2}}$—$z\ {}^2G^\circ_{3\frac{1}{2}}$
15	1534. 587	65164. 1	----------
20	1534. 860	65152. 5	$a\ {}^4F_{2\frac{1}{2}}$—$y\ {}^4G^\circ_{3\frac{1}{2}}$
10	1535. 055	65144. 2	----------
50	1535. 426	65128. 5	$a\ {}^4F_{3\frac{1}{2}}$—$x\ {}^4D^\circ_{2\frac{1}{2}}$
5	1536. 603	65078. 6	----------
3	1537. 057	65059. 4	$a\ {}^4P_{2\frac{1}{2}}$—$w\ {}^4D^\circ_{1\frac{1}{2}}$
20	1537. 806	65027. 7	$a\ {}^4P_{2\frac{1}{2}}$—$w\ {}^4D^\circ_{2\frac{1}{2}}$
30	1538. 624	64993. 1	$a\ {}^4F_{1\frac{1}{2}}$—$x\ {}^4D^\circ_{0\frac{1}{2}}$
1	1539. 478	64957. 1	$a\ {}^4P_{2\frac{1}{2}}$—$y\ {}^6P^\circ_{3\frac{1}{2}}$
5	1541. 167	64885. 9	$a\ {}^4P_{2\frac{1}{2}}$—$w\ {}^4F^\circ_{3\frac{1}{2}}$
15	1541. 718	64862. 7	$a\ {}^2P_{1\frac{1}{2}}$—$w\ {}^2D^\circ_{2\frac{1}{2}}$
15	1542. 188	64842. 9	$a\ {}^4F_{1\frac{1}{2}}$—$y\ {}^4G^\circ_{2\frac{1}{2}}$
15	5142. 293	64838. 5	$a\ {}^4P_{1\frac{1}{2}}$—$w\ {}^4D^\circ_{1\frac{1}{2}}$
1	1542. 844	64815. 4	$a\ {}^4F_{3\frac{1}{2}}$—$y\ {}^4D^\circ_{3\frac{1}{2}}$
10	1543. 042	64807. 0	$a\ {}^4P_{1\frac{1}{2}}$—$w\ {}^4D^\circ_{2\frac{1}{2}}$
5	1543. 299	64796. 3	$a\ {}^4F_{1\frac{1}{2}}$—$y\ {}^4D^\circ_{1\frac{1}{2}}$
30	1544. 414	64749. 5	$a\ {}^4F_{4\frac{1}{2}}$—$y\ {}^4F^\circ_{3\frac{1}{2}}$
15	1545. 152	64718. 6	$a\ {}^4P_{1\frac{1}{2}}$—$x\ {}^4P^\circ_{0\frac{1}{2}}$
15	1545. 961	64684. 7	$a\ {}^2G_{3\frac{1}{2}}$—$w\ {}^2F^\circ_{3\frac{1}{2}}$
30	1547. 756	64609. 7	$a\ {}^4F_{2\frac{1}{2}}$—$x\ {}^4D^\circ_{1\frac{1}{2}}$
1	1547. 856	64605. 5	$a\ {}^4F_{2\frac{1}{2}}$—$z\ {}^2F^\circ_{2\frac{1}{2}}$
10	1548. 679	64571. 2	$a\ {}^2G_{4\frac{1}{2}}$—$w\ {}^2G^\circ_{3\frac{1}{2}}$
15	1549. 571	64534. 0	$a\ {}^2D_{2\frac{1}{2}}$—$v\ {}^2F^\circ_{2\frac{1}{2}}$
2	1550. 065	64513. 4	----------
3	1550. 640	64489. 5	$a\ {}^4F_{3\frac{1}{2}}$—$z\ {}^2F^\circ_{3\frac{1}{2}}$
30	1550. 740	64485. 3	$a\ {}^2G_{4\frac{1}{2}}$—$w\ {}^2G^\circ_{4\frac{1}{2}}$
5	1553. 141	64385. 7	$a\ {}^4F_{4\frac{1}{2}}$—$z\ {}^4I^\circ_{4\frac{1}{2}}$
0	1553. 532	64369. 4	----------
0	1553. 777	64359. 3	----------
5	1554. 334	64336. 2	$a\ {}^2P_{1\frac{1}{2}}$—$y\ {}^2P^\circ_{1\frac{1}{2}}$
3	1556. 341	64253. 3	$a\ {}^4F_{3\frac{1}{2}}$—$z\ {}^2G^\circ_{4\frac{1}{2}}$
3	1558. 655	64157. 9	$a\ {}^4F_{2\frac{1}{2}}$—$x\ {}^4D^\circ_{3\frac{1}{2}}$
3h	1560. 180	64095. 2	$a\ {}^2G_{3\frac{1}{2}}$—$w\ {}^2H^\circ_{4\frac{1}{2}}$
50	1560. 998	64061. 6	$a\ {}^6D_{4\frac{1}{2}}$—$y\ {}^6P^\circ_{3\frac{1}{2}}$
5	1561. 603	64036. 4	$a\ {}^2D_{2\frac{1}{2}}$—$w\ {}^2D^\circ_{1\frac{1}{2}}$
30	1562. 607	63995. 6	$a\ {}^4F_{1\frac{1}{2}}$—$z\ {}^2F^\circ_{2\frac{1}{2}}$
20	1562. 726	63990. 7	$a\ {}^6D_{4\frac{1}{2}}$—$w\ {}^4F^\circ_{3\frac{1}{2}}$
15	1563. 928	63941. 6	$a\ {}^4F_{4\frac{1}{2}}$—$z\ {}^4G^\circ_{3\frac{1}{2}}$ $a\ {}^4P_{0\frac{1}{2}}$—$w\ {}^4D^\circ_{1\frac{1}{2}}$
0	1564. 620	63913. 3	----------
1	1565. 029	63896. 6	$a\ {}^6D_{3\frac{1}{2}}$—$x\ {}^2G^\circ_{4\frac{1}{2}}$
100	1566. 128	63851. 7	$a\ {}^4F_{4\frac{1}{2}}$—$z\ {}^4G^\circ_{4\frac{1}{2}}$
20	1566. 965	63817. 6	$a\ {}^2P_{0\frac{1}{2}}$—$w\ {}^2D^\circ_{1\frac{1}{2}}$
50	1567. 308	63803. 7	$a\ {}^4F_{3\frac{1}{2}}$—$y\ {}^4F^\circ_{4\frac{1}{2}}$
15	1567. 656	63789. 5	----------
3	1568. 525	63754. 2	$a\ {}^4P_{2\frac{1}{2}}$—$y\ {}^2F^\circ_{3\frac{1}{2}}$
3	1568. 933	63737. 6	----------
3	1569. 316	63722. 0	$a\ {}^4F_{3\frac{1}{2}}$—$z\ {}^2D^\circ_{2\frac{1}{2}}$
15	1570. 104	63690. 0	$a\ {}^4F_{3\frac{1}{2}}$—$z\ {}^2G^\circ_{3\frac{1}{2}}$
30	1570. 371	63679. 2	$a\ {}^2H_{4\frac{1}{2}}$—$v\ {}^2F^\circ_{3\frac{1}{2}}$
20	1571. 280	63642. 4	----------
1	1571. 671	63626. 5	----------
20	1572. 089	63609. 6	$a\ {}^4P_{2\frac{1}{2}}$—$x\ {}^4P^\circ_{1\frac{1}{2}}$
1	1573. 129	63567. 6	----------
2	1573. 407	63556. 3	----------
3	1573. 639	63547. 0	$a\ {}^4F_{1\frac{1}{2}}$—$x\ {}^4D^\circ_{2\frac{1}{2}}$
500d?	1574. 337	63518. 8	$a\ {}^4F_{4\frac{1}{2}}$—$z\ {}^4G^\circ_{5\frac{1}{2}}$
1	1575. 127	63486. 9	----------
0	1575. 297	63480. 1	----------
15	1576. 971	63412. 7	$a\ {}^4P_{0\frac{1}{2}}$—$2^\circ_{1\frac{1}{2}}$
1	1577. 115	63406. 9	----------
10	1577. 573	63388. 5	$a\ {}^4P_{1\frac{1}{2}}$—$x\ {}^4P^\circ_{1\frac{1}{2}}$
20	1577. 816	63378. 7	$a\ {}^2H_{4\frac{1}{2}}$—$3^\circ_{3\frac{1}{2}}$
30	1578. 728	63342. 1	$a\ {}^4P_{2\frac{1}{2}}$—$y\ {}^2F^\circ_{2\frac{1}{2}}$
10	1579. 578	63308. 0	$a\ {}^4F_{4\frac{1}{2}}$—$z\ {}^4H^\circ_{5\frac{1}{2}}$
10	1580. 816	63258. 5	----------
1	1580. 974	63252. 1	----------

TABLE 6. *The second spectrum of ruthenium* (Ru II)—Continued

1 Intensity	2 λ (vacuum)	3 σ	4 Term combination	1 Intensity	2 λ (vacuum)	3 σ	4 Term combination
	A	*K*			*A*	*K*	
15	1581. 328	63238. 0	$a\ ^2D_{2\frac{1}{2}}—w\ ^2D^{\circ}_{2\frac{1}{2}}$	5	1621. 728	61662. 6	$a\ ^4P_{0\frac{1}{2}}—z\ ^2S^{\circ}_{0\frac{1}{2}}$
10	1581. 636	63225. 7	$a\ ^4F_{3\frac{1}{2}}—y\ ^4F^{\circ}_{3\frac{1}{2}}$	20	1622. 431	61635. 9	$a\ ^2P_{1\frac{1}{2}}—x\ ^2D^{\circ}_{1\frac{1}{2}}$
5	1581. 791	63219. 5		20	1623. 231	61605. 5	$a\ ^6D_{1\frac{1}{2}}—y\ ^6P^{\circ}_{2\frac{1}{2}}$
10	1582. 652	63185. 1	$a\ ^2G_{4\frac{1}{2}}—x\ ^2G^{\circ}_{4\frac{1}{2}}$	20	1623. 390	61599. 5	$a\ ^2D_{1\frac{1}{2}}—w\ ^2D^{\circ}_{1\frac{1}{2}}$
1	1582. 903	63175. 1		1	1624. 563	61555. 0	$b\ ^2D_{1\frac{1}{2}}—v\ ^4D^{\circ}_{1\frac{1}{2}}$
200	1583. 819	63138. 5	$a\ ^2G_{3\frac{1}{2}}—w\ ^2G^{\circ}_{3\frac{1}{2}}$	100	1625. 178	61531. 7	$a\ ^4F_{2\frac{1}{2}}—z\ ^4G^{\circ}_{2\frac{1}{2}}$
30	1584. 256	63121. 1	$a\ ^4P_{1\frac{1}{2}}—y\ ^2F^{\circ}_{2\frac{1}{2}}$	50	1625. 565	61517. 1	$a\ ^2G_{3\frac{1}{2}}—x\ ^2G^{\circ}_{3\frac{1}{2}}$
50	1585. 040	63089. 9	$a\ ^2G_{4\frac{1}{2}}—x\ ^2H^{\circ}_{5\frac{1}{2}}$	50	1627. 138	61457. 6	$a\ ^6D_{1\frac{1}{2}}—y\ ^6P^{\circ}_{1\frac{1}{2}}$
30	1585. 740	63062. 0	$a\ ^6D_{3\frac{1}{2}}—y\ ^6P^{\circ}_{3\frac{1}{2}}$	100	1627. 397	61447. 8	$a\ ^4F_{2\frac{1}{2}}—z\ ^4G^{\circ}_{3\frac{1}{2}}$
15	1585. 965	63053. 1	$a\ ^2G_{3\frac{1}{2}}—w\ ^2G^{\circ}_{4\frac{1}{2}}$	10	1628. 541	61404. 7	$a\ ^4D_{1\frac{1}{2}}—w\ ^4P^{\circ}_{0\frac{1}{2}}$
1	1586. 945	63014. 2	$a\ ^4F_{2\frac{1}{2}}—y\ ^4P^{\circ}_{1\frac{1}{2}}$	5	1628. 986	61387. 9	$a\ ^2G_{4\frac{1}{2}}—x\ ^2F^{\circ}_{3\frac{1}{2}}$
5	1587. 517	62991. 5	$a\ ^6D_{3\frac{1}{2}}—w\ ^4F^{\circ}_{3\frac{1}{2}}$	15	1629. 092	61383. 9	$a\ ^4F_{3\frac{1}{2}}—z\ ^4H^{\circ}_{4\frac{1}{2}}$
1	1587. 852	62978. 2		5	1629. 721	61360. 2	$a\ ^4F_{1\frac{1}{2}}—y\ ^4F^{\circ}_{2\frac{1}{2}}$
5	1588. 797	62940. 7	$a\ ^4F_{3\frac{1}{2}}—y\ ^4F^{\circ}_{2\frac{1}{2}}$	15	1631. 284	61301. 4	
15	1589. 645	62907. 1	$a\ ^4F_{4\frac{1}{2}}—z\ ^4H^{\circ}_{4\frac{1}{2}}$	30	1632. 321	61262. 5	$a\ ^2H_{5\frac{1}{2}}—y\ ^2I^{\circ}_{5\frac{1}{2}}$
30	1590. 774	62862. 5	$a\ ^4F_{3\frac{1}{2}}—z\ ^4I^{\circ}_{4\frac{1}{2}}$	10	1633. 802	61206. 9	$a\ ^4D_{2\frac{1}{2}}—w\ ^4P^{\circ}_{2\frac{1}{2}}$
30	1590. 882	62858. 2	$a\ ^4P_{2\frac{1}{2}}—x\ ^4P^{\circ}_{2\frac{1}{2}}$	1	1634. 306	61188. 1	
15	1591. 744	62824. 2	$a\ ^2G_{3\frac{1}{2}}—x\ ^2D^{\circ}_{2\frac{1}{2}}$	30	1635. 129	61157. 3	$a\ ^6D_{0\frac{1}{2}}—y\ ^6P^{\circ}_{1\frac{1}{2}}$
40	1593. 403	62758. 8	$a\ ^6D_{3\frac{1}{2}}—y\ ^6P^{\circ}_{2\frac{1}{2}}$	50	1635. 333	61149. 6	$a\ ^2G_{4\frac{1}{2}}—y\ ^2F^{\circ}_{3\frac{1}{2}}$
30	1594. 398	62719. 6	$a\ ^4F_{2\frac{1}{2}}—z\ ^2G^{\circ}_{3\frac{1}{2}}$	100	1635. 948	61126. 6	$a\ ^2H_{5\frac{1}{2}}—y\ ^2I^{\circ}_{6\frac{1}{2}}$
30	1594. 603	62711. 5	$a\ ^2D_{2\frac{1}{2}}—y\ ^2P^{\circ}_{1\frac{1}{2}}$	30	1637. 446	61070. 7	$a\ ^2G_{3\frac{1}{2}}—x\ ^2H^{\circ}_{4\frac{1}{2}}$
10	1596. 482	62637. 7	$a\ ^4P_{1\frac{1}{2}}—x\ ^4P^{\circ}_{2\frac{1}{2}}$	40	1637. 591	61065. 3	$a\ ^2G_{4\frac{1}{2}}—y\ ^2H^{\circ}_{4\frac{1}{2}}$
1	1597. 172	62610. 7		20	1638. 366	61036. 4	
0	1597. 890	62582. 5		15	1639. 209	61005. 0	$a\ ^4D_{0\frac{1}{2}}—w\ ^4P^{\circ}_{0\frac{1}{2}}$
20	1598. 491	62559. 0	$a\ ^4P_{1\frac{1}{2}}—z\ ^2S^{\circ}_{0\frac{1}{2}}$	20	1639. 371	60999. 0	$a\ ^2H_{5\frac{1}{2}}—w\ ^2H^{\circ}_{5\frac{1}{2}}$
15	1599. 309	62527. 0	$a\ ^4F_{4\frac{1}{2}}—z\ ^4H^{\circ}_{5\frac{1}{2}}$	15	1639. 530	60993. 1	$a\ ^4D_{1\frac{1}{2}}—w\ ^4P^{\circ}_{1\frac{1}{2}}$
10	1599. 937	62502. 5	$a\ ^4F_{3\frac{1}{2}}—z\ ^4G^{\circ}_{2\frac{1}{2}}$; $a\ ^2G_{4\frac{1}{2}}—x\ ^2H^{\circ}_{4\frac{1}{2}}$	5	1639. 963	60977. 0	
30	1600. 183	62492. 9	$a\ ^4P_{0\frac{1}{2}}—x\ ^4P^{\circ}_{1\frac{1}{2}}$; $a\ ^2P_{0\frac{1}{2}}—y\ ^2P^{\circ}_{1\frac{1}{2}}$	2	1640. 756	60947. 5	
100	1602. 095	62418. 3	$a\ ^4F_{3\frac{1}{2}}—z\ ^4G^{\circ}_{3\frac{1}{2}}$	100	1641. 460	60921. 4	$a\ ^4F_{1\frac{1}{2}}—z\ ^4G^{\circ}_{2\frac{1}{2}}$
1	1602. 447	62404. 6	$a\ ^4F_{1\frac{1}{2}}—y\ ^4P^{\circ}_{1\frac{1}{2}}$	10	1643. 312	60852. 7	$a\ ^2H_{4\frac{1}{2}}—w\ ^2F^{\circ}_{3\frac{1}{2}}$
15	1602. 653	62396. 5	$a\ ^2D_{2\frac{1}{2}}—w\ ^2F^{\circ}_{3\frac{1}{2}}$	2	1643. 434	60848. 2	$a\ ^2G_{3\frac{1}{2}}—w\ ^4F^{\circ}_{3\frac{1}{2}}$
10	1603. 572	62360. 8	$a\ ^6D_{2\frac{1}{2}}—y\ ^6P^{\circ}_{3\frac{1}{2}}$	15	1644. 914	60793. 5	$a\ ^2P_{1\frac{1}{2}}—w\ ^4D^{\circ}_{0\frac{1}{2}}$
3	1603. 819	62351. 2	$a\ ^2G_{4\frac{1}{2}}—y\ ^6P^{\circ}_{3\frac{1}{2}}$	10	1645. 706	60764. 2	
30	1604. 029	62343. 0	$a\ ^4D_{3\frac{1}{2}}—w\ ^4P^{\circ}_{2\frac{1}{2}}$	20	1647. 615	60693. 8	$a\ ^4F_{1\frac{1}{2}}—y\ ^4P^{\circ}_{2\frac{1}{2}}$
100	1604. 405	62328. 4	$a\ ^4F_{3\frac{1}{2}}—z\ ^4G^{\circ}_{4\frac{1}{2}}$	5	1647. 913	60682. 8	$a\ ^2H_{5\frac{1}{2}}—w\ ^2G^{\circ}_{4\frac{1}{2}}$
1	1604. 767	62314. 3	$a\ ^4P_{2\frac{1}{2}}—y\ ^2D^{\circ}_{2\frac{1}{2}}$	15	1648. 069	60677. 1	$a\ ^2G_{3\frac{1}{2}}—w\ ^4F^{\circ}_{2\frac{1}{2}}$
20	1605. 111	62301. 0	$a\ ^4P_{1\frac{1}{2}}—y\ ^2D^{\circ}_{1\frac{1}{2}}$; $a\ ^2G_{3\frac{1}{2}}—w\ ^4D^{\circ}_{3\frac{1}{2}}$	3	1650. 327	60594. 1	$a\ ^4D_{0\frac{1}{2}}—w\ ^4P^{\circ}_{1\frac{1}{2}}$
15	1605. 616	62281. 4	$a\ ^2G_{4\frac{1}{2}}—w\ ^4F^{\circ}_{3\frac{1}{2}}$	1	1650. 659	60581. 9	
30	1605. 787	62274. 8	$a\ ^4F_{3\frac{1}{2}}—y\ ^4P^{\circ}_{2\frac{1}{2}}$	30	1651. 898	60536. 4	$a\ ^2D_{2\frac{1}{2}}—x\ ^2D^{\circ}_{2\frac{1}{2}}$
5	1608. 733	62160. 7	$a\ ^2P_{1\frac{1}{2}}—x\ ^2D^{\circ}_{2\frac{1}{2}}$	1	1652. 363	60519. 4	
10	1610. 372	62097. 5	$a\ ^2D_{1\frac{1}{2}}—v\ ^2F^{\circ}_{2\frac{1}{2}}$	2	1653. 564	60475. 4	$a\ ^4D_{1\frac{1}{2}}—w\ ^4P^{\circ}_{2\frac{1}{2}}$
10	1610. 464	62093. 9	$a\ ^4P_{1\frac{1}{2}}—y\ ^2D^{\circ}_{2\frac{1}{2}}$	3	1654. 477	60442. 1	
50	1611. 415	62057. 3	$a\ ^6D_{2\frac{1}{2}}—y\ ^6P^{\circ}_{2\frac{1}{2}}$?	1	1656. 747	60359. 2	$a\ ^2P_{1\frac{1}{2}}—w\ ^4D^{\circ}_{2\frac{1}{2}}$
1	1613. 158	61990. 2	$b\ ^4D_{3\frac{1}{2}}—v\ ^4D^{\circ}_{3\frac{1}{2}}$	30	1657. 217	60342. 1	$a\ ^2G_{4\frac{1}{2}}—y\ ^2H^{\circ}_{5\frac{1}{2}}$
3	1613. 685	61969. 9	$a\ ^4F_{2\frac{1}{2}}—y\ ^4F^{\circ}_{2\frac{1}{2}}$	1	1657. 617	60327. 6	$a\ ^2P_{1\frac{1}{2}}—w\ ^4D^{\circ}_{2\frac{1}{2}}$
20	1615. 064	61917. 1		10	1658. 457	60297. 0	$a\ ^4P_{1\frac{1}{2}}—y\ ^4D^{\circ}_{2\frac{1}{2}}$
20	1615. 267	61909. 3	$a\ ^6D_{2\frac{1}{2}}—y\ ^6P^{\circ}_{1\frac{1}{2}}$	100	1659. 364	60264. 1	$a\ ^2H_{4\frac{1}{2}}—w\ ^2H^{\circ}_{4\frac{1}{2}}$
1	1615. 656	61894. 4	$a\ ^4P_{2\frac{1}{2}}—1^{\circ}_{1\frac{1}{2}}$	0	1659. 871	60245. 6	$a\ ^4P_{0\frac{1}{2}}—x\ ^4F^{\circ}_{1\frac{1}{2}}$
15	1617. 663	61817. 6	$a\ ^4F_{1\frac{1}{2}}—y\ ^4F^{\circ}_{1\frac{1}{2}}$	2	1660. 059	60238. 8	$a\ ^2P_{1\frac{1}{2}}—x\ ^4P^{\circ}_{0\frac{1}{2}}$
1	1618. 781	61774. 9		0	1662. 684	60143. 7	
1	1618. 986	61767. 1		10*eh*	1666. 312	60012. 8	$a\ ^2P_{1\frac{1}{2}}—w\ ^4F^{\circ}_{2\frac{1}{2}}$; $a\ ^2D_{2\frac{1}{2}}—w\ ^4D^{\circ}_{3\frac{1}{2}}$
20	1619. 365	61752. 6	$a\ ^2G_{3\frac{1}{2}}—x\ ^2G^{\circ}_{4\frac{1}{2}}$	2	1667. 426	59972. 7	$a\ ^4P_{2\frac{1}{2}}—x\ ^4D^{\circ}_{3\frac{1}{2}}$
20	1620. 102	61724. 5	$a\ ^4D_{2\frac{1}{2}}—w\ ^4P^{\circ}_{1\frac{1}{2}}$	3	1667. 912	59955. 2	$a\ ^2G_{3\frac{1}{2}}—x\ ^2F^{\circ}_{3\frac{1}{2}}$
30	1620. 865	61695. 5		3	1670. 788	59852. 0	
5	1621. 445	61673. 4	$a\ ^4P_{1\frac{1}{2}}—1^{\circ}_{1\frac{1}{2}}$	5	1671. 412	59829. 7	$a\ ^2P_{1\frac{1}{2}}—2^{\circ}_{1\frac{1}{2}}$

TABLE 6. *The second spectrum of ruthenium* (Ru II)—Continued

1 Intensity	2 λ (vacuum)	3 σ	4 Term combination	1 Intensity	2 λ (vacuum)	3 σ	4 Term combination
	A	*K*			*A*	*K*	
0	1671. 819	59815. 1	----------	0	1748. 441	57193. 8	$a\ ^2P_{1½}—1i^0_{1½}$
30	1672. 225	59800. 6	$a\ ^2H_{4½}—y\ ^2I^0_{5½}$	3	1750. 239	57135. 1	$a\ ^2H_{5½}—z\ ^2K^0_{6½}$
5	1672. 445	59792. 7	$a\ ^2P_{0½}—x\ ^2D^0_{1½}$	2	1750. 979	57110. 9	$a\ ^2G_{3½}—x\ ^4F^0_{3½}$
3	1676. 922	59633. 1	$a\ ^2G_{3½}—y\ ^2H^0_{4½}$	1	1752. 835	57050. 4	----------
2	1678. 781	59567. 0	$a\ ^2P_{1½}—w\ ^4F^0_{1½}$?	1	1753. 173	57039. 4	$a\ ^2G_{4½}—x\ ^4F^0_{4½}$
30	1679. 620	59537. 3	$a\ ^2H_{4½}—w\ ^2H^0_{5½}$	30	1753. 441	57030. 7	$a\ ^4P_{1½}—y\ ^4P^0_{1½}$
1	1683. 810	59389. 1	$a\ ^4P_{2½}—y\ ^4G^0_{3½}$	5	1754. 756	56988. 0	$a\ ^4P_{2½}—z\ ^2D^0_{2½}$
50	1683. 985	59383. 0	$a\ ^2H_{5½}—x\ ^2G^0_{4½}$	5	1755. 728	56956. 4	$a\ ^4P_{2½}—z\ ^2G^0_{3½}$
1	1684. 311	59371. 5	----------	10	1757. 854	56887. 5	$a\ ^2G_{3½}—y\ ^2G^0_{4½}$
15c	1686. 161	59306. 3	$a\ ^2G_{3½}—y\ ^2F^0_{2½}$	3	1759. 769	56825. 6	$a\ ^2F_{3½}—v\ ^2F^0_{2½}$
100	1686. 691	59287. 7	$a\ ^2H_{5½}—x\ ^2H^0_{5½}$	20	1761. 030	56784. 9	$a\ ^2G_{4½}—y\ ^4G^0_{3½}$
10	1688. 357	59229. 2	$a\ ^2D_{2½}—x\ ^2G^0_{3½}$	15	1761. 580	56767. 2	$a\ ^4P_{1½}—z\ ^2D^0_{2½}$
1	1692. 828	59072. 7	$a\ ^4P_{0½}—z\ ^2P^0_{1½}$	1	1763. 996	56689. 5	$a\ ^2P_{1½}—x\ ^4F^0_{2½}$
2	1694. 677	59008. 3	----------	0	1764. 829	56662. 7	$a\ ^2P_{1½}—x\ ^4F^0_{1½}$
20	1697. 943	58894. 8	----------	20	1765. 525	56640. 4	$a\ ^2G_{4½}—z\ ^2H^0_{5½}$
0	1699. 330	58846. 7	$a\ ^4P_{2½}—x\ ^4D^0_{1½}$ $a\ ^6D_{1½}—1i^0_{1½}$	20	1768. 666	56539. 8	$a\ ^2H_{5½}—y\ ^2H^0_{5½}$
20	1699. 442	58842. 8	$a\ ^4P_{2½}—z\ ^2F^0_{2½}$?	5	1770. 160	56492. 1	$a\ ^4P_{2½}—y\ ^4F^0_{3½}$
3	1700. 049	58821. 8	$a\ ^2G_{3½}—x\ ^4P^0_{2½}$	15	1770. 446	56482. 9	$a\ ^2P_{1½}—z\ ^2P^0_{0½}$
1	1700. 839	58794. 5	$a\ ^2G_{4½}—y\ ^4H^0_{3½}$	50	1776. 061	56304. 4	$a\ ^2G_{4½}—y\ ^4G^0_{4½}$
30	1701. 080	58786. 2	$a\ ^2G_{4½}—y\ ^4H^0_{5½}$	5	1777. 432	56260. 9	$a\ ^2F_{2½}—w\ ^2D^0_{2½}$
3	1702. 061	58752. 3	$a\ ^2G_{4½}—y\ ^4H^0_{4½}$	10	1778. 206	56236. 4	$a\ ^2P_{0½}—z\ ^2S^0_{0½}$
1	1702. 572	58734. 7	$a\ ^2D_{2½}—w\ ^4D^0_{1½}$	5	1779. 124	56207. 4	$a\ ^4P_{2½}—y\ ^4F^0_{3½}$
50	1703. 562	58700. 5	$a\ ^2H_{5½}—x\ ^2H^0_{4½}$	0	1779. 420	56198. 1	$a\ ^2D_{2½}—y\ ^2D^0_{1½}$
10	1703. 818	58691. 7	$a\ ^2G_{4½}—x\ ^4G^0_{3½}$	0	1780. 057	56178. 0	$a\ ^2D_{1½}—x\ ^4P^0_{0½}$
5	1705. 263	58642. 0	$a\ ^2P_{1½}—y\ ^2F^0_{2½}$	0	1781. 407	56135. 4	$a\ ^4P_{0½}—y\ ^4P^0_{1½}$
2	1705. 572	58631. 4	$a\ ^2D_{2½}—y\ ^6P^0_{3½}$?	5	1781. 792	56123. 3	$a\ ^2H_{4½}—x\ ^2F^0_{3½}$
1	1705. 735	58625. 8	$a\ ^4P_{1½}—x\ ^4D^0_{1½}$	0	1784. 767	56029. 7	----------
1	1705. 840	58622. 1	$a\ ^4P_{1½}—z\ ^2F^0_{2½}$	20	1786. 032	55990. 0	$a\ ^2D_{2½}—y\ ^2D^0_{2½}$
10	1707. 608	58561. 4	$a\ ^2D_{2½}—w\ ^4F^0_{3½}$	1	1786. 155	55986. 2	$a\ ^4P_{1½}—y\ ^4F^0_{2½}$
15	1708. 620	58526. 8	$a\ ^4P_{0½}—y\ ^4D^0_{1½}$	2	1786. 347	55980. 2	$a\ ^2P_{0½}—y\ ^2D^0_{1½}$
20	1710. 299	58469. 3	$a\ ^2H_{4½}—w\ ^4D^0_{3½}$	10	1787. 233	55952. 4	$a\ ^2D_{1½}—w\ ^4F^0_{2½}$
20	1712. 456	58395. 7	$a\ ^2P_{0½}—x\ ^4P^0_{0½}$	1	1787. 770	55935. 6	$a\ ^2G_{3½}—x\ ^4D^0_{3½}$
3	1714. 667	58320. 4	$a\ ^2G_{4½}—y\ ^2G^0_{4½}$	1	1789. 383	55885. 2	$a\ ^2H_{4½}—y\ ^2F^0_{3½}$
3	1717. 160	58235. 7	----------	20	1791. 253	55826. 8	$a\ ^2G_{3½}—z\ ^2H^0_{4½}$
20	1718. 975	58174. 2	$a\ ^4P_{1½}—x\ ^4D^0_{2½}$	20	1791. 560	55817. 3	$a\ ^2P_{1½}—y\ ^4D^0_{2½}$
10	1721. 171	58100. 0	$a\ ^2D_{1½}—x\ ^2D^0_{2½}$	2	1792. 072	55801. 3	$a\ ^2H_{4½}—y\ ^2H^0_{4½}$
15	1721. 712	58081. 7	$a\ ^4P_{2½}—y\ ^4D^0_{2½}$	1	1797. 118	55644. 6	$a\ ^6S_{2½}—x\ ^6P^0_{1½}$?
15	1721. 778	58079. 5	$a\ ^2P_{1½}—z\ ^2S^0_{0½}$	10	1799. 549	55569. 5	$a\ ^2D_{2½}—1i^0_{1½}$
0	1725. 761	57945. 5	$a\ ^2F_{2½}—3i^0_{3½}$	15	1800. 470	55541. 1	$a\ ^4P_{2½}—y\ ^6P^0_{2½}$
5	1729. 417	57823. 0	$a\ ^2P_{1½}—y\ ^2D^0_{1½}$	15	1806. 599	55352. 6	$a\ ^2G_{3½}—y\ ^4G^0_{3½}$
1	1731. 110	57766. 4	----------	5	1807. 658	55320. 2	$a\ ^4P_{1½}—y\ ^4P^0_{2½}$
50	1731. 415	57756. 2	$a\ ^4P_{2½}—z\ ^2F^0_{3½}$	5	1813. 558	55140. 2	$a\ ^2P_{1½}—x\ ^4D^0_{0½}$
10	1732. 209	57729. 8	$a\ ^4P_{0½}—x\ ^4D^0_{1½}$	1	1815. 607	55078. 0	$a\ ^2H_{4½}—y\ ^2H^0_{5½}$
20	1733. 537	57685. 5	$a\ ^2H_{4½}—x\ ^2G^0_{3½}$	5	1816. 030	55065. 2	$a\ ^2D_{2½}—x\ ^4F^0_{3½}$
5	1734. 069	57667. 8	$a\ ^2D_{2½}—x\ ^2F^0_{3½}$	3	1818. 527	54989. 6	$a\ ^2P_{1½}—y\ ^4G^0_{2½}$
15	1735. 654	57615. 2	$a\ ^2P_{1½}—y\ ^2D^0_{2½}$				
10	1737. 389	57557. 6	$a\ ^2F_{2½}—v\ ^2F^0_{2½}$	20	1818. 724	54983. 6	$a\ ^2H_{5½}—y\ ^4H^0_{5½}$
15	1738. 666	57515. 4	$a\ ^2F_{3½}—v\ ^2F^0_{3½}$	30	1819. 125	54971. 5	$a\ ^6S_{2½}—x\ ^6P^0_{2½}$
15	1740. 114	57467. 5	$a\ ^2G_{4½}—x\ ^4G^0_{3½}$	3	1819. 852	54949. 5	$a\ ^2H_{5½}—y\ ^4H^0_{4½}$
20	1741. 262	57429. 6	$a\ ^2D_{2½}—y\ ^2F^0_{3½}$	5	1820. 059	54943. 3	$a\ ^2P_{1½}—y\ ^4D^0_{1½}$
				2	1820. 999	54914. 9	$a\ ^2G_{4½}—z\ ^2G^0_{4½}$
1	1743. 514	57355. 4	----------				
5	1744. 614	57319. 3	$a\ ^2G_{3½}—y\ ^4H^0_{4½}$	1	1822. 238	54877. 6	----------
30	1746. 446	57259. 1	$a\ ^2G_{4½}—z\ ^2H^0_{4½}$ $a\ ^2G_{3½}—x\ ^4G^0_{3½}$	1	1822. 427	54871. 9	$a\ ^2G_{3½}—y\ ^4G^0_{4½}$
3	1747. 804	57214. 7	$a\ ^2F_{3½}—3i^0_{3½}$	10	1824. 619	54806. 0	$a\ ^2G_{3½}—z\ ^2F^0_{3½}$
1	1748. 310	57198. 1	----------	0	1828. 521	54689. 0	$a\ ^2F_{3½}—w\ ^2F^0_{3½}$?
				5	1829. 894	54648. 0	$a\ ^2H_{5½}—y\ ^4H^0_{5½}$

TABLE 6. *The second spectrum of ruthenium* (Ru II)—Continued

1 Intensity	2 λ (vacuum)	3 σ	4 Term combination	1 Intensity	2 λ (vacuum)	3 σ	4 Term combination
	A	*K*			*A*	*K*	
0	1830. 163	54639. 9	$a\ ^2P_{0\frac{1}{2}}$—$z\ ^2P^\circ_{0\frac{1}{2}}$	3	1904. 679	52502. 3	$a\ ^2H_{5\frac{1}{2}}$—$y\ ^4G^\circ_{4\frac{1}{2}}$
3	1830. 296	54636. 0		5	1906. 378	52455. 5	$a\ ^2G_{3\frac{1}{2}}$—$y\ ^4F^\circ_{3\frac{1}{2}}$
0	1831. 130	54611. 1	$a\ ^2G_{4\frac{1}{2}}$—$z\ ^4I^\circ_{5\frac{1}{2}}$				$a\ ^4D_{2\frac{1}{2}}$—$w\ ^4F^\circ_{3\frac{1}{2}}$
20	1832. 144	54580. 9	$a\ ^2D_{1\frac{1}{2}}$—$y\ ^2F^\circ_{2\frac{1}{2}}$	0	1907. 601	52421. 9	$a\ ^2D_{1\frac{1}{2}}$—$z\ ^2P^\circ_{0\frac{1}{2}}$
3	1834. 262	54517. 8	$a\ ^2H_{5\frac{1}{2}}$—$y\ ^2G^\circ_{4\frac{1}{2}}$	1	1910. 093	52353. 5	
				10	1911. 888	52304. 3	$a\ ^2P_{0\frac{1}{2}}$—$x\ ^4D^\circ_{1\frac{1}{2}}$
50	1836. 013	54465. 8	$a\ ^2G_{4\frac{1}{2}}$—$y\ ^4F^\circ_{4\frac{1}{2}}$				
15	1841. 375	54307. 2	$a\ ^6S_{2\frac{1}{2}}$—$x\ ^6P^\circ_{3\frac{1}{2}}$	50	1912. 036	52300. 3	$a\ ^4F_{2\frac{1}{2}}$—$z\ ^4F^\circ_{2\frac{1}{2}}$
5	1842. 642	54269. 9	$a\ ^4P_{2\frac{1}{2}}$—$z\ ^4H^\circ_{3\frac{1}{2}}$	30	1912. 484	52288. 0	$a\ ^2P_{1\frac{1}{2}}$—$z\ ^2D^\circ_{2\frac{1}{2}}$
200	1844. 138	54225. 9	$a\ ^4F_{4\frac{1}{2}}$—$z\ ^4F^\circ_{3\frac{1}{2}}$	20	1913. 797	52252. 1	$a\ ^2F_{2\frac{1}{2}}$—$x\ ^2G^\circ_{3\frac{1}{2}}$
2	1844. 886	54203. 9	$a\ ^6D_{1\frac{1}{2}}$—$y\ ^4P^\circ_{1\frac{1}{2}}$	1	1914. 999	52219. 3	$a\ ^4D_{3\frac{1}{2}}$—$y\ ^2F^\circ_{2\frac{1}{2}}$
				1	1915. 597	52203. 0	$a\ ^2H_{4\frac{1}{2}}$—$x\ ^4G^\circ_{5\frac{1}{2}}$
100	1845. 368	54189. 7	$a\ ^4P_{2\frac{1}{2}}$—$z\ ^4S^\circ_{1\frac{1}{2}}$	200	1916. 829	52169. 5	$a\ ^4F_{2\frac{1}{2}}$—$z\ ^4D^\circ_{1\frac{1}{2}}$
30	1845. 974	54171. 9	$a\ ^4F_{2\frac{1}{2}}$—$z\ ^4P^\circ_{1\frac{1}{2}}$	50	1918. 650	52120. 0	$a\ ^4F_{1\frac{1}{2}}$—$z\ ^4F^\circ_{1\frac{1}{2}}$
			$a\ ^4F_{3\frac{1}{2}}$—$z\ ^4P^\circ_{2\frac{1}{2}}$	2	1919. 292	52102. 5	$d\ ^2D_{2\frac{1}{2}}$—$w\ ^4G^\circ_{3\frac{1}{2}}$
1	1846. 147	54166. 9		3	1919. 431	52098. 8	
1	1846. 983	54142. 3	$a\ ^2P_{1\frac{1}{2}}$—$z\ ^2F^\circ_{2\frac{1}{2}}$	3	1919. 679	52092. 0	$a\ ^2G_{3\frac{1}{2}}$—$z\ ^4I^\circ_{4\frac{1}{2}}$
15	1848. 515	54097. 5	$a\ ^2D_{1\frac{1}{2}}$—$x\ ^4P^\circ_{2\frac{1}{2}}$				
				5	1921. 377	52046. 0	$a\ ^2G_{4\frac{1}{2}}$—$z\ ^4H^\circ_{4\frac{1}{2}}$
5	1851. 213	54018. 6	$a\ ^2D_{1\frac{1}{2}}$—$z\ ^2S^\circ_{0\frac{1}{2}}$	0	1921. 695	52037. 4	$a\ ^2D_{1\frac{1}{2}}$—$x\ ^4G^\circ_{3\frac{1}{2}}$
3	1853. 683	53946. 7					$a\ ^4D_{1\frac{1}{2}}$—$w\ ^4D^\circ_{2\frac{1}{2}}$
0	1856. 193	53873. 7	$a\ ^2F_{2\frac{1}{2}}$—$w\ ^2G^\circ_{3\frac{1}{2}}$	2	1923. 250	51995. 3	$a\ ^2H_{4\frac{1}{2}}$—$z\ ^2H^\circ_{5\frac{1}{2}}$
5	1856. 503	53864. 7	$a\ ^2D_{2\frac{1}{2}}$—$z\ ^2P^\circ_{1\frac{1}{2}}$	0	1925. 000	51948. 1	$a\ ^4D_{1\frac{1}{2}}$—$x\ ^4P^\circ_{0\frac{1}{2}}$
10	1860. 065	53761. 6	$a\ ^2D_{1\frac{1}{2}}$—$y\ ^2D^\circ_{1\frac{1}{2}}$	0	1926. 867	51897. 7	
10	1861. 527	53719. 3	$a\ ^2G_{3\frac{1}{2}}$—$z\ ^2F^\circ_{3\frac{1}{2}}$	100	1927. 623	51877. 4	$a\ ^4F_{1\frac{1}{2}}$—$z\ ^4D^\circ_{0\frac{1}{2}}$
0	1862. 386	53694. 6	$a\ ^2P_{1\frac{1}{2}}$—$x\ ^4D^\circ_{2\frac{1}{2}}$	100	1930. 717	51794. 2	$a\ ^4F_{3\frac{1}{2}}$—$z\ ^4D^\circ_{3\frac{1}{2}}$
0	1863. 023	53676. 2	$a\ ^2P_{1\frac{1}{2}}$—$y\ ^4D^\circ_{0\frac{1}{2}}$	15	1931. 763	51766. 2	
500	1863. 404	53665. 2	$a\ ^2H_{5\frac{1}{2}}$—$x\ ^4G^\circ_{5\frac{1}{2}}$				$a\ ^2D_{2\frac{1}{2}}$—$y\ ^4D^\circ_{3\frac{1}{2}}$
5*h*	1864. 030	53647. 2	$a\ ^2P_{0\frac{1}{2}}$—$z\ ^2P^\circ_{1\frac{1}{2}}$	50	1932. 118	51756. 7	$a\ ^2D_{1\frac{1}{2}}$—$y\ ^4D^\circ_{2\frac{1}{2}}$
							$a\ ^2F_{3\frac{1}{2}}$—$x\ ^2G^\circ_{4\frac{1}{2}}$
0	1868. 088	53530. 7	$a\ ^2H_{4\frac{1}{2}}$—$y\ ^4H^\circ_{5\frac{1}{2}}$	1	1932. 892	51736. 0	$a\ ^4D_{3\frac{1}{2}}$—$x\ ^4P^\circ_{2\frac{1}{2}}$
10	1868. 308	53524. 4	$a\ ^2G_{4\frac{1}{2}}$—$z\ ^4I^\circ_{4\frac{1}{2}}$				
2	1869. 588	53487. 7	$a\ ^2H_{4\frac{1}{2}}$—$y\ ^4H^\circ_{4\frac{1}{2}}$	15	1933. 055	51731. 6	$a\ ^4F_{2\frac{1}{2}}$—$z\ ^4F^\circ_{3\frac{1}{2}}$
2	1869. 763	53482. 7	$a\ ^2G_{3\frac{1}{2}}$—$z\ ^2G^\circ_{4\frac{1}{2}}$	20	1934. 615	51689. 9	$a\ ^4F_{1\frac{1}{2}}$—$z\ ^4F^\circ_{2\frac{1}{2}}$
5	1870. 657	53457. 2	$a\ ^2H_{5\frac{1}{2}}$—$z\ ^2H^\circ_{4\frac{1}{2}}$	2	1935. 210	51674. 0	$a\ ^6D_{2\frac{1}{2}}$—$z\ ^4H^\circ_{3\frac{1}{2}}$
				100	1937. 089	51623. 9	
5	1871. 692	53427. 6	$a\ ^2H_{4\frac{1}{2}}$—$x\ ^4G^\circ_{3\frac{1}{2}}$	50	1937. 715	51607. 2	
0	1873. 874	53365. 4	$a\ ^2D_{2\frac{1}{2}}$—$y\ ^4G^\circ_{2\frac{1}{2}}$				
500	1875. 564	53317. 3	$a\ ^4F_{4\frac{1}{2}}$—$z\ ^4D^\circ_{3\frac{1}{2}}$	20	1938. 193	51594. 4	$a\ ^6D_{2\frac{1}{2}}$—$z\ ^6S^\circ_{1\frac{1}{2}}$
100	1877. 186	53271. 2	$a\ ^4F_{3\frac{1}{2}}$—$z\ ^4F^\circ_{2\frac{1}{2}}$	200	1939. 056	51571. 5	$a\ ^4F_{2\frac{1}{2}}$—$z\ ^4D^\circ_{2\frac{1}{2}}$
5	1878. 364	53237. 8	$a\ ^2H_{5\frac{1}{2}}$—$x\ ^4F^\circ_{4\frac{1}{2}}$	200	1939. 521	51559. 1	$a\ ^4F_{1\frac{1}{2}}$—$z\ ^4D^\circ_{1\frac{1}{2}}$
				5	1939. 911	51548. 8	$a\ ^4F_{4\frac{1}{2}}$—$z\ ^6P^\circ_{3\frac{1}{2}}$
5	1883. 220	53100. 5	$a\ ^2P_{0\frac{1}{2}}$—$y\ ^4D^\circ_{1\frac{1}{2}}$	30	1940. 422	51535. 2	$a\ ^2H_{5\frac{1}{2}}$—$z\ ^4I^\circ_{5\frac{1}{2}}$
10?	1884. 154	53074. 2	$a\ ^4P_{0\frac{1}{2}}$—$z\ ^6S^\circ_{1\frac{1}{2}}$?				
15	1884. 484	53064. 9	$a\ ^2D_{2\frac{1}{2}}$—$y\ ^4G^\circ_{3\frac{1}{2}}$	5	1940. 964	51520. 8	$a\ ^2H_{4\frac{1}{2}}$—$y\ ^4G^\circ_{3\frac{1}{2}}$
15	1884. 801	53056. 0	$a\ ^2H_{4\frac{1}{2}}$—$y\ ^2G^\circ_{4\frac{1}{2}}$				$a\ ^2F_{3\frac{1}{2}}$—$x\ ^2G^\circ_{3\frac{1}{2}}$
			$a\ ^2G_{3\frac{1}{2}}$—$y\ ^4F^\circ_{4\frac{1}{2}}$	10	1942. 628	51476. 7	$a\ ^2H_{4\frac{1}{2}}$—$y\ ^4G^\circ_{3\frac{1}{2}}$
50*h*	1885. 559	53034. 7	$a\ ^2F_{2\frac{1}{2}}$—$x\ ^2D^\circ_{1\frac{1}{2}}$	20	1943. 966	51441. 2	$a\ ^4F_{3\frac{1}{2}}$—$z\ ^4F^\circ_{4\frac{1}{2}}$
				10	1946. 421	51376. 3	$a\ ^2H_{4\frac{1}{2}}$—$z\ ^2H^\circ_{5\frac{1}{2}}$?
15	1887. 134	52990. 4	$a\ ^2G_{4\frac{1}{2}}$—$z\ ^4G^\circ_{4\frac{1}{2}}$	3	1947. 393	51350. 7	$a\ ^4D_{2\frac{1}{2}}$—$x\ ^4P^\circ_{1\frac{1}{2}}$
500	1888. 045	52964. 8	$a\ ^4F_{4\frac{1}{2}}$—$z\ ^4F^\circ_{4\frac{1}{2}}$	10	1947. 638	51344. 2	
15	1889. 655	52919. 7	$a\ ^2G_{3\frac{1}{2}}$—$z\ ^2G^\circ_{3\frac{1}{2}}$	30	1949. 196	51303. 2	
1	1890. 774	52888. 4		15	1949. 423	51297. 2	$a\ ^4F_{3\frac{1}{2}}$—$z\ ^6P^\circ_{2\frac{1}{2}}$
2	1891. 702	52862. 4		3	1953. 081	51201. 2	
				0	1953. 468	51191. 0	$a\ ^4F_{2\frac{1}{2}}$—$z\ ^6P^\circ_{1\frac{1}{2}}$
5	1892. 570	52838. 2	$a\ ^2H_{5\frac{1}{2}}$—$z\ ^2H^\circ_{5\frac{1}{2}}$	15	1954. 559	51162. 4	
20	1892. 926	52828. 3	$a\ ^2F_{3\frac{1}{2}}$—$x\ ^2D^\circ_{2\frac{1}{2}}$	5	1956. 462	51112. 7	$a\ ^2H_{5\frac{1}{2}}$—$z\ ^2G^\circ_{4\frac{1}{2}}$
100	1896. 441	52730. 4	$a\ ^4F_{2\frac{1}{2}}$—$z\ ^4F^\circ_{1\frac{1}{2}}$	1	1957. 748	51079. 1	$a\ ^2D_{1\frac{1}{2}}$—$x\ ^4D^\circ_{0\frac{1}{2}}$
1	1897. 132	52711. 1		5	1957. 931	51074. 3	$a\ ^2F_{3\frac{1}{2}}$—$x\ ^2H^\circ_{4\frac{1}{2}}$
100	1897. 437	52702. 7	$a\ ^4F_{3\frac{1}{2}}$—$z\ ^4F^\circ_{3\frac{1}{2}}$	1	1962. 144	50964. 7	$a\ ^2F_{2\frac{1}{2}}$—$w\ ^4F^\circ_{1\frac{1}{2}}$
3	1901. 073	52601. 9	$a\ ^2D_{1\frac{1}{2}}$—$x\ ^4F^\circ_{1\frac{1}{2}}$	20	1962. 285	50961. 0	$a\ ^4F_{1\frac{1}{2}}$—$z\ ^4D^\circ_{2\frac{1}{2}}$
1	1902. 897	52551. 5	$a\ ^2P_{1\frac{1}{2}}$—$y\ ^4P^\circ_{1\frac{1}{2}}$	20	1962. 503	50955. 3	
500	1903. 227	52542. 3	$a\ ^4F_{3\frac{1}{2}}$—$z\ ^4D^\circ_{2\frac{1}{2}}$	200	1965. 293	50883. 0	$a\ ^2H_{5\frac{1}{2}}$—$z\ ^2I^\circ_{6\frac{1}{2}}$
2	1903. 966	52521. 9	$a\ ^2D_{2\frac{1}{2}}$—$x\ ^4D^\circ_{1\frac{1}{2}}$	200	1966. 076	50862. 7	$a\ ^4F_{4\frac{1}{2}}$—$z\ ^6F^\circ_{5\frac{1}{2}}$
2	1904. 393	52510. 2		2	1966. 467	50852. 6	$a\ ^2F_{3\frac{1}{2}}$—$w\ ^4F^\circ_{3\frac{1}{2}}$

TABLE 6. *The second spectrum of ruthenium* (Ru II)—Continued

1 Intensity	2 λ (vacuum)	3 σ	4 Term combination	1 Intensity	2 λ (air)	3 σ	4 Term combination
	A	*K*			*A*	*K*	
200	1966. 746	50845. 4	$a\ {}^4F_{4\frac{1}{2}}$—$z\ {}^6F^\circ_{4\frac{1}{2}}$	5	2085. 037	47945. 5	$a\ {}^2D_{2\frac{1}{2}}$—$z\ {}^4H^\circ_{3\frac{1}{2}}$
10	1966. 926	50840. 8	$a\ {}^2P_{1\frac{1}{2}}$—$y\ {}^4P^\circ_{2\frac{1}{2}}$	3	2085. 683	47930. 7	$a\ {}^4D_{2\frac{1}{2}}$—$z\ {}^2P^\circ_{1\frac{1}{2}}$
5	1967. 515	50825. 5		20	2087. 463	47889. 8	$a\ {}^4P_{0\frac{1}{2}}$—$z\ {}^4P^\circ_{0\frac{1}{2}}$
20	1967. 610	50823. 1	$a\ {}^4F_{2\frac{1}{2}}$—$z\ {}^4D^\circ_{3\frac{1}{2}}$	1	2088. 543	47865. 1	$a\ {}^2D_{2\frac{1}{2}}$—$z\ {}^4S^\circ_{1\frac{1}{2}}$
0	1969. 862	50765. 0		1	2091. 668	47793. 5	$a\ {}^4D_{0\frac{1}{2}}$—$z\ {}^2P^\circ_{0\frac{1}{2}}$
1	1970. 115	50758. 5	$a\ {}^4F_{4\frac{1}{2}}$—$z\ {}^6F^\circ_{3\frac{1}{2}}$	15	2091. 979	47786. 4	$a\ {}^4D_{3\frac{1}{2}}$—$y\ {}^6G^\circ_{4\frac{1}{2}}$
2	1970. 381	50751. 6		10	2103. 377	47527. 5	$a\ {}^4D_{1\frac{1}{2}}$—$y\ {}^4D^\circ_{2\frac{1}{2}}$
5	1972. 061	50708. 4	$a\ {}^2P_{0\frac{1}{2}}$—$y\ {}^4P^\circ_{1\frac{1}{2}}$	2	2104. 747	47496. 6	$a\ {}^2F_{2\frac{1}{2}}$—$x\ {}^4G^\circ_{3\frac{1}{2}}$
5	1972. 770	50690. 1	$a\ {}^2P_{2\frac{1}{2}}$—$x\ {}^2F^\circ_{3\frac{1}{2}}$?	500	2107. 322	47438. 6	$a\ {}^4P_{2\frac{1}{2}}$—$z\ {}^4P^\circ_{2\frac{1}{2}}$
10	1973. 811	50663. 4	$a\ {}^2D_{2\frac{1}{2}}$—$z\ {}^2D^\circ_{2\frac{1}{2}}$ $a\ {}^2H_{3\frac{1}{2}}$—$y\ {}^4F^\circ_{4\frac{1}{2}}$	1	2110. 538	47366. 3	$a\ {}^2F_{3\frac{1}{2}}$—$y\ {}^4H^\circ_{3\frac{1}{2}}$
				10	2110. 945	47357. 2	$a\ {}^2F_{3\frac{1}{2}}$—$x\ {}^4F^\circ_{3\frac{1}{2}}$
10	1975. 048	50631. 7	$a\ {}^2D_{2\frac{1}{2}}$—$z\ {}^2G^\circ_{3\frac{1}{2}}$	200	2113. 895	47291. 1	$a\ {}^4P_{0\frac{1}{2}}$—$z\ {}^4P^\circ_{1\frac{1}{2}}$
5	1987. 023	50326. 5	$a\ {}^4F_{2\frac{1}{2}}$—$z\ {}^6P^\circ_{2\frac{1}{2}}$	100	2117. 190	47217. 5	$a\ {}^4P_{1\frac{1}{2}}$—$z\ {}^4P^\circ_{2\frac{1}{2}}$
200	1990. 720	50233. 1	$a\ {}^2G_{3\frac{1}{2}}$—$z\ {}^4H^\circ_{3\frac{1}{2}}$	1	2121. 077	47131. 0	$a\ {}^4D_{2\frac{1}{2}}$—$y\ {}^4G^\circ_{3\frac{1}{2}}$
10	1993. 078	50173. 7	$a\ {}^4D_{3\frac{1}{2}}$—$x\ {}^4G^\circ_{3\frac{1}{2}}$	2	2121. 701	47117. 1	$b\ {}^2H_{4\frac{1}{2}}$—$v\ {}^2F^\circ_{3\frac{1}{2}}$
5	1994. 127	50147. 3		3	2122. 086	47108. 5	$a\ {}^4H_{3\frac{1}{2}}$—$w\ {}^4F^\circ_{4\frac{1}{2}}$
				10	2128. 836	46959. 2	$a\ {}^4D_{3\frac{1}{2}}$—$y\ {}^4D^\circ_{3\frac{1}{2}}$
100	1995. 048	50124. 1	$a\ {}^2H_{4\frac{1}{2}}$—$z\ {}^2I^\circ_{5\frac{1}{2}}$	100	2131. 898	46891. 7	$a\ {}^2F_{3\frac{1}{2}}$—$y\ {}^2G^\circ_{4\frac{1}{2}}$
5	1996. 748	50081. 4	$a\ {}^2D_{1\frac{1}{2}}$—$z\ {}^2F^\circ_{2\frac{1}{2}}$	3	2133. 029	46866. 9	
2	1997. 770	50055. 8	$a\ {}^4D_{2\frac{1}{2}}$—$y\ {}^2D^\circ_{2\frac{1}{2}}$	30	2135. 40?	46814. 9	$a\ {}^4H_{3\frac{1}{2}}$—$w\ {}^4D^\circ_{2\frac{1}{2}}$
30	1998. 988	50025. 3	$a\ {}^4F_{3\frac{1}{2}}$—$z\ {}^6P^\circ_{3\frac{1}{2}}$				
	λ (air)			2	2137. 661	46765. 4	$a\ {}^2F_{3\frac{1}{2}}$—$x\ {}^4G^\circ_{3\frac{1}{2}}$
20	2002. 168	49929. 7		30	2140. 120	46711. 6	$a\ {}^4F_{4\frac{1}{2}}$—$z\ {}^6D^\circ_{3\frac{1}{2}}$
				1	2140. 29?	46707. 9	$a\ {}^2F_{2\frac{1}{2}}$—$y\ {}^2G^\circ_{3\frac{1}{2}}$
2	2003. 860	49887. 6	$a\ {}^2H_{4\frac{1}{2}}$—$z\ {}^2F^\circ_{3\frac{1}{2}}$	5	2143. 697	46633. 7	$a\ {}^4D_{3\frac{1}{2}}$—$z\ {}^2F^\circ_{3\frac{1}{2}}$
3	2005. 278	49852. 3		3	2145. 793	46588. 1	$a\ {}^4D_{2\frac{1}{2}}$—$x\ {}^4D^\circ_{1\frac{1}{2}}$
2	2008. 180	49780. 2					
10	2010. 542	49721. 8	$a\ {}^2H_{3\frac{1}{2}}$—$z\ {}^4I^\circ_{4\frac{1}{2}}$ $a\ {}^2F_{3\frac{1}{2}}$—$y\ {}^2F^\circ_{3\frac{1}{2}}$	2	2145. 989	46583. 9	$a\ {}^4D_{2\frac{1}{2}}$—$z\ {}^2F^\circ_{2\frac{1}{2}}$
5	2010. 774	49716. 0	$a\ {}^4F_{1\frac{1}{2}}$—$z\ {}^6P^\circ_{2\frac{1}{2}}$	10	2148. 103	46538. 1	$a\ {}^4P_{2\frac{1}{2}}$—$z\ {}^4F^\circ_{2\frac{1}{2}}$ $a\ {}^4G_{3\frac{1}{2}}$—$w\ {}^2F^\circ_{3\frac{1}{2}}$
				2	2151. 124	46472. 7	$b\ {}^4D_{3\frac{1}{2}}$—$v\ {}^2F^\circ_{3\frac{1}{2}}$
30	2013. 189	49656. 4	$a\ {}^4F_{3\frac{1}{2}}$—$z\ {}^6F^\circ_{2\frac{1}{2}}$	2	2152. 124	46451. 1	$a\ {}^4D_{0\frac{1}{2}}$—$x\ {}^4D^\circ_{0\frac{1}{2}}$
10	2013. 979	49636. 6	$a\ {}^2F_{3\frac{1}{2}}$—$y\ {}^2H^\circ_{4\frac{1}{2}}$	30	2154. 427	46401. 5	$a\ {}^2H_{4\frac{1}{2}}$—$z\ {}^4H^\circ_{3\frac{1}{2}}$
5	2014. 977	49612. 3					
5	2018. 433	49527. 4	$a\ {}^4D_{3\frac{1}{2}}$—$x\ {}^4G^\circ_{4\frac{1}{2}}$	5	2155. 028	46388. 5	$a\ {}^2F_{2\frac{1}{2}}$—$y\ {}^4G^\circ_{3\frac{1}{2}}$
100	2026. 838	49322. 1	$a\ {}^4F_{3\frac{1}{2}}$—$z\ {}^6F^\circ_{4\frac{1}{2}}$	1	2155. 337	46381. 9	$a\ {}^6S_{2\frac{1}{2}}$—$w\ {}^4P^\circ_{1\frac{1}{2}}$
				1	2157. 188	46342. 1	$a\ {}^2F_{2\frac{1}{2}}$—$y\ {}^4D^\circ_{1\frac{1}{2}}$
10	2030. 979	49221. 5	$a\ {}^2F_{2\frac{1}{2}}$—$y\ {}^2D^\circ_{1\frac{1}{2}}$	20	2158. 373	46316. 6	$a\ {}^4P_{1\frac{1}{2}}$—$z\ {}^4F^\circ_{2\frac{1}{2}}$
5	2031. 804	49201. 5	$a\ {}^2H_{4\frac{1}{2}}$—$y\ {}^4F^\circ_{4\frac{1}{2}}$	3	2160. 766	46265. 4	$b\ {}^4F_{4\frac{1}{2}}$—$x\ {}^2G^\circ_{3\frac{1}{2}}$
1	2032. 35	49188. 3	$a\ {}^2H_{3\frac{1}{2}}$—$z\ {}^4G^\circ_{4\frac{1}{2}}$				
1	2033. 77	49154. 0	$b\ {}^4F_{2\frac{1}{2}}$—$y\ {}^2P^\circ_{1\frac{1}{2}}$	1	2161. 270	46254. 6	$a\ {}^4D_{0\frac{1}{2}}$—$y\ {}^4D^\circ_{1\frac{1}{2}}$
10	2034. 348	49140. 0	$a\ {}^4D_{2\frac{1}{2}}$—$y\ {}^4H^\circ_{3\frac{1}{2}}$	20	2164. 480	46186. 0	$a\ {}^4P_{1\frac{1}{2}}$—$z\ {}^4D^\circ_{1\frac{1}{2}}$
				20	2166. 828	46135. 9	$a\ {}^4D_{2\frac{1}{2}}$—$x\ {}^4D^\circ_{2\frac{1}{2}}$
5	2034. 732	49130. 7	$a\ {}^4D_{2\frac{1}{2}}$—$x\ {}^4F^\circ_{2\frac{1}{2}}$?	3	2169. 076	46088. 1	$a\ {}^2F_{2\frac{1}{2}}$—$y\ {}^4G^\circ_{3\frac{1}{2}}$
1	2036. 187	49095. 6		3	2169. 401	46081. 2	
5	2036. 506	49087. 9	$a\ {}^2H_{4\frac{1}{2}}$—$z\ {}^2G^\circ_{3\frac{1}{2}}$	100	2174. 713	45968. 7	$a\ {}^4P_{2\frac{1}{2}}$—$z\ {}^4F^\circ_{3\frac{1}{2}}$
5	2037. 867	49055. 1	$a\ {}^4F_{2\frac{1}{2}}$—$z\ {}^6P^\circ_{3\frac{1}{2}}$	10	2176. 070	45940. 0	$a\ {}^2F_{3\frac{1}{2}}$—$x\ {}^4D^\circ_{3\frac{1}{2}}$
10	2039. 626	49012. 8	$a\ {}^2F_{2\frac{1}{2}}$—$y\ {}^2D^\circ_{2\frac{1}{2}}$	30	2176. 476	45931. 4	
				1	2179. 574	45866. 2	$a\ {}^4D_{3\frac{1}{2}}$—$z\ {}^2D^\circ_{2\frac{1}{2}}$
20	2043. 301	48924. 7	$a\ {}^2H_{3\frac{1}{2}}$—$z\ {}^4H^\circ_{6\frac{1}{2}}$	3	2179. 683	45863. 9	$a\ {}^6S_{2\frac{1}{2}}$—$w\ {}^4P^\circ_{2\frac{1}{2}}$
2	2044. 800	48888. 9	$a\ {}^4D_{2\frac{1}{2}}$—$x\ {}^4F^\circ_{3\frac{1}{2}}$				
30	2047. 561	48822. 7	$a\ {}^4F_{2\frac{1}{2}}$—$z\ {}^6F^\circ_{1\frac{1}{2}}$	15	2180. 063	45855. 9	$a\ {}^4D_{1\frac{1}{2}}$—$x\ {}^4D^\circ_{1\frac{1}{2}}$
200	2049. 111	48786. 0	$a\ {}^4P_{1\frac{1}{2}}$—$z\ {}^4P^\circ_{0\frac{1}{2}}$	30	2181. 254	45830. 8	$a\ {}^2F_{3\frac{1}{2}}$—$z\ {}^2H^\circ_{4\frac{1}{2}}$
5	2060. 257	48522. 1	$a\ {}^4D_{3\frac{1}{2}}$—$x\ {}^4F^\circ_{4\frac{1}{2}}$	30	2181. 622	45823. 1	$a\ {}^4D_{2\frac{1}{2}}$—$y\ {}^4D^\circ_{3\frac{1}{2}}$
				10	2182. 081	45813. 5	$a\ {}^6D_{2\frac{1}{2}}$—$z\ {}^4P^\circ_{1\frac{1}{2}}$
2	2062. 992	48457. 8		10	2184. 536	45762. 0	$a\ {}^4F_{3\frac{1}{2}}$—$z\ {}^6D^\circ_{2\frac{1}{2}}$
100	2065. 110	48408. 1	$a\ {}^4P_{2\frac{1}{2}}$—$z\ {}^4P^\circ_{1\frac{1}{2}}$	2	2186. 692	45716. 9	
5	2065. 474	48399. 6	$a\ {}^4D_{1\frac{1}{2}}$—$x\ {}^4F^\circ_{2\frac{1}{2}}$	1	2189. 554	45657. 1	
30	2070. 515	48281. 8	$a\ {}^2F_{3\frac{1}{2}}$—$y\ {}^2D^\circ_{2\frac{1}{2}}$	20	2191. 923	45607. 8	$a\ {}^4P_{0\frac{1}{2}}$—$z\ {}^4D^\circ_{0\frac{1}{2}}$
15	2070. 768	48275. 8	$a\ {}^4F_{1\frac{1}{2}}$—$z\ {}^6F^\circ_{0\frac{1}{2}}$	10	2192. 419	45597. 5	$b\ {}^4F_{4\frac{1}{2}}$—$w\ {}^4F^\circ_{3\frac{1}{2}}$
				200	2192. 889	45587. 7	$a\ {}^4P_{1\frac{1}{2}}$—$z\ {}^4D^\circ_{2\frac{1}{2}}$
3	2072. 151	48243. 6	$a\ {}^2H_{3\frac{1}{2}}$—$z\ {}^4H^\circ_{4\frac{1}{2}}$	20	2194. 970	45544. 5	$a\ {}^6D_{3\frac{1}{2}}$—$z\ {}^4P^\circ_{2\frac{1}{2}}$
200	2074. 581	48187. 3	$a\ {}^4P_{1\frac{1}{2}}$—$z\ {}^4P^\circ_{1\frac{1}{2}}$	5	2195. 130	45541. 2	$a\ {}^2F_{2\frac{1}{2}}$—$z\ {}^2F^\circ_{2\frac{1}{2}}$
100	2078. 455	48097. 3	$a\ {}^2F_{2\frac{1}{2}}$—$y\ {}^4H^\circ_{3\frac{1}{2}}$	5	2195. 185	45540. 0	
50	2079. 967	48062. 3	$a\ {}^2F_{2\frac{1}{2}}$—$x\ {}^4F^\circ_{1\frac{1}{2}}$	20	2199. 165	45457. 6	$a\ {}^4D_{0\frac{1}{2}}$—$x\ {}^4D^\circ_{1\frac{1}{2}}$
30	2082. 916	47994. 3	$a\ {}^2F_{2\frac{1}{2}}$—$x\ {}^4G^\circ_{3\frac{1}{2}}$	10	2201. 736	45404. 5	$a\ {}^4D_{1\frac{1}{2}}$—$x\ {}^4D^\circ_{2\frac{1}{2}}$

TABLE 6. *The second spectrum of ruthenium* (Ru II)—Continued

1 Intensity	2 λ (air)	3 σ	4 Term combination	1 Intensity	2 λ (vacuum)	3 σ	4 Term combination
	A	*K*			*A*	*K*	
10	2203. 837	45361. 3	$a\ ^6D_{1½}—z\ ^4P°_{1½}$	100	2276. 43	43914. 9	$a\ ^6D_{3½}—z\ ^4D°_{3½}$
20	2204. 055	45356. 8	$a\ ^2F_{3½}—y\ ^4G°_{3½}$	10	2278. 84	43868. 4	$b\ ^4P_{2½}—y\ ^2D°_{1½}$
20	2205. 108	45335. 2	$b\ ^4F_{3½}—w\ ^4D°_{2½}$	10	2281. 15	43824. 0	$b\ ^2D_{1½}—w\ ^2D°_{1½}$
100	2207. 328	45289. 5	$a\ ^4P_{0½}—z\ ^4D°_{1½}$	300	2281. 72	43813. 1	$a\ ^6D_{4½}—z\ ^4F°_{4½}$
30	2209. 067	45253. 9	$b\ ^4F_{1½}—w\ ^4D°_{0½}$	30	2283. 02	43788. 1	$b\ ^2D_{2½}—w\ ^2D°_{1½}$ $b\ ^2G_{4½}—v\ ^2F°_{3½}$
10	2209. 218	45250. 8	$a\ ^4H_{6½}—y\ ^2H°_{5½}$				
1	2210. 997	45214. 4	$a\ ^4F_{2½}—z\ ^6D°_{1½}$	4	2283. 41	43780. 6	$b\ ^2F_{3½}—w\ ^2D°_{2½}$
10	2211. 325	45207. 7	$a\ ^4P_{1½}—z\ ^6P°_{1½}$	2	2283. 71	43774. 9	
10	2212. 845	45176. 6	$b\ ^4F_{2½}—w\ ^4D°_{1½}$	2*h*	2284. 31	43763. 4	
20	2213. 161	45170. 2		7*h*	2285. 10	43748. 3	
5	2214. 392	45145. 0	$b\ ^4F_{2½}—w\ ^4D°_{2½}$	2	2286. 20	43727. 2	$b\ ^4F_{2½}—x\ ^4P°_{1½}$
5	2216. 945	45093. 1	$a\ ^2F_{2½}—x\ ^4D°_{2½}$ $a\ ^4H_{3½}—y\ ^2H°_{3½}$	1*H*	2286. 39	43723. 6	$a\ ^2F_{3½}—z\ ^2F°_{3½}$
5	2217. 371	45084. 4	$a\ ^4H_{4½}—y\ ^2H°_{3½}$	3	2287. 21	43707. 7	$a\ ^2P_{1½}—z\ ^4P°_{1½}$
5	2217. 766	45076. 4	$b\ ^2F_{3½}—v\ ^2F°_{2½}$	15	2287. 51	43702. 2	$b\ ^2H_{4½}—w\ ^2H°_{4½}$
3	2217. 880	45074. 1	$a\ ^6D_{4½}—z\ ^4F°_{3½}$	10	2288. 32	43686. 7	$a\ ^2F_{2½}—z\ ^2D°_{2½}$
				15	2288. 80	43677. 5	$a\ ^6D_{1½}—z\ ^4D°_{0½}$
3	2218. 312	45065. 3					
500	2218. 552	45060. 4	$a\ ^4P_{2½}—z\ ^4D°_{3½}$	10	2289. 80	43658. 5	$b\ ^4F_{4½}—y\ ^2H°_{5½}$
15	2218. 887	45053. 6		10	2289. 98	43654. 9	$a\ ^2F_{2½}—z\ ^2G°_{3½}$
10	2220. 194	45027. 1	$a\ ^4G_{3½}—x\ ^2G°_{4½}$	5	2290. 52	43644. 8	$b\ ^4D_{3½}—w\ ^2F°_{3½}$
3	2220. 483	45021. 2	$b\ ^4F_{3½}—w\ ^4F°_{2½}$	50	2291. 82	43620. 2	$a\ ^6D_{0½}—z\ ^4F°_{1½}$
				15	2294. 10	43576. 6	
10	2222. 774	44974. 8	$b\ ^2D_{2½}—v\ ^2F°_{3½}$	10	2295. 09	43557. 9	$b\ ^2P_{1½}—y\ ^2P°_{1½}$
3	2224. 173	44946. 6	$a\ ^4F_{3½}—z\ ^6D°_{4½}$	30	2295. 71	43546. 1	
50	2229. 284	44843. 5	$a\ ^6D_{2½}—z\ ^4P°_{2½}$	150	2296. 18	43537. 2	$a\ ^4H_{3½}—y\ ^4H°_{3½}$ $a\ ^4H_{4½}—y\ ^4H°_{3½}$
5	2230. 449	44820. 0	$b\ ^4F_{1½}—w\ ^4D°_{1½}$	15	2296. 64	43528. 5	$a\ ^4D_{3½}—z\ ^4H°_{4½}$ $a\ ^4H_{4½}—y\ ^4H°_{3½}$
1	2231. 004	44808. 9					
3	2231. 144	44806. 1		30	2297. 97	43503. 3	$a\ ^4H_{3½}—y\ ^4H°_{4½}$
1	2232. 770	44773. 5					
30	2237. 73	44674. 3	$b\ ^2D_{2½}—3°_{3½}$	40	2298. 45	43494. 1	$a\ ^4H_{4½}—y\ ^4H°_{4½}$
80	2243. 27	44564. 0	$a\ ^4P_{2½}—z\ ^6P°_{2½}$	90	2298. 63	43490. 8	$a\ ^6D_{1½}—z\ ^4F°_{2½}$
2	2246. 21	44505. 6	$b\ ^2F_{2½}—v\ ^2F°_{3½}$	1	2301. 46	43437. 3	
				1	2301. 64	43433. 9	$a\ ^4H_{4½}—x\ ^4G°_{3½}$
1	2247. 87	44472. 8	$a\ ^4D_{3½}—z\ ^4G°_{4½}$	100	2304. 63	43377. 6	$a\ ^6D_{0½}—z\ ^4D°_{0½}$
2	2248. 79	44454. 6	$a\ ^2F_{2½}—z\ ^2F°_{3½}$				
7	2252. 20	44387. 3		200	2304. 82	43374. 0	$a\ ^6D_{2½}—z\ ^4F°_{3½}$
1	2252. 96	44372. 3	$a\ ^6D_{2½}—z\ ^4F°_{1½}$	200	2305. 61	43359. 1	$a\ ^6D_{1½}—z\ ^4D°_{1½}$ $a\ ^4H_{6½}—y\ ^4H°_{6½}$
100	2254. 45	44343. 0	$a\ ^4P_{1½}—z\ ^6P°_{2½}$	10*H*	2306. 68	43339. 0	
100	2256. 07	44311. 1	$a\ ^4P_{0½}—z\ ^6P°_{1½}$	10*H*	2306. 88	43335. 3	
20	2256. 25	44307. 6	$a\ ^4P_{1½}—z\ ^4P°_{0½}$	3	2307. 76	43318. 7	$b\ ^2F_{2½}—w\ ^2D°_{1½}$
50	2256. 67	44299. 6	$b\ ^4F_{3½}—x\ ^2F°_{3½}$				
80	2257. 12	44290. 5	$b\ ^4F_{1½}—2°_{1½}$ $b\ ^2H_{4½}—w\ ^2F°_{3½}$	40	2308. 63	43302. 4	$b\ ^2H_{5½}—y\ ^2I°_{5½}$
				70	2309. 14	43292. 9	$a\ ^4P_{2½}—z\ ^6P°_{3½}$
60	2260. 03	44233. 5	$a\ ^4D_{2½}—y\ ^4F°_{3½}$	10	2309. 38	43288. 2	$b\ ^2G_{3½}—v\ ^2F°_{3½}$
				50	2309. 52	43285. 9	$a\ ^4H_{4½}—x\ ^4F°_{3½}$
15	2261. 56	44203. 6	$b\ ^4P_{2½}—x\ ^4P°_{2½}$	40*H*	2311. 21	43254. 1	
100	2261. 78	44199. 1	$a\ ^4G_{3½}—w\ ^4F°_{4½}$				
10	2262. 11	44192. 8	$b\ ^4P_{1½}—w\ ^4D°_{2½}$	60*H*	2312. 01	43239. 1	$b\ ^2H_{4½}—y\ ^2I°_{5½}$?
300	2263. 51	44165. 5	$a\ ^6D_{4½}—z\ ^4D°_{3½}$	10*H*	2312. 74	43225. 5	
400	2268. 14	44075. 4	$a\ ^6D_{3½}—z\ ^4F°_{3½}$	3	2313. 18	43217. 2	$a\ ^4D_{1½}—y\ ^4F°_{2½}$?
				150	2313. 37	43213. 7	$a\ ^6D_{2½}—z\ ^4D°_{2½}$
30*H*	2272. 76	43985. 8		50	2314. 02	43201. 6	$a\ ^4H_{5½}—y\ ^4H°_{6½}$
2	2273. 19	43977. 4	$b\ ^4F_{3½}—y\ ^2H°_{4½}$				
3*h*	2273. 66	43968. 4		50	2314. 78	43187. 2	$a\ ^4H_{3½}—y\ ^4H°_{3½}$
150	2275. 00	43942. 5	$a\ ^6D_{2½}—z\ ^4F°_{2½}$	2	2315. 04	43182. 5	
100	2276. 14	43920. 5	$a\ ^6D_{1½}—z\ ^4F°_{1½}$	10	2315. 27	43178. 2	$a\ ^4H_{3½}—x\ ^4F°_{2½}$

TABLE 6. *The second spectrum of ruthenium* (Ru II)—Continued

1 Intensity	2 λ (air)	3 σ	4 Term combination	5 Type	6 Δg	7 g	8 g	9 Strong p	10 Strong n
	A	*K*							
50	2315. 90	43166. 5	$a\ ^6D_{3½}—z\ ^4D^o_{3½}$ $b\ ^2H_{3½}—y\ ^2I^o_{6½}$	-----	-----	-----	-----	-----	-----
20*H*	2316. 52	43154. 9	----------	-----	-----	-----	-----	-----	-----
5	2316. 88	43148. 2	$a\ ^4D_{3½}—z\ ^4H^o_{3½}$	-----	-----	-----	-----	-----	-----
5	2317. 07	43144. 7	$a\ ^4H_{3½}—y\ ^4H^o_{4½}$	-----	-----	-----	-----	-----	-----
50	2318. 46	43118. 8	$a\ ^4G_{4½}—w\ ^4F^o_{4½}$	-----	-----	-----	-----	-----	-----
50*h*	2319. 28	43103. 6	$b\ ^4F_{1½}—y\ ^2F^o_{2½}$	-----	-----	-----	-----	-----	-----
80	2321. 66	43059. 5	$a\ ^6D_{0½}—z\ ^4D^o_{1½}$ $a\ ^4P_{2½}—z\ ^6F^o_{1½}$	-----	-----	-----	-----	-----	-----
20	2322. 57	43042. 5	$a\ ^4G_{4½}—w\ ^4F^o_{3½}$	-----	-----	-----	-----	-----	-----
2	2322. 74	43039. 4	$b\ ^2H_{5½}—w\ ^2H^o_{5½}$	-----	-----	-----	-----	-----	-----
60	2322. 83	43037. 7	$a\ ^2F_{3½}—y\ ^4F^o_{4½}$	5	-------	(1. 141)	1. 17	0	1. 29
3	2323. 50	43025. 4	$b\ ^2D_{1½}—w\ ^2D^o_{2½}$	-----	-----	-----	-----	-----	-----
3	2323. 66	43022. 3	$a\ ^4G_{2½}—w\ ^4D^o_{1½}$	-----	-----	-----	-----	-----	-----
40	2323. 76	43020. 5	----------	-----	-----	-----	-----	-----	-----
6	2325. 41	42990. 0	$b\ ^2D_{2½}—w\ ^2D^o_{2½}$	-----	-----	-----	-----	-----	-----
10	2325. 51	42988. 1	$b\ ^2G_{3½}—3^o_{3½}$	-----	-----	-----	-----	-----	-----
5	2326. 21	42974. 8	$b\ ^2H_{4½}—w\ ^2H^o_{5½}$	-----	-----	-----	-----	-----	-----
40	2328. 16	42939. 2	$b\ ^2F_{3½}—w\ ^2F^o_{3½}$	-----	-----	-----	-----	-----	-----
40	2328. 33	42936. 0	$a\ ^4H_{3½}—x\ ^4F^o_{3½}$	-----	-----	-----	-----	-----	-----
150	2329. 02	42923. 4	$a\ ^4P_{2½}—z\ ^6F^o_{3½}$ $a\ ^4G_{3½}—x\ ^2H^o_{4½}$	6	0. 27	(1. 57)	1. 30	0. 67	1. 43
30	2330. 14	42902. 7	$a\ ^4P_{1½}—z\ ^6F^o_{6½}$	5	-------	-------	-------	1. 08	2. 75
40*H*	2331. 70	42874. 0	----------	-----	-----	-----	-----	-----	-----
50*H*	2332. 31	42862. 8	----------	-----	-----	-----	-----	-----	-----
5	2332. 90	42851. 9	----------	-----	-----	-----	-----	-----	-----
20	2333. 30	42844. 6	$a\ ^4G_{3½}—w\ ^4D^o_{2½}$	-----	-----	-----	-----	-----	-----
150	2333. 57	42839. 7	$a\ ^4P_{1½}—z\ ^4F^o_{1½}$	-----	-----	-----	-----	-----	-----
200	2333. 89	42833. 8	$a\ ^6D_{2½}—z\ ^6P^o_{1½}$	4	0. 722	1. 660	2. 382	0. 361	0. 577
8	2334. 27	42826. 8	$b\ ^4P_{0½}—w\ ^4D^o_{1½}$	-----	-----	-----	-----	-----	-----
300	2334. 96	42814. 2	$a\ ^6D_{3½}—z\ ^4F^o_{4½}$	4	. 229	1. 575	1. 346	. 111	0. 543
60	2335. 88	42797. 2	$a\ ^4H_{5½}—x\ ^4G^o_{4½}$	-----	-----	-----	-----	-----	-----
25	2336. 38	42788. 2	$a\ ^4H_{4½}—x\ ^4G^o_{4½}$	-----	-----	-----	-----	-----	-----
200*H*	2336. 83	42779. 9	----------	-----	-----	-----	-----	-----	-----
0	2337. 09	42775. 1	$b\ ^4P_{1½}—x\ ^4P^o_{1½}$	-----	-----	-----	-----	-----	-----
100	2337. 84	42761. 4	$a\ ^6D_{1½}—z\ ^4D^o_{2½}$	4	. 494	(1. 843)	1. 349	. 247	?
20	2338. 74	42745. 0	$b\ ^2H_{4½}—w\ ^2G^o_{3½}$	-----	-----	-----	-----	-----	-----
20	2339. 10	42738. 4	$a\ ^2P_{1½}—z\ ^4P^o_{2½}$	-----	-----	-----	-----	-----	-----
15	2339. 92	42723. 5	$b\ ^2H_{5½}—w\ ^2G^o_{4½}$	-----	-----	-----	-----	-----	-----
60	2339. 95	42722. 9	----------	-----	-----	-----	-----	-----	-----
5	2339. 98	42722. 3	----------	-----	-----	-----	-----	-----	-----
30	2340. 51	42712. 7	$a\ ^4H_{3½}—y\ ^2G^o_{4½}$	-----	-----	-----	-----	-----	-----
100	2341. 06	42702. 6	$a\ ^4P_{1½}—z\ ^6F^o_{2½}$ $a\ ^4G_{3½}—w\ ^4F^o_{3½}$	4	. 36	1. 68	1. 32	. 18	0. 78
10	2342. 37	42679. 4	----------	-----	-----	-----	-----	-----	-----
300	2342. 85	42670. 0	$a\ ^6D_{3½}—z\ ^6P^o_{2½}$	4	. 254	1. 576	1. 830	. 126	0. 942
30	2343. 43	42659. 4	$b\ ^2H_{4½}—w\ ^2G^o_{4½}$	-----	-----	-----	-----	-----	-----
20	2344. 46	42640. 7	$b\ ^4F_{2½}—y\ ^2D^o_{1½}$	-----	-----	-----	-----	-----	-----
100*H*	2344. 84	42633. 8	----------	-----	-----	-----	-----	-----	-----
12	2345. 48	42622. 1	$b\ ^4F_{3½}—y\ ^2D^o_{2½}$	-----	-----	-----	-----	-----	-----
150	2346. 38	42605. 8	$a\ ^4P_{2½}—z\ ^6F^o_{3½}$	-----	-----	-----	-----	-----	-----
3	2348. 74	42563. 0	----------	-----	-----	-----	-----	-----	-----
5*h*	2350. 08	42538. 8	----------	-----	-----	-----	-----	-----	-----
200	2350. 53	42530. 6	$a\ ^4G_{3½}—w\ ^4F^o_{4½}$	7*	-------	-------	-------	0	1. 032
10	2350. 59	42529. 5	----------	-----	-----	-----	-----	-----	-----
15	2351. 07	42520. 8	$b\ ^2F_{2½}—w\ ^2D^o_{2½}$	-----	-----	-----	-----	-----	-----
3	2351. 63	42510. 7	----------	-----	-----	-----	-----	-----	-----
3	2351. 79	42507. 8	$b\ ^4P_{1½}—y\ ^2F^o_{2½}$	-----	-----	-----	-----	-----	-----
4	2352. 25	42499. 5	$b\ ^2D_{1½}—y\ ^2P^o_{1½}$	-----	-----	-----	-----	-----	-----

TABLE 6. *The second spectrum of ruthenium* (Ru II)—Continued

1 Intensity	2 λ (air)	3 σ	4 Term combination	5 Type	6 Δg	7 g	8 g	9 Strong p	10 Strong n
	A	*K*							
3	2352. 63	42492. 7	$\left\{\begin{matrix} b\ {}^4P_{2\frac{1}{2}}—x\ {}^4F^\circ_{3\frac{1}{2}} \\ a\ {}^4G_{2\frac{1}{2}}—2^\circ_{1\frac{1}{2}} \end{matrix}\right\}$	-----	-------	-------	-------	-------	-------
40	2354. 24	42463. 6	$\left\{\begin{matrix} a\ {}^2P_{0\frac{1}{2}}—z\ {}^4P^\circ_{0\frac{1}{2}} \\ b\ {}^2D_{2\frac{1}{2}}—y\ {}^2P^\circ_{1\frac{1}{2}} \end{matrix}\right\}$	-----	-------	-------	-------	-------	-------
5*h*	2354. 43	42460. 1	$a\ {}^2F_{3\frac{1}{2}}—y\ {}^4F^\circ_{3\frac{1}{2}}$	-----	-------	-------	-------	-------	-------
25	2355. 63	42438. 4	$a\ {}^4H_{3\frac{1}{2}}—x\ {}^4G^\circ_{4\frac{1}{2}}$	-----	-------	-------	-------	-------	-------
20	2355. 97	42432. 4	$b\ {}^4F_{2\frac{1}{2}}—y\ {}^2D^\circ_{2\frac{1}{2}}$	-----	-------	-------	-------	-------	-------
6*H*	2356. 47	42423. 4	$a\ {}^2S_{0\frac{1}{2}}—w\ {}^4P^\circ_{0\frac{1}{2}}$	-----	-------	-------	-------	-------	-------
600	2357. 92	42397. 4	$a\ {}^6D_{4\frac{1}{2}}—z\ {}^6P^\circ_{3\frac{1}{2}}$	-----	-------	-------	-------	-------	-------
400	2358. 79	42381. 7	$a\ {}^6D_{1\frac{1}{2}}—z\ {}^6P^\circ_{1\frac{1}{2}}$	6	0. 517	1. 844	2. 361	0. 770	2. 102
150	2359. 10	42376. 0	$a\ {}^4H_{6\frac{1}{2}}—x\ {}^4G^\circ_{5\frac{1}{2}}$	-----	-------	-------	-------	-------	-------
40*H*	2360. 61	42349. 0	$b\ {}^2F_{3\frac{1}{2}}—w\ {}^2H^\circ_{4\frac{1}{2}}$	-----	-------	-------	-------	-------	-------
5*H*	2361. 91	42325. 7	----------	-----	-------	-------	-------	-------	-------
6	2363. 02	42305. 8	$a\ {}^4H_{3\frac{1}{2}}—y\ {}^4D^\circ_{2\frac{1}{2}}$	-----	-------	-------	-------	-------	-------
5*H*	2363. 32	42300. 4	----------	-----	-------	-------	-------	-------	-------
5*H*	2363. 92	42289. 7	----------	-----	-------	-------	-------	-------	-------
50	2364. 23	42284. 2	$b\ {}^4F_{1\frac{1}{2}}—y\ {}^2D^\circ_{1\frac{1}{2}}$	-----	-------	-------	-------	-------	-------
3*h*	2366. 01	42252. 3	----------	-----	-------	-------	-------	-------	-------
150	2367. 22	42230. 7	$a\ {}^4G_{2\frac{1}{2}}—w\ {}^4F^\circ_{1\frac{1}{2}}$	5	0. 161	0. 642	0. 480	0. 080	0. 884
15	2367. 88	42219. 0	$a\ {}^4H_{5\frac{1}{2}}—x\ {}^4G^\circ_{5\frac{1}{2}}$	-----	-------	-------	-------	-------	-------
5	2368. 37	42210. 2	$a\ {}^4H_{4\frac{1}{2}}—x\ {}^4G^\circ_{5\frac{1}{2}}$	-----	-------	-------	-------	-------	-------
20	2369. 65	42187. 4	----------	-----	-------	-------	-------	-------	-------
10	2369. 83	42184. 2	$a\ {}^4G_{3\frac{1}{2}}—y\ {}^2H^\circ_{3\frac{1}{2}}$	-----	-------	-------	-------	-------	-------
80	2371. 84	42148. 5	$\left\{\begin{matrix} a\ {}^4G_{4\frac{1}{2}}—x\ {}^2F^\circ_{3\frac{1}{2}} \\ b\ {}^2D_{2\frac{1}{2}}—w\ {}^2F^\circ_{3\frac{1}{2}}? \end{matrix}\right\}$	5	-------	(1. 167)	1. 14	*w*	1. 24
100	2371. 91	42147. 2	$a\ {}^4H_{4\frac{1}{2}}—y\ {}^2G^\circ_{3\frac{1}{2}}$	5	-------	(1. 14)	1. 06	o	1. 41
2*H*	2373. 05	42127. 0	----------	-----	-------	-------	-------	-------	-------
20	2373. 96	42110. 8	$\left\{\begin{matrix} a\ {}^4H_{4\frac{1}{2}}—x\ {}^4D^\circ_{3\frac{1}{2}} \\ b\ {}^4F_{4\frac{1}{2}}—y\ {}^4H^\circ_{3\frac{1}{2}} \end{matrix}\right\}$	-----	-------	-------	-------	-------	-------
7	2374. 67	42098. 3	$b\ {}^4D_{2\frac{1}{2}}—x\ {}^2D^\circ_{2\frac{1}{2}}$	-----	-------	-------	-------	-------	-------
400	2375. 63	42081. 3	$a\ {}^6D_{0\frac{1}{2}}—z\ {}^6P^\circ_{1\frac{1}{2}}$	4	0. 920	3. 271	2. 351	0. 460	1. 890
30	2376. 23	42070. 6	$c\ {}^2G_{4\frac{1}{2}}—\ 3^\circ_{3\frac{1}{2}}$	-----	-------	-------	-------	-------	-------
5	2376. 35	42068. 5	$b\ {}^4F_{4\frac{1}{2}}—y\ {}^4H^\circ_{4\frac{1}{2}}$	-----	-------	-------	-------	-------	-------
4*h*	2378. 84	42024. 5	$a\ {}^2P_{1\frac{1}{2}}—z\ {}^4D^\circ_{1\frac{1}{2}}$	-----	-------	-------	-------	-------	-------
2	2379. 07	42020. 4	----------	-----	-------	-------	-------	-------	-------
100	2379. 60	42011. 0	$a\ {}^4H_{3\frac{1}{2}}—z\ {}^2H^\circ_{4\frac{1}{2}}$	-----	-------	-------	-------	-------	-------
100	2379. 84	42006. 8	$a\ {}^4P_{0\frac{1}{2}}—z\ {}^6F^\circ_{0\frac{1}{2}}$	6	3. 21	2. 61	−0. 60	1. 60	1. 00
1	2380. 39	41997. 1	----------	-----	-------	-------	-------	-------	-------
400	2381. 99	41968. 9	$a\ {}^6D_{2\frac{1}{2}}—z\ {}^6P^\circ_{2\frac{1}{2}}$	6	0. 189	1. 646	1. 835	0. 475	1. 741
10	2382. 74	41955. 7	$a\ {}^4G_{2\frac{1}{2}}—x\ {}^2F^\circ_{3\frac{1}{2}}$	-----	-------	-------	-------	-------	-------
90	2383. 42	41943. 8	$a\ {}^4P_{0\frac{1}{2}}—z\ {}^6F^\circ_{1\frac{1}{2}}$	4	1. 55	2. 61	1. 06	. 77	0. 30
5	2383. 96	41934. 2	----------	-----	-------	-------	-------	-------	-------
1	2384. 95	41916. 8	----------	-----	-------	-------	-------	-------	-------
2	2385. 29	41910. 8	$a\ {}^4G_{4\frac{1}{2}}—y\ {}^2F^\circ_{3\frac{1}{2}}$	-----	-------	-------	-------	-------	-------
10*h*	2386. 19	41895. 0	----------	-----	-------	-------	-------	-------	-------
20*H*	2386. 71	41885. 9	----------	-----	-------	-------	-------	-------	-------
10	2388. 04	41862. 5	$b\ {}^4P_{2\frac{1}{2}}—y\ {}^4D^\circ_{3\frac{1}{2}}$	-----	-------	-------	-------	-------	-------
40	2388. 23	41859. 3	$b\ {}^4F_{4\frac{1}{2}}—x\ {}^4F^\circ_{3\frac{1}{2}}$	-----	-------	-------	-------	-------	-------
3*h*	2388. 53	41854. 0	----------	-----	-------	-------	-------	-------	-------
2*h*	2388. 67	41851. 5	----------	-----	-------	-------	-------	-------	-------
2	2389. 47	41837. 5	$a\ {}^2P_{1\frac{1}{2}}—z\ {}^4F^\circ_{2\frac{1}{2}}$	-----	-------	-------	-------	-------	-------
15	2390. 09	41826. 7	$a\ {}^4G_{4\frac{1}{2}}—y\ {}^2H^\circ_{4\frac{1}{2}}$	-----	-------	-------	-------	-------	-------
20	2390. 32	41822. 6	$c\ {}^2G_{3\frac{1}{2}}—v\ {}^2F^\circ_{3\frac{1}{2}}$	-----	-------	-------	-------	-------	-------
20	2391. 10	41809. 1	$a\ {}^4G_{3\frac{1}{2}}—x\ {}^2F^\circ_{3\frac{1}{2}}$	-----	-------	-------	-------	-------	-------
30	2391. 44	41803. 0	----------	-----	-------	-------	-------	-------	-------
60	2391. 77	41797. 4	$a\ {}^4H_{3\frac{1}{2}}—y\ {}^2G^\circ_{3\frac{1}{2}}$	-----	-------	-------	-------	-------	-------
3	2392. 59	41784. 7	$b\ {}^4D_{3\frac{1}{2}}—x\ {}^2D^\circ_{2\frac{1}{2}}$	-----	-------	-------	-------	-------	-------
200	2393. 84	41761. 1	$a\ {}^4H_{3\frac{1}{2}}—x\ {}^4D^\circ_{3\frac{1}{2}}$	6	0. 202	(0. 753)	0. 955	0. 707	?
600	2396. 71	41711. 2	$a\ {}^6D_{4\frac{1}{2}}—z\ {}^6F^\circ_{3\frac{1}{2}}$	5	-------	(1. 54)	1. 47	0	1. 78

TABLE 6. *The second spectrum of ruthenium* (Ru II)—Continued

1 Intensity	2 λ (air)	3 σ	4 Term combination	5 Type	6 Δg	7 g	8 g	9 Strong p	10 Strong a
	A	*K*							
80	2396. 97	41706. 6	$\left\{\begin{matrix} a\ {}^2P_{1\frac{1}{2}}—z\ {}^4D^\circ_{1\frac{1}{2}} \\ b\ {}^4F_{3\frac{1}{2}}—y\ {}^4H^\circ_{3\frac{1}{2}} \end{matrix}\right.$						
40	2397. 49	41697. 6	$b\ {}^4F_{3\frac{1}{2}}—x\ {}^4F^\circ_{2\frac{1}{2}}$						
100	2397. 69	41694. 1	$a\ {}^6D_{4\frac{1}{2}}—z\ {}^6F^\circ_{4\frac{1}{2}}$	6 *us*					
5	2399. 52	41662. 3							
5	2400. 10	41652. 2	$\left\{\begin{matrix} a\ {}^2F_{3\frac{1}{2}}—z\ {}^4G^\circ_{3\frac{1}{2}} \\ a\ {}^4H_{3\frac{1}{2}}—z\ {}^2H^\circ_{4\frac{1}{2}} \end{matrix}\right.$						
3*H*	2400. 44	41646. 4							
20	2401. 02	41636. 4	$b\ {}^4F_{4\frac{1}{2}}—y\ {}^2G^\circ_{4\frac{1}{2}}$						
3	2401. 26	41632. 1	$b\ {}^4D_{0\frac{1}{2}}—x\ {}^2D^\circ_{1\frac{1}{2}}$?						
40	2401. 85	41621. 9							
800	2402. 72	41606. 9	$a\ {}^6D_{4\frac{1}{2}}—z\ {}^6F^\circ_{5\frac{1}{2}}$	4	(0. 10)	(1. 54)	1. 44	0. 48*w*	0. 97+
3	2404. 66	41573. 2	$\left\{\begin{matrix} a\ {}^4G_{2\frac{1}{2}}—x\ {}^4P^\circ_{1\frac{1}{2}} \\ b\ {}^4D_{2\frac{1}{2}}—x\ {}^2D^\circ_{1\frac{1}{2}} \end{matrix}\right.$						
10	2404. 79	41571. 0	$a\ {}^4G_{3\frac{1}{2}}—y\ {}^2F^\circ_{3\frac{1}{2}}$						
10	2405. 28	41562. 6	$a\ {}^2F_{3\frac{1}{2}}—z\ {}^4G^\circ_{4\frac{1}{2}}$						
2*h*	2405. 65	41556. 2							
20	2406. 06	41549. 1	$a\ {}^4H_{6\frac{1}{2}}—z\ {}^2H^\circ_{5\frac{1}{2}}$						
4	2406. 65	41538. 8							
20	2407. 31	41527. 5	$a\ {}^4H_{4\frac{1}{2}}—y\ {}^4G^\circ_{3\frac{1}{2}}$						
300	2407. 92	41517. 1	$a\ {}^6D_{1\frac{1}{2}}—z\ {}^6P^\circ_{2\frac{1}{2}}$	7		(1. 843)	1. 88	0	1. 82
50	2408. 44	41508. 0	$b\ {}^4F_{2\frac{1}{2}}—x\ {}^4F^\circ_{2\frac{1}{2}}$	6	(0. 04)	0. 94	0. 98	0. 12	0. 96
2	2409. 34	41492. 5	$a\ {}^4H_{5\frac{1}{2}}—y\ {}^4G^\circ_{5\frac{1}{2}}$						
25	2409. 68	41486. 7	$a\ {}^4G_{3\frac{1}{2}}—y\ {}^2H^\circ_{3\frac{1}{2}}$						
150	2410. 15	41478. 6	$a\ {}^4H_{3\frac{1}{2}}—y\ {}^4G^\circ_{2\frac{1}{2}}$	5	(0. 07)	(0. 753)	. 68	. 17*w*	. 92−
100	2411. 51	41455. 2	$b\ {}^4F_{3\frac{1}{2}}—x\ {}^4F^\circ_{3\frac{1}{2}}$						
40	2413. 40	41422. 8	$b\ {}^2H_{5\frac{1}{2}}—x\ {}^2G^\circ_{4\frac{1}{2}}$						
20*H*	2413. 80	41415. 9							
20	2413. 92	41413. 8	$b\ {}^4F_{2\frac{1}{2}}—x\ {}^4G^\circ_{3\frac{1}{2}}$						
150	2414. 82	41398. 4	$a\ {}^6D_{3\frac{1}{2}}—z\ {}^6P^\circ_{3\frac{1}{2}}$	7		(1. 576)	1. 592	0	1. 584
120	2415. 20	41391. 9	$a\ {}^4H_{5\frac{1}{2}}—z\ {}^2H^\circ_{5\frac{1}{2}}$	6*us*					1. 36
100	2415. 72	41383. 0	$a\ {}^4H_{4\frac{1}{2}}—z\ {}^2H^\circ_{5\frac{1}{2}}$						
2	2416. 06	41377. 1	$b\ {}^4P_{0\frac{1}{2}}—x\ {}^4P^\circ_{1\frac{1}{2}}$						
120	2416. 96	41361. 7	$b\ {}^4F_{4\frac{1}{2}}—x\ {}^4G^\circ_{4\frac{1}{2}}$	6	(0. 04)	1. 17	1. 21	. 16−	1. 19
60	2418. 96	41327. 6	$b\ {}^2H_{5\frac{1}{2}}—x\ {}^2H^\circ_{4\frac{1}{2}}$	7		(1. 053)	1. 05	0	1. 04
15	2420. 10	41308. 0	$b\ {}^2F_{3\frac{1}{2}}—w\ {}^2G^\circ_{4\frac{1}{2}}$						
10	2420. 24	41305. 6	$a\ {}^4G_{2\frac{1}{2}}—y\ {}^2F^\circ_{2\frac{1}{2}}$						
3	2421. 28	41288. 0							
5*H*	2422. 08	41274. 3							
3	2422. 68	41264. 0	$b\ {}^2H_{4\frac{1}{2}}—x\ {}^2H^\circ_{5\frac{1}{2}}$						
40	2422. 84	41261. 3	$b\ {}^4D_{3\frac{1}{2}}—w\ {}^4D^\circ_{3\frac{1}{2}}$						
5*H*	2423. 62	41248. 1							
70	2424. 56	41232. 0	$b\ {}^4F_{3\frac{1}{2}}—y\ {}^2G^\circ_{4\frac{1}{2}}$	4		(1. 093)	1. 06	0	1. 00+
3*H*	2425. 46	41216. 8							
50	2426. 59	41197. 6	$b\ {}^2P_{0\frac{1}{2}}—y\ {}^2P^\circ_{1\frac{1}{2}}$	5	0. 408	0. 890	1. 298	0. 204	1. 502
40	2426. 99	41190. 8		6				. 59	?
60	2427. 75	41177. 9	$a\ {}^4H_{3\frac{1}{2}}—y\ {}^4G^\circ_{3\frac{1}{2}}$	6	. 26	. 76	1. 02	. 920	0. 89
10	2428. 86	41159. 0	$a\ {}^4G_{3\frac{1}{2}}—y\ {}^2F^\circ_{2\frac{1}{2}}$						
10	2429. 01	41156. 6							
60	2430. 40	41133. 0	$c\ {}^2G_{3\frac{1}{2}}—v\ {}^2F^\circ_{2\frac{1}{2}}$	7		(0. 942)	0. 96	0	. 900
3*h*	2430. 72	41127. 6							
50	2430. 94	41123. 9	$\left\{\begin{matrix} b\ {}^2H_{4\frac{1}{2}}—x\ {}^2G^\circ_{3\frac{1}{2}} \\ b\ {}^4F_{1\frac{1}{2}}—x\ {}^4F^\circ_{1\frac{1}{2}} \end{matrix}\right.$	6	. 20	0. 415	. 62	0. 40	?
2*h*	2431. 21	41119. 3	$a\ {}^6S_{2\frac{1}{2}}—w\ {}^2F^\circ_{3\frac{1}{2}}$						
2	2431. 82	41109. 0	$a\ {}^2P_{1\frac{1}{2}}—z\ {}^4D^\circ_{2\frac{1}{2}}$						
40	2432. 16	41103. 2	$a\ {}^4G_{4\frac{1}{2}}—y\ {}^2H^\circ_{5\frac{1}{2}}$	4*				. 30*w*	0. 76+
40	2433. 58	41079. 2	$b\ {}^2F_{3\frac{1}{2}}—x\ {}^2D^\circ_{2\frac{1}{2}}$						
30	2433. 86	41074. 4							
2	2434. 03	41071. 7							

TABLE 6. *The second spectrum of ruthenium* (Ru II)—Continued

1 Intensity	2 λ (air)	3 σ	4 Term combination	5 Type	6 Δ *g*	7 *g*	8 *g*	9 Strong *p*	10 Strong *n*
	A	*K*							
6	2434.74	41059.6	*b* $^4P_{1\frac{1}{2}}$—$1\hat{i}_{1\frac{1}{2}}$	-----	-------	-------	-------	-------	-------
80	2434.98	41055.7	*a* $^4H_{3\frac{1}{2}}$—*y* $^4G^{\circ}_{4\frac{1}{2}}$	-----	-------	-------	-------	-------	-------
4	2435.33	41049.8	----------	-----	-------	-------	-------	-------	-------
200	2435.51	41046.8	*a* $^4H_{4\frac{1}{2}}$—*y* $^4G^{\circ}_{4\frac{1}{2}}$	6*us*	-------	-------	-------	.38	1.37±
2	2436.23	41034.6	*b* $^4P_{2\frac{1}{2}}$—*y* $^4G^{\circ}_{2\frac{1}{2}}$	-----	-------	-------	-------	-------	-------
5	2436.55	41029.3	*a* $^6D_{3\frac{1}{2}}$—*z* $^6F^{\circ}_{3\frac{1}{2}}$	-----	-------	-------	-------	-------	-------
1*h*	2438.94	40989.0	*b* $^4P_{2\frac{1}{2}}$—*y* $^4D\hat{i}_{1\frac{1}{2}}$	-----	-------	-------	-------	-------	-------
2*h*	2439.15	40985.5	----------	-----	-------	-------	-------	-------	-------
150*H*	2439.69	40976.3	----------	-----	-------	-------	-------	-------	-------
2	2440.13	40969.0	*a* $^2F_{2\frac{1}{2}}$—*z* $^4H^{\circ}_{3\frac{1}{2}}$	-----	-------	-------	-------	-------	-------
80	2440.80	40957.7	*b* $^4F_{3\frac{1}{2}}$—*x* $^4G^{\circ}_{4\frac{1}{2}}$	-----	-------	-------	-------	-------	-------
70	2441.37	40948.3	----------	-----	-------	-------	-------	0.25*w*	?
30	2441.61	40944.1	*b* $^4F_{1\frac{1}{2}}$—*z* $^2P^{\circ}_{0\frac{1}{2}}$	4	0.42	0.42	0.84	.21	0.21
100*Hw*	2443.30	40915.8	*b* $^4F_{2\frac{1}{2}}$—*x* $^4G^{\circ}_{2\frac{1}{2}}$	-----	-------	-------	-------	-------	-------
40*H*	2445.55	40878.2	----------	-----	-------	-------	-------	-------	-------
8	2446.55	40861.5	*b* $^4D_{1\frac{1}{2}}$—*w* $^4D^{\circ}_{0\frac{1}{2}}$?	-----	-------	-------	-------	-------	-------
8	2446.77	40857.8	*b* $^2P_{1\frac{1}{2}}$—*x* $^2D\hat{i}_{1\frac{1}{2}}$	-----	-------	-------	-------	-------	-------
5	2448.36	40831.4	----------	-----	-------	-------	-------	-------	-------
10	2448.91	40822.1	*a* $^4G_{2\frac{1}{2}}$—*x* $^4P^{\circ}_{2\frac{1}{2}}$ *c* $^2D_{2\frac{1}{2}}$—*v* $^2F^{\circ}_{3\frac{1}{2}}$	-----	-------	-------	-------	-------	-------
200*H*	2449.58	40811.0	*z* $^6D^{\circ}_{3\frac{1}{2}}$—*e* $^4D_{2\frac{1}{2}}$	-----	-------	-------	-------	-------	-------
30	2450.88	40789.3	*b* $^4D_{0\frac{1}{2}}$—*w* $^4D^{\circ}_{0\frac{1}{2}}$	6	.43	.13	.56	.216	.34?
40	2451.23	40783.5	*b* $^4F_{4\frac{1}{2}}$—*x* $^4G^{\circ}_{5\frac{1}{2}}$	4	(0.04)	1.20	1.16	.19*w*	.96+
10	2451.66	40776.3	----------	-----	-------	-------	-------	-------	-------
5	2452.53	40761.9	----------	-----	-------	-------	-------	-------	-------
60	2453.82	40740.5	*b* $^2H_{5\frac{1}{2}}$—*x* $^2H\hat{i}_{4\frac{1}{2}}$	-----	-------	-------	-------	-------	-------
10	2454.16	40734.8	*b* $^4P_{2\frac{1}{2}}$—*y* $^4G^{\circ}_{3\frac{1}{2}}$	-----	-------	-------	-------	-------	-------
10	2454.99	40721.0	*b* $^4F_{4\frac{1}{2}}$—*y* $^2G^{\circ}_{3\frac{1}{2}}$	-----	-------	-------	-------	-------	-------
600	2455.53	40712.0	*a* $^6D_{3\frac{1}{2}}$—*z* $^6F^{\circ}_{3\frac{1}{2}}$	6*us*	(0.11)	1.58	1.47	.39—	1.53±
500	2456.44	40697.0	*a* $^6D_{2\frac{1}{2}}$—*z* $^6P^{\circ}_{3\frac{1}{2}}$	4	-------	(1.637)	1.57	*w*	1.39+
500	2456.57	40694.8	*a* $^6D_{3\frac{1}{2}}$—*z* $^6F^{\circ}_{4\frac{1}{2}}$	4	-------	(1.576)	1.43	.39*w*	0.93+
20	2457.19	40684.6	*b* $^4F_{4\frac{1}{2}}$—*x* $^4D^{\circ}_{3\frac{1}{2}}$	5	0.24	(1.200)	0.96	.12	-------
10	2459.24	40650.7	----------	-----	-------	-------	-------	-------	-------
20	2459.42	40647.6	----------	-----	-------	-------	-------	-------	-------
20	2460.18	40635.2	*b* $^4F_{2\frac{1}{2}}$—*y* $^4D^{\circ}_{2\frac{1}{2}}$	-----	-------	-------	-------	-------	-------
20	2460.43	40631.1	*a* $^4H_{3\frac{1}{2}}$—*z* $^2F^{\circ}_{2\frac{1}{2}}$	4	-------	(0.753)	.82	*w*	.60
20	2460.59	40628.4	*a* $^4G_{3\frac{1}{2}}$—*y* $^4H^{\circ}_{3\frac{1}{2}}$	-----	-------	-------	-------	-------	-------
5	2461.54	40612.8	----------	-----	-------	-------	-------	-------	-------
20	2462.17	40602.3	*b* $^2D_{2\frac{1}{2}}$—*w* $^2G^{\circ}_{3\frac{1}{2}}$	-----	-------	-------	-------	-------	-------
25	2462.65	40594.4	*a* $^4G_{5\frac{1}{2}}$—*y* $^4H\hat{i}_{4\frac{1}{2}}$	5	0.243	(1.237)	0.994	0.122	?
1	2463.86	40574.4	----------	-----	-------	-------	-------	-------	-------
2	2464.24	40568.1	----------	-----	-------	-------	-------	-------	-------
100	2464.76	40559.7	*b* $^4F_{1\frac{1}{2}}$—*x* $^4G^{\circ}_{2\frac{1}{2}}$	5	2.74	0.442	.716	.141	1.127
25	2465.00	40555.6	*b* $^4P_{1\frac{1}{2}}$—*x* $^4F^{\circ}_{2\frac{1}{2}}$ *b* $^2F_{3\frac{1}{2}}$—*w* $^4D^{\circ}_{3\frac{1}{2}}$	-----	-------	-------	-------	-------	-------
1	2465.52	40547.1	*b* $^4P_{0\frac{1}{2}}$—*z* $^2S^{\circ}_{0\frac{1}{2}}$	-----	-------	-------	-------	-------	-------
1	2466.61	40529.2	*b* $^4P_{1\frac{1}{2}}$—*x* $^4F\hat{i}_{1\frac{1}{2}}$?	-----	-------	-------	-------	-------	-------
1	2467.05	40522.0	*c* $^2D_{2\frac{1}{2}}$—$3^{\circ}_{3\frac{1}{2}}$	-----	-------	-------	-------	-------	-------
30	2467.33	40517.4	----------	-----	-------	-------	-------	-------	-------
2*H*	2468.71	40494.7	----------	-----	-------	-------	-------	-------	-------
20	2469.25	40485.9	*a* $^4G_{2\frac{1}{2}}$—*y* $^2D\hat{i}_{1\frac{1}{2}}$?	-----	-------	-------	-------	-------	-------
40	2469.77	40477.4	*b* $^4D_{3\frac{1}{2}}$—*x* $^2G^{\circ}_{3\frac{1}{2}}$	6	.275	(1.397)	1.122	.963	-------
60	2470.51	40465.3	*a* $^6D_{2\frac{1}{2}}$—*z* $^6F\hat{i}_{1\frac{1}{2}}$	5	.582	1.629	1.047	.294	2.502
30	2471.05	40456.4	*b* $^2H_{4\frac{1}{2}}$—*w* $^4F^{\circ}_{3\frac{1}{2}}$	*	-------	-------	-------	*w*	1.36
3*H*	2471.76	40444.8	----------	-----	-------	-------	-------	-------	-------
20	2472.44	40433.7	----------	6	-------	-------	-------	.28	0.98
30	2472.83	40427.2	*b* $^4D_{1\frac{1}{2}}$—*w* $^4D\hat{i}_{1\frac{1}{2}}$	7	-------	(1.200)	1.214	0	1.207

TABLE 6. *The second spectrum of ruthenium* (Ru II)—Continued

1 Intensity	2 λ (air)	3 σ	4 Term combination	5 Type	6 Δ *g*	7 *g*	8 *g*	9 Strong *p*	10 Strong *s*
	A	*K*							
8	2472. 99	40424. 7	*a* $^2P_{0\frac{1}{2}}$—*z* $^4F^\circ_{1\frac{1}{2}}$	-----	-----	-----	-----	-----	-----
10	2473. 57	40415. 1	----------	-----	-----	-----	-----	-----	-----
5*h*	2473. 83	40410. 9	----------	-----	-----	-----	-----	-----	-----
30	2474. 76	40395. 7	*b* $^4D_{1\frac{1}{2}}$—*w* $^4D^\circ_{2\frac{1}{2}}$	5	-------	(1. 200)	1. 30	*w*	1. 44
4	2476. 15	40373. 1	*b* $^2G_{4\frac{1}{2}}$—*w* $^2H^\circ_{4\frac{1}{2}}$	-----	-----	-----	-----	-----	-----
10	2477. 17	40356. 4	*b* $^4F_{4\frac{1}{2}}$—*x* $^4F^\circ_{4\frac{1}{2}}$	-----	-----	-----	-----	-----	-----
50	2477. 26	40355. 0	*b* $^4D_{0\frac{1}{2}}$—*w* $^4D^\circ_{1\frac{1}{2}}$	-----	-----	-----	-----	-----	-----
8	2477. 98	40343. 3	----------	-----	-----	-----	-----	-----	-----
20	2478. 36	40337. 2	----------	-----	-----	-----	-----	-----	-----
500	2478. 93	40327. 9	*a* $^6D_{2\frac{1}{2}}$—*z* $^6F^\circ_{2\frac{1}{2}}$	6	0. 334	1. 635	1. 301	0. 851	1. 468
5	2480. 20	40307. 0	*b* $^4F_{2\frac{1}{2}}$—*z* $^2P^\circ_{1\frac{1}{2}}$ *b* $^4D_{1\frac{1}{2}}$—*x* $^4P^\circ_{2\frac{1}{2}}$	-----	-----	-----	-----	-----	-----
30	2480. 81	40297. 1	*a* $^4H_{6\frac{1}{2}}$—*z* $^2I^\circ_{5\frac{1}{2}}$	5	. 181	(1. 23)	1. 05	. 09	2. 16?
200	2481. 11	40292. 4	*a* $^4G_{3\frac{1}{2}}$—*y* $^4H^\circ_{4\frac{1}{2}}$	4	-------	(1. 237)	1. 20	. 20*w*	1. 02+
15	2481. 85	40280. 4	*b* $^4F_{3\frac{1}{2}}$—*x* $^4D^\circ_{3\frac{1}{2}}$	-----	-----	-----	-----	-----	-----
60	2482. 78	40265. 2	*b* $^4D_{2\frac{1}{2}}$—*w* $^4D^\circ_{2\frac{1}{2}}$	6	(0. 044)	1. 345	1. 301	. 110	1. 323
1	2483. 20	40258. 5	----------	-----	-----	-----	-----	-----	-----
3	2483. 54	40253. 0	----------	-----	-----	-----	-----	-----	-----
50	2483. 96	40246. 2	*a* $^4H_{6\frac{1}{2}}$—*z* $^4I^\circ_{6\frac{1}{2}}$	6	(0. 10)	1. 23	1. 03	. 67−	1. 13±
5	2484. 49	40237. 5	*a* $^2F_{3\frac{1}{2}}$—*z* $^4H^\circ_{3\frac{1}{2}}$	-----	-----	-----	-----	-----	-----
10	2484. 67	40234. 6	*b* $^4D_{0\frac{1}{2}}$—*x* $^4P^\circ_{0\frac{1}{2}}$	6	1. 62	0. 14	1. 76	. 81	0. 95
8	2487. 20	40193. 7	*b* $^4D_{2\frac{1}{2}}$—*y* $^6P^\circ_{3\frac{1}{2}}$	5*	0. 268	1. 306	1. 574	. 135	2. 244?
4*H*	2487. 51	40188. 7	*b* $^4P_{2\frac{1}{2}}$—*z* $^2F^\circ_{2\frac{1}{2}}$	-----	-----	-----	-----	-----	-----
3	2487. 90	40182. 4	*a* $^4H_{3\frac{1}{2}}$—*x* $^4D^\circ_{3\frac{1}{2}}$?	-----	-----	-----	-----	-----	-----
30	2488. 57	40171. 6	*b* $^4F_{3\frac{1}{2}}$—*z* $^2H^\circ_{4\frac{1}{2}}$	4	-------	(1. 093)	1. 02	. 23*w*	0. 76+
3	2488. 88	40166. 6	----------	-----	-----	-----	-----	-----	-----
50	2489. 34	40159. 2	*a* $^2I_{5\frac{1}{2}}$—*w* $^2H^\circ_{4\frac{1}{2}}$	4	-------	(0. 90)	0. 91	*w*	. 87
6	2490. 54	40139. 8	*a* $^4H_{5\frac{1}{2}}$—*z* $^2I^\circ_{5\frac{1}{2}}$	-----	-----	-----	-----	-----	-----
50	2491. 08	40131. 2	*a* $^4G_{3\frac{1}{2}}$—*y* $^2D^\circ_{2\frac{1}{2}}$	-----	-----	-----	-----	-----	-----
40	2491. 10	40130. 8	*a* $^4H_{4\frac{1}{2}}$—*z* $^2I^\circ_{5\frac{1}{2}}$	-----	-----	-----	-----	-----	-----
5	2491. 34	40127. 0	*b* $^4F_{2\frac{1}{2}}$—*y* $^2G^\circ_{3\frac{1}{2}}$	5	-------	(0. 943)	1. 028	*w*	1. 24−
40	2491. 56	40123. 4	*b* $^4D_{2\frac{1}{2}}$—*w* $^4F^\circ_{3\frac{1}{2}}$	7, 4	-------	(1. 344)	1. 32	0	1. 26
5	2493. 59	40090. 9	*b* $^4F_{2\frac{1}{2}}$—*x* $^4D^\circ_{3\frac{1}{2}}$	-----	-----	-----	-----	-----	-----
300	2493. 68	40089. 2	*a* $^4H_{5\frac{1}{2}}$—*z* $^4I^\circ_{6\frac{1}{2}}$	7*	-------	-------	-------	0	1. 124
10	2494. 16	40081. 6	*b* $^4D_{1\frac{1}{2}}$—*w* $^4F^\circ_{2\frac{1}{2}}$	-----	-----	-----	-----	-----	-----
40	2494. 48	40076. 4	*a* $^6D_{1\frac{1}{2}}$—*z* $^6F^\circ_{0\frac{1}{2}}$	5	2. 50	1. 83	−0. 67	1. 25	3. 08
2*h*	2495. 35	40062. 4	----------	-----	-----	-----	-----	-----	-----
200	2495. 69	40057. 0	*b* $^4F_{4\frac{1}{2}}$—*y* $^4G^\circ_{5\frac{1}{2}}$	4	-------	(1. 200)	1. 17	*w*	1. 03+
2*h*	2495. 94	40053. 0	----------	-----	-----	-----	-----	-----	-----
25	2496. 86	40038. 2	----------	6	-------	-------	-------	0. 26−	0. 98±
1	2497. 36	40030. 2	*b* $^4D_{3\frac{1}{2}}$—*x* $^2H^\circ_{4\frac{1}{2}}$?	-----	-----	-----	-----	-----	-----
200	2498. 41	40013. 4	*a* $^6D_{1\frac{1}{2}}$—*z* $^6F^\circ_{1\frac{1}{2}}$	?					
200	2498. 58	40010. 7	*a* $^6D_{2\frac{1}{2}}$—*z* $^6F^\circ_{3\frac{1}{2}}$	4	0. 180	1. 637	1. 457	. 091	1. 007
8	2499. 38	39997. 8	*b* $^4F_{3\frac{1}{2}}$—*y* $^4G^\circ_{2\frac{1}{2}}$	-----	-----	-----	-----	-----	-----
3	2499. 56	39994. 9	----------	-----	-----	-----	-----	-----	-----
50	2500. 14	39985. 6	*a* $^2I_{6\frac{1}{2}}$—*y* $^2I^\circ_{5\frac{1}{2}}$	5	(0. 08)	1. 08	1. 00	. 41*w*	1. 52−
100	2501. 95	39956. 8	*b* $^4F_{4\frac{1}{2}}$—*z* $^2H^\circ_{5\frac{1}{2}}$	4	(0. 06)	1. 20	1. 14	. 25*w*	0. 87+
40*h*	2502. 30	39951. 3	*b* $^4D_{2\frac{1}{2}}$—*w* $^4F^\circ_{3\frac{1}{2}}$ *b* $^4D_{3\frac{1}{2}}$—*w* $^4D^\circ_{2\frac{1}{2}}$	-----	-----	-----	-----	-----	-----
5*H*	2503. 22	39936. 5	----------	-----	-----	-----	-----	-----	-----
10	2504. 92	39909. 5	*b* $^2G_{4\frac{1}{2}}$—*y* $^2I^\circ_{5\frac{1}{2}}$	-----	-----	-----	-----	-----	-----
10	2505. 64	39897. 9	*a* $^2G_{4\frac{1}{2}}$—*z* $^6F^\circ_{3\frac{1}{2}}$ *b* $^4D_{1\frac{1}{2}}$—$2^\circ_{1\frac{1}{2}}$	-----	-----	-----	-----	-----	-----
15	2505. 89	39894. 0	*a* $^4H_{4\frac{1}{2}}$—*z* $^2F^\circ_{3\frac{1}{2}}$	-----	-----	-----	-----	-----	-----
25	2506. 25	39888. 2	*a* $^4G_{3\frac{1}{2}}$—*x* $^4G^\circ_{4\frac{1}{2}}$	-----	-----	-----	-----	-----	-----
25	2506. 42	39885. 5	*b* $^4D_{3\frac{1}{2}}$—*w* $^4F^\circ_{4\frac{1}{2}}$	-----	-----	-----	-----	-----	-----
300	2507. 00	39876. 3	*a* $^6D_{1\frac{1}{2}}$—*z* $^6F^\circ_{2\frac{1}{2}}$	4	0. 536	1. 869	1. 333	. 267	0. 592
4	2507. 50	39868. 4	----------	-----	-----	-----	-----	-----	-----

TABLE 6. *The second spectrum of ruthenium* (Ru II)—Continued

1 Intensity	2 λ (air)	3 σ	4 Term combination	5 Type	6 Δg	7 g	8 g	9 Strong p	10 Strong n
	A	*K*							
100	2508. 67	39849. 8	$a\ {}^2I_{6\frac{1}{2}}$—$y\ {}^2I^\circ_{6\frac{1}{2}}$	7	(0. 00)	1. 08	1. 08	0	1. 08
3	2509. 42	39837. 8	$c\ {}^2G_{3\frac{1}{2}}$—$w\ {}^2D^\circ_{2\frac{1}{2}}$	-----	-------	-------	-------	-------	-------
6*H*	2511. 22	39809. 3	$b\ {}^4D_{3\frac{1}{2}}$—$w\ {}^4F^\circ_{3\frac{1}{2}}$	-----	-------	-------	-------	-------	-------
1	2511. 59	39803. 4	----------	-----	-------	-------	-------	-------	-------
5*H*	2512. 52	39788. 7	----------	-----	-------	-------	-------	-------	-------
150	2513. 32	39776. 0	$a\ {}^6D_{0\frac{1}{2}}$—$z\ {}^6F^\circ_{0\frac{1}{2}}$	6	3. 87	3. 28	−0. 59	1. 935	1. 347
1	2513. 61	39771. 5	$b\ {}^2F_{3\frac{1}{2}}$—$x\ {}^2G^\circ_{3\frac{1}{2}}$	-----	-------	-------	-------	-------	-------
3*h*	2514. 16	39762. 8	$b\ {}^2D_{2\frac{1}{2}}$—$x\ {}^2D^\circ_{1\frac{1}{2}}$	-----	-------	-------	-------	-------	-------
8	2515. 63	39739. 5	$b\ {}^4P_{2\frac{1}{2}}$—$x\ {}^4D^\circ_{2\frac{1}{2}}$	6*us*	-------	-------	-------	-------	-------
10	2516. 71	39722. 4	$a\ {}^2I_{6\frac{1}{2}}$—$w\ {}^2H^\circ_{5\frac{1}{2}}$	-----	-------	-------	-------	-------	-------
200	2517. 32	39712. 8	$a\ {}^6D_{0\frac{1}{2}}$—$z\ {}^6F^\circ_{1\frac{1}{2}}$	4	2. 21	3. 26	1. 05	1. 11	−0. 06?
100	2518. 41	39695. 6	$a\ {}^2I_{5\frac{1}{2}}$—$y\ {}^2I^\circ_{5\frac{1}{2}}$	6	(0. 05)	0. 90	0. 95	0. 29	. 93
75	2519. 20	39683. 2	$b\ {}^4P_{1\frac{1}{2}}$—$y\ {}^4D^\circ_{2\frac{1}{2}}$	4	0. 327	1. 634	1. 307	. 164	. 817
10	2520. 57	39661. 6	$b\ {}^4P_{0\frac{1}{2}}$—$1^\circ_{1\frac{1}{2}}$	-----	-------	-------	-------	-------	-------
40	2520. 82	39657. 6	$a\ {}^4H_{4\frac{1}{2}}$—$z\ {}^2G^\circ_{4\frac{1}{2}}$	6*us*	-------	1. 14	1. 00	. 20	1. 07
3	2522. 26	39634. 9	$b\ {}^4D_{1\frac{1}{2}}$—$w\ {}^4F^\circ_{1\frac{1}{2}}$	-----	-------	-------	-------	-------	-------
25	2522. 59	39629. 9	----------	-----	-------	-------	-------	0	1. 101
1	2522. 74	39627. 5	----------	-----	-------	-------	-------	-------	-------
8	2523. 16	39620. 9	$b\ {}^4F_{4\frac{1}{2}}$—$y\ {}^4G^\circ_{4\frac{1}{2}}$	6	(0. 05)	(1. 200)	1. 15	0. 23	?
1	2523. 72	39612. 1	----------	-----	-------	-------	-------	-------	-------
20	2524. 39	39601. 7	$b\ {}^4F_{1\frac{1}{2}}$—$x\ {}^4D^\circ_{0\frac{1}{2}}$	7	-------	(0. 415)	0. 40	0	0. 42
100	2524. 85	39594. 4	$a\ {}^4H_{6\frac{1}{2}}$—$z\ {}^2I^\circ_{6\frac{1}{2}}$	6	(0. 08)	1. 20	1. 12	0. 51	1. 16±
200*H*	2525. 42	39585. 5	----------	-----	-------	-------	-------	-------	-------
25	2526. 88	39562. 5	$b\ {}^4D_{0\frac{1}{2}}$—$w\ {}^4F^\circ_{1\frac{1}{2}}$	5	0. 368	0. 131	0. 499	. 184	0. 683
20	2527. 07	39559. 6	$a\ {}^2I_{5\frac{1}{2}}$—$y\ {}^2I^\circ_{6\frac{1}{2}}$	-----	-------	-------	-------	-------	-------
3	2527. 30	39556. 0	$a\ {}^4G_{4\frac{1}{2}}$—$y\ {}^4H^\circ_{3\frac{1}{2}}$	-----	-------	-------	-------	-------	-------
200	2527. 86	39547. 2	$a\ {}^4G_{4\frac{1}{2}}$—$y\ {}^4H^\circ_{5\frac{1}{2}}$	4	(0. 06)	1. 17	1. 11	0. 29*w*	. 84+
100	2528. 05	39544. 3	$c\ {}^2G_{4\frac{1}{2}}$—$w\ {}^2F^\circ_{3\frac{1}{2}}$	7	-------	-------	-------	0	1. 04
20	2529. 61	39520. 0	$a\ {}^4H_{6\frac{1}{2}}$—$z\ {}^4I^\circ_{5\frac{1}{2}}$	5	0. 184?	(1. 23)	1. 05	0. 09	?
10	2530. 04	39513. 2	$a\ {}^4G_{4\frac{1}{2}}$—$y\ {}^4H^\circ_{4\frac{1}{2}}$	-----	-------	-------	-------	-------	-------
70	2530. 41	39507. 4	$b\ {}^4F_{2\frac{1}{2}}$—$y\ {}^4G^\circ_{3\frac{1}{2}}$	5	(0. 08)	0. 92	1. 00	. 19*w*	1. 20−
2	2531. 68	39487. 6	----------	-----	-------	-------	-------	-------	-------
10	2533. 03	39466. 6	----------	-----	-------	-------	-------	-------	-------
6	2533. 39	39461. 0	$b\ {}^2P_{1\frac{1}{2}}$—$x\ {}^4P^\circ_{2\frac{1}{2}}$	4	0. 56	(1. 188)	1. 748	0. 28	?
100	2533. 97	39451. 9	$b\ {}^4F_{1\frac{1}{2}}$—$y\ {}^4G^\circ_{2\frac{1}{2}}$	5	. 268	0. 426	0. 694	. 134	1. 096
80	2534. 92	39437. 1	$a\ {}^4H_{5\frac{1}{2}}$—$z\ {}^2I^\circ_{6\frac{1}{2}}$	?	-------	-------	-------	-------	-------
50	2535. 23	39432. 4	$a\ {}^2I_{5\frac{1}{2}}$—$w\ {}^2H^\circ_{5\frac{1}{2}}$	-----	-------	-------	-------	-------	-------
100	2535. 60	39426. 6	$b\ {}^4P_{2\frac{1}{2}}$—$y\ {}^4D^\circ_{3\frac{1}{2}}$	4	0. 226	1. 565	1. 339	0. 111	0. 774
5	2536. 30	39415. 7	$b\ {}^2G_{4\frac{1}{2}}$—$w\ {}^2G^\circ_{3\frac{1}{2}}$	-----	-------	-------	-------	-------	-------
3	2536. 68	39409. 8	----------	-----	-------	-------	-------	-------	-------
10*Hw*	2537. 34	39399. 5	----------	-----	-------	-------	-------	-------	-------
100	2539. 72	39362. 6	$a\ {}^4H_{5\frac{1}{2}}$—$z\ {}^4I^\circ_{5\frac{1}{2}}$ $a\ {}^4G_{2\frac{1}{2}}$—$y\ {}^4H^\circ_{3\frac{1}{2}}$	-----	-------	-------	-------	-------	-------
100	2540. 30	39353. 6	$a\ {}^4H_{4\frac{1}{2}}$—$z\ {}^4I^\circ_{5\frac{1}{2}}$	-----	-------	-------	-------	-------	-------
1	2540. 84	39345. 2	----------	-----	-------	-------	-------	-------	-------
1	2541. 80	39330. 4	$b\ {}^2G_{4\frac{1}{2}}$—$w\ {}^2G^\circ_{4\frac{1}{2}}$	-----	-------	-------	-------	-------	-------
25	2542. 04	39326. 7	$a\ {}^4G_{2\frac{1}{2}}$—$x\ {}^4F^\circ_{1\frac{1}{2}}$	7	(0. 00)	0. 648	0. 648	0	. 648
20	2542. 23	39323. 7	$b\ {}^2H_{4\frac{1}{2}}$—$y\ {}^2F^\circ_{3\frac{1}{2}}$	4	0. 172	. 958	1. 130	0. 086	?
100	2542. 146	39309. 6	$a\ {}^4G_{5\frac{1}{2}}$—$x\ {}^4G^\circ_{5\frac{1}{2}}$	-----	-------	-------	-------	-------	-------
100	2543. 216	39308. 5	$a\ {}^4H_{3\frac{1}{2}}$—$z\ {}^2G^\circ_{4\frac{1}{2}}$	-----	-------	-------	-------	-------	-------
300	2543. 272	39307. 6	$a\ {}^4H_{6\frac{1}{2}}$—$z\ {}^4I^\circ_{7\frac{1}{2}}$	4	(0. 03)	1. 235	1. 205	. 20*w*	1. 02+
100	2543. 47	39304. 6	$a\ {}^4G_{4\frac{1}{2}}$—$x\ {}^4F^\circ_{3\frac{1}{2}}$	-----	-------	-------	-------	-------	-------
2	2544. 18	39293. 6	$b\ {}^2F_{2\frac{1}{2}}$—$x\ {}^2D^\circ_{1\frac{1}{2}}$	-----	-------	-------	-------	-------	-------
1	2545. 29	39276. 5	----------	-----	-------	-------	-------	-------	-------
3H*w*	2545. 81	39268. 4	----------	-----	-------	-------	-------	-------	-------
2*H*	2546. 40	39259. 3	$a\ {}^4G_{2\frac{1}{2}}$—$x\ {}^4G^\circ_{3\frac{1}{2}}$	-----	-------	-------	-------	-------	-------

TABLE 6. *The second spectrum of ruthenium* (Ru II)—Continued

1 Intensity	2 λ (air)	3 σ	4 Term combination	5 Type	6 Δg	7 g	8 g	9 Strong p	10 Strong s
	A	*K*							
20	2547. 66	39239. 9	$b\ ^2H_{4\frac{1}{2}}—y\ ^2H^o_{4\frac{1}{2}}$	7	-------	0. 95	0. 96	0	0. 955
8	2547. 95	39235. 5	$b\ ^2P_{1\frac{1}{2}}—w\ ^4F^o_{2\frac{1}{2}}$	4	0. 184	1. 168	. 984	0. 092	0. 709
2	2548. 31	39229. 9	$b\ ^4D_{2\frac{1}{2}}—x\ ^2F^o_{3\frac{1}{2}}$	-----	-------	-------	-------	-------	-------
3	2548. 78	39222. 7	----------	-----	-------	-------	-------	-------	-------
50	2549. 121	39217. 4	$a\ ^4H_{5\frac{1}{2}}—y\ ^4F^o_{4\frac{1}{2}}$	-----	-------	-------	-------	-------	-------
100	2549. 171	39216. 7	$b\ ^4F_{3\frac{1}{2}}—y\ ^4G^o_{4\frac{1}{2}}$	5*us*	-------	-------	-------	*w*	-------
80	2549. 79	39207. 1	$a\ ^4G_{3\frac{1}{2}}—x\ ^4F^o_{2\frac{1}{2}}$	7, 5	-------	(1. 021)	1. 00	0	1. 06
5	2551. 56	39179. 8	$b\ ^2F_{3\frac{1}{2}}—w\ ^4F^o_{4\frac{1}{2}}$	5	. 22	1. 06	1. 28	0. 11	2. 05?
150	2551. 98	39173. 5	$a\ ^4G_{3\frac{1}{2}}—y\ ^4H^o_{4\frac{1}{2}}$	5*us*	-------	(1. 021)	1. 00	*w*	0. 96
8	2553. 49	39150. 4	$b\ ^4F_{3\frac{1}{2}}—z\ ^2F^o_{2\frac{1}{2}}$	-----	-------	-------	-------	-------	-------
1*h*	2554. 29	39138. 1	----------	-----	-------	-------	-------	-------	-------
1*h*	2554. 82	39130. 0	$b\ ^4P_{0\frac{1}{2}}—x\ ^4F^o_{1\frac{1}{2}}$	-----	-------	-------	-------	-------	-------
5	2555. 70	39116. 6	$a\ ^2I_{5\frac{1}{2}}—w\ ^2G^o_{4\frac{1}{2}}$	-----	-------	-------	-------	-------	-------
30	2555. 93	39113. 0	$a\ ^4G_{3\frac{1}{2}}—x\ ^4G^o_{3\frac{1}{2}}$	7	(0. 00)	1. 00	1. 00	0	1. 00
30	2556. 08	39110. 7	$a\ ^4G_{2\frac{1}{2}}—x\ ^4F^o_{3\frac{1}{2}}$	5	0. 40	0. 65	1. 054	0. 20	2. 05
15	2556. 72	39100. 9	$b\ ^4P_{2\frac{1}{2}}—z\ ^2F^o_{3\frac{1}{2}}$	4	. 38	1. 584	1. 204	. 191	0. 254
15	2557. 15	39094. 2	$a\ ^4H_{4\frac{1}{2}}—z\ ^2G^o_{3\frac{1}{2}}$?	7*us*	-------	-------	-------	*w*	1. 13
3	2558. 02	39081. 0	$a\ ^4G_{4\frac{1}{2}}—y\ ^2G^o_{4\frac{1}{2}}$	6	(0. 107)	1. 16	1. 05	0. 48—	1. 11±
15	2559. 56	39057. 6	----------	7	-------	-------	-------	0	0. 874
3	2559. 96	39051. 4	$b\ ^2P_{1\frac{1}{2}}—2^o_{1\frac{1}{2}}$	6	0. 16	1. 18	1. 34	0. 24	1. 26
1	2561. 22	39032. 2	----------	-----	-------	-------	-------	-------	-------
1	2561. 45	39028. 7	$a\ ^4P_{2\frac{1}{2}}—z\ ^6D^o_{2\frac{1}{2}}$	-----	-------	-------	-------	-------	-------
2	2562. 94	39026. 0	$b\ ^2P_{1\frac{1}{2}}—y\ ^6P^o_{1\frac{1}{2}}$	6*	. 42	2. 07	2. 49	. 64	2. 28
1	2563. 28	39000. 8	----------	-----	-------	-------	-------	-------	-------
1	2563. 61	38995. 8	$c\ ^2G_{3\frac{1}{2}}—w\ ^2F^o_{3\frac{1}{2}}$	-----	-------	-------	-------	-------	-------
8	2563. 91	38991. 2	$b\ ^4D_{2\frac{1}{2}}—y\ ^2F^o_{3\frac{1}{2}}$	4	. 225	1. 345	1. 120	0. 114	0. 558
1	2564. 83	38977. 2	$b\ ^4D_{1\frac{1}{2}}—x\ ^4P^o_{1\frac{1}{2}}$	-----	-------	-------	-------	-------	-------
40	2565. 69	38964. 2	$b\ ^4F_{2\frac{1}{2}}—x\ ^4D^o_{1\frac{1}{2}}$	4	. 252	0. 940	1. 192	1. 25	. 562
5	2565. 94	38960. 4	$b\ ^4F_{2\frac{1}{2}}—z\ ^2F^o_{2\frac{1}{2}}$	-----	-------	-------	-------	-------	-------
40	2566. 25	38955. 7	$c\ ^2G_{4\frac{1}{2}}—w\ ^2H^o_{4\frac{1}{2}}$	6	(0. 14)	(1. 078)	0. 94	. 62—	?
20	2566. 59	38950. 5	$b\ ^4P_{0\frac{1}{2}}—z\ ^2P^o_{0\frac{1}{2}}$	-----	-------	-------	-------	-------	-------
100	2568. 88	38915. 9	$b\ ^4D_{3\frac{1}{2}}—x\ ^2F^o_{3\frac{1}{2}}$	6	0. 250	1. 39	1. 14	. 877	1. 27
1	2569. 41	38907. 7	----------	-----	-------	-------	-------	-------	-------
8	2569. 58	38905. 3	$b\ ^4D_{0\frac{1}{2}}—x\ ^4P^o_{1\frac{1}{2}}$ $c\ ^2D_{1\frac{1}{2}}—w\ ^2D^o_{1\frac{1}{2}}$	}	-------	-------	-------	-------	-------
150	2571. 09	38882. 3	$a\ ^4G_{5\frac{1}{2}}—x\ ^4F^o_{4\frac{1}{2}}$	5	-------	(1. 237)	1. 20	*w*	1. 39—
1	2571. 44	38877. 1	----------	-----	-------	-------	-------	-------	-------
1	2571. 73	38872. 6	----------	-----	-------	-------	-------	-------	-------
10	2572. 67	38858. 5	$a\ ^4H_{3\frac{1}{2}}—y\ ^4F^o_{4\frac{1}{2}}$	5	0. 400	0. 752	1. 152	0. 200	2. 552
3*Hw*	2573. 11	38851. 8	----------	-----	-------	-------	-------	-------	-------
50	2573. 44	38846. 9	$b\ ^4D_{2\frac{1}{2}}—x\ ^4P^o_{1\frac{1}{2}}$	4	. 225	1. 335	1. 560	. 114	0. 997
25	2574. 06	38837. 5	$c\ ^2D_{2\frac{1}{2}}—w\ ^2D^o_{2\frac{1}{2}}$	6	(0. 10)	1. 17	1. 07	. 297—	1. 12±
5	2574. 53	38830. 4	$b\ ^2G_{3\frac{1}{2}}—w\ ^2G^o_{4\frac{1}{2}}$	-----	-------	-------	-------	-------	-------
1*h*	2575. 58	38814. 6	----------	-----	-------	-------	-------	-------	-------
2	2575. 93	38809. 2	$b\ ^4P_{1\frac{1}{2}}—y\ ^4D^o_{1\frac{1}{2}}$	-----	-------	-------	-------	-------	-------
50	2576. 09	38806. 9	$a\ ^4G_{4\frac{1}{2}}—x\ ^4G^o_{4\frac{1}{2}}$	7	(0. 00)	1. 19	1. 19	0	1. 185
10	2576. 99	38793. 4	$b\ ^4F_{4\frac{1}{2}}—y\ ^4D^o_{3\frac{1}{2}}$	4	(0. 14)	1. 20	1. 34	0. 51*w*	0. 71+
5	2577. 31	38788. 5	$b\ ^2P_{1\frac{1}{2}}—w\ ^4F^o_{1\frac{1}{2}}$	-----	-------	-------	-------	-------	-------
2	2578. 11	38776. 5	$a\ ^4H_{3\frac{1}{2}}—z\ ^2D^o_{2\frac{1}{2}}$	4	0. 56	(0. 753)	1. 31	. 28	?
60	2579. 10	38761. 7	$a\ ^4G_{2\frac{1}{2}}—x\ ^4G^o_{2\frac{1}{2}}$	6	(0. 044)	0. 666	0. 710	. 108	. 688
5	2580. 22	38744. 8	$a\ ^4H_{3\frac{1}{2}}—z\ ^2G^o_{3\frac{1}{2}}$	-----	-------	-------	-------	-------	-------
5	2580. 45	38741. 3	$a\ ^4G_{3\frac{1}{2}}—y\ ^2G^o_{4\frac{1}{2}}$	-----	-------	-------	-------	-------	-------
5	2581. 43	38726. 6	----------	-----	-------	-------	-------	. 31	?
3	2582. 54	38710. 0	$b\ ^4D_{1\frac{1}{2}}—y\ ^2F^o_{2\frac{1}{2}}$	7	-------	(1. 200)	1. 20	0	1. 19?
10	2582. 90	38704. 7	$b\ ^4F_{4\frac{1}{2}}—z\ ^2I^o_{5\frac{1}{2}}$	-----	-------	-------	-------	-------	-------
20	2583. 07	38702. 0	$b\ ^4F_{3\frac{1}{2}}—x\ ^4D^o_{2\frac{1}{2}}$	4	0. 19	1. 10	1. 29	0. 093	0. 633

TABLE 6. *The second spectrum of ruthenium* (Ru II)—Continued

1 Intensity	2 λ (air)	3 σ	4 Term combination	5 Type	6 Δg	7 g	8 g	9 Strong p	10 Strong n
	A	*K*							
10*H*	2586. 83	38645. 8							
75	2587. 87	38630. 2	$a\ {}^4H_{4\frac{1}{2}}—y\ {}^4F^o_{3\frac{1}{2}}$						
1	2588. 68	38618. 2							
2	2588. 88	38615. 2	$a\ {}^4G_{3\frac{1}{2}}—x\ {}^4G^o_{2\frac{1}{2}}$						
100*w*	2589. 43	38607. 0	$b\ {}^4F_{1\frac{1}{2}}—x\ {}^4D^o_{1\frac{1}{2}}$						
75	2591. 04	38583. 0	$a\ {}^4G_{5\frac{1}{2}}—y\ {}^4G^o_{5\frac{1}{2}}$	6	(0. 07)	1. 23	1. 16	. 37—	1. 19±
75	2591. 26	38579. 7	$b\ {}^2H_{5\frac{1}{2}}—y\ {}^2H^o_{5\frac{1}{2}}$ $b\ {}^4D_{2\frac{1}{2}}—y\ {}^2F^o_{2\frac{1}{2}}$						
1	2593. 15	38551. 6	$a\ {}^2G_{3\frac{1}{2}}—z\ {}^6F^o_{4\frac{1}{2}}$						
50*H*	2594. 41	38532. 9							
4	2595. 54	38516. 1	$b\ {}^2H_{4\frac{1}{2}}—y\ {}^2H^o_{5\frac{1}{2}}$						
50	2595. 81	38512. 1	$b\ {}^4F_{2\frac{1}{2}}—x\ {}^4D^o_{2\frac{1}{2}}$	6	0. 338	0. 942	1. 28	0. 854	1. 111
1	2596. 81	38497. 3	$b\ {}^2P_{0\frac{1}{2}}—x\ {}^2D^o_{1\frac{1}{2}}$						
10	2597. 14	38492. 4	$c\ {}^2G_{4\frac{1}{2}}—y\ {}^2I^o_{5\frac{1}{2}}$						
5	2597. 79	38482. 8	$a\ {}^4G_{3\frac{1}{2}}—z\ {}^2H^o_{3\frac{1}{2}}$						
15	2598. 80	38467. 7	$b\ {}^4F_{4\frac{1}{2}}—z\ {}^2F^o_{3\frac{1}{2}}$	7		(1. 200)	1. 20	0	1. 220
15	2599. 68	38454. 7	$b\ {}^2D_{2\frac{1}{2}}—w\ {}^4D^o_{2\frac{1}{2}}$? $a\ {}^4P_{2\frac{1}{2}}—z\ {}^6D^o_{3\frac{1}{2}}$	7		(1. 57)	1. 56	0	1. 550
30	2602. 26	38416. 6		4				0. 24*w*	1. 03+
5	2602. 88	38407. 4	$c\ {}^2G_{3\frac{1}{2}}—w\ {}^2H^o_{3\frac{1}{2}}$	7, 5		(0. 942)	0. 948	0	0. 967
1	2603. 25	38402. 1	$b\ {}^2D_{1\frac{1}{2}}—x\ {}^4P^o_{0\frac{1}{2}}$						
10	2604. 13	38389. 1	$b\ {}^4F_{3\frac{1}{2}}—y\ {}^4D^o_{3\frac{1}{2}}$	6	. 254	1. 094	1. 348	0. 902	1. 221
10*Hw*	2606. 21	38358. 4		7				0	0. 861
5	2606. 91	38348. 1							
1	2607. 49	38339. 6							
5	2607. 79	38335. 2	$a\ {}^4P_{0\frac{1}{2}}—z\ {}^6D^o_{1\frac{1}{2}}$		. 73	2. 57	(1. 84)	0. 365	?
20	2607. 92	38333. 4	$b\ {}^4P_{2\frac{1}{2}}—z\ {}^2D^o_{2\frac{1}{2}}$	6	. 246	1. 573	1. 327	. 626	1. 450
1	2609. 30	38312. 9	$b\ {}^2D_{2\frac{1}{2}}—w\ {}^4F^o_{3\frac{1}{2}}$						
25	2610. 09	38301. 4	$b\ {}^4P_{2\frac{1}{2}}—z\ {}^2G^o_{3\frac{1}{2}}$	4	. 547	1. 608	1. 060	. 276	−0. 310
40	2611. 50	38280. 7	$a\ {}^4H_{3\frac{1}{2}}—y\ {}^4F^o_{3\frac{1}{2}}$	6	. 300	0. 798	1. 042	1. 064	. 890
3	2611. 84	38275. 7	$a\ {}^4H_{5\frac{1}{2}}—z\ {}^4I^o_{4\frac{1}{2}}$						
5	2612. 44	38266. 9	$a\ {}^4H_{4\frac{1}{2}}—z\ {}^4I^o_{4\frac{1}{2}}$						
40	2612. 52	38265. 8	$b\ {}^4D_{3\frac{1}{2}}—y\ {}^2F^o_{2\frac{1}{2}}$	5	. 192	1. 385	1. 193	0. 094	1. 865
5*H*	2613. 31	38254. 2							
50	2614. 86	38231. 5	$b\ {}^4F_{4\frac{1}{2}}—z\ {}^2G^o_{4\frac{1}{2}}$	6	0. 203	1. 200	0. 994	0. 927	
75	2615. 05	38228. 8	$a\ {}^4G_{4\frac{1}{2}}—x\ {}^4G^o_{5\frac{1}{2}}$ $c\ {}^2G_{4\frac{1}{2}}—w\ {}^2H^o_{5\frac{1}{2}}$	4		(1. 167)	1. 15	*w*	1. 074
1	2615. 43	38223. 2	$a\ {}^2P_{1\frac{1}{2}}—z\ {}^6F^o_{2\frac{1}{2}}$						
25	2616. 33	38210. 1	$b\ {}^2F_{3\frac{1}{2}}—x\ {}^2F^o_{3\frac{1}{2}}$	6	(0. 05)	(1. 083)	1. 13	0. 17	?
40	2617. 08	38199. 2	$b\ {}^4F_{2\frac{1}{2}}—y\ {}^4D^o_{3\frac{1}{2}}$	5	0. 410	0. 933	1. 343	. 206	2. 368
10	2617. 45	38193. 7							
1*h*	2618. 59	38177. 0	$b\ {}^2D_{1\frac{1}{2}}—w\ {}^4F^o_{2\frac{1}{2}}$						
50	2619. 35	38166. 0	$a\ {}^4G_{4\frac{1}{2}}—y\ {}^2G^o_{3\frac{1}{2}}$	5	. 138	1. 166	1. 028	. 067	1. 649
5	2620. 06	38155. 6	$b\ {}^4F_{1\frac{1}{2}}—x\ {}^4D^o_{2\frac{1}{2}}$	5	. 91	0. 38	1. 29	. 46	2. 65
20	2620. 69	38146. 5	$a\ {}^4G_{5\frac{1}{2}}—y\ {}^4G^o_{4\frac{1}{2}}$						
20	2621. 28	38138. 0	$b\ {}^4F_{1\frac{1}{2}}—y\ {}^4D^o_{0\frac{1}{2}}$	4	. 372	0. 421	0. 793	. 186	0. 235
3	2621. 74	38131. 3	$b\ {}^2P_{1\frac{1}{2}}—x\ {}^4P^o_{1\frac{1}{2}}$						
2	2621. 85	38129. 6	$a\ {}^4G_{4\frac{1}{2}}—x\ {}^4D^o_{3\frac{1}{2}}$						
3*Hw*	2622. 26	38123. 7							
10*Hw*	2623. 43	38106. 6	$c\ {}^2D_{1\frac{1}{2}}—w\ {}^2D^o_{2\frac{1}{2}}$						
40	2624. 17	38095. 9	$b\ {}^4D_{2\frac{1}{2}}—x\ {}^4P^o_{2\frac{1}{2}}$	6	(0. 09)	1. 34	1. 25	. 22—	1. 30±
5	2624. 71	38088. 1							
25	2625. 39	38078. 2	$b\ {}^2G_{3\frac{1}{2}}—w\ {}^4D^o_{3\frac{1}{2}}$	6	0. 248	0. 886	1. 134	. 877	1. 010
10	2625. 58	38075. 5	$b\ {}^4D_{0\frac{1}{2}}—z\ {}^2S^o_{0\frac{1}{2}}$						
30	2626. 41	38063. 4	$b\ {}^4F_{3\frac{1}{2}}—z\ {}^2F^o_{3\frac{1}{2}}$	6	(0. 106)	1. 095	1. 201	. 37—	1. 148±
15	2627. 31	38050. 3		7				0	1. 20
5	2627. 82	38043. 0		7				0	0. 861
5*Hw*	2628. 15	38038. 2							

TABLE 6. *The second spectrum of ruthenium* (Ru II)—Continued

1 Intensity	2 λ (air)	3 σ	4 Term combination	5 Type	6 Δg	7 g	8 g	9 Strong p	10 Strong n
	A	*K*							
75	2628. 75	38029. 5	$b\ ^2G_{4\frac{1}{2}}—x\ ^2G^0_{3\frac{1}{2}}$	7[a]				d?	1. 08
5	2629. 37	38020. 6	$a\ ^4G_{4\frac{1}{2}}—z\ ^2H^0_{4\frac{1}{2}}$	6	0. 159	(1. 167)	1. 008	0. 716	?
150	2630. 04	38010. 9	$a\ ^2I_{6\frac{1}{2}}—x\ ^2H^0_{5\frac{1}{2}}$	7, 4		(1. 08)	1. 09	0	1. 051
20	2631. 09	37995. 7	$a\ ^4H_{3\frac{1}{2}}—y\ ^4F^0_{2\frac{1}{2}}$	4	. 259	0. 758	1. 017	0. 126	0. 110
25	2632. 73	37972. 0	$a\ ^4G_{2\frac{1}{2}}—y\ ^2G^0_{3\frac{1}{2}}$	5	0. 381	0. 652	1. 035	0. 191	1. 604
5	2633. 50	37961. 0							
20	2633. 82	37956. 4	$b\ ^4P_{0\frac{1}{2}}—z\ ^2P^0_{1\frac{1}{2}}$	4	1. 372	2. 541	1. 169	−. 686	0. 483
10	2635. 21	37936. 3	$a\ ^4G_{2\frac{1}{2}}—x\ ^4D^0_{3\frac{1}{2}}$	5	0. 305	0. 647	0. 953	. 154	1. 718
10	2635. 34	37934. 4	$b\ ^2G_{4\frac{1}{2}}—x\ ^2H^0_{5\frac{1}{2}}$						
70	2635. 84	37927. 2	$b\ ^4F_{4\frac{1}{2}}—z\ ^4I^0_{5\frac{1}{2}}$	4	. 165	1. 207	1. 042	. 082	0. 300
100	2636. 54	37917. 2	$a\ ^4H_{3\frac{1}{2}}—z\ ^4I^0_{4\frac{1}{2}}$	5	. 200	0. 748	0. 948	. 100	1. 648
20	2636. 84	37912. 9	$c\ ^2G_{4\frac{1}{2}}—w\ ^2G^0_{4\frac{1}{2}}$	6	(0. 06)	1. 09	1. 03	. 27—	1. 065±
10	2638. 35	37891. 2	$b\ ^4D_{1\frac{1}{2}}—y\ ^2D^0_{1\frac{1}{2}}$	6	0. 457	1. 205	0. 748	. 697	0. 977
1	2639. 34	37877. 0							
15	2639. 58	37873. 5	$b\ ^4F_{2\frac{1}{2}}—z\ ^2F^0_{3\frac{1}{2}}$	5	. 254	1. 193	. 939	. 127	1. 828
50	2641. 63	37844. 2	$b\ ^2F_{2\frac{1}{2}}—w\ ^4F^0_{3\frac{1}{2}}$	7				0	1. 038
5	2642. 10	37837. 4	$b\ ^4P_{2\frac{1}{2}}—y\ ^4F^0_{3\frac{1}{2}}$	4	. 525	(1. 572)	1. 047	0. 262	
20	2642. 80	37827. 4	$b\ ^4F_{3\frac{1}{2}}—z\ ^2G^0_{4\frac{1}{2}}$						
30	2642. 88	37826. 2	$a\ ^4G_{3\frac{1}{2}}—y\ ^2G^0_{3\frac{1}{2}}$						
20	2643. 14	37822. 6	$a\ ^4H_{4\frac{1}{2}}—z\ ^4G^0_{3\frac{1}{2}}$						
3	2643. 40	37818. 7	$b\ ^4D_{0\frac{1}{2}}—y\ ^2D^0_{1\frac{1}{2}}$						
3	2643. 60	37815. 9	$a\ ^2I_{5\frac{1}{2}}—x\ ^2G^0_{4\frac{1}{2}}$						
40	2644. 62	37801. 4	$a\ ^4G_{4\frac{1}{2}}—x\ ^4F^0_{3\frac{1}{2}}$	6		(1. 167)	1. 19	*w*	1. 18±
75	2645. 97	37782. 0	$b\ ^4F_{4\frac{1}{2}}—y\ ^4F^0_{4\frac{1}{2}}$	6		1. 20	1. 15	. 23—	1. 18±
100	2648. 78	37742. 0	$a\ ^4H_{5\frac{1}{2}}—z\ ^4G^0_{4\frac{1}{2}}$					*us*	1. 16*us*
3	2650. 26	37720. 9	$a\ ^2I_{5\frac{1}{2}}—x\ ^2H^0_{5\frac{1}{2}}$						
10	2652. 94	37682. 8	$b\ ^4D_{1\frac{1}{2}}—y\ ^2D^0_{2\frac{1}{2}}$	4		(1. 200)	1. 15	*us*	1. 07*us*
8	2653. 10	37680. 6	$a\ ^4G_{3\frac{1}{2}}—z\ ^2H^0_{4\frac{1}{2}}$	7		(1. 021)	1. 016	0	1. 006
25	2653. 95	37668. 5	$b\ ^4F_{4\frac{1}{2}}—z\ ^2G^0_{3\frac{1}{2}}$	5	. 170	1. 202	1. 032	0. 086	1. 797
1*h*	2654. 524	37660. 33							
10	2654. 876	37655. 34	$b\ ^2P_{0\frac{1}{2}}—w\ ^4D^0_{0\frac{1}{2}}$?						
5	2655. 008	37653. 47	$a\ ^4G_{2\frac{1}{2}}—y\ ^4G^0_{2\frac{1}{2}}$						
300	2656. 235	37636. 07	$a\ ^4H_{6\frac{1}{2}}—z\ ^4H^0_{6\frac{1}{2}}$	6	(0. 08)	1. 22	1. 14	0. 51—	1. 18±
25	2657. 198	37622. 43							
10	2657. 326	37620. 62							
15	2658. 244	37607. 63	$b\ ^4P_{0\frac{1}{2}}—x\ ^4D^0_{0\frac{1}{2}}$	6		2. 53	0. 37	1. 08	1. 45
1	2658. 672	37601. 58							
1	2658. 922	37598. 04							
1	2660. 152	37580. 66	$c\ ^2D_{1\frac{1}{2}}—y\ ^2P^0_{1\frac{1}{2}}$						
200	2661. 169	37566. 30	$a\ ^4H_{6\frac{1}{2}}—z\ ^4G^0_{5\frac{1}{2}}$	7		(1. 23)	1. 24	0	1. 143
300	2661. 610	37560. 07	$a\ ^6D_{4\frac{1}{2}}—z\ ^6D^0_{3\frac{1}{2}}$	7		(1. 54)	1. 56	0	1. 502
20	2661. 82	37557. 11	$a\ ^4H_{3\frac{1}{2}}—z\ ^4G^0_{2\frac{1}{2}}$						
15	2662. 183	37551. 99	$b\ ^4D_{2\frac{1}{2}}—y\ ^2D^0_{2\frac{1}{2}}$						
25	2662. 880	37542. 16	$b\ ^4P_{1\frac{1}{2}}—y\ ^4D^0_{0\frac{1}{2}}$	5	0. 856	1. 652	0. 796	0. 428	2. 080
10	2663. 754	37529. 84	$b\ ^2G_{3\frac{1}{2}}—x\ ^2G^0_{4\frac{1}{2}}$	4	. 174	(0. 883)	. 709	. 087	?
2	2665. 376	37507. 00	$a\ ^4G_{3\frac{1}{2}}—y\ ^4G^0_{2\frac{1}{2}}$	5	. 330	(1. 021)	. 691	. 162	?
100	2667. 390	37478. 68	$a\ ^4H_{5\frac{1}{2}}—z\ ^4H^0_{5\frac{1}{2}}$	4*us*		(1. 16)	1. 14	*w*	1. 02
10	2667. 79	37473. 07	$a\ ^4H_{3\frac{1}{2}}—z\ ^4G^0_{3\frac{1}{2}}$	6	. 228	0. 752	0. 980	0. 798	0. 866
5	2668. 632	37461. 25	$a\ ^4G_{3\frac{1}{2}}—x\ ^4F^0_{3\frac{1}{2}}$						
75	2669. 43	37450. 05	$c\ ^2G_{3\frac{1}{2}}—w\ ^2G^0_{3\frac{1}{2}}$	6	(0. 031)	. 943	. 913	. 107	. 928
15	2670. 527	37434. 66		6				. 117	1. 120±
25	2672. 212	37411. 06	$b\ ^4P_{0\frac{1}{2}}—y\ ^4D^0_{1\frac{1}{2}}$						
25	2672. 354	37409. 07	$a\ ^4H_{5\frac{1}{2}}—z\ ^4G^0_{5\frac{1}{2}}$						
10	2672. 880	37401. 71	$a\ ^4G_{4\frac{1}{2}}—z\ ^2H^0_{5\frac{1}{2}}$						
30	2673. 004	37399. 98	$a\ ^4H_{4\frac{1}{2}}—z\ ^4G^0_{5\frac{1}{2}}$						

TABLE 6. *The second spectrum of ruthenium* (Ru II)—Continued

1 Intensity	2 λ (air)	3 σ	4 Term combination	5 Type	6 Δ *g*	7 *g*	8 *g*	9 Strong *p*	10 Strong *n*
	A	*K*							
10	2674. 219	37382. 99	$a\ ^4H_{3\frac{1}{2}}—z\ ^4G^\circ_{4\frac{1}{2}}$	5	0. 380	(0. 753)	1. 133	. 190	?
10	2675. 197	37369. 32	$b\ ^4F_{2\frac{1}{2}}—y\ ^4P^\circ_{1\frac{1}{2}}$	-----	-------	-------	-------	-------	-------
25	2675. 543	37364. 49	$c\ ^2G_{3\frac{1}{2}}—w\ ^2G^\circ_{4\frac{1}{2}}$	-----	-------	-------	-------	-------	-------
100	2676. 183	37355. 55	$\begin{cases} a\ ^4H_{6\frac{1}{2}}—z\ ^4H^\circ_{5\frac{1}{2}} \\ a\ ^6S_{2\frac{1}{2}}—y\ ^6P^\circ_{3\frac{1}{2}} \end{cases}$	5	0. 143	1. 24	1. 10	0. 79*w*	2. 03—
4	2676. 775	37347. 29	$b\ ^2G_{4\frac{1}{2}}—x\ ^2H^\circ_{4\frac{1}{2}}$	6	. 104	(1. 067)	0. 96	. 47	?
3	2678. 054	37329. 46	$a\ ^4H_{3\frac{1}{2}}—y\ ^4P^\circ_{2\frac{1}{2}}$	-----	-------	-------	-------	-------	-------
800	2678. 759	37319. 63	$a\ ^6D_{4\frac{1}{2}}—z\ ^6D^\circ_{4\frac{1}{2}}$	7	-------	1. 532	(1. 530)	0	1. 531
5	2679. 450	37310. 01	----------	-----	-------	-------	-------	0	1. 55
100	2680. 585	37294. 21	$b\ ^2G_{3\frac{1}{2}}—x\ ^2G^\circ_{3\frac{1}{2}}$	6	. 221	0. 893	1. 114	0. 794	1. 003
2	2681. 293	37284. 36	$a\ ^6S_{2\frac{1}{2}}—w\ ^4F^\circ_{3\frac{1}{2}}$	-----	-------	-------	-------	-------	-------
1	2681. 417	37282. 64	----------	-----	-------	-------	-------	-------	-------
3	2682. 632	37265. 76	----------	-----	-------	-------	-------	-------	-------
5	2682. 754	37264. 06	$b\ ^4F_{3\frac{1}{2}}—z\ ^2G^\circ_{3\frac{1}{2}}$	6	(0. 05)	1. 09	1. 04	. 19—	1. 07±
3	2682. 894	37262. 12	$b\ ^4D_{1\frac{1}{2}}—1^\circ_{1\frac{1}{2}}$	-----	-------	-------	-------	-------	-------
15	2684. 613	37238. 26	$b\ ^4D_{3\frac{1}{2}}—y\ ^2D^\circ_{2\frac{1}{2}}$	5	0. 249	1. 406	1. 157	. 125	2. 028
15	2685. 152	37230. 78	$a\ ^4G_{3\frac{1}{2}}—z\ ^2I^\circ_{3\frac{1}{2}}$	6	. 197	(1. 237)	1. 040	1. 084	?
2	2685. 581	37224. 84	$b\ ^2F_{2\frac{1}{2}}—w\ ^4F^\circ_{1\frac{1}{2}}$	-----	-------	-------	-------	-------	-------
2	2685. 893	37220. 51	$b\ ^2P_{0\frac{1}{2}}—w\ ^4D^\circ_{1\frac{1}{2}}$	-----	-------	-------	-------	-------	-------
3	2686. 418	37213. 24	----------	-----	-------	-------	-------	-------	-------
15	2686. 889	37206. 72	$a\ ^4G_{3\frac{1}{2}}—y\ ^4G^\circ_{3\frac{1}{2}}$	4?	-------	(1. 021)	1. 03	*w*	1. 02+
25	2687. 071	37204. 20	$b\ ^4F_{4\frac{1}{2}}—y\ ^4F^\circ_{3\frac{1}{2}}$	5	. 147	1. 186	1. 039	0. 072	1. 700—
100	2687. 494	37198. 34	$a\ ^4H_{5\frac{1}{2}}—z\ ^4H^\circ_{5\frac{1}{2}}$	-----	-------	-------	-------	-------	-------
80	2688. 147	37189. 31	$a\ ^4H_{4\frac{1}{2}}—z\ ^4H^\circ_{5\frac{1}{2}}$	-----	-------	-------	-------	-------	-------
1	2689. 431	37171. 55	----------	-----	-------	-------	-------	-------	-------
10	2690. 208	37160. 81	$c\ ^2G_{4\frac{1}{2}}—w\ ^4D^\circ_{3\frac{1}{2}}$	4	-------	(1. 078)	1. 11	*w*	0. 97+
400	2692. 120	37134. 43	$a\ ^6D_{3\frac{1}{2}}—z\ ^6D^\circ_{2\frac{1}{2}}$	4	-------	(1. 576)	1. 71	*w*	1. 44+
1	2692. 716	37126. 21	$b\ ^2G_{4\frac{1}{2}}—w\ ^4F^\circ_{3\frac{1}{2}}$	-----	-------	-------	-------	-------	-------
20	2693. 628	37113. 64	$b\ ^4P_{2\frac{1}{2}}—z\ ^4G^\circ_{2\frac{1}{2}}$	-----	-------	-------	-------	-------	-------
1	2694. 199	37105. 77	$b\ ^4F_{2\frac{1}{2}}—z\ ^2D^\circ_{2\frac{1}{2}}$	-----	-------	-------	-------	-------	-------
1	2694. 598	37100. 28	$b\ ^2P_{0\frac{1}{2}}—x\ ^4P^\circ_{0\frac{1}{2}}$	-----	-------	-------	-------	-------	-------
2	2696. 495	37074. 18	$b\ ^4F_{2\frac{1}{2}}—z\ ^2G^\circ_{3\frac{1}{2}}$	-----	-------	-------	-------	-------	-------
20	2697. 07	37066. 3	$a\ ^2S_{0\frac{1}{2}}—y\ ^2P^\circ_{1\frac{1}{2}}$	4	0. 516	1. 284	1. 800	0. 258	1. 026
10	2697. 12	37065. 6	$a\ ^4G_{4\frac{1}{2}}—y\ ^4G^\circ_{4\frac{1}{2}}$	-----	-------	-------	-------	-------	-------
10	2698. 167	37051. 21	$a\ ^6S_{2\frac{1}{2}}—y\ ^6P^\circ_{2\frac{1}{2}}$	-----	-------	-------	-------	-------	-------
20	2698. 268	37049. 82	----------	-----	-------	-------	-------	*w*	1. 16?
3*h*	2698. 767	37042. 97	----------	-----	-------	-------	-------	-------	-------
5	2699. 228	37036. 64	$b\ ^2D_{2\frac{1}{2}}—x\ ^4P^\circ_{1\frac{1}{2}}$	4	. 480	(1. 102)	1. 582	0. 240	?
50	2700. 163	37023. 82	$b\ ^2H_{5\frac{1}{2}}—y\ ^4H^\circ_{6\frac{1}{2}}$	6	(0. 031)	1. 077	1. 108	. 172	1. 092
25	2700. 999	37012. 36	$b\ ^4F_{1\frac{1}{2}}—y\ ^4P^\circ_{1\frac{1}{2}}$?	-----	-------	-------	-------	-------	-------
10	2702. 639	36989. 90	$b\ ^2H_{5\frac{1}{2}}—y\ ^4H^\circ_{4\frac{1}{2}}$	-----	-------	-------	-------	-------	-------
15	2704. 192	36968. 66	$b\ ^2H_{4\frac{1}{2}}—y\ ^4H^\circ_{3\frac{1}{2}}$	5	0. 146	0. 958	0. 812	. 073	1. 469
80	2704. 585	36963. 29	$a\ ^2I_{6\frac{1}{2}}—z\ ^2K^\circ_{7\frac{1}{2}}$	4	-------	(1. 08)	1. 07	*w*	0. 99+
10	2704. 830	36959. 94	$b\ ^2H_{4\frac{1}{2}}—y\ ^4H^\circ_{5\frac{1}{2}}$	5	. 160	0. 98	1. 14	0. 080	1. 70?
1	2705. 568	36949. 86	$b\ ^2F_{2\frac{1}{2}}—x\ ^2F^\circ_{3\frac{1}{2}}$	-----	-------	-------	-------	-------	-------
1*h*	2706. 936	36931. 19	----------	-----	-------	-------	-------	-------	-------
50	2707. 310	36926. 09	$b\ ^2H_{4\frac{1}{2}}—y\ ^4H^\circ_{4\frac{1}{2}}$	6	(0. 04)	. 95	0. 99	. 19—	0. 97
2	2707. 555	36922. 74	----------	-----	-------	-------	-------	-------	-------
1	2709. 000	36903. 05	$a\ ^6S_{2\frac{1}{2}}—y\ ^6P^\circ_{1\frac{1}{2}}$	-----	-------	-------	-------	-------	-------
100	2710. 228	36886. 33	$b\ ^4P_{2\frac{1}{2}}—y\ ^4P^\circ_{2\frac{1}{2}}$	6	0. 281	1. 576	1. 295	. 709	1. 436
300	2712. 409	36856. 67	$a\ ^6D_{2\frac{1}{2}}—z\ ^6D^\circ_{1\frac{1}{2}}$	4	. 201	1. 637	1. 838	. 101	1. 335
40	2713. 071	36847. 68	$b\ ^2G_{3\frac{1}{2}}—x\ ^2H^\circ_{4\frac{1}{2}}$	-----	-------	-------	-------	-------	-------
40	2713. 585	36840. 70	$b\ ^4F_{4\frac{1}{2}}—z\ ^4I^\circ_{4\frac{1}{2}}$	6	. 247	1. 203	0. 956	1. 120	1. 080
1	2714. 717	36825. 34	----------	-----	-------	-------	-------	-------	-------
1	2715. 101	36820. 13	----------	-----	-------	-------	-------	-------	-------
30	2716. 132	36806. 16	$a\ ^4G_{2\frac{1}{2}}—z\ ^2F^\circ_{2\frac{1}{2}}$	6	. 19	0. 65	. 84	0. 46	0. 745

TABLE 6. *The second spectrum of ruthenium* (Ru II)—Continued

1 Intensity	2 λ (air)	3 σ	4 Term combination	5 Type	6 Δ g	7 g	8 g	9 Strong p	10 Strong s
	A	*K*							
10	2716. 580	36800. 09	*b* $^4F_{3\frac{1}{2}}$—*y* $^4F^{\circ}_{3\frac{1}{2}}$	6	(0. 03)	1. 09	1. 06	0. 10	1. 08*h*
1	2716. 78	36797. 38	*a* $^4H_{5\frac{1}{2}}$—*z* $^4H^{\circ}_{4\frac{1}{2}}$						
80	2717. 447	36788. 35	*a* $^4H_{4\frac{1}{2}}$—*z* $^4H^{\circ}_{3\frac{1}{2}}$	6	(0. 05)	1. 08	1. 03	. 22*w*	1. 06±
10	2717. 855	36782. 82	*b* $^4F_{2\frac{1}{2}}$—*y* $^4F^{\circ}_{1\frac{1}{2}}$	5	0. 514	0. 941	0. 427	. 257	1. 712
20	2719. 717	36757. 64	*a* $^4G_{3\frac{1}{2}}$—*z* $^2G^{\circ}_{4\frac{1}{2}}$	5	. 238	1. 218	. 982	. 118	2. 280
1	2720. 336	36749. 28	*b* $^4F_{1\frac{1}{2}}$—*z* $^2D^{\circ}_{2\frac{1}{2}}$						
1	2722. 081	36725. 72	*a* $^4G_{3\frac{1}{2}}$—*y* $^4G^{\circ}_{4\frac{1}{2}}$						
20	2723. 126	36711. 63	*b* $^2F_{2\frac{1}{2}}$—*y* $^2F^{\circ}_{3\frac{1}{2}}$	5	. 165	0. 947	1. 112	. 082	1. 524
2	2723. 812	36702. 38	*b* $^2G_{3\frac{1}{2}}$—*w* $^4F^{\circ}_{4\frac{1}{2}}$						
2	2724. 630	36691. 36	*b* $^2P_{0\frac{1}{2}}$—$2^{\circ}_{1\frac{1}{2}}$						
100	2724. 864	36688. 21	*b* $^2H_{5\frac{1}{2}}$—*y* $^4H^{\circ}_{5\frac{1}{2}}$	5	. 127	1. 053	1. 180	. 062	1. 878
300	2725. 465	36680. 13	*a* $^6D_{1\frac{1}{2}}$—*z* $^6D^{\circ}_{0\frac{1}{2}}$	4	1. 448	1. 840	3. 288	. 724	1. 116
20	2727. 03	36659. 08	*b* $^4D_{0\frac{1}{2}}$—*x* $^4F^{\circ}_{1\frac{1}{2}}$						
2	2728. 691	36636. 76	*b* $^4D_{2\frac{1}{2}}$—*y* $^4H^{\circ}_{3\frac{1}{2}}$						
2	2729. 39	36627. 38	*b* $^4D_{2\frac{1}{2}}$—*x* $^4F^{\circ}_{2\frac{1}{2}}$	6	0. 36	(1. 344)	0. 98	. 90	
5*w*	2730. 413	36613. 65	*b* $^4P_{0\frac{1}{2}}$—*x* $^4D^{\circ}_{1\frac{1}{2}}$						
5	2730. 688	36609. 97	*b* $^4F_{2\frac{1}{2}}$—*y* $^4F^{\circ}_{3\frac{1}{2}}$						
3	2731. 389	36600. 58	*b* $^4D_{2\frac{1}{2}}$—*x* $^4F^{\circ}_{1\frac{1}{2}}$						
3	2732. 685	36583. 22							
500	2734. 345	36561. 01	*a* $^6D_{3\frac{1}{2}}$—*z* $^6D^{\circ}_{3\frac{1}{2}}$	7, 6		(1. 576)	1. 584	0	1. 580
40	2736. 456	36532. 81	*b* $^2F_{3\frac{1}{2}}$—*y* $^2D^{\circ}_{2\frac{1}{2}}$						
60	2736. 826	36527. 87	*a* $^4G_{5\frac{1}{2}}$—*z* $^2I^{\circ}_{6\frac{1}{2}}$	4	(0. 11)	1. 26	1. 15	0. 53*w*	0. 62+
1	2737. 384	36520. 42							
10	2737. 606	36517. 46	*c* $^2G_{4\frac{1}{2}}$—*x* $^2H^{\circ}_{5\frac{1}{2}}$	7		(1. 078)	1. 074	0	1. 056
20	2737. 783	36515. 10	*b* $^4F_{3\frac{1}{2}}$—*y* $^4F^{\circ}_{2\frac{1}{2}}$	5	(0. 07)	1. 09	1. 02	0. 17*w*	1. 26−
20	2739. 372	36493. 92	*b* $^2H_{4\frac{1}{2}}$—*y* $^2G^{\circ}_{4\frac{1}{2}}$	6	0. 12	0. 95	1. 07	. 53−	1. 01±
5*h*	2741. 178	36469. 88							
25	2742. 401	36453. 61	*a* $^4G_{3\frac{1}{2}}$—*z* $^4I^{\circ}_{4\frac{1}{2}}$	6	. 195	1. 245	1. 050	1. 073	1. 148
1	2742. 691	36449. 76	*c* $^2D_{2\frac{1}{2}}$—*w* $^2G^{\circ}_{3\frac{1}{2}}$						
25	2743. 513	36438. 84	*a* $^4H_{3\frac{1}{2}}$—*z* $^4H^{\circ}_{4\frac{1}{2}}$	5	0. 265	0. 761	1. 026	0. 134	1. 953
5	2743. 700	36436. 36	*b* $^4F_{3\frac{1}{2}}$—*z* $^4I^{\circ}_{4\frac{1}{2}}$						
60	2743. 934	36433. 25	*a* $^6D_{2\frac{1}{2}}$—*z* $^6D^{\circ}_{2\frac{1}{2}}$	7		(1. 637)	1. 643	0	1. 640
1	2744. 29	36428. 5	*b* $^2P_{0\frac{1}{2}}$—*w* $^4F^{\circ}_{1\frac{1}{2}}$						
100	2745. 158	36417. 00	*b* $^4P_{1\frac{1}{2}}$—*y* $^4P^{\circ}_{1\frac{1}{2}}$						
50	2745. 827	36408. 15	*a* $^4H_{4\frac{1}{2}}$—*z* $^4H^{\circ}_{3\frac{1}{2}}$						
20	2746. 068	36404. 94	*a* $^6D_{1\frac{1}{2}}$—*z* $^6D^{\circ}_{1\frac{1}{2}}$	7, 6		(1. 843)	1. 80	0	1. 82?
25	2746. 695	36396. 63	*b* $^4F_{4\frac{1}{2}}$—*z* $^4G^{\circ}_{3\frac{1}{2}}$	5	. 219	1. 192	0. 973	0. 110	1. 958
10	2747. 563	36385. 13	*b* $^4D_{2\frac{1}{2}}$—*x* $^4F^{\circ}_{3\frac{1}{2}}$	4	. 297	1. 361	1. 064	. 148	0. 322
50	2747. 963	36379. 83	*a* $^6D_{0\frac{1}{2}}$—*z* $^6D^{\circ}_{0\frac{1}{2}}$	7		(3. 271)	3. 273	0	3. 272
5	2749. 100	36364. 79	*d* $^2D_{1\frac{1}{2}}$—*v* $^2F^{\circ}_{2\frac{1}{2}}$						
15	2749. 230	36363. 07		7				0	0. 93
5*h*	2749. 64	36357. 65	*a* $^4G_{2\frac{1}{2}}$—*x* $^4D^{\circ}_{2\frac{1}{2}}$						
10	2752. 110	36325. 02	*b* $^4F_{2\frac{1}{2}}$—*y* $^4F^{\circ}_{2\frac{1}{2}}$	6	(0. 08)	1. 03	1. 11	0. 21−	1. 07±
30	2752. 447	36320. 57	*a* $^6D_{3\frac{1}{2}}$—*z* $^6D^{\circ}_{4\frac{1}{2}}$	4	(0. 04)	1. 59	1. 55	. 15*w*	1. 39+
50	2752. 763	36316. 40	*a* $^4D_{2\frac{1}{2}}$—*z* $^4P^{\circ}_{2\frac{1}{2}}$	4	0. 175	1. 399	1. 574	. 088	0. 961
20	2753. 508	36306. 58	*b* $^4F_{4\frac{1}{2}}$—*z* $^4G^{\circ}_{4\frac{1}{2}}$	6	(0. 08)	1. 26	1. 18	. 35−	1. 22±
2	2753. 831	36302. 32							
20	2755. 258	36283. 52	*b* $^2H_{5\frac{1}{2}}$—*x* $^4G^{\circ}_{4\frac{1}{2}}$	4	(0. 09)	1. 03	1. 12	. 39*w*	0. 64+
4	2755. 519	36280. 08	*b* $^4D_{3\frac{1}{2}}$—*y* $^4H^{\circ}_{4\frac{1}{2}}$						
1	2755. 748	36277. 07							
15	2756. 411	36268. 34							
1*h*	2756. 899	36261. 92							
5	2758. 347	36242. 89	*b* $^2D_{1\frac{1}{2}}$—*z* $^2S^{\circ}_{0\frac{1}{2}}$	4	1. 087	0. 975	2. 062	. 544	. 431
2	2758. 692	36238. 35	*a* $^4G_{4\frac{1}{2}}$—*y* $^4D^{\circ}_{3\frac{1}{2}}$						
10	2759. 159	36232. 22	*b* $^2G_{4\frac{1}{2}}$—*x* $^2F^{\circ}_{3\frac{1}{2}}$	4	(0. 06)	1. 08	1. 14	. 21*w*	. 87+

TABLE 6. *The second spectrum of ruthenium* (Ru II)—Continued

1 Intensity	2 λ (air)	3 σ	4 Term combination	5 Type	6 Δg	7 g	8 g	9 Strong p	10 Strong n
	A	*K*							
8	2760. 115	36219. 67	*b* $^2H_{4\frac{1}{2}}$—*x* $^4G^\circ_{4\frac{1}{2}}$						
20	2760. 745	36211. 41	*a* $^4G_{3\frac{1}{2}}$—*x* $^4D^\circ_{2\frac{1}{2}}$	4	0. 260	1. 021	1. 281	. 130	. 371
3	2761. 473	36201. 86							
40	2762. 071	36194. 03	*d* $^2D_{2\frac{1}{2}}$—*v* $^2F^\circ_{3\frac{1}{2}}$	4	0. 160	1. 206	1. 046	0. 080	0. 646
20	2765. 134	36153. 93	*b* $^4P_{1\frac{1}{2}}$—*z* $^2D^\circ_{2\frac{1}{2}}$	4	. 322	1. 643	1. 321	. 160	. 838
100	2765. 429	36150. 08	*a* $^4D_{2\frac{1}{2}}$—*z* $^4P^\circ_{1\frac{1}{2}}$	4	. 372	1. 339	1. 711	. 186	. 781
15	2765. 889	36144. 06	*b* $^4P_{0\frac{1}{2}}$—*y* $^4D^\circ_{0\frac{1}{2}}$						
80	2766. 563	36135. 26	*c* $^2D_{2\frac{1}{2}}$—*x* $^2D^\circ_{2\frac{1}{2}}$	7	.....	(1. 18)	1. 20	0	1. 19
250	2768. 926	36104. 42	*a* $^6D_{0\frac{1}{2}}$—*z* $^6D^\circ_{1\frac{1}{2}}$						
1	2770. 088	36089. 28							
50	2771. 060	36076. 62	*b* $^4F_{3\frac{1}{2}}$—*z* $^4G^\circ_{2\frac{1}{2}}$	5	. 446	1. 085	0. 639	. 223	2. 200
5	2771. 464	36071. 36	*b* $^4D_{2\frac{1}{2}}$—*x* $^4F^\circ_{3\frac{1}{2}}$						
3	2772. 011	36064. 24	*c* $^2G_{3\frac{1}{2}}$—*x* $^2G^\circ_{4\frac{1}{2}}$						
100	2772. 459	36058. 42	*x* $^4H_{3\frac{1}{2}}$—*z* $^4H^\circ_{3\frac{1}{2}}$	6	. 200	0. 764	. . 964	. 708	0. 864
10	2774. 197	36035. 83	*b* $^4D_{2\frac{1}{2}}$—*x* $^4G^\circ_{2\frac{1}{2}}$						
30	2775. 631	36017. 21	*a* $^4D_{1\frac{1}{2}}$—*z* $^4P^\circ_{0\frac{1}{2}}$	4	1. 452	1. 189	2. 641	. 728	. 463
50	2777. 401	35994. 26	*b* $^2G_{4\frac{1}{2}}$—*y* $^2F^\circ_{3\frac{1}{2}}$	4	.....	(1. 067)	1. 10	*w*	. 95+
50	2777. 54	35992. 46	*b* $^4F_{3\frac{1}{2}}$—*z* $^4G^\circ_{3\frac{1}{2}}$	6	0. 11	1. 10	0. 99	0. 38−	1. 05±
1	2778. 024	35986. 19	*b* $^2D_{1\frac{1}{2}}$—*y* $^2D^\circ_{1\frac{1}{2}}$						
150	2778. 388	35981. 48	*a* $^6D_{1\frac{1}{2}}$—*z* $^6D^\circ_{2\frac{1}{2}}$	4	. 210	1. 843	1. 633	. 105	1. 317
30	2778. 975	35973. 87	*b* $^4F_{4\frac{1}{2}}$—*z* $^4G^\circ_{5\frac{1}{2}}$	5	(0. 03)	1. 23	1. 26	. 14*w*	1. 40−
15	2779. 406	35968. 30	*b* $^4F_{1\frac{1}{2}}$—*y* $^4F^\circ_{2\frac{1}{2}}$	5	0. 614	0. 415	1. 029	. 308	1. 948?
8*h*	2780. 817	35950. 05	*b* $^2D_{2\frac{1}{2}}$—*y* $^2D^\circ_{1\frac{1}{2}}$	5	. 354	1. 107	. 753	. 177	1. 638
8	2782. 23	35931. 79		5	. 228	1. 053	. 825	. 114	1. 623
10	2782. 361	35930. 10	*c* $^2G_{4\frac{1}{2}}$—*x* $^2H^\circ_{4\frac{1}{2}}$	6	. 12	1. 08	. 96	. 53−	1. 02±
8	2783. 69	35912. 95	*a* $^4G_{4\frac{1}{2}}$—*z* $^4F^\circ_{3\frac{1}{2}}$	7	.....	(1. 167)	1. 18	0	1. 117
4	2783. 799	35911. 54	*b* $^2P_{1\frac{1}{2}}$—*x* $^4F^\circ_{2\frac{1}{2}}$						
40	2784. 516	35902. 29	*b* $^4F_{3\frac{1}{2}}$—*z* $^4G^\circ_{4\frac{1}{2}}$	5	.....	(1. 093)	1. 14	*w*	1. 23−
10	2785. 186	35893. 66	*d* $^2D_{2\frac{1}{2}}$—$3^\circ_{3\frac{1}{2}}$	4	. 194	1. 227	1. 033	0. 097	0. 548
75	2785. 741	35886. 51	*b* $^4F_{2\frac{1}{2}}$—*z* $^4G^\circ_{3\frac{1}{2}}$	6	. 292	0. 944	0. 652	. 743	. 798
25	2785. 87	35884. 84	*b* $^2P_{1\frac{1}{2}}$—*x* $^4F^\circ_{1\frac{1}{2}}$						
15	2786. 383	35878. 24							
20	2787. 25	35867. 08	*d* $^2D_{1\frac{1}{2}}$—*w* $^2D^\circ_{1\frac{1}{2}}$	6	(0. 07)	0. 80	0. 87	0. 10−	0. 83±
200	2787. 823	35859. 71	*a* $^6D_{2\frac{1}{2}}$—*z* $^6D^\circ_{3\frac{1}{2}}$	4	(0. 08)	1. 68	1. 60	. 21*w*	1. 39+
25	2788. 729	35848. 06	*b* $^4D_{3\frac{1}{2}}$—*y* $^2G^\circ_{4\frac{1}{2}}$	4	0. 333	(1. 397)	1. 063	. 167	?
3	2789. 453	35838. 75							
5	2790. 082	35830. 67	*b* $^4P_{1\frac{1}{2}}$—*y* $^4F^\circ_{1\frac{1}{2}}$						
15	2790. 240	35828. 65	*c* $^2G_{3\frac{1}{2}}$—*x* $^2G^\circ_{3\frac{1}{2}}$						
5	2791. 193	35816. 41	*b* $^2F_{2\frac{1}{2}}$—*x* $^4P^\circ_{2\frac{1}{2}}$						
100	2792. 32	35801. 96	*b* $^4F_{2\frac{1}{2}}$—*z* $^4G^\circ_{3\frac{1}{2}}$	5	.....	(0. 943)	0. 99	*w*	1. 09−
5	2794. 092	35779. 25	*b* $^2D_{1\frac{1}{2}}$—*y* $^2D^\circ_{2\frac{1}{2}}$?						
20*h*	2794. 278	35776. 87		5	. 182	1. 120	. 938	0. 092	1. 393
10	2795. 349	35763. 17	*b* $^4F_{4\frac{1}{2}}$—*z* $^4H^\circ_{5\frac{1}{2}}$	4	. 134	(1. 200)	1. 064	. 068	?
8	2795. 555	35760. 53							
5	2795. 993	35754. 93	*b* $^4D_{2\frac{1}{2}}$—*y* $^4D^\circ_{2\frac{1}{2}}$						
8	2796. 461	35748. 94							
2*H*	2797. 077	35741. 07	*a* $^6S_{2\frac{1}{2}}$—*y* $^2F^\circ_{2\frac{1}{2}}$						
10	2797. 747	35732. 51	*b* $^2G_{3\frac{1}{2}}$—*x* $^2F^\circ_{3\frac{1}{2}}$	6	. 254	(0. 883)	1. 137	. 889	?
25	2798. 779	35719. 34	*a* $^4G_{2\frac{1}{2}}$—*z* $^2F^\circ_{3\frac{1}{2}}$	5	. 545	0. 649	1. 194	. 274	2. 557
8	2799. 587	35709. 03	*c* $^2G_{4\frac{1}{2}}$—*w* $^4F^\circ_{3\frac{1}{2}}$						
15	2799. 927	35704. 70	*b* $^2P_{1\frac{1}{2}}$—*z* $^2P^\circ_{0\frac{1}{2}}$	5	. 368	1. 197	0. 829	. 186	1. 381
1	2800. 408	35698. 56							
2	2800. 586	35696. 29	*a* $^2I_{5\frac{1}{2}}$—*y* $^2H^\circ_{4\frac{1}{2}}$			(0. 90)	. 91	*w*	0. 86*h*
30	2802. 152	35676. 34	*a* $^4G_{4\frac{1}{2}}$—*z* $^2G^\circ_{4\frac{1}{2}}$	6	. 173	1. 168	. 995	0. 776	1. 082
3	2802. 717	35669. 15							

TABLE 6. *The second spectrum of ruthenium* (Ru II)—Continued

1 Intensity	2 λ (air)	3 σ	4 Term combination	5 Type	6 Δg	7 g	8 g	9 Strong p	10 Strong s
	A	*K*							
4	2803. 535	35658. 75	$b\ ^4F_{2\frac{5}{2}}—y\ ^4P^\circ_{2\frac{5}{2}}$	6	. 353	(0. 943)	1. 296	. 883	?
50	2804. 903	35641. 36	$b\ ^2H_{4\frac{1}{2}}—x\ ^4G^\circ_{3\frac{1}{2}}$	5	. 198	0. 954	1. 152	. 099	2. 043
100	2806. 77	35617. 65	$a\ ^4D_{0\frac{1}{2}}—z\ ^4P^\circ_{0\frac{1}{2}}$	6	2. 654	0	2. 654	1. 327	1. 327
25	2807. 200	35612. 19	$c\ ^2D_{2\frac{1}{2}}—w\ ^4D^\circ_{3\frac{1}{2}}$	4	-------	1. 16	(1. 13)	*w*	1. 06*h*
5	2807. 350	35610. 29	$a\ ^2G_{4\frac{1}{2}}—z\ ^6D^\circ_{4\frac{1}{2}}$ $c\ ^2D_{2\frac{1}{2}}—x\ ^2D^\circ_{1\frac{1}{2}}$	-----	-------	-------	-------	-------	-------
20	2807. 554	35607. 70	$b\ ^2F_{3\frac{1}{2}}—x\ ^4F^\circ_{2\frac{1}{2}}$	5	(0. 08)	1. 09	1. 01	0. 20*w*	1. 29—?
8	2810. 249	35573. 56	$b\ ^4D_{3\frac{1}{2}}—x\ ^4G^\circ_{4\frac{1}{2}}$	-----	-------	-------	-------	-------	-------
250	2810. 649	35568. 50	$a\ ^2I_{5\frac{1}{2}}—z\ ^2K^\circ_{6\frac{1}{2}}$	7	-------	(0. 90)	0. 91	0	0. 94
10	2811. 545	35557. 16	$b\ ^4D_{1\frac{1}{2}}—z\ ^2P^\circ_{1\frac{1}{2}}$	-----	-------	(1. 200)	1. 18	-------	1. 19
10	2811. 931	35552. 28	----------	-----	-------	-------	-------	-------	-------
1	2812. 689	35542. 70	$b\ ^2H_{4\frac{1}{2}}—x\ ^4D^\circ_{3\frac{1}{2}}$	-----	-------	-------	-------	-------	-------
100	2813. 311	35534. 84	$b\ ^4P_{2\frac{1}{2}}—z\ ^4S^\circ_{1\frac{1}{2}}$	4	0. 234	1. 564	1. 798	0. 118	1. 213
60	2813. 694	35530. 00	$b\ ^4F_{1\frac{1}{2}}—z\ ^4G^\circ_{2\frac{1}{2}}$	5	. 230	0. 418	0. 648	. 115	0. 994
2	2814. 952	35514. 13	$b\ ^2F_{3\frac{1}{2}}—x\ ^4G^\circ_{3\frac{1}{2}}$	-----	-------	-------	-------	-------	-------
2	2815. 685	35504. 88	$d\ ^2D_{2\frac{1}{2}}—v\ ^2F^\circ_{3\frac{1}{2}}$	-----	-------	-------	-------	-------	-------
1	2816. 281	35497. 37	$b\ ^2H_{5\frac{1}{2}}—z\ ^2H^\circ_{4\frac{1}{2}}$	-----	-------	-------	-------	-------	-------
1	2817. 255	35485. 10	$b\ ^4D_{0\frac{1}{2}}—z\ ^2P^\circ_{1\frac{1}{2}}$	-----	-------	-------	-------	-------	-------
50	2817. 591	35480. 87	$b\ ^2F_{2\frac{1}{2}}—y\ ^2D^\circ_{1\frac{1}{2}}$	5	. 212	. 945	. 733	. 106	1. 263?
100	2821. 34	35433. 72	$b\ ^2H_{4\frac{1}{2}}—z\ ^2H^\circ_{4\frac{1}{2}}$	6	-------	. 95	1. 01	. 29—	0. 98±
1	2821. 883	35426. 90	$b\ ^4D_{2\frac{1}{2}}—z\ ^2P^\circ_{1\frac{1}{2}}$	-----	-------	-------	-------	-------	-------
150	2822. 542	35418. 63	$a\ ^4D_{1\frac{1}{2}}—z\ ^4P^\circ_{1\frac{1}{2}}$	6	. 528	1. 185	1. 713	. 795	1. 448
10	2822. 778	35415. 67	$a\ ^4D_{3\frac{1}{2}}—z\ ^4F^\circ_{2\frac{1}{2}}$	-----	-------	-------	-------	-------	-------
75	2823. 176	35410. 68	$b\ ^2G_{3\frac{1}{2}}—y\ ^2H^\circ_{4\frac{1}{2}}$	5	. 05	0. 93	0. 98	. 19*w*	1. 17—
1	2823. 596	35405. 41	$c\ ^2D_{1\frac{1}{2}}—x\ ^2D^\circ_{2\frac{1}{2}}$	-----	-------	-------	-------	-------	-------
30	2825. 071	35386. 93	----------	5	. 168	1. 202	1. 034	. 085	1. 454
10	2825. 162	35385. 79	----------	-----	-------	-------	-------	-------	-------
40	2825. 484	35381. 75	$c\ ^2G_{3\frac{1}{2}}—x\ ^2H^\circ_{4\frac{1}{2}}$	5	-------	(0. 942)	0. 96	*w*	1. 02—
50	2826. 230	35372. 41	$a\ ^4G_{4\frac{1}{2}}—z\ ^4I^\circ_{5\frac{1}{2}}$	-----	-------	-------	-------	-------	-------
50	2826. 674	35366. 86	$a\ ^4G_{5\frac{1}{2}}—z\ ^4I^\circ_{4\frac{1}{2}}$	5	. 278	1. 234	. 956	0. 140	2. 485
2	2827. 053	35362. 12	$b\ ^4F_{4\frac{1}{2}}—z\ ^4H^\circ_{4\frac{1}{2}}$	-----	-------	-------	-------	-------	-------
2	2827. 433	35357. 36	$b\ ^2D_{1\frac{1}{2}}—1^\circ_{1\frac{1}{2}}$	-----	-------	-------	-------	-------	-------
2	2827. 604	35355. 23	----------	-----	-------	-------	-------	-------	-------
20	2829. 092	35336. 63	$a\ ^4G_{3\frac{1}{2}}—z\ ^2G^\circ_{4\frac{1}{2}}$	7	-------	(1. 021)	1. 01	0	0. 975
50	2831. 84	35302. 34	$b\ ^4F_{1\frac{1}{2}}—y\ ^4P^\circ_{2\frac{1}{2}}$	5	0. 884	0. 405	1. 289	0. 442	2. 615
50	2833. 806	35277. 86	$b\ ^2H_{5\frac{1}{2}}—x\ ^4F^\circ_{4\frac{1}{2}}$	4	. 12	1. 04	1. 16	. 52*w*	0. 52+
2*h*	2834. 232	35272. 55	$b\ ^2F_{2\frac{1}{2}}—y\ ^2D^\circ_{2\frac{1}{2}}$	-----	-------	-------	-------	-------	-------
2*h*	2836. 319	35246. 60	$b\ ^4D_{2\frac{1}{2}}—y\ ^2G^\circ_{3\frac{1}{2}}$	-----	-------	-------	-------	-------	-------
3	2837. 112	35236. 75	$c\ ^2G_{3\frac{1}{2}}—w\ ^4F^\circ_{4\frac{1}{2}}$	-----	-------	-------	-------	-------	-------
3	2837. 898	35226. 99	$a\ ^4G_{4\frac{1}{2}}—y\ ^4F^\circ_{4\frac{1}{2}}$	-----	-------	(1. 167)	1. 39	*w*	1. 28*h*
10*h*	2838. 875	35214. 87	$a\ ^4G_{2\frac{1}{2}}—y\ ^4P^\circ_{1\frac{1}{2}}$	-----	-------	-------	-------	-------	-------
10	2839. 385	35208. 54	$b\ ^4D_{1\frac{1}{2}}—x\ ^4D^\circ_{0\frac{1}{2}}$	-----	-------	-------	-------	-------	-------
50	2841. 147	35186. 71	$b\ ^2G_{4\frac{1}{2}}—y\ ^2H^\circ_{5\frac{1}{2}}$	7	-------	(1. 067)	1. 315	0	1. 116
100	2841. 680	35180. 11	$a\ ^4D_{2\frac{1}{2}}—z\ ^4P^\circ_{2\frac{1}{2}}$	6	. 235	1. 339	1. 574	0. 592	1. 456
75	2844. 716	35142. 56	$b\ ^2F_{3\frac{1}{2}}—y\ ^2G^\circ_{4\frac{1}{2}}$	7	-------	(1. 083)	1. 07	0	1. 029
15	2845. 229	35136. 23	$b\ ^4D_{0\frac{1}{2}}—x\ ^4D^\circ_{0\frac{1}{2}}$	6	. 240	0. 145	0. 385	0. 120	0. 265
10	2847. 087	35113. 30	$a\ ^4G_{4\frac{1}{2}}—z\ ^2G^\circ_{3\frac{1}{2}}$	-----	-------	-------	-------	-------	-------
20	2847. 574	35107. 29	$a\ ^2F_{2\frac{1}{2}}—z\ ^4P^\circ_{1\frac{1}{2}}$	4	. 850	. 86	1. 71	. 425	—. 42
50*d*	2849. 289	35086. 16	----------	-----	-------	-------	-------	. 45	. 45
15	2849. 591	35082. 45	$b\ ^2G_{3\frac{1}{2}}—y\ ^2F^\circ_{2\frac{1}{2}}$	4	. 314	(0. 883)	1. 20	. 157	?
2	2850. 024	35077. 12	----------	-----	-------	-------	-------	-------	-------
20	2850. 697	35068. 83	$d\ ^2D_{1\frac{1}{2}}—w\ ^2D^\circ_{2\frac{1}{2}}$	5	. 265	0. 803	1. 068	. 133	1. 466
5	2852. 993	35040. 62	----------	-----	-------	-------	-------	-------	-------
10	2853. 126	35038. 98	$b\ ^2P_{1\frac{1}{2}}—y\ ^4D^\circ_{2\frac{1}{2}}$	5	. 12	1. 19	1. 31	. 17*w*	1. 48—
40	2854. 722	35019. 39	$a\ ^4D_{0\frac{1}{2}}—z\ ^4P^\circ_{1\frac{1}{2}}$	5	1. 730	—0. 030	1. 700	. 865	2. 565
15	2854. 980	35016. 23	$b\ ^2F_{3\frac{1}{2}}—x\ ^4G^\circ_{2\frac{1}{2}}$	-----	-------	-------	-------	-------	-------

TABLE 6. *The second spectrum of ruthenium* (Ru II)—Continued

1 Intensity	2 λ (air)	3 σ	4 Term combination	5 Type	6 Δ g	7 g	8 g	9 Strong p	10 Strong n
	A	*K*							
20	2855. 357	35011. 60	$b\ ^4D_{1\frac{1}{2}}—y\ ^4D^\circ_{1\frac{1}{2}}$	-----	-------	-------	-------	-------	-------
3*h*	2855. 710	35007. 28	$d\ ^2D_{2\frac{1}{2}}—w\ ^2D^\circ_{1\frac{1}{2}}$	-----	-------	-------	-------	-------	-------
30	2856. 570	34996. 74	----------	4, 5	0. 162	-------	-------	. 081	?
10	2857. 240	34988. 53	$c\ ^2G_{3\frac{1}{2}}—w\ ^4F^\circ_{2\frac{1}{2}}$	4	(0. 04)	(0. 942)	0. 98	0. 11*w*	-------
2	2857. 590	34984. 25	----------	-----	-------	-------	-------	-------	-------
50	2857. 780	34981. 92	$b\ ^4F_{4\frac{1}{2}}—z\ ^4H^\circ_{3\frac{1}{2}}$	5	0. 240	1. 205	. 965	. 120	2. 045
1	2858. 042	34978. 72	$b\ ^2H_{3\frac{1}{2}}—y\ ^4G^\circ_{3\frac{1}{2}}$	-----	-------	-------	-------	-------	-------
3	2858. 506	34973. 04	$a\ ^2I_{5\frac{1}{2}}—y\ ^2H^\circ_{5\frac{1}{2}}$	-----	-------	-------	-------	-------	-------
10	2859. 622	34959. 39	$b\ ^2H_{4\frac{1}{2}}—y\ ^4G^\circ_{3\frac{1}{2}}$	4	-------	(0. 958)	1. 03	*w*	0. 70+
10	2859. 749	34957. 84	$b\ ^4F_{3\frac{1}{2}}—z\ ^4H^\circ_{4\frac{1}{2}}$	-----	-------	-------	-------	-------	-------
8	2861. 108	34941. 23	$b\ ^2P_{0\frac{1}{2}}—z\ ^2S^\circ_{0\frac{1}{2}}$	6	1. 165	0. 866	2. 031	0. 583	1. 448
5	2861. 686	34934. 17	$b\ ^4P_{1\frac{1}{2}}—z\ ^4G^\circ_{2\frac{1}{2}}$	-----	-------	-------	-------	-------	-------
10*h*	2862. 848	34920. 00	$a\ ^4G_{2\frac{1}{2}}—z\ ^2G^\circ_{3\frac{1}{2}}$	5	0. 376	. 658	1. 034	. 192	1. 974
50*h*	2863. 261	34914. 96	$b\ ^2H_{4\frac{1}{2}}—y\ ^4G^\circ_{3\frac{1}{2}}$	5	. 212	. 954	1. 166	. 106	2. 120
10	2865. 544	34887. 15	$a\ ^4G_{3\frac{1}{2}}—y\ ^4F^\circ_{4\frac{1}{2}}$	5	. 14	1. 01	1. 15	. 070	1. 64?
15	2866. 096	34880. 43	$c\ ^2D_{1\frac{1}{2}}—x\ ^2D^\circ_{1\frac{1}{2}}$	-----	-------	(0. 789)	0. 87	0	0. 83*h*
15	2866. 276	34878. 24	$b\ ^2H_{5\frac{1}{2}}—z\ ^2H^\circ_{5\frac{1}{2}}$	6	(0. 06)	1. 08	1. 14	0. 36—	1. 11±
10	2867. 107	34868. 13	$b\ ^2F_{3\frac{1}{2}}—x\ ^4G^\circ_{4\frac{1}{2}}$	5	(0. 08)	(1. 083)	1. 16	. 27*w*	-------
2	2868. 832	34847. 16	$a\ ^4D_{3\frac{1}{2}}—z\ ^4F^\circ_{3\frac{1}{2}}$	6	0. 12	(1. 403)	1. 28	. 42—	?
30	2870. 573	34826. 03	$b\ ^2D_{2\frac{1}{2}}—y\ ^4H^\circ_{3\frac{1}{2}}$	4	. 301	1. 098	0. 797	. 150	0. 044
30	2871. 493	34814. 87	$b\ ^2H_{4\frac{1}{2}}—z\ ^2H^\circ_{5\frac{1}{2}}$	5	. 188	0. 942	1. 130	. 093	1. 976
30	2873. 329	34792. 63	----------	4	-------	-------	-------	*w*	1. 15+
15	2873. 752	34787. 50	$b\ ^4D_{3\frac{1}{2}}—z\ ^2H^\circ_{4\frac{1}{2}}$	4	. 380	(1. 397)	1. 017	0. 190	?
6	2878. 056	34735. 48	$b\ ^2F_{3\frac{1}{2}}—y\ ^4D^\circ_{2\frac{1}{2}}$	4	. 228	1. 080	1. 308	. 114	0. 510
20	2879. 078	34723. 15	$b\ ^2D_{2\frac{1}{2}}—x\ ^4G^\circ_{3\frac{1}{2}}$	4	(0. 01)	(1. 102)	0. 99	. 25*w*	. 72+
4	2880. 091	34710. 94	$b\ ^2P_{1\frac{1}{2}}—z\ ^2P^\circ_{1\frac{1}{2}}$	-----	-------	-------	-------	-------	-------
5	2880. 440	34706. 74	$b\ ^4P_{1\frac{1}{2}}—y\ ^4P^\circ_{2\frac{1}{2}}$	4	0. 353	1. 655	1. 302	. 177	. 772
200	2882. 112	34686. 61	$a\ ^4D_{3\frac{1}{2}}—z\ ^4D^\circ_{2\frac{1}{2}}$	5	-------	(1. 403)	1. 35	*w*	1. 53—
3	2885. 473	34646. 20	$b\ ^2D_{1\frac{1}{2}}—z\ ^2P^\circ_{0\frac{1}{2}}$	5	. 14	(0. 965)	0. 82	0. 07	?
4*h*	2887. 084	34626. 87	$b\ ^4D_{2\frac{1}{2}}—y\ ^4G^\circ_{3\frac{1}{2}}$	-----	-------	-------	-------	-------	-------
8	2889. 396	34599. 17	$b\ ^2G_{3\frac{1}{2}}—x\ ^4P^\circ_{2\frac{1}{2}}$	4	0. 364	0. 884	1. 248	0. 180	−0. 026
20*Hw*	2890. 476	34586. 24	----------	-----	-------	-------	-------	-------	-------
20	2891. 219	34577. 35	$c\ ^2G_{4\frac{1}{2}}—y\ ^2F^\circ_{3\frac{1}{2}}$	-----	-------	-------	-------	-------	-------
2	2891. 987	34568. 17	$b\ ^4D_{3\frac{1}{2}}—x\ ^4F^\circ_{4\frac{1}{2}}$	-----	-------	-------	-------	-------	-------
1	2894. 148	34542. 36	$b\ ^2H_{5\frac{1}{2}}—y\ ^4G^\circ_{4\frac{1}{2}}$; $d\ ^2D_{1\frac{1}{2}}—y\ ^2P^\circ_{1\frac{1}{2}}$?	-----	-------	-------	-------	-------	-------
40	2897. 713	34499. 86	$a\ ^4G_{5\frac{1}{2}}—z\ ^4G^\circ_{5\frac{1}{2}}$	7	-------	(1. 237)	1. 231	0	1. 234
40	2898. 242	34493. 57	$c\ ^2G_{4\frac{1}{2}}—y\ ^2H^\circ_{4\frac{1}{2}}$?	4	(0. 04)	1. 06	1. 02	0. 17*w*	1. 04+
10	2899. 502	34478. 58	$b\ ^2H_{4\frac{1}{2}}—y\ ^4G^\circ_{4\frac{1}{2}}$	6	0. 196	0. 962	1. 158	. 882	1. 06?
50	2900. 441	34467. 42	----------	4	-------	-------	-------	. 19*w*	1. 35—
10	2901. 431	34455. 66	$a\ ^4G_{2\frac{1}{2}}—y\ ^4F^\circ_{3\frac{1}{2}}$	5	. 407	. 647	1. 054	. 203	2. 072
75	2902. 026	34448. 59	$a\ ^4D_{1\frac{1}{2}}—z\ ^4P^\circ_{2\frac{1}{2}}$	5	. 384	1. 182	1. 566	. 192	2. 142
2*h*	2902. 572	34442. 11	----------	-----	-------	-------	-------	-------	-------
3	2903. 394	34432. 36	$b\ ^4P_{0\frac{1}{2}}—y\ ^4F^\circ_{1\frac{1}{2}}$	-----	-------	-------	-------	-------	-------
1	2906. 937	34390. 40	----------	-----	-------	-------	-------	-------	-------
1	2907. 160	34387. 76	$b\ ^4F_{2\frac{1}{2}}—z\ ^4H^\circ_{3\frac{1}{2}}$	-----	-------	-------	-------	-------	-------
1	2909. 329	34362. 12	$b\ ^2P_{1\frac{1}{2}}—x\ ^4D^\circ_{0\frac{1}{2}}$	-----	-------	-------	-------	-------	-------
25	2909. 750	34357. 15	$b\ ^2F_{2\frac{1}{2}}—y\ ^4H^\circ_{3\frac{1}{2}}$	4	. 143	0. 926	0. 783	. 072	0. 426
25	2909. 845	34356. 03	----------	5	-------	-------	-------	*w*	1. 08—
1*h*	2912. 185	34328. 42	$a\ ^2P_{1\frac{1}{2}}—z\ ^6D^\circ_{2\frac{1}{2}}$	-----	-------	-------	-------	-------	-------
8*h*	2912. 804	34321. 13	$b\ ^2F_{2\frac{1}{2}}—x\ ^4F^\circ_{1\frac{1}{2}}$	-----	-------	-------	-------	-------	-------
1	2913. 462	34313. 38	$b\ ^4D_{3\frac{1}{2}}—y\ ^4G^\circ_{3\frac{1}{2}}$	-----	-------	-------	-------	-------	-------
2	2913. 803	34309. 36	$a\ ^4G_{3\frac{1}{2}}—y\ ^4F^\circ_{3\frac{1}{2}}$	-----	-------	-------	-------	-------	-------
20	2913. 999	34307. 06	$b\ ^4F_{2\frac{1}{2}}—z\ ^4S^\circ_{1\frac{1}{2}}$	4*	-------	-------	-------	0. 13*w*	1. 10+
50	2916. 370	34279. 17	$a\ ^4D_{2\frac{1}{2}}—z\ ^4F^\circ_{2\frac{1}{2}}$	6	. 261	1. 332	1. 071	. 651	1. 201
3	2917. 416	34266. 88	$c\ ^2G_{3\frac{1}{2}}—x\ ^2F^\circ_{3\frac{1}{2}}$	-----	-------	-------	-------	-------	-------

TABLE 6. *The second spectrum of ruthenium* (Ru II)—Continued

1 Intensity	2 λ (air)	3 σ	4 Term combination	5 Type	6 Δg	7 g	8 g	9 Strong p	10 Strong n
	A	*K*							
50	2918. 521	34253. 90	$b\ ^2F_{2\frac{1}{2}}$—$x\ ^4G^\circ_{3\frac{1}{2}}$	5	(0. 04)	0. 94	0. 98	. 11*w*	1. 09−
1*h*	2920. 514	34230. 53							
10	2920. 949	34225. 43	$b\ ^2D_{2\frac{1}{2}}$—$x\ ^4G^\circ_{2\frac{1}{2}}$	6	0. 402	1. 10	0. 70	1. 006	0. 90
3	2921. 880	34214. 53	$b\ ^4D_{1\frac{1}{2}}$—$x\ ^4D^\circ_{1\frac{1}{2}}$						
1*h*	2922. 192	34210. 87	$b\ ^4D_{1\frac{1}{2}}$—$z\ ^2F^\circ_{2\frac{1}{2}}$						
25	2922. 347	34209. 06	$d\ ^2D_{2\frac{1}{2}}$—$w\ ^2D^\circ_{2\frac{1}{2}}$	6	. 131	(1. 20)	1. 07	0. 328	?
10	2923. 112	34200. 11		7				0	0. 871
40	2923. 906	34190. 82	$b\ ^2F_{3\frac{1}{2}}$—$x\ ^4D^\circ_{3\frac{1}{2}}$	6	. 122	1. 086	0. 964	0. 429	1. 025
3*H*	2926. 519	34160. 29	$c\ ^2D_{2\frac{1}{2}}$—$w\ ^4F^\circ_{3\frac{1}{2}}$						
200	2927. 535	34148. 44	$a\ ^4D_{2\frac{1}{2}}$—$z\ ^4D^\circ_{1\frac{1}{2}}$	5	. 193	1. 337	1. 144	. 096	1. 626
2	2928. 063	34142. 28	$b\ ^4D_{0\frac{1}{2}}$—$x\ ^4D^\circ_{1\frac{1}{2}}$						
2	2928. 487	34137. 34	$a\ ^2F_{2\frac{1}{2}}$—$z\ ^4P^\circ_{2\frac{1}{2}}$						
20	2931. 209	34105. 64	$b\ ^2F_{2\frac{1}{2}}$—$x\ ^4F^\circ_{3\frac{1}{2}}$	5	(0. 09)	0. 97	1. 06	. 23*w*	1. 29−
3	2933. 059	34084. 13	$b\ ^4D_{2\frac{1}{2}}$—$x\ ^4D^\circ_{1\frac{1}{2}}$	5	0. 151	1. 333	1. 182	. 075	1. 56?
50	2933. 232	34082. 12	$b\ ^2F_{3\frac{1}{2}}$—$z\ ^2H^\circ_{4\frac{1}{2}}$	4	(0. 066)	(1. 083)	1. 02	. 23*w*	0. 78+
1	2933. 710	34076. 57							
40	2935. 517	34055. 59	$b\ ^2P_{0\frac{1}{2}}$—$1^\circ_{1\frac{1}{2}}$	5	0. 333	0. 876	1. 209	. 166	1. 375
25	2937. 043	34037. 89	$c\ ^2D_{1\frac{1}{2}}$—$w\ ^4D^\circ_{0\frac{1}{2}}$	5	. 242	. 794	0. 552	. 121	0. 915
1*h*	2938. 967	34015. 61							
5	2941. 979	33980. 79	$b\ ^2D_{1\frac{1}{2}}$—$y\ ^4D^\circ_{2\frac{1}{2}}$						
50	2942. 244	33977. 73	$a\ ^4D_{1\frac{1}{2}}$—$z\ ^4F^\circ_{1\frac{1}{2}}$	6	. 724	1. 192	. 468	1. 089	. 830
10	2945. 098	33944. 81	$c\ ^2G_{3\frac{1}{2}}$—$y\ ^2H^\circ_{4\frac{1}{2}}$	7		(0. 942)	. 95	0	. 970
500	2945. 661	33938. 32	$a\ ^4D_{3\frac{1}{2}}$—$z\ ^4D^\circ_{3\frac{1}{2}}$	7		(1. 403)	1. 397	0	1. 400
1*h*	2948. 279	33908. 18	$b\ ^2F_{3\frac{1}{2}}$—$y\ ^4G^\circ_{2\frac{1}{2}}$						
1	2948. 847	33901. 65							
20	2950. 028	33888. 08	$a\ ^4G_{3\frac{1}{2}}$—$z\ ^4H^\circ_{3\frac{1}{2}}$	5	. 211	1. 231	1. 020	0. 106	2. 181
10	2952. 246	33862. 62	$b\ ^2F_{3\frac{1}{2}}$—$x\ ^4F^\circ_{3\frac{1}{2}}$	5	. 13	1. 08	1. 21	. 47*w*	1. 54−
10	2952. 706	33857. 35							
25	2954. 084	33841. 55	$a\ ^4G_{4\frac{1}{2}}$—$z\ ^4G^\circ_{3\frac{1}{2}}$	5	. 184	1. 167	0. 983	. 093	1. 811
1	2954. 855	33832. 72	$e\ ^4D_{3\frac{1}{2}}$—$y\ ^4G^\circ_{4\frac{1}{2}}$						
25	2960. 216	33771. 45		4	0. 180	1. 367	1. 547	0. 091	0. 917
20	2961. 538	33756. 38	$b\ ^2F_{2\frac{1}{2}}$—$x\ ^4G^\circ_{2\frac{1}{2}}$	6	. 248	0. 953	0. 705	. 623	. 830
10*H*	2962. 08	33750. 20							
60	2963. 398	33735. 19	$a\ ^4D_{1\frac{1}{2}}$—$z\ ^4D^\circ_{0\frac{1}{2}}$	5	1. 200	1. 200	. 000	. 601	1. 800
200	2965. 554	33710. 67	$a\ ^4D_{2\frac{1}{2}}$—$z\ ^4F^\circ_{3\frac{1}{2}}$	4		(1. 337)	1. 28	*w*	1. 14+
5	2965. 879	33706. 98	$a\ ^2I_{6\frac{1}{2}}$—$y\ ^4H^\circ_{5\frac{1}{2}}$						
10	2966. 399	33701. 07		5				0. 18*w*	1. 35−
10	2968. 022	33682. 64	$d\ ^2D_{2\frac{1}{2}}$—$y\ ^2P^\circ_{1\frac{1}{2}}$	4	(0. 08)	1. 21	1. 29	. 12*w*	1. 09+
4*h*	2970. 672	33652. 59	$b\ ^2D_{1\frac{1}{2}}$—$z\ ^2P^\circ_{1\frac{1}{2}}$	6	0. 21	(0. 965)	1. 17	. 31	?
2*h*	2971. 057	33648. 23	$a\ ^4G_{2\frac{1}{2}}$—$z\ ^4G^\circ_{3\frac{1}{2}}$	5	. 333	0. 645	0. 978	. 166	1. 811
15	2972. 466	33632. 28	$b\ ^4D_{2\frac{1}{2}}$—$x\ ^4D^\circ_{3\frac{1}{2}}$	6	(0. 07)	1. 35	1. 28	. 17−	1. 32±
10	2972. 578	33631. 02	$b\ ^2G_{4\frac{1}{2}}$—$y\ ^4H^\circ_{5\frac{1}{2}}$						
8	2972. 98	33626. 47	$b\ ^2H_{5\frac{1}{2}}$—$z\ ^2I^\circ_{5\frac{1}{2}}$	6	(0. 03)	1. 08	1. 05	. 16−	1. 06±
8*h*	2973. 826	33616. 90	$b\ ^2D_{2\frac{1}{2}}$—$z\ ^2P^\circ_{1\frac{1}{2}}$ $c\ ^2G_{3\frac{1}{2}}$—$y\ ^2F^\circ_{2\frac{1}{2}}$						
4	2974. 643	33607. 67	$b\ ^2F_{3\frac{1}{2}}$—$y\ ^4G^\circ_{3\frac{1}{2}}$	6	(0. 05)	1. 08	1. 03	. 19−	1. 05±
4	2974. 882	33604. 97		4, 5	0. 158			. 080	?
200	2976. 578	33585. 82	$a\ ^4D_{3\frac{1}{2}}$—$z\ ^4F^\circ_{4\frac{1}{2}}$	4	(0. 05)	1. 38	1. 33	. 19*w*	1. 14+
30	2977. 219	33578. 59	$a\ ^4D_{0\frac{1}{2}}$—$z\ ^4F^\circ_{1\frac{1}{2}}$	5	0. 46	0. 47	0. 01	. 229	0. 700?
25	2977. 471	33575. 75	$b\ ^2H_{5\frac{1}{2}}$—$z\ ^4I^\circ_{5\frac{1}{2}}$	4?	(0. 04)	1. 08	1. 12	. 21*w*	1. 33+
50	2978. 638	33562. 59	$b\ ^2H_{4\frac{1}{2}}$—$z\ ^2I^\circ_{5\frac{1}{2}}$	5	(0. 09)	0. 93	1. 02	. 42*w*	1. 45−
60	2979. 713	33550. 49	$a\ ^4D_{2\frac{1}{2}}$—$z\ ^4D^\circ_{2\frac{1}{2}}$	7		(1. 337)	1. 331	0	1. 334
70	2979. 946	33547. 87	$a\ ^4D_{1\frac{1}{2}}$—$z\ ^4F^\circ_{2\frac{1}{2}}$	4	0. 14	1. 26	1. 12	0. 22*w*	0. 90+
25	2980. 966	33536. 39	$b\ ^2G_{4\frac{1}{2}}$—$x\ ^4G^\circ_{3\frac{1}{2}}$	5	(0. 08)	1. 09	1. 01	. 27*w*	1. 36−?
10*H*	2982. 026	33524. 47	$b\ ^2P_{0\frac{1}{2}}$—$x\ ^4F^\circ_{1\frac{1}{2}}$						
1	2983. 781	33504. 75	$a\ ^4G_{2\frac{1}{2}}$—$y\ ^4P^\circ_{2\frac{1}{2}}$						

TABLE 6. *The second spectrum of ruthenium* (Ru II)—Continued

1 Intensity	2 λ (air)	3 σ	4 Term combination	5 Type	6 Δ g	7 g	8 g	9 Strong p	10 Strong n
	A	K							
5h	2985. 676	33483. 49	c $^2D_{1½}$—x $^4P°_{½}$	4	0. 940	0. 809	1. 749	. 471	0. 339
10	2991. 453	33418. 82	a $^4G_{4½}$—z $^4G°_{3½}$	5	(0. 06)	1. 18	1. 24	. 28w	1. 52—
70	2991. 621	33416. 95	a $^4D_{1½}$—z $^4D°_{½}$	7	-------	(1. 188)	1. 156	0	1. 172
15	2992. 083	33411. 79	a $^4G_{3½}$—z $^4G°_{4½}$	-----	-------	-------	-------	-------	-------
20h	2992. 601	33406. 01	a $^2F_{3½}$—z $^4P°_{2½}$	4	0. 440	(1. 14)	1. 58	0. 220	?
10	2993. 142	33399. 97	b $^2D_{2½}$—x $^4D°_{3½}$	-----	-------	-------	-------	-------	-------
5h	2994. 650	33383. 15	a $^2I_{5½}$—y $^4H°_{4½}$	-----	-------	-------	-------	-------	-------
20h	2996. 002	33368. 09	b $^2P_{1½}$—x $^4D°_{½}$	7, 6	-------	(1. 188)	1. 21	0	1. 20
1	2996. 331	33364. 42	b $^2P_{1½}$—z $^2F°_{2½}$	-----	-------	-------	-------	-------	-------
3h	2998. 126	33344. 45	b $^2P_{0½}$—z $^2P°_{½}$	-----	-------	-------	-------	-------	-------
75	2998. 886	33336. 00	a $^4D_{0½}$—z $^4D°_{½}$	Unaffected			-------	0	0
50	2999. 789	33325. 96	b $^2H_{4½}$—z $^2F°_{3½}$	4	0. 248	0. 960	1. 208	0. 124	0. 092
10	3000. 465	33318. 46	b $^4D_{3½}$—x $^4D°_{2½}$	-----	-------	-------	-------	-------	-------
25	3005. 141	33266. 61	c $^2D_{2½}$—x $^2F°_{3½}$	4	-------	1. 17	(1. 137)	w	1. 05+
1	3005. 891	33258. 31	c $^2D_{1½}$—w $^4F°_{2½}$	-----	-------	-------	-------	-------	-------
10	3006. 716	33249. 19	----------	7	-------	-------	-------	0	1. 27
2h	3007. 88	33236. 32	a $^2F_{2½}$—z $^4F°_{2½}$	6	. 21	0. 86	(1. 07)	0. 105	?
30	3010. 450	33207. 95	a $^4G_{4½}$—z $^4H°_{5½}$	4	(0. 09)	1. 13	1. 04	. 40w	0. 64+
1h	3014. 360	33164. 88	b $^2G_{4½}$—y $^2G°_{4½}$	-----	-------	-------	-------	-------	-------
30	3015. 410	33153. 33	b $^2H_{5½}$—z $^2G°_{4½}$ b $^2D_{1½}$—y $^4G°_{2½}$	5	(0. 06)	1. 05	0. 99	0. 29w	1. 32—
5	3015. 956	33147. 33	b $^2F_{2½}$—z $^2P°_{1½}$	4	0. 200	0. 951	1. 151	. 100	0. 651
30	3017. 816	33126. 90	b $^2F_{3½}$—y $^4G°_{4½}$	5	(0. 06)	1. 09	1. 15	. 22w	1. 37—
1h	3018. 690	33117. 31	b $^2D_{2½}$—y $^4G°_{2½}$	-----	-------	-------	-------	-------	-------
1	3019. 642	33106. 87	b $^2D_{1½}$—y $^4D°_{1½}$	-----	-------	-------	-------	-------	-------
5	3019. 76	33105. 57	a $^2F_{2½}$—z $^4D°_{1½}$	4	0. 270	0. 871	1. 141	. 134	0. 466
1	3020. 549	33096. 92	b $^2G_{3½}$—y $^4H°_{4½}$	-----	-------	-------	-------	-------	-------
1h	3021. 23	33089. 47	b $^2H_{4½}$—z $^2G°_{4½}$ a $^2S_{0½}$—w $^4D°_{1½}$	-----	-------	-------	-------	-------	-------
1h	3021. 977	33081. 29	a $^2I_{5½}$—y $^4H°_{5½}$	-----	-------	-------	-------	-------	-------
10h	3022. 61	33074. 36	c $^2D_{1½}$—$2°_{1½}$	6	-------	(0. 789)	0. 85	w	0. 82
10h	3022. 946	33070. 68	b $^2D_{2½}$—y $^4D°_{1½}$	4	0. 133	1. 106	1. 239	0. 066	. 91
8	3023. 841	33060. 90	b $^2F_{3½}$—z $^2F°_{2½}$	5	. 232	1. 087	0. 855	. 117	1. 667
8h	3026. 817	33028. 39	c $^2D_{2½}$—y $^2F°_{3½}$	-----	-------	-------	-------	-------	-------
30	3027. 780	33017. 88	a $^4D_{0½}$—z $^4D°_{1½}$	5	1. 144	0. 000	1. 444	. 573	1. 716
1	3028. 271	33012. 53	----------	-----	-------	-------	-------	-------	-------
5	3028. 928	33005. 37	b $^4D_{2½}$—y $^4D°_{3½}$	6	(0. 04)	1. 38	1. 34	. 13—	1. 36±
5	3032. 250	32969. 21	a $^2S_{0½}$—x $^4P°_{½}$	-----	-------	-------	-------	-------	-------
7	3032. 442	32967. 13	b $^2F_{2½}$—y $^2G°_{3½}$	5	(0. 06)	0. 99	1. 05	. 15w	1. 20—
5	3032. 624	32965. 15	----------	-----	-------	-------	-------	-------	-------
8	3033. 911	32951. 16	a $^2I_{5½}$—y $^2G°_{4½}$	-----	-------	-------	-------	-------	-------
15h	3035. 792	32930. 75	b $^2F_{2½}$—x $^4D°_{3½}$	7	-------	(0. 945)	0. 95	0	0. 967
75	3036. 463	32923. 47	b $^2H_{5½}$—z $^2I°_{6½}$	5	(0. 07)	1. 08	1. 15	0. 36w	1. 51—
2h	3037. 116	32916. 40	a $^6S_{2½}$—y $^4D°_{2½}$	-----	-------	-------	-------	-------	-------
15	3038. 758	32898. 61	b $^2P_{1½}$—y $^4D°_{0½}$	5	0. 410	1. 187	0. 777	. 205	1. 392
1h	3039. 50	32890. 58	b $^2G_{4½}$—x $^4G°_{4½}$	-----	-------	-------	-------	-------	-------
2	3040. 096	32884. 13	c $^2D_{2½}$—x $^4P°_{1½}$	-----	-------	-------	-------	-------	-------
1	3042. 367	32859. 58	z $^4D°_{1½}$—e $^4D_{2½}$	-----	-------	-------	-------	-------	-------
1h	3043. 342	32849. 06	b $^2H_{5½}$—z $^4I°_{5½}$	-----	-------	-------	-------	-------	-------
10	3046. 132	32818. 97	a $^4D_{1½}$—z $^4D°_{2½}$	5	. 155	1. 193	1. 348	. 077	1. 580
1h	3046. 827	32811. 49	c $^2D_{1½}$—w $^4F°_{1½}$	-----	-------	-------	-------	-------	-------
1	3047. 223	32807. 22	a $^4G_{4½}$—z $^4H°_{4½}$	-----	-------	-------	-------	-------	-------
25	3047. 702	32802. 07	a $^4D_{2½}$—z $^4D°_{3½}$	5	-------	(1. 337)	1. 38	w	1. 50—
50	3049. 246	32785. 46	b $^2H_{4½}$—z $^4I°_{5½}$	5	(0. 08)	0. 98	1. 06	0. 38w	1. 44—
1	3053. 80	32736. 57	----------	-----	-------	-------	-------	-------	-------
5H	3054. 563	32728. 39	z $^4F°_{2½}$—e $^4D_{2½}$	-----	-------	-------	-------	-------	-------
100	3056. 855	32703. 85	b $^2H_{5½}$—y $^4F°_{4½}$	4	(0. 08)	1. 07	1. 15	0. 35w	0. 72+

TABLE 6. *The second spectrum of ruthenium* (Ru II)—Continued

1 Intensity	2 λ (air)	3 σ	4 Term combination	5 Type	6 Δ *g*	7 *g*	8 *g*	9 Strong *p*	10 Strong *s*
	A	*K*							
20	3059. 101	32679. 84	*b* $^4D_{3½}$—*z* $^2F^o_{3½}$						
30	3060. 217	32667. 93	*a* $^2F_{2½}$—*z* $^4F^o_{3½}$	5	0. 416	0. 846	1. 262	. 209	2. 302
30	3060. 500	32664. 90	*b* $^2G_{3½}$—*y* $^2G^o_{4½}$	5	. 179	. 869	1. 048	. 089	1. 67?
8*h*	3062. 07	32648. 16	*b* $^2F_{2½}$—*y* $^4G^o_{2½}$	6	. 260	. 942	0. 682	. 651	0. 812
1	3062. 819	32640. 17	*b* $^2H_{4½}$—*y* $^4F^o_{4½}$						
1	3064. 366	32623. 69							
20	3066. 435	32601. 69	*b* $^2F_{2½}$—*y* $^4D^o_{1½}$	4	. 278	. 954	1. 232	. 139	. 537
3	3067. 575	32589. 57	*c* $^2G_{3½}$—*y* $^2D^o_{2½}$						
4	3070. 317	32560. 47							
30	3072. 341	32539. 02	*b* $^2G_{3½}$—*x* $^4G^o_{2½}$	5	. 186	. 880	0. 694	. 093	1. 345
40	3073. 548	32526. 24	*b* $^2H_{4½}$—*z* $^2G^o_{3½}$	4	(0. 07)	. 92	. 99	. 26*w*	0. 66+
20	3075. 33	32507. 39	*a* $^2F_{2½}$—*z* $^4D^o_{2½}$	6	0. 475	. 873	1. 348	1. 191	1. 111
4	3079. 120	32467. 38	*a* $^4G_{3½}$—*z* $^4H^o_{4½}$	7		(1. 021)	1. 026	0	1. 043
25	3081. 396	32443. 40	*b* $^4D_{3½}$—*z* $^2G^o_{4½}$	4	. 391	1. 384	0. 993	—0. 197	—0. 386
10	3081. 847	32438. 65	*a* $^4D_{1½}$—*z* $^6P^o_{1½}$						
1	3082. 963	32426. 91	*a* $^4G_{4½}$—*z* $^4H^o_{3½}$						
25	3086. 624	32388. 45	*a* $^2I_{6½}$—*x* $^4G^o_{5½}$	4	(0. 07)	1. 04	1. 11	. 40*w*	. 64+
1	3087. 924	32374. 82	*z* $^4D^o_{2½}$—*e* $^4D_{3½}$						
10	3089. 689	32356. 32	*b* $^4D_{1½}$—*z* $^2D^o_{2½}$						
5	3090. 523	32347. 59	*b* $^2F_{2½}$—*y* $^4G^o_{3½}$						
100	3093. 902	32312. 26	*b* $^2G_{4½}$—*x* $^4G^o_{5½}$	5	(0. 08)	1. 06	1. 14	. 34*w*	1. 48—
25	3094. 565	32305. 34	*a* $^4D_{2½}$—*z* $^6P^o_{3½}$	6	0. 500	1. 340	1. 840	1. 248	1. 591
20	3097. 960	32269. 94	*b* $^2D_{2½}$—*z* $^2F^o_{2½}$	6	. 26	(1. 102)	0. 84	0. 65	?
3	3099. 908	32249. 66	*b* $^2G_{4½}$—*y* $^2G^o_{3½}$						
2*h*	3101. 462	32233. 51	*a* $^4G_{2½}$—*z* $^4H^o_{3½}$						
1*h*	3102. 532	32222. 39	*c* $^2G_{4½}$—*y* $^4H^o_{3½}$						
30	3103. 422	32213. 15	*b* $^2G_{4½}$—*x* $^4D^o_{3½}$	5	0. 116	1. 067	0. 951	0. 058	1. 473
30	3107. 586	32169. 99	*a* $^4D_{3½}$—*z* $^6P^o_{3½}$	6	. 178	1. 407	1. 585	. 626	1. 496
5*h*	3111. 148	32133. 16	*c* $^2D_{2½}$—*x* $^4P^o_{2½}$	6	(0. 07)	1. 18	(1. 246)	. 18—	?
10*H*	3113. 947	32104. 28	*b* $^2G_{4½}$—*z* $^2H^o_{4½}$	6	(0. 06)	1. 07	1. 01	. 26—	1. 04±
5*h*	3115. 606	32087. 18	*a* $^4G_{3½}$—*z* $^4H^o_{3½}$						
20?	3118. 03	32062. 2	*b* $^2H_{4½}$—*y* $^4F^o_{3½}$	4	0. 10	0. 93	1. 03	. 36*w*	0. 58+
3	3120. 234	32039. 59	*a* $^4D_{0½}$—*z* $^6P^o_{1½}$						
25	3120. 872	32033. 04	*b* $^4D_{1½}$—*y* $^4F^o_{1½}$	6	. 780	1. 200	0. 420	1. 169	. 810
10	3123. 892	32002. 07	*b* $^2P_{0½}$—*x* $^4D^o_{0½}$	6	. 51	0. 88	. 37	0. 254	. 627
25	3124. 678	31994. 02	*b* $^4D_{3½}$—*y* $^4F^o_{4½}$						
20	3126. 613	31974. 22	*b* $^2F_{3½}$—*z* $^2F^o_{3½}$	6	. 116	1. 082	1. 198	. 415	1. 140
25	3127. 923	31960. 83	*b* $^4D_{0½}$—*y* $^4F^o_{1½}$	5	. 298	0. 139	0. 437	. 149	0. 586
10	3132. 701	31912. 09	*b* $^4D_{3½}$—*z* $^2D^o_{3½}$	5	(0. 06)	1. 40	1. 34	. 15*w*	1. 55—
25	3134. 817	31890. 55	*a* $^2I_{5½}$—*z* $^2H^o_{4½}$	4	(0. 08)	0. 94	1. 02	. 37*w*	0. 57+
10	3135. 199	31886. 66	*c* $^2D_{1½}$—*y* $^2F^o_{2½}$						
25	3135. 807	31880. 48	*b* $^4D_{3½}$—*z* $^2G^o_{3½}$	6	0. 362	1. 391	1. 029	1. 270	1. 210
1	3138. 022	31857. 98	*b* $^2D_{1½}$—*x* $^4D^o_{2½}$						
2	3139. 576	31842. 21	*d* $^2D_{1½}$—*x* $^2D^o_{1½}$						
10	3141. 594	31821. 76	*b* $^2D_{2½}$—*x* $^4D^o_{2½}$	6	. 180	1. 097	1. 277	0. 453	1. 187
40	3143. 240	31805. 09	*b* $^2P_{0½}$—*y* $^4D^o_{1½}$	5	. 361	0. 868	1. 230	. 181	1. 411
60	3143. 650	31800. 94	*b* $^2F_{2½}$—*z* $^2F^o_{2½}$	6	. 12	0. 99	0. 87	. 29—	0. 93±
15	3146. 09	31776. 28	*a* $^2F_{3½}$—*z* $^4D^o_{2½}$	4	. 206	1. 139	1. 345	. 103	. 624
3	3146. 395	31773. 20	*b* $^2P_{1½}$—*y* $^4P^o_{1½}$						
50	3147. 456	31762. 49	*b* $^2H_{5½}$—*z* $^4I^o_{4½}$	5	. 120	1. 06	0. 94	. 06	1. 60—
2	3148. 716	31749. 78	*b* $^2G_{3½}$—*y* $^2G^o_{3½}$						
3	3148. 913	31747. 80	*c* $^2G_{4½}$—*y* $^2G^o_{4½}$						
1	3149. 901	31737. 84	*b* $^2F_{3½}$—*z* $^2G^o_{4½}$						
2	3152. 311	31713. 57	*b* $^2G_{3½}$—*x* $^4D^o_{3½}$						
2	3157. 173	31664. 74	*c* $^2G_{3½}$—*x* $^4F^o_{2½}$						

TABLE 6. *The second spectrum of ruthenium* (Ru II)—Continued

1 Intensity	2 λ (air)	3 σ	4 Term combination	5 Type	6 Δ g	7 g	8 g	9 Strong p	10 Strong n
	A	*K*							
75	3160. 631	31630. 10	*b* $^2G_{4\frac{1}{2}}$—*y* $^4G^{\circ}_{3\frac{1}{2}}$	5	(0. 05)	1. 08	1. 03	0. 18*w*	1. 26—
100	3163. 188	31604. 53	*b* $^2G_{3\frac{1}{2}}$—*z* $^2H^{\circ}_{4\frac{1}{2}}$	5	0. 123	0. 896	1. 019	. 062	1. 451
10	3164. 719	31589. 24	*c* $^2D_{2\frac{1}{2}}$—*y* $^2D^{\circ}_{2\frac{1}{2}}$	6	(0. 04)	1. 18	1. 14	. 09*h*	1. 16*h*
50	3165. 071	31585. 73	*b* $^2G_{4\frac{1}{2}}$—*y* $^4G^{\circ}_{3\frac{1}{2}}$	5	(0. 08)	1. 12	1. 20	. 36*w*	1. 56—
15	3166. 091	31575. 55	*b* $^4D_{1\frac{1}{2}}$—*y* $^4F^{\circ}_{2\frac{1}{2}}$	4	0. 174	1. 194	1. 020	. 087	0. 759
15	3166. 542	31571. 05	*c* $^2G_{3\frac{1}{2}}$—*x* $^4G^{\circ}_{3\frac{1}{2}}$	6	(0. 05)	0. 96	1. 01	. 18—	. 98±
75	3167. 458	31561. 92	*a* $^2I_{6\frac{1}{2}}$—*z* $^2H^{\circ}_{5\frac{1}{2}}$	4	(0. 06)	1. 05	1. 11	. 34*w*	. 71+
80	3172. 669	31510. 09	*b* $^2P_{1\frac{1}{2}}$—*z* $^2D^{\circ}_{2\frac{1}{2}}$	5	0. 140	1. 185	1. 325	0. 70	1. 536
5	3172. 946	31507. 34	*d* $^2D_{2\frac{1}{2}}$—*x* $^2D^{\circ}_{2\frac{1}{2}}$	7	0	1. 19	1. 19	0*h*	1. 19*h*
20	3175. 143	31485. 54	*b* $^2G_{4\frac{1}{2}}$—*z* $^2H^{\circ}_{5\frac{1}{2}}$	5	(0. 08)	0. 96	1. 04	0. 36*w*	1. 40—
10	3175. 312	31483. 86	*a* $^4D_{3\frac{1}{2}}$—*z* $^6F^{\circ}_{3\frac{1}{2}}$	-----	-------	-------	-------	-------	-------
150	3177. 048	31466. 66	*a* $^4D_{3\frac{1}{2}}$—*z* $^6F^{\circ}_{4\frac{1}{2}}$	5	-------	(1. 403)	1. 42	*w*	1. 46—
10	3179. 24	31444. 96	*b* $^4D_{2\frac{1}{2}}$—*y* $^4F^{\circ}_{2\frac{1}{2}}$	-----	-------	-------	-------	-------	-------
1	3182. 144	31416. 27	*b* $^4D_{3\frac{1}{2}}$—*y* $^4F^{\circ}_{3\frac{1}{2}}$	-----	-------	-------	-------	-------	-------
25	3183. 479	31403. 09	*c* $^2D_{1\frac{1}{2}}$—*x* $^4P^{\circ}_{2\frac{1}{2}}$	5	0. 457	0. 789	1. 246	0. 229	1. 932
1	3184. 177	31396. 21	----------	-----	-------	-------	-------	-------	-------
10	3185. 294	31385. 20	*b* $^2G_{3\frac{1}{2}}$—*x* $^4F^{\circ}_{4\frac{1}{2}}$	5	. 304	(0. 883)	1. 187	. 152	
2	3192. 568	31313. 69	----------	-----	-------	-------	-------	-------	?
100	3195. 148	31288. 41	*b* $^2F_{3\frac{1}{2}}$—*y* $^4F^{\circ}_{4\frac{1}{2}}$	5	(0. 07)	1. 09	1. 16	. 24*w*	1. 40—
5	3195. 746	31282. 55	----------	-----	-------	-------	-------	-------	-------
20	3198. 624	31254. 41	*b* $^2H_{4\frac{1}{2}}$—*z* $^4G^{\circ}_{3\frac{1}{2}}$	4	(0. 03)	0. 94	0. 97	. 10*w*	0. 84+
50	3201. 260	31228. 68	*b* $^2H_{5\frac{1}{2}}$—*z* $^4G^{\circ}_{4\frac{1}{2}}$	4	(0. 03)?	. 96?	. 99?	. 13*w*	. 83+
10	3203. 555	31206. 30	*b* $^2F_{3\frac{1}{2}}$—*z* $^2D^{\circ}_{2\frac{1}{2}}$	4	0. 242	1. 083	1. 325	. 122	. 478
20	3204. 287	31199. 18	*c* $^2G_{3\frac{1}{2}}$—*y* $^2G^{\circ}_{4\frac{1}{2}}$	5	. 120	0. 942	1. 062	. 060	1. 482
2	3205. 567	31186. 72	*b* $^2P_{1\frac{1}{2}}$—*y* $^4F^{\circ}_{1\frac{1}{2}}$	-----	-------	-------	-------	-------	-------
50	3206. 799	31174. 74	*b* $^2F_{2\frac{1}{2}}$—*z* $^2G^{\circ}_{3\frac{1}{2}}$	6	(0. 05)	1. 08	1. 03	0. 16—	1. 05±
10	3207. 421	31168. 69	*c* $^2D_{2\frac{1}{2}}$—*s*$1^{\circ}_{\frac{1}{2}}$	7	-------	1. 193	(1. 209)	0	1. 169
15	3207. 841	31164. 61	*b* $^2H_{4\frac{1}{2}}$—*z* $^4G^{\circ}_{4\frac{1}{2}}$	6	0. 180	0. 956	1. 136	0. 811	1. 046
3	3209. 422	31149. 26	*b* $^2G_{4\frac{1}{2}}$—*y* $^4G^{\circ}_{4\frac{1}{2}}$	-----	-------	-------	-------	-------	-------
2	3210. 688	31136. 98	*b* $^4D_{1\frac{1}{2}}$—*z* $^4G^{\circ}_{2\frac{1}{2}}$	-----	-------	-------	-------	-------	-------
5	3211. 381	31130. 26	*b* $^2G_{3\frac{1}{2}}$—*y* $^4G^{\circ}_{3\frac{1}{2}}$	-----	-------	-------	-------	-------	-------
10	3217. 863	31067. 55	*c* $^2D_{1\frac{1}{2}}$—*y* $^2D^{\circ}_{1\frac{1}{2}}$	6	(0. 06)	. 80	0. 74	. 088	0. 77±
50	3219. 418	31052. 55	*b* $^4D_{3\frac{1}{2}}$—*z* $^4I^{\circ}_{4\frac{1}{2}}$	4	0. 438	1. 416	. 978	—. 219	—. 555
25	3221. 360	31033. 83	*a* $^4D_{2\frac{1}{2}}$—*z* $^6P^{\circ}_{3\frac{1}{2}}$	5	. 241	1. 334	1. 575	. 122	2. 179
30	3221. 970	31027. 95	*a* $^2F_{3\frac{1}{2}}$—*z* $^4D^{\circ}_{3\frac{1}{2}}$	6	. 254	1. 134	1. 388	. 889	1. 261?
4	3224. 041	31008. 02	*b* $^2P_{0\frac{1}{2}}$—*x* $^4D^{\circ}_{1\frac{1}{2}}$	-----	-------	-------	-------	-------	-------
15	3224. 938	30999. 40	*d* $^2D_{1\frac{1}{2}}$—*w* $^4D^{\circ}_{0\frac{1}{2}}$	-----	-------	-------	-------	-------	-------
3	3226. 526	30984. 14	*d* $^2D_{2\frac{1}{2}}$—*w* $^4D^{\circ}_{3\frac{1}{2}}$	-----	-------	-------	-------	-------	-------
150	3228. 49	30965. 29	*b* $^2H_{5\frac{1}{2}}$—*z* $^4H^{\circ}_{5\frac{1}{2}}$	5	(0. 07)	1. 06	1. 13	. 39*w*	1. 52—
10	3231. 586	30935. 63	*a* $^2I_{5\frac{1}{2}}$—*y* $^4G^{\circ}_{4\frac{1}{2}}$	4	0. 220	0. 938	(1. 158)	. 110	?
50	3234. 339	30909. 30	*b* $^4D_{1\frac{1}{2}}$—*y* $^4P^{\circ}_{2\frac{1}{2}}$	5	(0 09)	1. 21	1. 30	. 13*w*	1. 43—
5	3235. 786	30895. 48	*b* $^2H_{3\frac{1}{2}}$—*z* $^4G^{\circ}_{3\frac{1}{2}}$	6	0. 17	(1. 053)	1. 22	. 929	?
25	3245. 611	30801. 95	*a* $^4D_{2\frac{1}{2}}$—*z* $^6F^{\circ}_{1\frac{1}{2}}$	5	. 272	1. 340	1. 068	. 138	1. 748
25	3246. 222	30796. 16	*c* $^2G_{4\frac{1}{2}}$—*x* $^4D^{\circ}_{3\frac{1}{2}}$	5	. 124	1. 078	0. 954	. 061	1. 512
3	3248. 04	30778. 92	*b* $^4D_{2\frac{1}{2}}$—*y* $^4P^{\circ}_{2\frac{1}{2}}$?	-----	-------	-------	-------	-------	-------
15	3253. 314	30729. 03	*b* $^2P_{1\frac{1}{2}}$—*y* $^4F^{\circ}_{2\frac{1}{2}}$	4	. 160	1. 023	1. 183	. 080	0. 783
2	3257. 159	30692. 75	*b* $^4D_{3\frac{1}{2}}$—*z* $^4G^{\circ}_{3\frac{1}{2}}$	-----	-------	-------	-------	-------	-------
20	3257. 748	30687. 20	*c* $^2G_{4\frac{1}{2}}$—*z* $^2H^{\circ}_{4\frac{1}{2}}$	6	(0. 07)	1. 10	1. 03	. 33—	1. 06±
75	3258. 970	30675. 69	*a* $^2F_{3\frac{1}{2}}$—*z* $^4F^{\circ}_{4\frac{1}{2}}$	5	0. 203	1. 345	1. 142	. 101	2. 045
10	3260. 147	30664. 62	*a* $^4D_{2\frac{1}{2}}$—*z* $^6F^{\circ}_{3\frac{1}{2}}$	-----	-------	-------	-------	-------	-------
2	3261. 747	30649. 58	*b* $^2G_{3\frac{1}{2}}$—*y* $^4G^{\circ}_{4\frac{1}{2}}$	-----	-------	-------	-------	-------	-------
25	3264. 795	30620. 97	*b* $^2H_{4\frac{1}{2}}$—*z* $^4H^{\circ}_{5\frac{1}{2}}$	5	. 122	1. 071	0. 949	. 061	1. 620
8	3266. 112	30608. 62	*b* $^4D_{3\frac{1}{2}}$—*z* $^4G^{\circ}_{3\frac{1}{2}}$	-----	-------	-------	-------	-------	-------
5	3267. 184	30598. 58	----------	-----	-------	-------	-------	-------	-------
60	3268. 803	30583. 42	*b* $^2G_{3\frac{1}{2}}$—*z* $^2F^{\circ}_{2\frac{1}{2}}$	5 *us*	-------	(0. 883)	0. 85	*w*	0. 97

TABLE 6. *The second spectrum of ruthenium* (Ru II)—Continued

1 Intensity	2 λ (air)	3 σ	4 Term combination	5 Type	6 Δ *g*	7 *g*	8 *g*	9 Strong *p*	10 Strong *n*
	A	*K*							
3	3270. 155	30570. 78	*c* $^2D_{2\frac{1}{2}}$—*x* $^4G^\circ_{3\frac{1}{2}}$	-----	-------	-------	-------	-------	-------
1	3272. 010	30553. 45	*a* $^2S_{0\frac{1}{2}}$—*y* $^2D^\circ_{1\frac{1}{2}}$	-----	-------	-------	-------	-------	-------
10	3273. 612	30538. 50	*b* $^2P_{0\frac{1}{2}}$—*y* $^4D^\circ_{0\frac{1}{2}}$	-----	-------	-------	-------	-------	-------
15	3275. 729	30518. 76	*b* $^4D_{3\frac{1}{2}}$—*z* $^4G^\circ_{4\frac{1}{2}}$	-----	-------	-------	-------	-------	-------
2	3276. 783	30508. 94	----------	-----	-------	-------	-------	-------	-------
2	3281. 193	30467. 94	*c* $^2G_{4\frac{1}{2}}$—*x* $^4F^\circ_{4\frac{1}{2}}$	-----	-------	-------	-------	-------	-------
8	3281. 518	30464. 93	*b* $^4D_{3\frac{1}{2}}$—*y* $^4P^\circ_{2\frac{1}{2}}$	-----	-------	-------	-------	-------	-------
60	3282. 973	30451. 42	*b* $^2D_{1\frac{1}{2}}$—*z* $^2D^\circ_{2\frac{1}{2}}$	5	0. 367	(0. 965)	1. 332	0. 184	?
30	3284. 343	30438. 72	*c* $^2D_{1\frac{1}{2}}$—$1^\circ_{1\frac{1}{2}}$	-----	-------	-------	-------	-------	-------
2	3285. 762	30425. 58	*b* $^2F_{3\frac{1}{2}}$—*y* $^4F^\circ_{2\frac{1}{2}}$	-----	-------	-------	-------	-------	-------
1	3286. 114	30422. 32	*c* $^2D_{2\frac{1}{2}}$—*x* $^4F^\circ_{3\frac{1}{2}}$	-----	-------	-------	-------	-------	-------
2	3286. 840	30415. 60	*b* $^2D_{2\frac{1}{2}}$—*z* $^2D^\circ_{2\frac{1}{2}}$	-----	-------	-------	-------	-------	-------
300	3294. 232	30347. 35	*a* $^4D_{2\frac{1}{2}}$—*z* $^6F^\circ_{3\frac{1}{2}}$	5 *us*	-------	-------	-------	.49*w*	1. 82—
5	3298. 321	30309. 73	*a* $^2I_{6\frac{1}{2}}$—*z* $^2I^\circ_{5\frac{1}{2}}$	-----	-------	-------	-------	-------	-------
2	3300. 115	30293. 25	----------	-----	-------	-------	-------	-------	-------
15	3301. 14	30283. 85	*b* $^2H_{5\frac{1}{2}}$—*z* $^4H^\circ_{4\frac{1}{2}}$ *c* $^2G_{3\frac{1}{2}}$—*y* $^2G^\circ_{3\frac{1}{2}}$	5	(0. 04)	1. 10	1. 06	.16*w*	1. 26—?
15	3301. 219	30283. 12	----------	-----	-------	-------	-------	-------	-------
3	3308. 102	30220. 11	*b* $^2H_{4\frac{1}{2}}$—*z* $^4H^\circ_{4\frac{1}{2}}$ *d* $^2D_{1\frac{1}{2}}$—*w* $^4F^\circ_{2\frac{1}{2}}$	-----	-------	-------	-------	-------	-------
10	3308. 885	30212. 96	*c* $^2G_{4\frac{1}{2}}$—*y* $^4G^\circ_{3\frac{1}{2}}$	-----	-------	-------	-------	-------	-------
10	3309. 233	30209. 79	*b* $^2F_{2\frac{1}{2}}$—*y* $^4P^\circ_{1\frac{1}{2}}$	-----	-------	-------	-------	-------	-------
15	3310. 283	30200. 21	*d* $^2D_{2\frac{1}{2}}$—*x* $^2G^\circ_{3\frac{1}{2}}$	-----	-------	-------	-------	-------	-------
10	3312. 831	30176. 98	----------	6	0. 265	-------	-------	. 397	?
1	3313. 010	30175. 35	----------	-----	-------	-------	-------	-------	-------
1	3313. 738	30168. 72	*c* $^2G_{4\frac{1}{2}}$—*y* $^4G^\circ_{4\frac{1}{2}}$	-----	-------	-------	-------	-------	-------
3	3317. 015	30138. 91	*c* $^2G_{3\frac{1}{2}}$—*z* $^2H^\circ_{4\frac{1}{2}}$	-----	-------	-------	-------	-------	-------
3	3317. 402	30135. 40	*b* $^2G_{3\frac{1}{2}}$—*x* $^4D^\circ_{2\frac{1}{2}}$	-----	-------	-------	-------	-------	-------
5	3317. 591	30133. 68	*a* $^4D_{1\frac{1}{2}}$—*z* $^6F^\circ_{0\frac{1}{2}}$	-----	-------	-------	-------	-------	-------
3	3322. 784	30086. 59	----------	-----	-------	-------	-------	-------	-------
2	3324. 553	30070. 58	*a* $^4D_{1\frac{1}{2}}$—*z* $^6F^\circ_{1\frac{1}{2}}$	-----	-------	-------	-------	-------	-------
1	3324. 800	30068. 35	*c* $^2G_{4\frac{1}{2}}$—*z* $^2H^\circ_{5\frac{1}{2}}$	-----	-------	-------	-------	-------	-------
25	3325. 407	30062. 86	*b* $^2P_{1\frac{1}{2}}$—*y* $^4P^\circ_{2\frac{1}{2}}$	5	0. 108	1. 189	1. 297	0. 052	1. 459—
1	3335. 852	29968. 73	*a* $^2I_{5\frac{1}{2}}$—*z* $^4I^\circ_{6\frac{1}{2}}$	-----	-------	-------	-------	-------	-------
1	3338. 329	29946. 49	*b* $^2F_{2\frac{1}{2}}$—*z* $^2D^\circ_{2\frac{1}{2}}$	-----	-------	-------	-------	-------	-------
75	3339. 788	29933. 41	*a* $^4D_{1\frac{1}{2}}$—*z* $^6F^\circ_{2\frac{1}{2}}$	5	. 126	1. 177	1. 303	. 064	1. 492
1	3340. 404	29927. 89	----------	-----	-------	-------	-------	-------	-------
2	3340. 789	29924. 45	*a* $^2S_{0\frac{1}{2}}$—$1^\circ_{1\frac{1}{2}}$	-----	-------	-------	-------	-------	-------
1	3341. 34	29919. 51	*b* $^2D_{2\frac{1}{2}}$—*y* $^4F^\circ_{3\frac{1}{2}}$ *c* $^2G_{3\frac{1}{2}}$—*x* $^4F^\circ_{4\frac{1}{2}}$	-----	-------	-------	-------	-------	-------
2	3342. 665	29907. 65	*c* $^2D_{1\frac{1}{2}}$—*x* $^4F^\circ_{1\frac{1}{2}}$	-----	-------	-------	-------	-------	-------
50	3343. 200	29902. 87	*b* $^2F_{3\frac{1}{2}}$—*z* $^4G^\circ_{3\frac{1}{2}}$	6	. 10	1. 08	0. 98	. 34—	1. 03±
100	3350. 246	29839. 98	*b* $^2H_{4\frac{1}{2}}$—*z* $^4H^\circ_{5\frac{1}{2}}$	7	-------	(0. 958)	. 964	0	0. 937
8	3353. 29	29812. 89	*b* $^2F_{3\frac{1}{2}}$—*z* $^4G^\circ_{4\frac{1}{2}}$	-----	-------	-------	-------	-------	-------
15	3359. 230	29760. 17	*b* $^2G_{4\frac{1}{2}}$—*z* $^2G^\circ_{4\frac{1}{2}}$	-----	-------	-------	-------	-------	-------
15	3359. 324	29759. 34	*b* $^2F_{3\frac{1}{2}}$—*y* $^4P^\circ_{2\frac{1}{2}}$ *a* $^2F_{2\frac{1}{2}}$—*z* $^6F^\circ_{1\frac{1}{2}}$	4	. 20	0. 86	(1. 058)	0. 099?	?
5	3359. 985	29753. 49	*b* $^4P_{2\frac{1}{2}}$—*z* $^4P^\circ_{1\frac{1}{2}}$	-----	-------	-------	-------	-------	-------
8	3362. 140	29734. 42	*a* $^4D_{0\frac{1}{2}}$—*z* $^6F^\circ_{0\frac{1}{2}}$	-----	-------	-------	-------	-------	-------
2	3365. 384	29705. 76	*d* $^2D_{2\frac{1}{2}}$—*w* $^4D^\circ_{1\frac{1}{2}}$	-----	-------	-------	-------	-------	-------
40	3369. 288	29671. 34	*a* $^4D_{0\frac{1}{2}}$—*z* $^6F^\circ_{1\frac{1}{2}}$	5	1. 06	. 00	1. 06	. 53	1. 59
30	3370. 061	29664. 53	*c* $^2G_{3\frac{1}{2}}$—*y* $^4G^\circ_{3\frac{1}{2}}$	6	(0. 08)	. 95	1. 03	. 27—	0. 99±
2	3373. 472	29634. 54	*b* $^2D_{2\frac{1}{2}}$—*y* $^4F^\circ_{2\frac{1}{2}}$	-----	-------	-------	-------	-------	-------
2	3376. 624	29606. 88	*a* $^2I_{6\frac{1}{2}}$—*z* $^2I^\circ_{6\frac{1}{2}}$	-----	-------	-------	-------	-------	-------
3	3380. 356	29574. 19	*b* $^4D_{3\frac{1}{2}}$—*z* $^4H^\circ_{4\frac{1}{2}}$?	-----	-------	-------	-------	-------	-------
2	3382. 229	29557. 82	*b* $^4D_{1\frac{1}{2}}$—*z* $^4S^\circ_{1\frac{1}{2}}$	-----	-------	-------	-------	-------	-------
3	3387. 963	29507. 79	*b* $^4D_{2\frac{1}{2}}$—*z* $^4H^\circ_{3\frac{1}{2}}$	4	0. 392	(1. 344)	0. 952	0. 196	?
2	3389. 208	29497. 0	*b* $^2G_{3\frac{1}{2}}$—*z* $^2F^\circ_{3\frac{1}{2}}$	-----	-------	-------	-------	-------	-------
1	3393. 904	29456. 14	*b* $^2G_{4\frac{1}{2}}$—*z* $^4I^\circ_{5\frac{1}{2}}$	-----	-------	-------	-------	-------	-------

TABLE 6. *The second spectrum of ruthenium* (Ru II)—Continued

1 Intensity	2 λ (air)	3 σ	4 Term combination	5 Type	6 Δ g	7 g	8 g	9 Strong p	10 Strong n
	A	*K*							
8	3398.862	29413.17	*b* $^2P_{0\frac{1}{2}}$—*y* $^4P^\circ_{1\frac{1}{2}}$	5*us*	-------	-------	-------	.84	1.58
5	3401.188	29393.06	*a* $^2S_{0\frac{1}{2}}$—*x* $^4F^\circ_{1\frac{1}{2}}$?	-----	-------	-------	-------	-------	-------
1	3410.03	29316.85	*a* $^2I_{5\frac{1}{2}}$—*z* $^2I^\circ_{6\frac{1}{2}}$	-----	-------	-------	-------	-------	-------
50	3410.742	29310.73	*b* $^2G_{4\frac{1}{2}}$—*y* $^4F^\circ_{4\frac{1}{2}}$	6	(0.08)	1.07	1.15	.35—	1.11+
10	3411.43	29304.8	*a* $^2F_{2\frac{1}{2}}$—*z* $^6F^\circ_{3\frac{1}{2}}$	-----	-------	-------	-------	-------	-------
5	3416.612	29260.37	*b* $^2G_{3\frac{1}{2}}$—*z* $^2G^\circ_{4\frac{1}{2}}$	-----	-------	-------	-------	-------	-------
1	3424.018	29197.08	*b* $^2G_{4\frac{1}{2}}$—*z* $^2G^\circ_{3\frac{1}{2}}$	-----	-------	-------	-------	-------	-------
1	3424.131	29196.12	*b* $^2D_{2\frac{1}{2}}$—*z* $^4G^\circ_{3\frac{1}{2}}$	-----	-------	-------	-------	-------	-------
5	3424.381	29193.99	*b* $^4D_{3\frac{1}{2}}$—*z* $^4H^\circ_{3\frac{1}{2}}$	-----	-------	-------	-------	-------	-------
6	3427.728	29165.48	*b* $^2F_{2\frac{1}{2}}$—*y* $^4F^\circ_{2\frac{1}{2}}$	6	(0.06)	(0.945)	1.00	.16	?
1	3433.10	29119.84	----------	-----	-------	-------	-------	-------	-------
2	3434.02	29112.04	*b* $^2D_{2\frac{1}{2}}$—*z* $^4G^\circ_{3\frac{1}{2}}$	-----	-------	-------	-------	-------	-------
10	3446.750	29004.53	*b* $^2D_{1\frac{1}{2}}$—*y* $^4P^\circ_{2\frac{1}{2}}$	5	0.339	0.954	1.293	.170	1.801
10	3462.983	28868.57	*b* $^2F_{3\frac{1}{2}}$—*z* $^4H^\circ_{3\frac{1}{2}}$	4	(0.04)	1.04	1.00	.15*w*	0.85+
10	3465.405	28848.39	*d* $^2D_{1\frac{1}{2}}$—*y* $^2F^\circ_{2\frac{1}{2}}$	-----	-------	-------	-------	-------	-------
5	3469.269	28816.26	*c* $^2G_{4\frac{1}{2}}$—*z* $^2I^\circ_{5\frac{1}{2}}$	-----	-------	-------	-------	-------	-------
1	3469.907	28810.97	*b* $^2G_{3\frac{1}{2}}$—*y* $^4F^\circ_{4\frac{1}{2}}$	-----	-------	-------	-------	-------	-------
1	3473.195	28783.69	*b* $^4P_{2\frac{1}{2}}$—*z* $^4P^\circ_{2\frac{1}{2}}$	-----	-------	-------	-------	-------	-------
5	3479.339	28732.87	*b* $^2G_{4\frac{1}{2}}$—*y* $^4F^\circ_{3\frac{1}{2}}$	7	-------	(1.067)	1.03	0	1.20
2	3480.060	28725.91	*b* $^2F_{2\frac{1}{2}}$—*z* $^4G^\circ_{2\frac{1}{2}}$	-----	-------	-------	-------	-------	-------
2	3481.928	28711.50	*b* $^2P_{1\frac{1}{2}}$—*z* $^4S^\circ_{1\frac{1}{2}}$	-----	-------	-------	-------	-------	-------
5	3483.649	28697.32	*b* $^2G_{3\frac{1}{2}}$—*z* $^2G^\circ_{3\frac{1}{2}}$	-----	-------	-------	-------	-------	-------
5	3487.672	28664.22	*c* $^2D_{2\frac{1}{2}}$—*y* $^4G^\circ_{3\frac{1}{2}}$	-----	-------	-------	-------	-------	-------
5	3490.277	28642.82	*b* $^2F_{3\frac{1}{2}}$—*z* $^4G^\circ_{3\frac{1}{2}}$	-----	-------	-------	-------	-------	-------
10	3500.86	28556.24	*a* $^2F_{3\frac{1}{2}}$—*z* $^6F^\circ_{4\frac{1}{2}}$	-----	-------	-------	-------	-------	-------
2	3504.56	28526.09	*b* $^4F_{2\frac{1}{2}}$—*z* $^4P^\circ_{1\frac{1}{2}}$	-----	-------	-------	-------	-------	-------
200	3509.217	28488.24	*b* $^2F_{3\frac{1}{2}}$—*z* $^4H^\circ_{3\frac{1}{2}}$	6	0.121	1.082	0.961	0.427	1.021
2	3511.40	28470.53	----------	-----	-------	-------	-------	-------	-------
20	3520.063	28400.46	*d* $^2D_{2\frac{1}{2}}$—*y* $^2F^\circ_{3\frac{1}{2}}$	-----	-------	-------	-------	-------	-------
6	3523.917	28369.40	*b* $^2G_{4\frac{1}{2}}$—*z* $^4I^\circ_{4\frac{1}{2}}$	6	.12	(1.067)	.95	.54—	?
20	3524.480	28364.87	*d* $^2D_{1\frac{1}{2}}$—*x* $^4P^\circ_{2\frac{1}{2}}$	-----	-------	-------	-------	-------	-------
20	3527.183	28343.13	*c* $^2G_{4\frac{1}{2}}$—*z* $^2G^\circ_{4\frac{1}{2}}$	-----	-------	-------	-------	-------	-------
2	3542.617	28219.65	*a* $^2S_{0\frac{1}{2}}$—*z* $^2P^\circ_{1\frac{1}{2}}$	-----	-------	-------	-------	-------	-------
10	3548.508	28172.81	*b* $^4P_{1\frac{1}{2}}$—*z* $^4P^\circ_{0\frac{1}{2}}$	-----	-------	-------	-------	-------	-------
10	3556.816	28107.01	*a* $^4H_{4\frac{1}{2}}$—*z* $^4F^\circ_{3\frac{1}{2}}$	-----	-------	-------	-------	-------	-------
5	3565.437	28039.05	*c* $^2G_{4\frac{1}{2}}$—*z* $^4I^\circ_{5\frac{1}{2}}$	-----	-------	-------	-------	-------	-------
10	3566.452	28031.07	*c* $^2G_{3\frac{1}{2}}$—*z* $^2F^\circ_{3\frac{1}{2}}$	-----	-------	-------	-------	-------	-------
6	3577.045	27948.06	*b* $^2G_{3\frac{1}{2}}$—*y* $^4F^\circ_{2\frac{1}{2}}$	-----	-------	-------	-------	-------	-------
1	3582.395	27906.32	*a* $^4D_{3\frac{1}{2}}$—*z* $^6D^\circ_{3\frac{1}{2}}$	-----	-------	-------	-------	-------	-------
20	3584.022	27893.65	*c* $^2G_{4\frac{1}{2}}$—*y* $^4F^\circ_{4\frac{1}{2}}$	6	(0.07)	1.11	1.18	.31—	1.15±
4	3585.43	27882.70	*b* $^4P_{2\frac{1}{2}}$—*z* $^4F^\circ_{2\frac{1}{2}}$	-----	-------	-------	-------	-------	-------
30	3591.518	27835.44	*b* $^2G_{4\frac{1}{2}}$—*z* $^4G^\circ_{4\frac{1}{2}}$	6	(0.05)	1.05	1.10	.24—	1.07±
2	3601.613	27757.42	*a* $^4H_{3\frac{1}{2}}$—*z* $^4F^\circ_{3\frac{1}{2}}$	-----	-------	-------	-------	-------	-------
2	3603.059	27746.28	*b* $^4F_{3\frac{1}{2}}$—*z* $^4P^\circ_{2\frac{1}{2}}$	-----	-------	-------	-------	-------	-------
5	3612.482	27673.91	*a* $^2S_{0\frac{1}{2}}$—*y* $^4D^\circ_{1\frac{1}{2}}$	-----	-------	-------	-------	-------	-------
2	3615.206	27653.05	*b* $^2D_{1\frac{1}{2}}$—*z* $^4S^\circ_{1\frac{1}{2}}$	-----	-------	-------	-------	-------	-------
2	3627.896	27556.33	*b* $^4F_{2\frac{1}{2}}$—*z* $^4P^\circ_{2\frac{1}{2}}$	-----	-------	-------	-------	-------	-------
4	3628.629	27550.76	----------	-----	-------	-------	-------	-------	-------
2	3645.201	27425.51	*b* $^2G_{3\frac{1}{2}}$—*z* $^4G^\circ_{3\frac{1}{2}}$	-----	-------	-------	-------	-------	-------
2	3649.771	27391.18	*c* $^2D_{1\frac{1}{2}}$—*x* $^4D^\circ_{1\frac{1}{2}}$	-----	-------	-------	-------	-------	-------
5	3652.836	27368.19	*a* $^2I_{6\frac{1}{2}}$—*z* $^4H^\circ_{5\frac{1}{2}}$	-----	-------	-------	-------	-------	-------
60	3657.571	27332.76	*a* $^4D_{3\frac{1}{2}}$—*z* $^6D^\circ_{3\frac{1}{2}}$	6	0.165	1.403	1.568	0.579	1.486
30	3660.070	27314.10	*b* $^4P_{2\frac{1}{2}}$—*z* $^4F^\circ_{3\frac{1}{2}}$	4	.296	1.581	1.285	.149	0.545?
1	3666.07?	27291.73	*b* $^2G_{4\frac{1}{2}}$—*z* $^4H^\circ_{5\frac{1}{2}}$	-----	-------	-------	-------	-------	-------
2	3666.88	27263.38	*c* $^2G_{3\frac{1}{2}}$—*z* $^2D^\circ_{2\frac{1}{2}}$	-----	-------	-------	-------	-------	-------

479794—58——6

TABLE 6. *The second spectrum of ruthenium* (Ru II)—Continued

1 Intensity	2 λ (air)	3 σ	4 Term combination	5 Type	6 Δ g	7 g	8 g	9 Strong p	10 Strong n
	A	*K*							
2	3675.603	27198.67	$a\ ^4H_{4\frac{1}{2}}$—$z\ ^4D^\circ_{3\frac{1}{2}}$	-----	-------	-------	-------	-------	-------
4	3676.289	27193.60	$a\ ^4D_{2\frac{1}{2}}$—$z\ ^6D^\circ_{1\frac{1}{2}}$	-----	-------	-------	-------	-------	-------
2	3681.658	27153.95	$b\ ^4P_{2\frac{1}{2}}$—$z\ ^4D^\circ_{2\frac{1}{2}}$	-----	-------	-------	-------	-------	-------
150	3690.030	27092.34	$a\ ^4D_{3\frac{1}{2}}$—$z\ ^6D^\circ_{4\frac{1}{2}}$	5	.129	1.401	1.530	.065	1.981
10	3690.995	27085.26	$b\ ^4F_{2\frac{1}{2}}$—$z\ ^4F^\circ_{1\frac{1}{2}}$	-----	-------	-------	-------	-------	-------
6	3707.976	26961.22	$d\ ^2D_{2\frac{1}{2}}$—$y\ ^2D^\circ_{2\frac{1}{2}}$	-----	-------	-------	-------	-------	-------
10	3709.21	26952.25	$c\ ^2G_{4\frac{1}{2}}$—$z\ ^4I^\circ_{4\frac{1}{2}}$	6	.13	(1.078)	0.95	.59	?
2	3710.998	26939.27	$c\ ^2D_{1\frac{1}{2}}$—$x\ ^4D^\circ_{2\frac{1}{2}}$	-----	-------	-------	-------	-------	-------
2	3713.432	26921.61	$c\ ^2D_{1\frac{1}{2}}$—$y\ ^4D^\circ_{0\frac{1}{2}}$	-----	-------	-------	-------	-------	-------
2	3720.627	26869.55	$d\ ^2D_{1\frac{1}{2}}$—$x\ ^4F^\circ_{1\frac{1}{2}}$	-----	-------	-------	-------	-------	-------
5	3722.645	26854.98	$a\ ^4H_{3\frac{1}{2}}$—$z\ ^4F^\circ_{4\frac{1}{2}}$	-----	-------	-------	-------	-------	-------
50	3734.455	26770.06	$a\ ^4D_{2\frac{1}{2}}$—$z\ ^6D^\circ_{3\frac{1}{2}}$	6	.296	1.338	1.634	.750	1.486
4	3734.834	26767.34	$c\ ^2G_{3\frac{1}{2}}$—$y\ ^4F^\circ_{3\frac{1}{2}}$	-----	-------	-------	-------	-------	-------
5	3740.230	26728.73	$b\ ^4F_{1\frac{1}{2}}$—$z\ ^4F^\circ_{1\frac{1}{2}}$	-----	-------	-------	-------	-------	-------
10	3746.932	26680.92	$b\ ^4F_{4\frac{1}{2}}$—$z\ ^4F^\circ_{3\frac{1}{2}}$	-----	-------	-------	-------	-------	-------
5	3747.453?	26677.21	$a\ ^2I_{5\frac{1}{2}}$—$z\ ^4H^\circ_{4\frac{1}{2}}$	-----	-------	-------	-------	-------	-------
8	3750.508	26655.48	$b\ ^4F_{2\frac{1}{2}}$—$z\ ^4F^\circ_{2\frac{1}{2}}$	6	.134	1.083	0.949	.344	1.016
2	3757.730	26604.25	$b\ ^4P_{1\frac{1}{2}}$—$z\ ^4P^\circ_{2\frac{1}{2}}$	-----	-------	-------	-------	-------	-------
1	3766.72	26540.76	$d\ ^2D_{2\frac{1}{2}}$—$1\ ^1I^\circ_{5\frac{1}{2}}$	-----	-------	-------	-------	-------	-------
10	3769.012	26524.62	$b\ ^4F_{2\frac{1}{2}}$—$z\ ^4D^\circ_{1\frac{1}{2}}$	4	.207	0.943	1.151	.103	0.634
10	3774.474	26486.23	$b\ ^4F_{1\frac{1}{2}}$—$z\ ^4D^\circ_{0\frac{1}{2}}$	5	.444	.422	0.022	.222	.644
6	3777.923	26462.05	$a\ ^4D_{1\frac{1}{2}}$—$z\ ^6D^\circ_{1\frac{1}{2}}$	6	0.652	1.189	1.841	0.978	1.515
10	3784.175	26418.34	$c\ ^2G_{4\frac{1}{2}}$—$z\ ^4G^\circ_{4\frac{1}{2}}$	6	(0.021)	(1.078)	1.099	.094	?
4	3795.691	26338.19	$a\ ^4D_{0\frac{1}{2}}$—$z\ ^6D^\circ_{0\frac{1}{2}}$	-----	-------	-------	-------	-------	-------
10	3804.572	26276.71	$b\ ^4F_{3\frac{1}{2}}$—$z\ ^4F^\circ_{3\frac{1}{2}}$	6	0.193	(1.093)	1.286	.675	?
5	3806.567	26262.93	$c\ ^2D_{2\frac{1}{2}}$—$z\ ^2D^\circ_{2\frac{1}{2}}$	-----	-------	-------	-------	-------	-------
4	3811.166	26231.25	$c\ ^2D_{2\frac{1}{2}}$—$z\ ^2G^\circ_{3\frac{1}{2}}$	-----	-------	-------	-------	-------	-------
2	3811.805	26226.85	----------	-----	-------	-------	-------	-------	-------
2	3816.207	26196.60	$a\ ^4D_{2\frac{1}{2}}$—$z\ ^6D^\circ_{3\frac{1}{2}}$	5	.233	(1.337)	1.570	.118	?
5	3820.386	26167.94	$b\ ^4F_{1\frac{1}{2}}$—$z\ ^4D^\circ_{1\frac{1}{2}}$	-----	-------	-------	-------	-------	-------
3	3827.92	26116.44	$b\ ^4F_{3\frac{1}{2}}$—$z\ ^4D^\circ_{2\frac{1}{2}}$	4	.255	(1.093)	1.348	.126	?
5	3832.272	26086.78	$b\ ^4F_{2\frac{1}{2}}$—$z\ ^4F^\circ_{3\frac{1}{2}}$	-----	-------	-------	-------	-------	-------
6	3843.462	26010.83	$b\ ^2G_{3\frac{1}{2}}$—$z\ ^4H^\circ_{3\frac{1}{2}}$	-----	-------	-------	-------	-------	-------
1	3863.68	25874.73	$c\ ^2G_{4\frac{1}{2}}$—$z\ ^4H^\circ_{3\frac{1}{2}}$	-----	-------	-------	-------	-------	-------
50	3879.023	25772.38	$b\ ^4F_{4\frac{1}{2}}$—$z\ ^4D^\circ_{3\frac{1}{2}}$	4	.186	1.208	1.394	0.92	0.557
2	3885.823	25727.28	$a\ ^2F_{2\frac{1}{2}}$—$z\ ^6D^\circ_{2\frac{1}{2}}$	-----	-------	-------	-------	-------	-------
1	3889.43	25703.42	$b\ ^4P_{1\frac{1}{2}}$—$z\ ^4F^\circ_{2\frac{1}{2}}$	-----	-------	-------	-------	-------	-------
10	3932.828	25419.80	$b\ ^4F_{4\frac{1}{2}}$—$z\ ^4F^\circ_{4\frac{1}{2}}$	-----	-------	-------	-------	-------	-------
60	4002.957	24974.47	$b\ ^4P_{1\frac{1}{2}}$—$z\ ^4D^\circ_{2\frac{1}{2}}$	4	.295	1.645	1.350	.148	.907
100	4009.928	24931.06	$a\ ^4G_{2\frac{1}{2}}$—$z\ ^4F^\circ_{1\frac{1}{2}}$	5	.186	0.654	0.468	.093	.933

Observed at pole of arc				Observed at pole of arc			
Intensity	λ (vacuum)	σ	Term combination	Intensity	λ (vacuum)	σ	Term combination
3	4011.30	24922.6	----------	2	4093.41	24422.3	$a\ ^2F_{3\frac{1}{2}}$—$z\ ^6D^\circ_{3\frac{1}{2}}$
2	4016.96	24887.4	----------	20	4104.80	24354.9	$a\ ^4G_{3\frac{1}{2}}$—$z\ ^4F^\circ_{2\frac{1}{2}}$
5	4025.28	24836.0	$d\ ^2D_{2\frac{1}{2}}$—$z\ ^2P^\circ_{1\frac{1}{2}}$	5	4134.10	24182.3	$a\ ^2F_{3\frac{1}{2}}$—$z\ ^6D^\circ_{4\frac{1}{2}}$
10	4040.25	24744.0	$a\ ^4H_{4\frac{1}{2}}$—$z\ ^6F^\circ_{3\frac{1}{2}}$	10	4135.466	24174.3	$b\ ^4P_{0\frac{1}{2}}$—$z\ ^4D^\circ_{1\frac{1}{2}}$
15	4041.56	24736.0	$a\ ^4H_{3\frac{1}{2}}$—$z\ ^6F^\circ_{4\frac{1}{2}}$	10	4143.74	24126.0	$a\ ^4G_{4\frac{1}{2}}$—$z\ ^4F^\circ_{3\frac{1}{2}}$
2	4041.72	24735.0	$b\ ^4P_{0\frac{1}{2}}$—$z\ ^4F^\circ_{1\frac{1}{2}}$	1	4164.76	24004.2	$b\ ^4F_{4\frac{1}{2}}$—$z\ ^6P^\circ_{3\frac{1}{2}}$
20	4043.04	24726.9	$a\ ^4H_{4\frac{1}{2}}$—$z\ ^6F^\circ_{4\frac{1}{2}}$	10	4173.991	23951.13	$b\ ^4P_{2\frac{1}{2}}$—$z\ ^6F^\circ_{3\frac{1}{2}}$
1	4045.55	24711.6	$a\ ^4H_{3\frac{1}{2}}$—$z\ ^6F^\circ_{2\frac{1}{2}}$	20	4174.912	23945.85	$a\ ^4G_{5\frac{1}{2}}$—$z\ ^4F^\circ_{4\frac{1}{2}}$
2	4064.81	24594.5	$b\ ^4P_{1\frac{1}{2}}$—$z\ ^6P^\circ_{1\frac{1}{2}}$	3	4191.95	23848.6	----------
1	4081.72	24492.6	$b\ ^4P_{0\frac{1}{2}}$—$z\ ^4D^\circ_{0\frac{1}{2}}$	3	4204.62	23776.7	$b\ ^4D_{1\frac{1}{2}}$—$z\ ^4P^\circ_{1\frac{1}{2}}$

TABLE 6. *The second spectrum of ruthenium* (Ru II)—Continued

Observed at pole of arc				Observed at pole of arc			
Intensity	λ (vacuum)	σ	Term combination	Intensity	λ (vacuum)	σ	Term combination
1	4205.39	23772.4	$a\ ^4G_{2\frac{1}{2}}—z\ ^4D^\circ_{2\frac{1}{2}}$	3	4563.77	21905.6	$b\ ^4D_{1\frac{1}{2}}—z\ ^4F^\circ_{2\frac{1}{2}}$
2	4215.51	23715.3		0	4578.44	21835.4	$b\ ^2D_{2\frac{1}{2}}—z\ ^4P^\circ_{1\frac{1}{2}}$
20	4227.831	23646.1	$b\ ^4D_{2\frac{1}{2}}—z\ ^4P^\circ_{1\frac{1}{2}}$	4	4606.50	21702.4	$b\ ^4D_{0\frac{1}{2}}—z\ ^4D^\circ_{1\frac{1}{2}}$
10	4231.437	23626.0	$a\ ^4G_{3\frac{1}{2}}—z\ ^4D^\circ_{2\frac{1}{2}}$	3	4607.44	21698.0	
1	4248.87	23529.1	$b\ ^2P_{1\frac{1}{2}}—z\ ^4P^\circ_{0\frac{1}{2}}$	3	4660.96	21448.8	$a\ ^4G_{4\frac{1}{2}}—z\ ^6P^\circ_{3\frac{1}{2}}$
2	4257.19	23483.1		2	4697.92	21280.1	
1	4287.33	23318.0	$b\ ^4F_{4\frac{1}{2}}—z\ ^6F^\circ_{3\frac{1}{2}}$	2	4699.03	21275.1	$d\ ^2D_{1\frac{1}{2}}—z\ ^4G^\circ_{2\frac{1}{2}}$
2	4302.51	23235.7		5	4714.17	21206.7	$b\ ^4D_{2\frac{1}{2}}—z\ ^4F^\circ_{3\frac{1}{2}}$
2	4303.39	23231.0	$b\ ^4F_{3\frac{1}{2}}—z\ ^6F^\circ_{2\frac{1}{2}}$	3	4731.98	21126.9	
30	4305.885	23217.5	$a\ ^4G_{4\frac{1}{2}}—z\ ^4D^\circ_{3\frac{1}{2}}$	20	4750.040	21046.57	$b\ ^4D_{2\frac{1}{2}}—z\ ^4D^\circ_{2\frac{1}{2}}$
1	4306.59	23213.7	$b\ ^4F_{4\frac{1}{2}}—z\ ^6F^\circ_{3\frac{1}{2}}$	5	4776.78	20928.8	$b\ ^2P_{1\frac{1}{2}}—z\ ^4D^\circ_{1\frac{1}{2}}$
2	4313.17	23178.3	$b\ ^4F_{2\frac{1}{2}}—z\ ^6F^\circ_{1\frac{1}{2}}$	2	4784.96	20893.0	$b\ ^4D_{3\frac{1}{2}}—z\ ^4F^\circ_{3\frac{1}{2}}$
1	4338.89	23040.9	$b\ ^4F_{2\frac{1}{2}}—z\ ^6F^\circ_{2\frac{1}{2}}$	1	4807.27	20796.0	$b\ ^4D_{1\frac{1}{2}}—z\ ^6P^\circ_{1\frac{1}{2}}$
3	4359.81	22930.3	$b\ ^2P_{1\frac{1}{2}}—z\ ^4P^\circ_{1\frac{1}{2}}$	0	4821.92	20732.8	$b\ ^4D_{3\frac{1}{2}}—z\ ^4D^\circ_{2\frac{1}{2}}$
5	4362.98	22913.7	$b\ ^4F_{3\frac{1}{2}}—z\ ^6F^\circ_{3\frac{1}{2}}$	3	4828.15	20706.1	
1	4368.51	22884.7	$b\ ^4F_{1\frac{1}{2}}—z\ ^6F^\circ_{0\frac{1}{2}}$	3	4922.12	20310.8	
2	4369.84	22877.7	$a\ ^4G_{3\frac{1}{2}}—z\ ^4D^\circ_{3\frac{1}{2}}$	2	4934.08	20261.6	
1	4380.57	22821.7	$b\ ^4F_{1\frac{1}{2}}—z\ ^6F^\circ_{1\frac{1}{2}}$	20	5002.46	19984.6	$b\ ^4D_{3\frac{1}{2}}—z\ ^4D^\circ_{3\frac{1}{2}}$
3	4406.78	22686.0		5	5004.74	19975.5	
10	4407.49	22682.3		2	5092.34	19631.9	$b\ ^4D_{3\frac{1}{2}}—z\ ^4F^\circ_{3\frac{1}{2}}$
15	4408.62	22676.5	$b\ ^4D_{2\frac{1}{2}}—z\ ^4P^\circ_{2\frac{1}{2}}$	3	5172.73	19326.8	
3	4434.95	22541.9		2	5270.28	18969.1	
2	4435.67	22538.2		50	5607.744	17827.45	$a\ ^6S_{2\frac{1}{2}}—z\ ^6P^\circ_{1\frac{1}{2}}$
5	4436.64	22533.3		50	5893.612	16962.82	$a\ ^6S_{2\frac{1}{2}}—z\ ^6P^\circ_{2\frac{1}{2}}$
15	4454.76	22441.6		2	6018.00	16612.2	$a\ ^4G_{4\frac{1}{2}}—z\ ^6D^\circ_{3\frac{1}{2}}$
100	4470.502	22362.58	$b\ ^4D_{3\frac{1}{2}}—z\ ^4P^\circ_{2\frac{1}{2}}$	2	6290.63	15892.3	
3	4499.26	22219.7	$a\ ^2S_{0\frac{1}{2}}—z\ ^4S^\circ_{1\frac{1}{2}}$	50	6371.29	15691.07	$a\ ^6S_{2\frac{1}{2}}—z\ ^6P^\circ_{3\frac{1}{2}}$
3	4518.95	22122.9					
5	4525.06	22093.0	$b\ ^4D_{1\frac{1}{2}}—z\ ^4D^\circ_{0\frac{1}{2}}$				
20	4539.93	22020.6	$b\ ^4D_{0\frac{1}{2}}—z\ ^4D^\circ_{0\frac{1}{2}}$				

WASHINGTON, D. C. July 22, 1958.

Journal of Research of the National Bureau of Standards Vol. 61, No. 5, November 1958 Research Paper 2909

Self-Ignition Temperatures of Materials From Kinetic-Reaction Data

Daniel Gross and A. F. Robertson

Results of experimental determinations of the kinetic constants of the self-heating reaction are presented for wood fiberboard, cotton linters, sugar pine, cork, crepe rubber, GRS rubber, natural, synthetic, and blended foam rubber (with and without additive), various oils (raw linseed, cottonseed, rapeseed, sperm, olive, castor, and neatsfoot) applied to cotton gauze in a ratio of 1 part of oil to 6 parts of cotton by weight, ammonium perchlorate, and nitrocellulose plastic. Under the assumption that self-heating follows a first-order reaction, these constants were used to calculate the critical radii of spherical piles for each of four surface temperatures likely to be experienced in long-period storage. Calculated self-ignition temperatures of piles of ½-inch-diameter to 22-inch-diameter spheres of wood fiberboard and ⅛-inch-diameter to 2-inch-diameter spheres of cotton linters were in reasonable agreement with previous measurements by N. D. Mitchell (National Fire Protection Association Quarterly **45:** 162, 1951).

1. Introduction

Previous workers studying the self-ignition behavior of materials have experienced difficulties in the determination and specification of a unique ignition temperature. Because of the critical heat balance that exists during the ignition process, the measured "ignition temperature" is dependent upon the characteristics of the testing apparatus, the degree of control of the ambient temperature conditions, the time of exposure, and other experimental factors. It is highly dependent also upon the size of the specimen under test. This is due to the fact that self-ignition of a material is only possible when the rate of heat generation within the material exceeds the rate at which heat is lost by radiation, convection, and conduction to the surroundings. Since the heat generated is a function of the volume of the material, while the heat lost is a function of its surface area, the measured ignition temperature should decrease as the linear dimensions increase.

The incidence of fires resulting from self-ignition makes desirable an understanding of the relationship between the self-heating reaction and the physical parameters involved. The present paper proposes and illustrates the manner in which kinetic-reaction data obtained under conditions of negligible heat loss may be used to predict critical surface and ambient temperatures as a function of size and shape for a variety of materials.

2. Analysis and Nomenclature

In the analysis, the following symbols and units will be used:

A	heat-generation coefficient	cal $sec^{-1}cm^{-3}$
B	radius or half-thickness	cm
B_c	critical radius of sphere	cm
c	specific heat	cal g^{-1}° K^{-1}
e	Napierian base	
E	activation energy	kcal $mole^{-1}$
h	surface heat-transfer coefficient	cal $sec^{-1}cm^{-2}$° K^{-1}
k	thermal conductivity	cal $sec^{-1}cm^{-1}$° K^{-1}
m	coefficient in eq (1)	
R	gas constant = 0.0019872	kcal $mole^{-1}$° K^{-1}
t	time	sec
T	temperature within material	° K
T_A	self-ignition (critical ambient) temperature	° K
T_B	critical surface temperature	° K
T_O	critical center temperature	° K
T_m	mean temperature $=(T_O+T_B)/2$	° K
x	space coordinate	cm
ρ	density	g cm^{-3}

Analyses of self-heating have been made under the assumption that heat is generated within the body according to a first-order reaction law. Although this may be an oversimplification for complex materials and over extended temperature ranges, the assumption appears to be applicable for many materials in the relatively low-temperature ranges where self-heating becomes important and the ignition process is initiated. Provided the rate of the self-heating process within the material is not limited by diffusion of the reactants and/or products, or by depletion of the fuel supply, a steady-state condition can exist when the heat generated within the material is equal to the heat lost to the surroundings. The particular condition of interest is the one that produces the maximum self-heating which is still steady state. Either a slightly higher ambient temperature or a slightly larger bulk size results in a greater quantity of heat being generated than can be dissipated, and ignition results. Since this steady-state condition is critical with respect to ignition, the corresponding surface temperature and size of material are referred to as the critical surface temperature and the critical size. The ambient temperature corresponding to given critical steady-state conditions with given heat losses is considered the critical ambient or self-ignition temperature. There exists for each material and for each set of heat-loss conditions a series of corresponding self-ignition temperatures and critical sizes.

Consider a homogeneous material of half-thickness B generating heat in accordance with the first-order reaction law $Ae^{x\rho}-E/RT$ and losing heat from its surface. The steady-state heat-conduction equation which applies for the condition when the heat lost

through the surface is equal to the heat generated within the material may be written:

$$k\left[\frac{d^2T}{dx^2}+\frac{m}{x}\frac{dT}{dx}\right]+Ae^{-\frac{E}{RT}}=0. \quad (1)$$

The critical condition of ignition in the theory of thermal explosions originally proposed by Frank-Kamenetzky [1] [1] requires the solution of this nonlinear equation. Chambré [2] presented analytic solutions in terms of known functions for the sphere ($m=2$) and cylinder ($m=1$) to supplement that for the semi-infinite slab ($m=0$). Recent analyses by Genensky [3] for a sphere and by Thomas [4] for all three geometries have been made employing the assumption common to the previous solutions, namely, that temperature differences within the material are small in comparison with the temperature. Enig, Shanks, and Southworth [5] have provided solutions in the form of convenient tables of the center and surface temperatures for sphere, cylinder, and semi-infinite slab geometries without this restrictive assumption. From the tables it is useful to note that for a given surface temperature T_B, the critical radius for the cylinder and the critical half-thickness for the semi-infinite slab are given very closely by 0.775 B_c and 0.514 B_c, respectively, where B_c is the critical radius for the sphere. Assuming that the heat generated within the material at a mean temperature T_m is lost from its surface according to Newton's law of cooling, the following relation may be used for calculating the critical ambient temperature for a sphere:

$$T_A=T_B-\frac{AB_c}{3h}e^{-\frac{E}{RT_m}} \quad (2)$$

where T_m is a mean temperature, here assumed as $T_o+T_B/2$.

Since the analysis by Thomas employs Newtonian surface cooling as a boundary condition, the ambient temperature is obtained directly. From the graphical relations given, it is again useful to note that for a given ambient temperature T_A, the critical radius for the cylinder and the critical half-thickness for the semi-infinite slab are given very closely by 0.782 B_c and 0.520 B_c respectively.

The experimental method used in this study for determination of the constants of the first-order reaction involved self-heating conditions which differed from those of the self-heating process described. Instead of a fixed ambient temperature, the temperature within the adiabatic test furnace surrounding the specimen was controlled to maintain negligible loss of heat. Under these conditions, the specimen temperature remained uniform throughout its mass and the heat generated within the body increased its temperature according to the relation:

$$\rho c\frac{dT}{dt}=Ae^{-\frac{E}{RT}}. \quad (3)$$

By transposing terms, taking logarithms and plotting ln dT/dt versus $1/T$, the resultant line has a slope of $-(E/R)$ and intercepts the ln dT/dt axis at ln $A/\rho c$. For each material the determination of the values of A and E, as well as of its more common thermal properties, permits the solution of the general self-heating problem including the case where size and temperature become critical and ignition results.

3. Experimental Apparatus

In the determination of the kinetic constants, use was made of an improved version, figures 1 and 2, of an adiabatic furnace previously described [6]. Although the basic operation remains the same, refinements have been made and are here summarized:

Addition of guard heaters and associated control system. In order to reduce heat losses and to maintain minimum temperature gradients within the furnace enclosure, the Dewar flask has been enclosed within a close-fitting cylindrical shell. The shell consists of two concentric stainless steel cylinders containing two electric heating elements and an insulating fill. The shell contains the bottom and center guard heating elements while a top-guard heating element has been placed within the Dewar flask plug composed of several layers of asbestos board. A thyratron control system as shown in figure 3 permits adjustment of the guard-heater cycle.

Use of multiple-junction thermocouple. The sensing element for the servo controller consists of eight No. 30 gage (B&S) copper-constantan thermojunctions arranged in series to measure the mean temperature-difference between the specimen and its ambient medium.

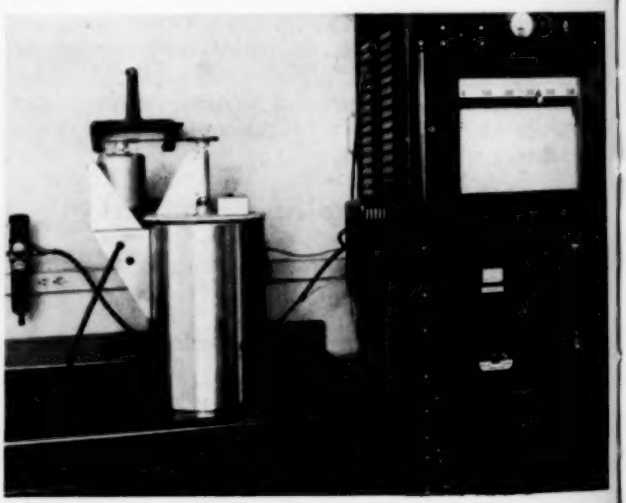

FIGURE 1. *Adiabatic furnace with control and recording equipment.*

[1] Figures in brackets indicate the literature reference at the end of this paper.

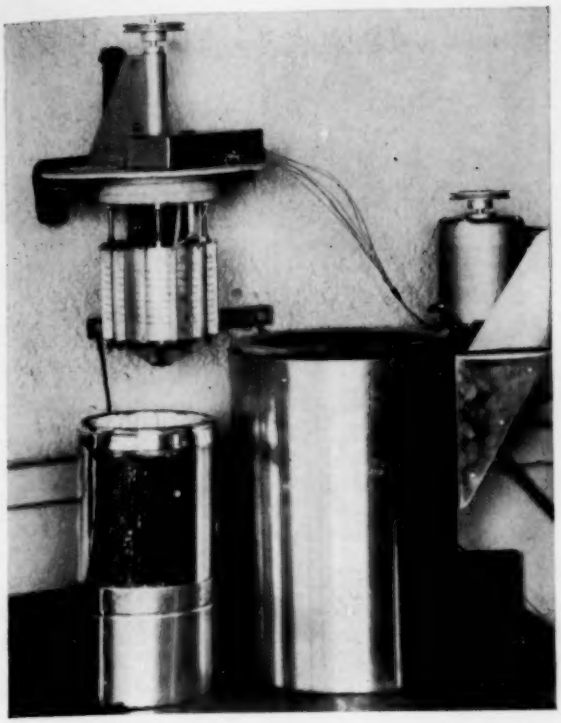

FIGURE 2. *Adiabatic furnace, showing Dewar flask and specimen container removed from insulating shell.*

The changes and additions described permit improved performance of the system. The controller can sense temperature differences of the order of 0.01° C while the rate of temperature drift as observed with an inert specimen has been reduced to approximately 0.25° C/hr over the temperature range 30° to 300° C.

4. Results

4.1. Determination of *A* and *E*

Table 1 lists some thermal and kinetic constants for a number of materials. Some of the values of k and c were determined during this investigation, while others were obtained from handbook sources. The values of A and E were determined over the indicated temperature ranges from experimental temperature-versus-time data and the use of eq (3). For some of these materials, there is reasonable agreement with published values obtained by other methods. These values were determined over limited temperature ranges before loss of weight became appreciable. An analysis that includes the effect of weight loss may be applied for the higher temperature ranges. Analysis of several cellulosic materials has actually shown that when weight changes are taken into consideration, the values of the kinetic constants were not much different from those obtained at the lower temperature ranges.

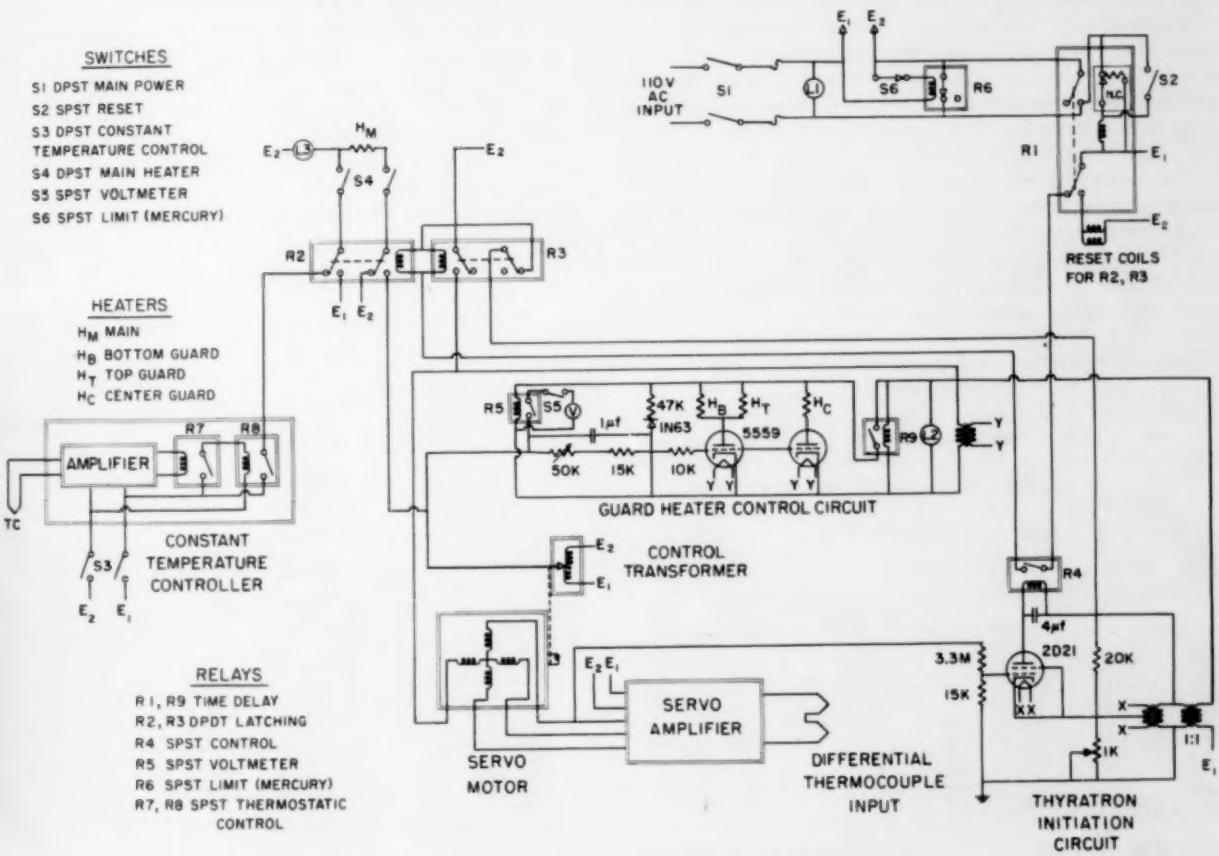

FIGURE 3. *Circuit diagram of furnace-control system.*

TABLE 1. *Physical and kinetic properties*

Material	Temperature range	Property				
		ρ	c	k	E	A
	°C	g cm^{-3}	cal g^{-1}°K	cal sec^{-1} cm^{-1}K^{-1}	kcal mole^{-1}	cal sec^{-1} cm^{-3}
Wood fiberboard	80–225	0.25	0.33	0.00012	25.7	1.97×10^{9}
Cotton linters	180–260	.32	.32	.00010	34.5	5.30×10^{11}
Sugar pine	140–310	.36	.32	.00024	20.3	2.11×10^{6}
Cork	170–225	.13	.48	.00010	19.1	2.50×10^{5}
Crepe rubber	210–310	.92	.5	.000282	23.4	1.06×10^{6}
GRS	220–330	1.10	.5	.000299	23.6	1.11×10^{7}
Foam rubber, 100% natural	100–180	.108	.5	.000096	27.6	7.48×10^{10}
Foam rubber, 100% synthetic	115–210	.129	.5	.000100	26.2	4.96×10^{9}
Foam rubber, blended, with additive	110–190	.118	.5	.000098	29.0	4.25×10^{11}
Foam rubber, blended, without additive	110–200	.104	.5	.000095	28.5	1.10×10^{11}
Raw linseed oil [a]	90–120	.309	.34	.00011	21.0	3.50×10^{9}
Cottonseed oil [a]	75–120	.338	.34	.00011	24.1	2.42×10^{11}
Rapeseed oil [a]	90–140	.316	.34	.00011	20.1	6.13×10^{8}
Sperm oil [a]	120–160	.313	.34	.00011	20.1	1.56×10^{7}
Olive oil [a]	115–160	.308	.34	.00011	18.7	2.41×10^{7}
Castor oil [a]	140–160	.314	.34	.00011	27.8	8.33×10^{11}
Neatsfoot oil [a]	140–170	.316	.34	.00011	24.7	3.82×10^{10}
Ammonium perchlorate	205–270	.91	.35	----------	41.2	1.22×10^{16}
Nitrocellulose plastic	135–170	.82	.34	.00051	42.0	2.43×10^{19}

[a] Applied to cotton gauze in ratio of 1 part of oil to 6 parts of cotton by weight. All property values refer to oil-cotton combination.

4.2. Determination of Critical Size and Temperature

The critical surface temperatures of spherical piles of wood fiberboard and cotton linters were computed, using the measured values of the kinetic and thermal constants, and the tables given in reference [5]. These computations were performed over the radius range corresponding to the specimen sizes reported by Mitchell [7]. Equation (2) was then used to calculate the corresponding critical ambient temperatures. The value of the surface heat-transfer coefficient was assumed as 4.4×10^{-4} cal/sec cm^2 °K. Using this value for the surface heat-transfer coefficient, the critical ambient temperature was also determined from the relations given in reference [4]. The results of these calculations are shown in table 2 for two materials for which published experimental data [7] are available. With the exception of the smallest size specimens, for which the assumption of an arithmetic mean temperature for eq (2) introduces considerable error in the calculated self-ignition temperature, the results are seen to be in reasonable agreement.

Table 3 lists the critical radius B_c of a sphere corresponding to several critical surface temperatures for each of the materials listed in table 1. Curves have been plotted in figure 4 showing this relationship for seven materials. In this temperature range (20° to 100° C), of practical interest for ordinary storage, the critical size calculations were based upon the assumption of the applicability of the kinetic constants which were determined over higher temperature ranges. It was further assumed that the thermal properties remained constant over the whole temperature range. Critical dimensions for cylinders and slabs may be estimated from the previously mentioned constants of $0.775B_c$ and $0.514B_c$, respectively. As h becomes very large, the self-ignition temperature is equal to the

TABLE 2. *Comparison between measured and calculated self-ignition temperatures, T_A*

Size		Wood fiberboard			Cotton linters		
		Self-ignition temperature			Self-ignition temperature		
Thickness $2B_e$	Half-thickness B_e	Measured [a]	Calculated [b]		Measured [a]	Calculated [b]	
		Ref 7	Ref 5 and eq 2	Ref 4	Ref 7	Ref 5 and eq 2	Ref 4
in.	cm	°C	°C	°C	°C	°C	°C
¼	.159	317	183	260	304	257	307
½	.318	252	218	243	270	274	291
½	.635	212	215	223	248	267	272
1	1.27	202	200	202	222	251	253
2	2.54	180	180	180	201	233	233
4	5.08	150	159	160			
8	10.2	130	140	140			
12	15.2	122	129	129			
22	27.9	109	114	114			

[a] Specimens ¼, ½, and ½ in. thick were cubes; specimens 1 in. and larger were octagonal prisms.
[b] Based on spheres of radius equal to half-thickness.

TABLE 3. *Computed critical radius of a sphere, B_c*

Material	Critical surface temperature			
	20° C	48.9° C	82.2° C	100° C
	cm	cm	cm	cm
Wood fiberboard	4.49×10^{3}	680	114	50
Cotton linters	4.25×10^{6}	3.29×10^{5}	2.86×10^{4}	9.43×10^{3}
Sugar pine	2.19×10^{3}	501	125	66
Cork	1.43×10^{3}	363	99	55
Crepe rubber	1.43×10^{4}	2.58×10^{3}	511	206
GRS rubber	1.71×10^{4}	3.03×10^{3}	591	280
Foam rubber, 100% natural	3.36×10^{3}	438	64	26
Foam rubber, 100% synthetic	4.00×10^{3}	588	95	41
Foam rubber, blended, with additive	4.65×10^{3}	542	71	27
Foam rubber, blended, without additive	4.53×10^{3}	565	78	34
Raw linseed oil [a]	66	14.3	3.6	1.7
Cottonseed oil [a]	101	17.3	3.3	1.5
Rapeseed oil [a]	72	17.0	4.3	2.3
Sperm oil [a]	143	34	8.5	4.5
Olive oil [a]	110	29	7.3	4.5
Castor oil [a]	1.16×10^{3}	150	69	9.0
Neatsfoot oil [a]	139	37	4.1	1.9
Nitrocellulose plastic	7.69×10^{4}	3.31×10^{3}	167	43

[a] Applied to cotton gauze in ratio of 1 part of oil to 6 parts of cotton by weight. All property values refer to oil-cotton combination.

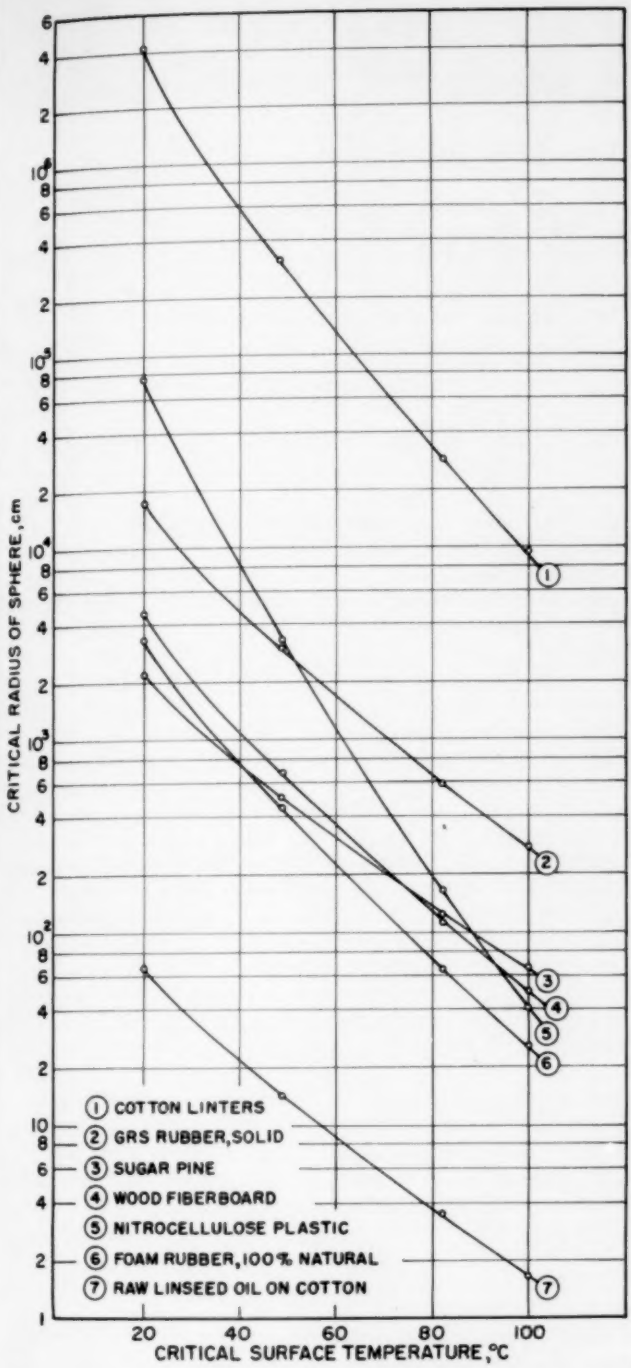

FIGURE 4. *Computed critical radii and critical-surface temperatures for spherical piles of various materials.*

critical surface temperature. For a finite h, the self-ignition temperature may be estimated from eq (2) or may be obtained directly from the relations presented in reference [4].

5. Conclusions

Recent analyses of self-ignition have been made under the assumption that self-heating follows a first-order reaction law. Experimental determinations of the kinetic constants of this reaction have been made for a number of materials and these constants have been used to calculate self-ignition (critical ambient) temperatures as a function of size and shape. The calculated self-ignition temperatures are in fair agreement with published experimental data for two materials, wood fiberboard, and cotton linters.

The experimental determinations and most of the computations were performed by Joseph J. Loftus to whom the authors are deeply appreciative. Thanks are due also to James S. Evans, Jr., who designed the thyratron control circuits and to William H. Bailey, who assembled the furnace and made the drawings.

An important contribution to this field has been made by Kazuo Akita of the Fire Research Institute, Tokyo, in a paper to be published in J. Chem. Soc. Japan, Section of Indust. Chem.

6. References

[1] D. A. Frank-Kamenetzky, Acta Physicochim. U. R. S. S. **10,** 365 (1939).
[2] P. L. Chambré, On the solution of the Poisson-Boltzman equation with application to the theory of thermal explosions, J. Chem. Phys. **20,** 1795 (1952).
[3] S. M. Genensky, A problem in self-heating of a spherical body, J. Research NBS **59,** 79 (1957) RP2773.
[4] P. H. Thomas, On the thermal conduction equation for self-heating materials with surface cooling, Trans. Faraday Soc. **54,** 60 (1958).
[5] J. W. Enig, D. Shanks, and R. W. Southworth, The numerical solution of the heat conduction equation occurring in the theory of thermal explosions, NAVORD Report 4377 (1956), Astia Document No. AD–116 873.
[6] W. H. Raskin and A. F. Robertson, An adiabatic apparatus for the study of self-heating of poorly conducting materials, Rev. Sci. Inst. **25,** 541 (1954).
[7] N. D. Mitchell, New light on self-ignition, Nat. Fire Protect. Assoc. Quart. **45,** 162 (1951).

WASHINGTON, June 11, 1958.

Journal of Research of the National Bureau of Standards Vol. 61, No. 5, November 1958 Research Paper 2910

Some Studies of Atmospheric Transmittance on Mauna Loa

Ralph Stair and Russell G. Johnston

Studies are described of the spectral intensity of solar radiation and its transmission through the atmosphere above a new 11,140-foot-altitude station on Mauna Loa, Hawaii, during May and June 1957. The spectral measurements covered the region from 300 millimicrons to 2.5 microns for different air masses from about 3.0 to 1.0. The amounts of ozone and of water vapor which were present in the upper atmosphere were calculated from spectral data obtained on several different days.

1. Introduction

During the past few years measurements on the spectral distribution of the radiant energy from the sun have been carried out at locations in Colorado and New Mexico [1–3] [1] because of high altitude and great distance from commercial activities. However, in each case there was a considerable amount of interference resulting from the presence of relatively great amounts of dust or water vapor much of the time. To get away from conditions of this type it was proposed that a station be set up at a high altitude in the Hawaiian Islands for this work.

Although few weather data were available for high altitude locations in the Hawaiian Islands, such data as existed indicated the superiority of a location on the north slope of Mauna Loa, on the island of Hawaii, for use in solar radiation and atmospheric transmission studies such as were being made. Furthermore, the available data and information indicated that an observing station situated at an altitude above 11,000 ft on this mountain would be above the normal atmospheric inversion layer much of the time and hence above most of the atmospheric dust and water vapor. Furthermore there are but few urban or rural land areas nearby to produce city and country air-pollution products.

For many years the U. S. Weather Bureau had been interested in a high altitude weather observing station on Mauna Loa. The first positive action in this direction occurred in 1951 when, through the efforts of various persons and agencies, a small shelter was erected at an altitude of approximately 13,450 ft near the Mokuaweoweo crater at the summit of Mauna Loa. As this location was difficult of access because of a rough lava terrain and the absence of an improved roadway it became advisable to establish the Mauna Loa Observatory at the terminus of the existing road just above 11,000 ft (at approximately 11,140 ft). This altitude has a further advantage over that of the summit location in affording conditions of atmospheric pressure (and hence oxygen concentration) more in keeping with the normal requirements of the average individual. Many observers would be unable to live and work at a much higher level.

Late in 1955 arrangements were set up between the U. S. Weather Bureau and the National Bureau of Standards for the latter institution to establish an observing station (with funds supplied by the U. S. Weather Bureau) on Mauna Loa, for the joint use of the two laboratories. Accordingly, through contacts with the Territorial Government of Hawaii a small parcel of land (4.05 acres) on the north slope of Mauna Loa, the land marker being set at an altitude of 11,134 ft, was transferred back to the Federal Government (Department of Commerce) and the Mauna Loa Observatory was constructed by the National Bureau of Standards during the early part of 1956.

Since this is a new station and location for spectral solar radiant energy measurements a few comments relating to the building and its facilities are in order. The main section of the Observatory (see figs. 1 and 2) consists of a one-story concrete block building (20 by 40 ft) partitioned into a 16- by 20-ft laboratory, three bedrooms, and a kitchenette, all furnished for pleasant and comfortable living and working quarters for six observers. A concrete platform (15 by 45 ft) on the south side, and a tower (8 by 8 ft) at the east end of the building, provide space for solar radiation measurements and for other experiments requiring outside exposures. Electrical power for the laboratory and housing facilities is provided by diesel-electric generators at 110 v, 60 cps single phase. Water is provided through a roof catchment, storage, and distribution system, while the fuel for the heating, cooking, and refrigeration is provided through the use of butane from tanks. A radio

FIGURE 1. *Mauna Loa Observatory; altitude 11,140 ft, looking southwest.*

[1] Figure in brackets indicate the literature references at the end of this paper.

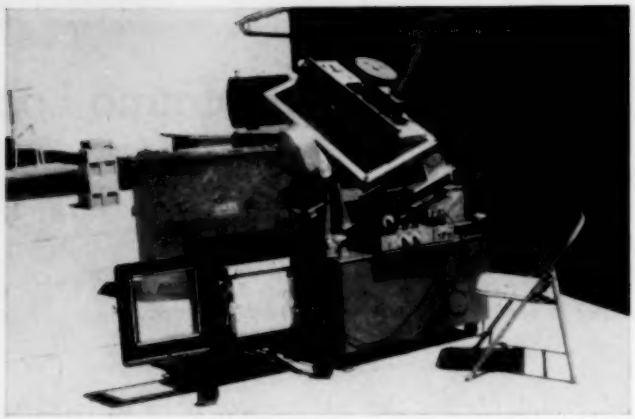

FIGURE 2. *Instrumental setup on outside platform in front of Mauna Loa Observatory.*

transmitter and receiver linked with a similar station at the U. S. Weather Bureau in Hilo furnishes continuous two-way contact with the outside world. A small library, supplemented by TV and radio broadcasts help in furnishing recreation at evenings and during bad weather. Other data about the Mauna Loa Observatory have been published elsewhere [4].

The observatory is reached by a cinder road, built and kept in repair by the Department of Institutions, Territory of Hawaii, and extending a distance of about 45 miles from near Hilo to just above the location of the observatory. Through most of the distance up the mountain the grade is gradual so that a stock automobile (having high clearance) can maneuver the 11,000-ft climb in less than 2 hr. It is, however, recommended that a 4-wheel-drive, high-slung vehicle be employed for general use in this area.

In the following paragraphs the spectroradiometric setup is briefly described and some results are given on atmospheric scattering and the amounts of ozone and water vapor above Mauna Loa on several days in May and June 1957, as deduced from measurements of solar spectral radiant energy.

2. Instruments and Method

The instrumental setup (see fig. 2) was essentially the same as employed at Sunspot, N. Mex., in 1955 [3]. New PbS cells (and associated housings and electronics) having higher sensitivities and less noise were employed in the present case. A further improvement was obtained by operating the PbS cells at lower temperatures (the ambient air temperature) rather than at a controlled elevated temperature as was the case in 1955. As a result the infrared data could be repeated more closely from time to time during each day with only small sensitivity drifts as the air temperature slowly changed. A type–935 phototube was employed in the ultraviolet spectral measurements.

An additional instrument for obtaining a measure of the amount of sky scattering was incorporated into the equipment. This consisted of a photoelectric photometer for comparative brightness measurement of the sun and an area of the sky nearby and surrounding the sun. Readings were alternately taken for the intensity of the solar disk and for that of an arbitrary area of the sky consisting of an annular ring of a few degrees immediately surrounding the sun. In each case the radiant energy was confined essentially to a narrow band in the yellow-green region of the visible spectrum through the use of a yellow-green filter (a dark-shade welding glass).

The electronics of the instrument for the measurement of sky scattering were arranged so that the same tuned amplifier and recorder could be readily shifted from the output of the spectroradiometer phototube to that of the auxiliary instrument without disrupting the recorder time scale. Thus the two records appeared on the same chart in proper sequence. Calibration was accomplished through an on-the-spot comparison with an Evans [5] visual photometer. Thus the portrayed data are given in terms of sky brightness within an annular conical angle near the sun relative to that of the solar disk

The use of electrical power from a small diesel-electric generating plant caused a number of problems in the practical operation of the equipment. First, it is very difficult to keep a small diesel-electric generating plant (in this case a 5-kw unit) in continuous operation at precisely 60 cps with the voltage constant, especially at this altitude and with considerable variation in the load. The power requirements of all other station activities were dependent upon the same power source. Furthermore, the need for regular servicing of the equipment required the alternate use of two similar units, which usually varied in output voltage and frequency. Because these difficulties had been anticipated previous to the setting up of the equipment, crystal-controlled electronic power supplies had been procured to handle the power requirements of all motors and amplifiers of the setup in which either voltage or frequency changes might result in erratic operation. Greatly improved operation resulted through the use of the crystal-controlled electronic power units. However, there remains no question but that commercial power would be preferred. Hence, a real need at the Mauna Loa Observatory is an extension of power lines for the remaining 12 miles up the mountain to the observatory.

In addition to the equipment employed in the spectral radiant-energy and sky-scattering measurements the standard U. S. Weather Bureau station instruments were available and were regularly read and the data transmitted to the Hilo office, and incidentally employed in the evaluation of the surface-humidity values reported herein.

3. Spectral Solar-Energy Distribution

On those days when the sky was clear, during a period of about 8 weeks in May and June 1957, spectral data were obtained either through the shorter-wavelength region, 300 to 550 mμ, by using a 935-type photoemission tube, or else through the longer-wavelength region, about 330 mμ to 2.5 μ, by using a PbS cell. These data were evaluated in

a manner similar to that previously followed and were found to be in general agreement with the earlier data [3] both as to spectral quality and absolute magnitude, except that they show a higher degree of scattering as a result of difficulties in keeping the power supply constant, or as the result of changes in atmospheric humidity.

4. Atmospheric Transmittance and Ozone

Following the same procedures as employed in previous work [1–3] the atmospheric transmission curve for the atmosphere above Mauna Loa (see figs. 3 and 4) was determined on the basis of two sets of ozone transmission coefficients—those of Fabry and Buisson [6], and those of Vigroux [7]—for the average data for 4 days in May (May 21, 28, 29, and 30).

In figure 3 the Fabry and Buisson ozone transmission coefficients were employed in the calculation of the two curves representing the amounts of ozone required for a specific amount of optical absorption. On the basis of these data, about 0.24 cm of ozone (ntp) was present above Mauna Loa at the time of

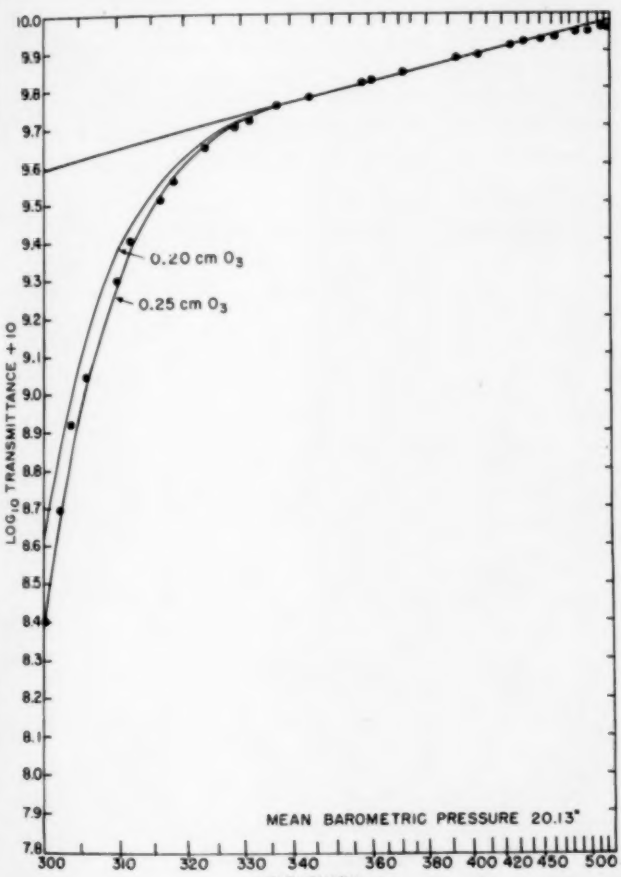

FIGURE 3. *Atmospheric transmittance above Mauna Loa Observatory, altitude 11,140 ft; also determination of total ozone using Fabry and Buisson transmission coefficients.*

Upper curve, scattering; lower curves, ozone; circles, measured atmospheric transmittance; air mass, 1.00; wavelength scale expanded as a function of $-(n-1)^2\lambda^{-4}$.

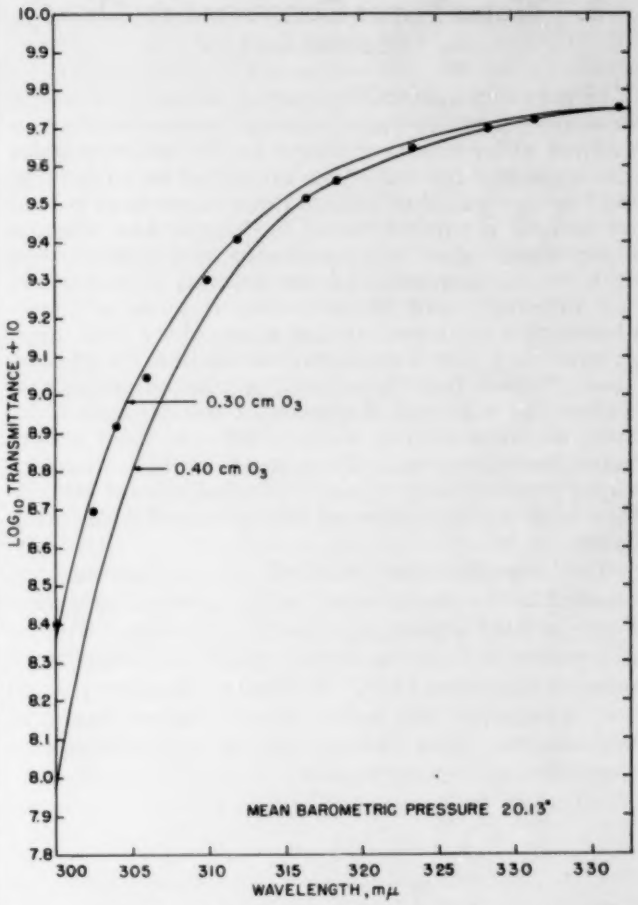

FIGURE 4. *Atmospheric transmittance above Mauna Loa Observatory, altitude 11,140 ft; also determination of total ozone using Vigroux transmission coefficients.*

Circles, measured atmospheric transmittance; air mass, 1.00.

the measurements. This value is in close agreement with the results of previous measurements of high altitude ozone at Climax, Colo. [1], and at Sunspot, N. Mex. [2, 3].

In figure 4 the same experimental data (for wavelengths shorter than about 337 mμ) are replotted, this time along with ozone curves calculated on the basis of Vigroux's transmission coefficients. New data by Inn and Tanaka [23] agree closely with those of Vigroux within the spectral region of 300 to 350 mμ. It is to be noted on the basis of these data that the calculated amount of ozone (ntp) becomes about 0.32 cm. Furthermore, if the data obtained at Climax and Sunspot are evaluated in terms of Vigroux's coefficients of ozone absorption, then the previously published ozone values should be increased to about 0.30 cm. Since the calculated value of atmospheric ozone depends upon the laboratory measurements of the absorption coefficients of ozone, and since there is considerable spread between the values obtained through using the two sets of data, it seems advisable to report both values until further experiment definitely determines the absorption coefficients of ozone.

5. Water Vapor Concentration Above Mauna Loa

In previous work at Sunspot, N. Mex. [2], changes in upper-air water-vapor concentrations resulted in marked absorption variations in the infrared solar spectrum (see fig. 5). As a matter of fact the large fluctuations noted at Sunspot were a primary reason for seeking the new location on Mauna Loa where a lower water-vapor concentration would interfere less with the measurement of the spectral intensities in the infrared. But water vapor is such a highly absorbing constituent of the atmosphere that even at the very low concentrations ordinarily present above Mauna Loa there is still a marked absorption within the principal water-vapor bands, even near noon on days having a relatively low total water-vapor concentration. Then small changes in water vapor produce large changes in total optical absorption within the regions of the principal absorption bands.

The spectroscopic method of evaluating the amount of the water vapor was originated by Fowle nearly a half century ago [8–11]. However, its use in routine studies has been greatly neglected until recent years when the U. S. Weather Bureau [12–17] and others [18, 19] have set up various types of hygrometers, filter radiometers, and spectroradiometers for water-vapor studies.

It should be noted that the water-vapor molecule has three principal modes of vibration resulting in three primary absorption bands located at 2.66, 2.74 and 6.26 μ [20]. The resulting combinations and overtones are responsible for the production of many bands (of lesser absorption) extending to shorter wavelengths. Principally among these are the bands centered at 0.942, 1.135, 1.370, and 1.872 μ, which increase in intensity of absorption with wavelength. Each of these bands produces a marked amount of optical absorption in the solar spectrum.

The relationship between the apparent absorption of water vapor (as measured with a prism instrument) and the amount of the vapor is not a simple one since each absorption band really consists of many fine lines of uneven intensity irregularly spaced. Furthermore, the attenuation at any wavelength due to water vapor is a complicated function of the pressure, temperature, and concentration of the vapor per unit volume. But the presence of all these complications does not prevent the use of the absorption-spectra method through the adoption of an empirical relationship between the optical absorption and the absolute amount of water in the atmosphere.

The spectroradiometric method for determining the water-vapor concentration in the upper atmosphere is rapid and practical for routine work—so long as the sun is not clouded over. It remains the most applicable of some 15 methods of water-vapor or moisture evaluation recently described [21]. This

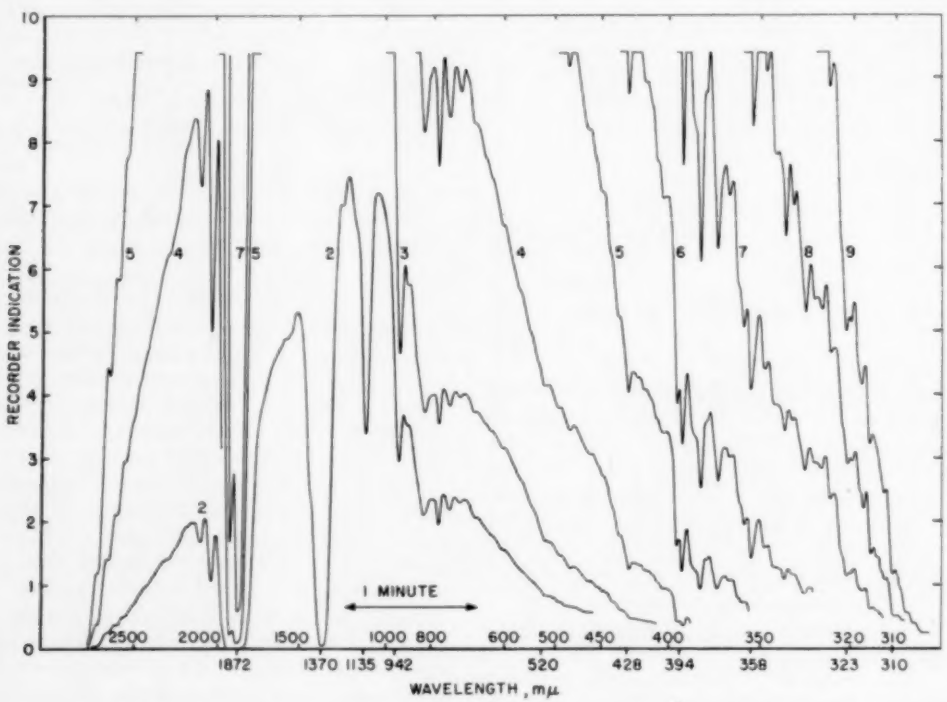

FIGURE 5. *Representative data taken from a section of the recorder chart while employing a PbS cell as a detector at Sunspot, New Mexico, in 1953.*

July 15, 1953, approximately 10:00 a. m. The numbers on the chart have no significance except to identify the curves and amplifier sensitivity settings. The data illustrated show the relative intensities of some of the principal water-vapor absorption bands. The time interval represented by the data approximates 18 min.

method, as developed by Fowle, permits calibration either in terms of total band absorption or of absorption at a single wavelength. In practice a combination of the two (the depth of a prismatic band) is simpler and has been found to yield more consistent results [10, 18] when a prism spectroradiometer is employed.

Any one of the water-vapor bands may be chosen for use in determining the total amount of precipitable water above the observer. In the present case, as noted above, the available bands for this purpose are located at 0.94, 1.135, 1.370, and 1.872 μ. (See figs. 5 and 6 which are representative of field data obtained at Sunspot, N. Mex. and on Mauna Loa, respectively.) It is important for highest accuracy to choose that band which is located in the part of the spectrum where the recorded intensities of solar spectral radiant energy are such that, in combination with the response properties of the spectroradiometer employed, a nearly horizontal curve results when the envelope of the recorder trace is drawn. Furthermore, greater sensitivity in detecting changes in the water-vapor content of the upper atmosphere can be obtained if the maximum of absorption falls between 25 and 75 percent. In the present case the band at 1.135 μ best meets these requirements. Hence this band has been chosen for use in evaluating the precipitable water above Mauna Loa.

Although the spectroradiometric method is rapid and highly practicable, its use entails certain assumptions relating to the characteristics of the shapes of the water-vapor absorption bands as affected by such things in the environment and instrument design as temperature, pressure, slit width, etc., which may and have been studied in the laboratory [8, 10, 11, 19], and their effects evaluated. Principal among these in importance is instrumental slit width or spectral purity. Fowle [10] determined a calibration employing specific slit widths through the use of a spectrobolometer by observing the depths of the water bands resulting from the absorption of a known amount of water vapor in a long tube. He furthermore determined that under the usual conditions of temperature and pressure of the upper atmosphere that in the practical case their effects could be neglected. This calibration of the total precipitable water in centimeters is given in figure 7 in terms of the intensity ratio for the water-vapor band at 1.135 μ when the spectral purity (slit width in wavelength) was 0.04 μ, as employed in the Mauna Loa work. We have used this calibration in the evaluation of the Mauna Loa data.

While this calibration and its application to the field data may not be of the highest accuracy owing to some question as to the total width of the band and its resultant effect upon depth measurements of the center of the band, it appears that the resulting errors are small since they would appear in a similar manner in both the field and laboratory data and would thus for the greater part cancel out.

The data for 4 days (June 7, 8, 12, and 13) have been analyzed and the amounts of precipitable water above the station plotted in figures 8 to 11, inclusive,

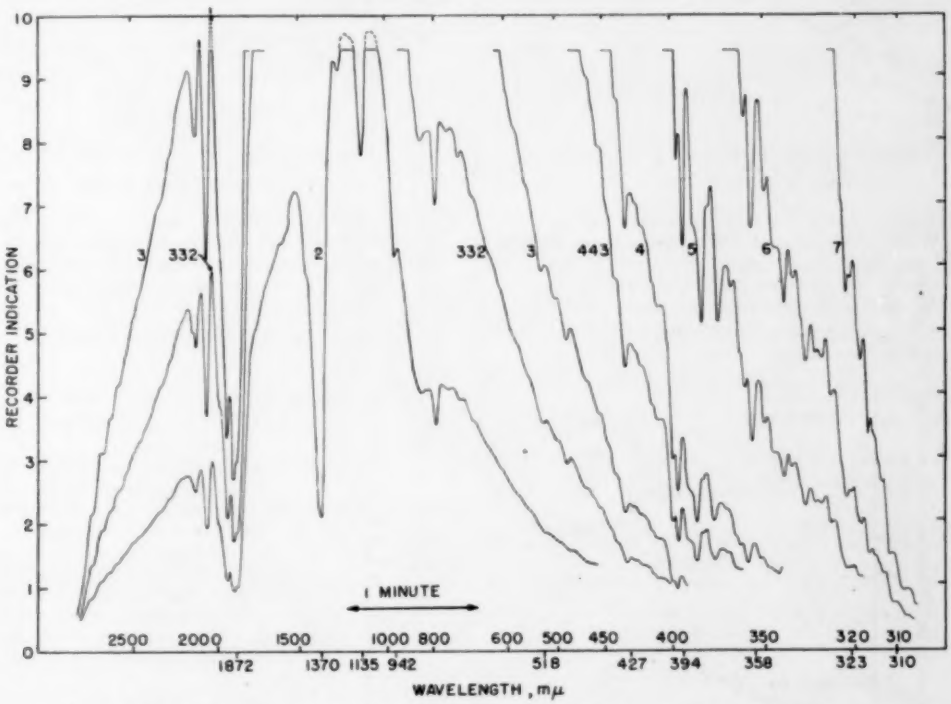

FIGURE 6. *Representative data taken from a section of the recorder chart while employing a PbS cell as a detector at Mauna Loa in 1957.*

June 12, 1957, approximately 10:00 a. m. The numbers on the chart have no significance except to identify the curves and amplifier sensitivity settings. (They should not be compared directly with those of figure 5 because of possible differences in spectrometer adjustment and the use of a different PbS cell.) The data illustrated show the relative intensities of some of the principal water-vapor absorption bands. The time interval represented by the data approximates 18 min.

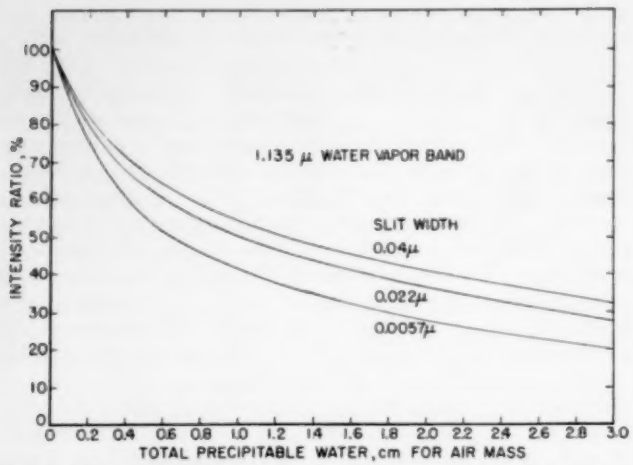

FIGURE 7. *Intensity ratios of radiation at the center of the 1.135 μ water-vapor band as a function of total precipitable water in the atmosphere for a prism instrument having specific spectral purity (effective slit widths).*

Data from Fowle, reference 10.

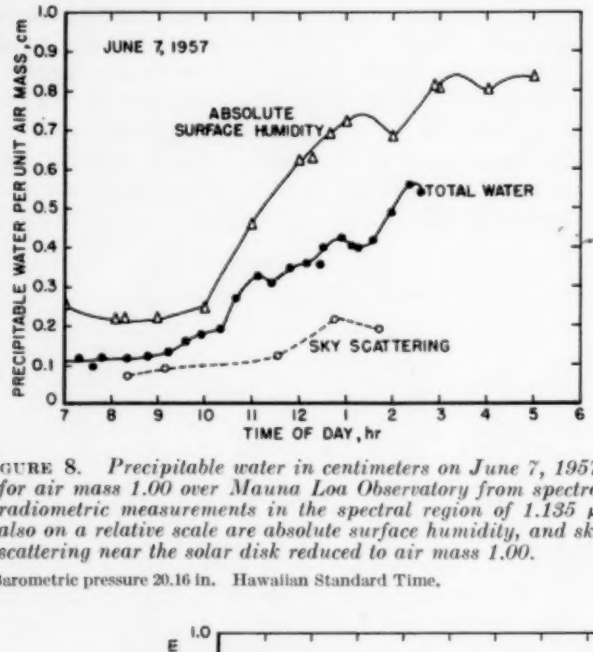

FIGURE 8. *Precipitable water in centimeters on June 7, 1957, for air mass 1.00 over Mauna Loa Observatory from spectroradiometric measurements in the spectral region of 1.135 μ; also on a relative scale are absolute surface humidity, and sky scattering near the solar disk reduced to air mass 1.00.*

Barometric pressure 20.16 in. Hawaiian Standard Time.

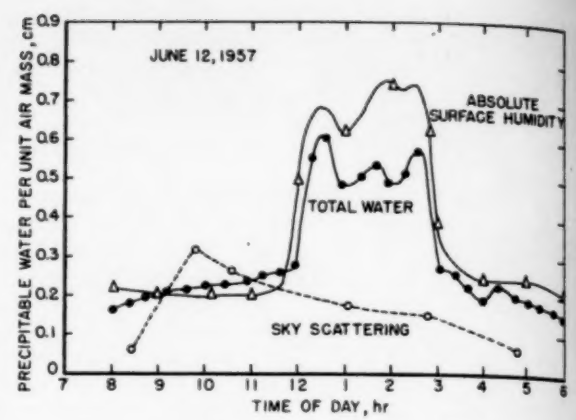

FIGURE 10. *Precipitable water in centimeters on June 12, 1957, for air mass 1.00 over the Mauna Loa Observatory from spectroradiometric measurements in the spectral region of 1.135 μ; also on a relative scale are absolute surface humidity, and sky scattering near the solar disk reduced to air mass 1.00.*

Barometric pressure 20.23 in. Hawaiian Standard Time.

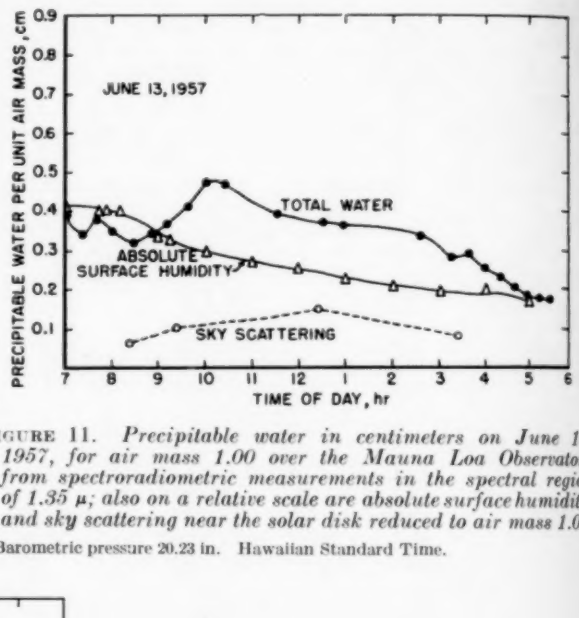

FIGURE 11. *Precipitable water in centimeters on June 13, 1957, for air mass 1.00 over the Mauna Loa Observatory from spectroradiometric measurements in the spectral region of 1.35 μ; also on a relative scale are absolute surface humidity, and sky scattering near the solar disk reduced to air mass 1.00.*

Barometric pressure 20.23 in. Hawaiian Standard Time.

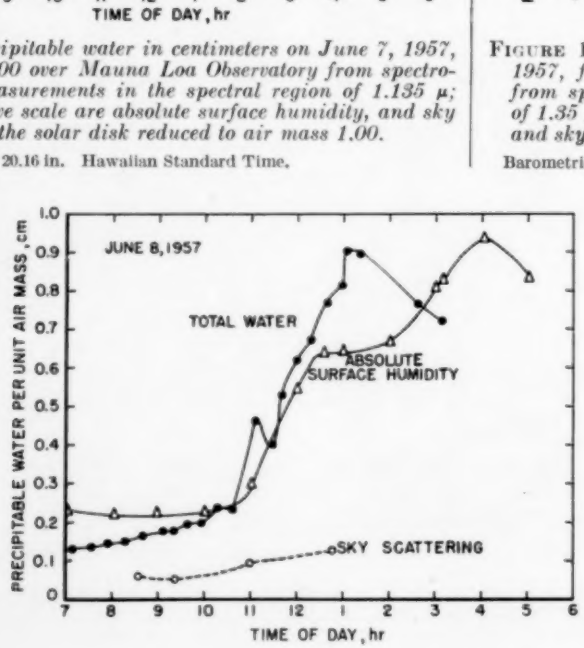

FIGURE 9. *Precipitable water in centimeters on June 8, 1957, for air mass 1.00 over the Mauna Loa Observatory from spectroradiometric measurements in the spectral region of 1.135 μ; also on a relative scale are absolute surface humidity, and sky scattering near the solar disk reduced to air mass 1.00.*

Barometric pressure 20.16 in. Hawaiian Standard Time.

as a function of the time of day. On these same plots are illustrated the relative amounts of precipitable water (absolute surface humidity) based on measurements of relative humidity and temperature at the station. These data are necessarily on a relative scale (but the same relative scale for the 4 days) as no means were available for determining the water at higher altitudes by this method. It is significant that on any one day there is a general correlation between the water-measurements at the station and the total amount of water as integrated for all altitudes by the spectroradiometric method. This probably indicates that the major part of the water above the station is near the station level.

A study of figures 8 to 11, coupled with the general observations of the sky at the station over a period of several months and with the experience of other observers in Martian studies [22] at this station, signifies that as a general rule there is a very low water concentration above Mauna Loa from late afternoon until late in the morning of the next day. Under certain weather conditions the low water concentration continues undisturbed throughout the 24-hr period. On many days, however, the inversion layer is disrupted near noon or in early afternoon thus allowing a mass of humid atmosphere to sweep up the mountain and enshroud the station either temporarily for an hour or two or until late afternoon or early evening. Except during unfavorable weather, however, the mass of humid atmosphere again descends the mountain during the late afternoon or early evening so that a picturesque sunset may be viewed—and on especially favorable occasions in such a way that the brilliant "green flash" may be observed immediately following the disappearance of the edge of the sun from view.

The amount of atmospheric scattering in the visible spectrum as measured in the annular conical angle surrounding the sun (figs. 8 to 11, inclusive) seems to have no definite relationship to the total precipitable water above the station. This is interesting and indicates the importance of additional study of atmospheric transmittance and scattering at high altitudes. It was noted that the sky appeared less blue when there was a minimum amount of water present; also that the sky usually appeared much bluer when viewed at the 5000- to 8000-ft levels than when viewed from the altitude of the Mauna Loa Observatory (11,140 ft).

The authors express their sincere appreciation to the Geophysics Research Directorate of Air Force Cambridge Research Center and the U. S. Weather Bureau for supporting this project, and to individual members of those organizations, in particular to P. R. Gast for helpful advice and assistance, and to R. G. Busniewski for much assistance in connection with the operation of the radio linkage and carrying out the field work at the observatory.

6. References

[1] Ralph Stair, Ultraviolet radiant energy from the sun observed at 11,190 feet, J. Research NBS **49,** 227 (1952) RP2357.

[2] Ralph Stair, Russell G. Johnston, and Thomas C. Bragg, Spectral distribution of energy from the sun, J. Research NBS **53,** 113 (1954) RP2523.

[3] Ralph Stair and Russell G. Johnston, Preliminary spectroradiometric measurements of the solar constant, J. Research NBS **57,** 205 (1956) RP2710.

[4] Roy L. Fox, New Mauna Loa Observatory unit, Nature **178,** 1272 (1956).

[5] John W. Evans, A photometer for measurement of sky brightness near the sun, J. Opt. Soc. Am. **38,** 1083 (1948).

[6] C. Fabry and H. Buisson, Data on ozone absorption, Compt. rend. **192,** 457 (1931).

[7] E. Vigroux, Contributions a l'étude expérimentale de l'absorption de l'ozone, Ann. phys. **8,** 709 (1953).

[8] F. E. Fowle, The spectroscopic determination of aqueous vapor, Astrophys. J. **35,** 149 (1912).

[9] F. E. Fowle, The determination of aqueous vapor above Mount Wilson, Astrophys. J. **37,** 359 (1913).

[10] F. E. Fowle, The transparency of aqueous vapor, Astrophys. J. **42,** 394 (1915).

[11] L. B. Aldrich, Note on Fowle's spectrographic method for the determination of aqueous vapor in the atmosphere, Smith. Misc. Collections **111,** No. 12, p. 1 (1949).

[12] L. W. Foskett and N. B. Foster, A spectroscopic hygrometer, Bull. Am. Meteorol. Soc. **24,** 146 (1943).

[13] Norman B. Foster and Laurence W. Foskett, A spectrophotometer for the determination of the water vapor in a vertical column of the atmosphere, J. Opt. Soc. Am. **35,** 601 (1945).

[14] L. W. Foskett, N. B. Foster, W. R. Thickstun, and R. C. Wood, Infrared absorption hygrometer, Monthly Weather Rev. **81,** 267 (1953).

[15] S. B. Solot, Computation of depth of precipitable water in a column of air, Monthly Weather Rev. **67,** 100 (1939).

[16] W. M. Elsasser, New values for infrared absorption coefficient of atmospheric water vapor, Monthly Weather Rev. **66,** 175 (1938).

[17] David S. Johnson, Field test of a total equivalent precipitable water hygrometer, Unpublished manuscript of the U. S. Weather Bureau.

[18] David M. Gates, Infrared determination of precipitable water vapor in a vertical column of the earth's atmosphere, J. Meteorol. **13,** 369 (1956).

[19] J. N. Howard, D. E. Burch, and D. Williams, Near infrared transmission through synthetic atmospheres, Geophysical Res. Pap., No. 40, G. R. D., AFCRC, ARDC (1955), ASTIA document No. AD–87679.

[20] E. K. Plyler and W. W. Sleator, Further study of the absorption of infrared radiation by water vapor, Phys. Rev., 2d Series **37,** 1493 (1931).

[21] Arnold Wexler and W. G. Brombacher, Methods of measuring humidity and testing hygrometers, NBS Circ. **512** (1951).

[22] C. C. Kiess, C. H. Corliss, Harriet K. Kiess, and Edith L. R. Corliss, High-dispersion spectra of Mars, Astrophys. J. **126,** 579 (1957).

[23] E. C. Y. Inn and Y. Tanaka, Comparison of recently recorded ozone absorption coefficients in the visible and ultraviolet regions, Conference on Ozone, Armour Research Foundation, Dec. 1956. See also, J. Opt. Soc. Am. **43,** 870 (1953).

WASHINGTON, June 18, 1958.

Journal of Research of the National Bureau of Standards Vol. 61, No. 5, November 1958 Research Paper 2911

Central Notations for the Revised ISCC-NBS Color-Name Blocks

Kenneth L. Kelly

Nickerson and Newhall published, in 1941, the central notations of the original ISCC-NBS (Inter-Society Color Council-National Bureau of Standards) color-name blocks which were used in the preparation of the soil and rock color-name charts. In 1955, the ISCC-NBS color-name blocks were revised to accord more closely with usage in the textile and other fields (NBS Circular 553). The central notations of these revised color-name blocks have been computed and are given in the present paper in tabular form. A color chart showing the central colors of the 267 ISCC-NBS color-name blocks would serve for rapid determination of the ISCC-NBS color designation, especially in field work where speed and ease of operation are more important than high accuracy.

1. Introduction

In 1941 Nickerson and Newhall published a paper [7][1] entitled Central Notations for ISCC-NBS Color Names based on the first description of the ISCC-NBS method of describing colors published in 1939 [2]. Since then, the ISCC-NBS color-name charts have been revised to accord more closely with usage in the textile and other fields and have been published in 1955 under the title The ISCC-NBS Method of Designating Colors and a Dictionary of Color Names [3]. The present paper contains the central notations of the revised color-name blocks.

2. Computation of Centroids

The color-name blocks into which the color solid has been divided are bounded at top and bottom by planes of constant Munsell value, at two of the sides by planes of constant Munsell hue, and at the other two sides by concentric cylindrical surfaces of constant Munsell chroma. The shape of such a block might be called a sector of a right cylindrical annulus (like a piece of pie with the point bitten off). The simplest such block is thus defined by six limits: two-value, two-hue, and two-chroma limits; the most complicated of these blocks may be broken down into three blocks of this simplest or elementary shape. The general method is to find the centroid of each such block and then find the volume-weighted centroid of the set of one to three such elementary centroids.

The hue and value of such an elementary centroid are simply the averages of the hue and value limits, respectively. The chroma of the centroid is not entirely a function of the chroma limits, but depends on the number of Munsell-hue steps ΔH in the block. Let the cross section of the block at constant Munsell value be laid out in cylindrical coordinates with the radius being Munsell chroma, C, and since there are 100 Munsell-hue steps in the complete hue circuit, the angle $\Delta\theta$ in radians will be given in terms of Munsell hue, H, as $2\pi\Delta H/100$. Further let $H=0$ correspond to the Munsell hue, $\overline{H}$, of the centroid of the block.

The chroma, $\overline{C}$, of the centroid [1] is defined as:

$$\overline{C}\equiv\frac{\int_{-\frac{\theta}{2}}^{\frac{\theta}{2}}\int_{C_n}^{C_x}C^2\,(\cos\theta)dCd\theta}{\int_{-\frac{\theta}{2}}^{\frac{\theta}{2}}\int_{C_n}^{C_x}CdCd\theta},\text{ or}$$

$$\overline{C}=\frac{2(C_x^2+C_xC_n+C_n^2)\sin(\pi\Delta H/100)}{3(C_x+C_n)(\pi\Delta H/100)},$$

where C_x and C_n are the upper and lower chroma limits of the block, respectively.

By this method, the central notation $(\overline{H},\ \overline{V}/\overline{C})$ of an elementary block like moderate red, hue range $1R$ to $7R$, value range from 3.5 to 5.5, and chroma range from 7 to 11, is determined as:

$$\overline{H}=(1R+7R)/2=4R;\ \overline{V}=(3.5+5.5)/2=4.5,$$

and

$$\overline{C}=\frac{2(11^2+7\times11+7^2)\sin(6\pi/100)}{3(11+7)(6\pi/100)}=\frac{2\times247\times0.1874}{3\times18\times0.1885}=9.1$$

The central notation of a compound block, that is, one in which two or more elementary blocks are joined together along common constant-hue planes, such as yellowish white or moderate blue, is found by computing the volume-weighted mean of the central notations of the simple blocks. The centroid of a two-component block, for instance, will lie on the straight line joining the centroids of the component blocks. Therefore, it is necessary to graph the respective centroids on circular graph paper, connect them by a straight line divided inversely according to the two volumes, and read off the hue and chroma of the resultant centroid. For a three-component block, the resultant centroid for two of the adjacent blocks is found and then combined by the same method with the centroid of the third block. The value notation of the resultant centroid is computed as the volume-weighted mean of the value notations of the separate centroids.

[1] Figures in brackets indicate the literature references at the end of this paper.

3. Peripheral Color-Name Blocks

The shape of the psychological color solid may be described as a grossly misshapen grapefruit, set so that the pithy core is vertical with an irregular outer surface or skin, determined by the MacAdam theoretical pigment limits [4]. The bounding surface has been determined in Munsell renotation terms by Nickerson and Newhall [8]. This solid, cut into 267 blocks each with a color name attached, forms the ISCC–NBS system of color names. Now consider the outermost or peripheral blocks, those that extend to the outer surface or skin. These represent colors of maximum saturation, maximum lightness or minimum lightness as determined from the MacAdam limits. These peripheral blocks, of which there are 120, have several simple boundary surfaces (plane and cylindrical) and are closed by the outer complicated curved surface of the color solid. The centroids of these peripheral blocks have been estimated graphically by plotting the MacAdam limits on the color-name charts.

4. Table of Central Notations of Color-Name Blocks

In table 1 the ISCC–NBS color-name blocks are identified by number and name, and the Munsell renotation of each centroid is given. The central notation of each of the 120 peripheral blocks, less certain because it was estimated rather than computed by formula, is marked with an asterisk. The numbers used to identify and order the color designations in table 1 are taken from table 1 of NBS Circular 553 [3]. Thus, for any hue name, the order of modifiers is vivid; brilliant, strong, deep, very deep; very light, light, moderate, dark, very dark; very pale (very light grayish), pale (light grayish), grayish, dark grayish, blackish; -ish white, light -ish gray; -ish gray, dark -ish gray, and -ish black. Not all of these modifiers are required with every hue name, as for instance there is no very dark pink or very pale olive. The notations of the centroids are given to one decimal place except that the value or chroma notations of the centroids of some of the peripheral blocks are given as whole numbers followed by a plus or minus sign, such as 4.5 *YR* 6.8/16+, indicating uncertainty in the next decimal place.

TABLE 1. *Central notations of ISCC–NBS color-name blocks.*

C553 number	ISCC–NBS color name	Central notation
1	vivid pink	1.5*R* 7 /13+*
2	strong pink	1.5*R* 7.5/9.1*
3	deep pink	1.9*R* 6.0/11.1
4	light pink	2.5*R* 8.6/5.2*
5	moderate pink	2.5*R* 7.2/5.2
6	dark pink	2.5*R* 6.0/6.0
7	pale pink	2.5*R* 8.8/2.3*
8	grayish pink	2.5*R* 7.2/2.3
9	pinkish white	7.6*R* 9.2/1.0*
10	pinkish gray	7.6*R* 7.5/1.0
11	vivid red	5–*R* 4 /15+*
12	strong red	4.0*R* 4.5/12.0
13	deep red	5.0*R* 2.8/9.9
14	very deep red	5.0*R* 1.4/9.0*
15	moderate red	4.0*R* 4.5/9.1
16	dark red	4.5*R* 2.8/6.8
17	very dark red	3.5*R* 1.2/4.9*
18	light grayish red	4.9*R* 6.0/3.4
19	grayish red	4.6*R* 4.5/4.7
20	dark grayish red	3.5*R* 2.7/2.2
21	blackish red	3.5*R* 1.1/1.6*
22	reddish gray	6.5*R* 5.5/1.1
23	dark reddish gray	6.0*R* 3.5/1.1
24	reddish black	6.0*R* 0.9/0.8*
25	vivid yellowish pink	8.0*R* 7 /13+*
26	strong yellowish pink	8.0*R* 7.5/9.0*
27	deep yellowish pink	5.6*R* 6.0/12.4
28	light yellowish pink	0.7*YR* 8.6/4.8*
29	moderate yellowish pink	0.7*YR* 7.2/4.8
30	dark yellowish pink	7.0*R* 6.0/6.0
31	pale yellowish pink	2.1*YR* 8.8/2.2*
32	grayish yellowish pink	0.5*YR* 7.2/2.3
33	brownish pink	6.5*YR* 7.2/2.2
34	vivid reddish orange	9.5+*R* 5.5/15.5+*
35	strong reddish orange	9.5*R* 5.5/12.0
36	deep reddish orange	9.5*R* 4.0/12.0
37	moderate reddish orange	9.5*R* 5.5/9.1
38	dark reddish orange	9.5*R* 4.0/9.1
39	grayish reddish orange	0.5*YR* 5.5/6.0
40	strong reddish brown	0.5*YR* 3.0/11.2*
41	deep reddish brown	9.8*R* 1.5+/7.5+*
42	light reddish brown	0.5*YR* 5.5/4.1
43	moderate reddish brown	9.6*R* 3.4/5.2
44	dark reddish brown	9.5*R* 1.3/3.6*
45	light grayish reddish brown	3.0*YR* 5.5/2.3
46	grayish reddish brown	9.9*R* 3.4/2.3
47	dark grayish reddish brown	9.5*R* 2.0/2.0
48	vivid orange	4.5*YR* 6.6/16+*
49	brilliant orange	4.5*YR* 8.0/12.1*
50	strong orange	4.5*YR* 6.5/12.1
51	deep orange	4.5*YR* 5.0/12.1
52	light orange	4.5*YR* 8 /8.1*
53	moderate orange	4.6*YR* 6.5/8.1
54	brownish orange	4.5*YR* 5.0/8.2
55	strong brown	5.0*YR* 3.5+/8+*
56	deep brown	5.0*YR* 2.1/6+*
57	light brown	5.5*YR* 5.5/4.6
58	moderate brown	5.5*YR* 3.5/3.9
59	dark brown	5.5*YR* 1.6/3.6*
60	light grayish brown	6.5*YR* 5.5/2.2
61	grayish brown	5.6*YR* 3.5/2.0
62	dark grayish brown	5.5*YR* 2.0/1.7
63	light brownish gray	6.8*YR* 5.5/1.0
64	brownish gray	6.4*YR* 3.5/0.9
65	brownish black	7.5*YR* 0.8/0.8*
66	vivid orange yellow	9.0*YR* 7.2/16+*
67	brilliant orange yellow	9.0*YR* 8.4/12.1*
68	strong orange yellow	9.0*YR* 7.2/12.1
69	deep orange yellow	9.0*YR* 6.0/12.1
70	light orange yellow	9.0*YR* 8.6/8.1*

TABLE 1. *Central notations of ISCC–NBS color-name blocks.*—Continued

TABLE 1. *Central notations of ISCC–NBS color-name blocks.*—Continued

C553 number	ISCC–NBS color name	Central notation
71	moderate orange yellow	9.0*YR* 7.2/8.1
72	dark orange yellow	9.0*YR* 6.0/8.1
73	pale orange yellow	9.1*YR* 8.6/4.4*
74	strong yellowish brown	9.0*YR* 4.6/9.6*
75	deep yellowish brown	9.5*YR* 2.9/6+*
76	light yellowish brown	9.2*YR* 6.6/4.7
77	moderate yellowish brown	9.5*YR* 4.5/4.0
78	dark yellowish brown	9.5*YR* 2.2/3.7*
79	light grayish yellowish brown	9.5*YR* 6.4/2.4
80	grayish yellowish brown	9.5*YR* 4.6/2.1
81	dark grayish yellow brown	9.5*Y R* 2.4/1.8
82	vivid yellow	4.0*Y* 7.8/14.5+*
83	brilliant yellow	4.0*Y* 8.8/9.5*
84	strong yellow	4.0*Y* 7.2/9.5
85	deep yellow	4.0*Y* 6.0/9.5
86	light yellow	4.0*Y* 8.8/6.6*
87	moderate yellow	4.0*Y* 7.2/6.6
88	dark yellow	4.0*Y* 6.0/6.6
89	pale yellow	4.2*Y* 8.9/3.6*
90	grayish yellow	4.2*Y* 7.2/3.6
91	dark grayish yellow	4.0*Y* 6.0/4.1
92	yellowish white	4.1*Y* 9.2/1.3*
93	yellowish gray	4.1*Y* 7.5/1.3
94	light olive brown	2.5*Y* 5.0/8.4*
95	moderate olive brown	2.5*Y* 3.5+/6+*
96	dark olive brown	2.5*Y* 1.8/2.5+*
97	vivid greenish yellow	9.5*Y* 7.8/14.5+*
98	brilliant greenish yellow	9.5*Y* 8.8/9.5*
99	strong greenish yellow	9.5*Y* 7.2/9.5
100	deep greenish yellow	9.5*Y* 6.0/9.5
101	light greenish yellow	9.5*Y* 8.8/6.6*
102	moderate greenish yellow	9.5*Y* 7.2/6.6
103	dark greenish yellow	9.5*Y* 6.0/6.6
104	pale greenish yellow	9.5*Y* 8.9/4.1*
105	grayish greenish yellow	9.5*Y* 7.2/4.1
106	light olive	8.1*Y* 5.1/8.0*
107	moderate olive	8.0*Y* 3.5+/5.8+*
108	dark olive	8.0*Y* 1.7/3.2*
109	light grayish olive	8.3*Y* 5.5/2.4
110	grayish olive	8.1*Y* 3.5/2.3
111	dark grayish olive	8.0*Y* 2.0/2.0
112	light olive gray	7.4*Y* 5.5/1.3
113	olive gray	8.1*Y* 3.5/1.0
114	olive black	9.0*Y* 0.9/0.8*
115	vivid yellow green	5.0*GY* 7.5/14.5+*
116	brilliant yellow green	5.0*GY* 8.5/9.1*
117	strong yellow green	5.0*GY* 6.0/9.1
118	deep yellow green	5.0*GY* 4.0/9.1
119	light yellow green	5.0*GY* 8.6/5.2*
120	moderate yellow green	5.0*GY* 6.0/5.2
121	pale yellow green	3.5*GY* 8.7/2.2*
122	grayish yellow green	4.4*GY* 6.1/2.2
123	strong olive green	5.0*GY* 3.2/7.8+*
124	deep olive green	5.0*GY* 2.4+/7.1+*
125	moderate olive green	5.0*GY* 3.5/5.2
126	dark olive green	5.0*GY* 1.8/3.7*
127	grayish olive green	5.0*GY* 3.5/2.2
128	dark grayish olive green	5.0*GY* 2.0/2.0
129	vivid yellowish green	0.5*G* 7 /15.5+*
130	brilliant yellowish green	0.5*G* 8.0/9.1*

TABLE 1. *Central notations of ISCC—NBC color-name blocks.*—Continued

C553 number	ISCC–NBS color name	Central notation
131	strong yellowish green	0.5*G* 5.5/9.1
132	deep yellowish green	0.5*G* 3.5/11.5+*
133	very deep yellowish green	0.5*G* 2.0/9.2+*
134	very light yellowish green	0.5*G* 9.1/5.1*
135	light yellowish green	0.5*G* 7.5/5.1
136	moderate yellowish green	0.5*G* 5.5/5.1
137	dark yellowish green	0.5*G* 3.5/5.1
138	very dark yellowish green	0.5*G* 1.5/4.9*
139	vivid green	6.5*G* 5.2/18+*
140	brilliant green	6.0*G* 7.4/9.1*
141	strong green	6.0*G* 4.5/9.1
142	deep green	6.0*G* 2.3/9.1*
143	very light green	6.0*G* 8.6/5.1*
144	light green	6.0*G* 6.5/5.1
145	moderate green	6.0*G* 4.5/5.1
146	dark green	6.0*G* 2.7/5.0
147	very dark green	6.0*G* 1.3/4.9*
148	very pale green	9.0*G* 8.7/1.8*
149	pale green	9.0*G* 6.5/1.8
150	grayish green	9.0*G* 4.5/1.8
151	dark grayish green	9.0*G* 2.8/1.6
152	blackish green	9.0*G* 1.1/1.4*
153	greenish white	7.0*G* 9.2/0.8*
154	light greenish gray	7.0*G* 7.5/0.8
155	greenish gray	7.0*G* 5.5/0.8
156	dark greenish gray	7.0*G* 3.5/0.8
157	greenish black	7.5*G* 0.9/0.7*
158	vivid bluish green	4.5*BG* 5.3/15.5+*
159	brilliant bluish green	4.5*BG* 7.3/9.0*
160	strong bluish green	4.5*BG* 4.5/9.0
161	deep bluish green	4.5*BG* 2.3/9.0*
162	very light bluish green	4.5*BG* 8.5/5.0*
163	light bluish green	4.5*BG* 6.5/5.0
164	moderate bluish green	4.5*BG* 4.5/5.0
165	dark bluish green	4.5*BG* 2.7/5.0
166	very dark bluish green	4.5*BG* 1.3/4.9*
167	vivid greenish blue	4.5*B* 5.2/13+*
168	brilliant greenish blue	4.5*B* 6.8/9.0*
169	strong greenish blue	4.5*B* 4.5/9.0
170	deep greenish blue	4.5*B* 2.5/9.0*
171	very light greenish blue	4.5*B* 8.2/5.2*
172	light greenish blue	4.5*B* 6.5/5.2
173	moderate greenish blue	4.5*B* 4.5/5.2
174	dark greenish blue	4.5*B* 2.7/5.0
175	very dark greenish blue	4.5*B* 1.3/4.9*
176	vivid blue	3.0*PB* 4.2/15+*
177	brilliant blue	3.0*PB* 6.4/11.0*
178	strong blue	3.0*PB* 4.2/11.0
179	deep blue	3.0*PB* 2.0/9.0*
180	very light blue	2.4*PB* 8.2/7.2*
181	light blue	2.7*PB* 6.5/7.3
182	moderate blue	2.9*PB* 4.2/7.2
183	dark blue	2.8*PB* 1.7/5.0*
184	very pale blue	0.9*PB* 8.4/3.0*
185	pale blue	0.9*PB* 6.5/3.0
186	grayish blue	0.9*PB* 4.2/3.0
187	dark grayish blue	9.5*B* 2.6/1.9
188	blackish blue	9.5*B* 1.1/1.5*
189	bluish white	9.5*B* 9.1/1.0*
190	light bluish gray	9.5*B* 7.5/1.0

TABLE 1. *Central notations of ISCC–NBS color-name blocks*—Continued

C553 number	ISCC–NBS color name	Central notation
191	bluish gray	9.5*B* 5.5/1.0
192	dark bluish gray	9.5*B* 3.5/1.0
193	bluish black	9.5*B* 1.0/0.7*
194	vivid purplish blue	8.0*PB* 2.5/22+*
195	brilliant purplish blue	8.0*PB* 6.0/10.8*
196	strong purplish blue	8.0*PB* 4.1/11.4
197	deep purplish blue	8.0*PB* 1.6/9.1*
198	very light purplish blue	7. *PB* 7.8+/6.1+*
199	light purplish blue	7.5*PB* 6.0/6.8
200	moderate purplish blue	8.0*PB* 3.5/6.9
201	dark purplish blue	7.9*PB* 1.1/4.7*
202	very pale purplish blue	7.0*PB* 8.2/4.1*
203	pale purplish blue	7.0*PB* 6.0/4.1
204	grayish purplish blue	7.2*PB* 3.3/4.0
205	vivid violet	1.0*P* 2.7/21+*
206	brilliant violet	1.0*P* 5.9/11.1*
207	strong violet	1.0*P* 3.5/11.1
208	deep violet	1.0*P* 1.4/10.3*
209	very light violet	1.0*P* 7.9/7*
210	light violet	1.0*P* 6.0/7.2
211	moderate violet	1.0*P* 3.5/7.2
212	dark violet	1.0*P* 1.3/5.0*
213	very pale violet	1.0*P* 8.2/4.1*
214	pale violet	1.0*P* 6.0/4.1
215	grayish violet	1.0*P* 3.3/4.1
216	vivid purple	6.0*P* 3.5/20+*
217	brilliant purple	6.0*P* 6.7/11.1*
218	strong purple	6.0*P* 4.5/11.1
219	deep purple	6.0*P* 2.8/10.2
220	very deep purple	6.0*P* 1.2/10.2*
221	very light purple	6.0*P* 8.0/7.2*
222	light purple	6.0*P* 6.5/7/2
223	moderate purple	6.0*P* 4.5/7.2
224	dark purple	6.0*P* 2.7/5.1
225	very dark purple	6.0*P* 1.1/4.9*
226	very pale purple	5.4*P* 8.4/3.3*
227	pale purple	6.8*P* 6.4/3.0
228	grayish purple	7.8*P* 4.5/2.9
229	dark grayish purple	10.0*P* 2.8/2.0
230	blackish purple	10.0*P* 1.0/1.4*

TABLE 1. *Central notations of ISCC–NBS color-name blocks.*—Continued

C553 number	ISCC–NBS color name	Central notations
231	purplish white	9.0*P* 9.1/1.0*
232	light purplish gray	9.0*P* 7.5/1.0
233	purplish gray	10.0*P* 5.5/1.0
234	dark purplish gray	10.0*P* 3.5/1.0
235	purplish black	10.0*P* 1.0/0.7*
236	vivid reddish purple	1.0*RP* 4+/19+*
237	strong reddish purple	1.0*RP* 4.5/11.1
238	deep reddish purple	1.0*RP* 2.8/10.3
239	very deep reddish purple	1.0*RP* 1.3/10.3*
240	light reddish purple	1.0*RP* 6.0/7.2
241	moderate reddish purple	1.0*RP* 4.5/7.2
242	dark reddish purple	1.0*RP* 2.7/5.1
243	very dark reddish purple	1.0*RP* 1.1/5.0*
244	pale reddish purple	1.0*RP* 6.0/4.1
245	grayish reddish purple	1.0*RP* 4.5/4.1
246	brilliant purplish pink	4.0*RP* 7.9+/11+*
247	strong purplish pink	4.0*RP* 7–/14.5*
248	deep purplish pink	4.0*RP* 6.0/12.0
249	light purplish pink	4.0*RP* 8.3/7.1*
250	moderate purplish pink	4.0*RP* 7.0/7.1
251	dark purplish pink	6.0*RP* 6.0/7.2
252	pale purplish pink	4.0*RP* 8.5/3.5*
253	grayish purplish pink	4.0*RP* 7.0/3.5
254	vivid purplish red	7.0*RP* 4+/17+*
255	strong purplish red	7.0*RP* 4.5/11.9
256	deep purplish red	7.0*RP* 2.8/11.0
257	very deep purplish red	7.0*RP* 1.3/9.0*
258	moderate purplish red	7.0*RP* 4.5/9.0
259	dark purplish red	7.0*RP* 2.7/6.3
260	very dark purplish red	7.0*RP* 1.2/4.9*
261	light grayish purplish red	7.0*RP* 6.0/4.0
262	grayish purplish red	7.0*RP* 4.5/5.2
263	white	3.0*Y* 9.25/0.06
264	light gray	3.0*Y* 7.5/0.06
265	medium gray	3.0*Y* 5.5/0.06
266	dark gray	*N* 3.5/
267	black	*N* 1.25/

5. Applications

For nonborderline colors it is much easier to determine the ISCC–NBS color name from a color chart containing 267 samples, one for each of the central notations of the 267 ISCC–NBS color-name blocks, than it is to determine the Munsell renotation of the color and then to find the ISCC–NBS designation from the color-name charts. In using such a color chart, the observer simply picks out the particular color most closely duplicating that of the specimen to be designated; he does not have to check for conformity to hue, lightness, and saturation limits separately. The production of such a color chart is now under consideration. It should be pointed out, however, that if the specimen color falls about equally near to two or more of the 267 central colors, it would be impossible to determine accurately which ISCC–NBS designation to apply to it. If necessary, such borderline cases would have to be resolved by recourse to the method described in NBS Circular 553 [3].

These central notations have a number of applications. Those published by Nickerson and Newhall [7] were used in designing the color-name charts used in the description of the colors of soils [5] and rocks [6]. In both of these color charts, the Munsell Color Company painted samples representing the central notations of each of the color-name blocks used. Matching to one central color rather than to several limit colors is a less exact but quicker method and was developed for field use where speed and ease of operation are more important than high accuracy.

The author acknowledges the assistance received from G. L. Gibson in checking the computation of the centroid locations.

6. References

[1] Dull, R. W., Mathematics for engineers, p. 753 (McGraw-Hill Book Company Inc., N. Y., N. Y., 1926).

[2] Judd, D. B., and Kelly, K. L., Method of designating colors, J. Research NBS **23,** 355 (1939) RP1239.

[3] Kelly, K. L. and Judd, D. B., The ISCC–NBS method of designating colors and a dictionary of color names, NBS Circ. 553 (1955), obtainable from the Superintendent of Documents, U. S. Government Printing Office, Washington 25, D. C. ($2.00).

[4] MacAdam, D. L., Maximum visual efficiency of colored materials, J. Opt. Soc. Am. **25,** 361 (1935).

[5] Munsell Color Company, Munsell Soil Color Charts, special form for use of soil scientists, geologists, and archaeologists (Munsell Color Company, 10 East Franklin Street, Baltimore 2, Md., 1950).

[6] National Research Council, Rock-Color Chart, prepared by the Rock-Color Chart Committee (sponsored by five geological organizations), National Research Council, Washington, D. C., 1948.

[7] Nickerson, Dorothy, and Newhall, Sidney M., Central notations for ISCC–NBS color names, J. Opt. Soc. Am. **31,** 587 (1941).

[8] Nickerson, Dorothy, and Newhall, Sidney M., A psychological color solid, J. Opt. Soc. Am. **33,** 419 (1943).

WASHINGTON, June 3, 1958.

Journal of Research of the National Bureau of Standards Vol. 61, No. 5, November 1958 Research Paper 2912

Viscosity of *n*-Hexadecane

Robert C. Hardy

Attempts to prepare high-purity *n*-hexadecane from commercial cetane by simple laboratory procedures were unsuccessful. Fractional distillation at reduced pressure, of material previously treated with silica gel, produced a few small fractions of about 99.5-mole-percent purity. The kinematic viscosities of the original material and of the fraction of highest purity, 99.63-mole percent, were found to be the same, 4.4635 centistokes at 20°. All other fractions had lower viscosities. The viscosity of NBS standard sample of *n*-hexadecane, 99.94-mole percent, was found to be 4.4642 centistokes or 3.4540 centipoises at 20°C. *n*-Hexadecane is not likely to be suitable for use as a second calibration standard for viscometry until a simple, easily defined routine of purification is developed.

1. Introduction

Most viscometers must be calibrated by the use of one or more liquids of known viscosity. The viscosity of water at 20°C has been accurately determined [1],[1] and water at this temperature is widely accepted as the calibration standard for viscometry. However, each viscometer has practical usefulness for measuring only a limited range of viscosities, which in general, does not include the viscosity of water. Consequently, most instruments must be calibrated with liquids other than water.

For about 30 years the Bureau has supplied a series of oils of known viscosity for use as viscometer calibrating liquids. The American Petroleum Institute with the cooperation of the American Society for Testing Materials provides a similar but more limited service, used principally by the petroleum industry. These oils are multicomponent solutions whose properties may change slightly over extended periods of time, depending on many factors including the conditions of storage. If deterioration due to age or contamination is suspected, fresh samples must be obtained from the supplier. There is no process by which their original viscosity can be reestablished or reaffirmed which does not require redetermination of the viscosity.

This suggests the desirability of using pure chemical compounds as calibration standards since if deterioration occurred or was suspected, the liquid could be reestablished as a standard by any purification process which would return it to its original purity. Chemical compounds to be suitable for use as calibration standards should be liquid at normal room temperatures, readily available, easy to purify, reasonably stable, and nonhygroscopic. They should have a low vapor pressure, and a surface tension value in the range of about 25 to 30 dynes/cm. The viscosity of the first of these compounds which would serve as a second calibration standard, preferably should be several times that of water. Cetane (*n*-hexadecane) meets the requirements relative to viscosity, surface tension, and vapor pressure. Presumably, it is also suitable with respect to stability and hygroscopicity. Also, a fairly pure grade (about 95%) is commercially available as ASTM Reference Fuel Cetane.

Although information developed prior to actual work on this project indicated that suitable purification of the commercially available cetane would be difficult, it was decided to proceed with the work since no more suitable commercial material was known to be available.

2. Materials and Test Procedures

Attempts to prepare highly purified *n*-hexadecaen from commercial cetane by recrystallization, by silica-gel filtration, and by the hydrocarbon-urea-clathrate complex, were unsuccessful. A first attempt to purify ASTM Reference Fuel Cetane by fractional distillation at reduced pressure, using a 10-ft-long rectifying column 1 in. in diameter was also unsuccessful. Practically all of the fractions had greenish-golden tints, apparently due to cracking of some of the impurities.

A successful fractional distillation was made using a Podbielniak column at 75-mm-Hg pressure. The starting material was ASTM Reference Fuel Cetane which had been filtered through silica gel to remove some impurities which it was thought may have been responsible for pyrolysis in the first attempt. The fractions from this distillation were not colored and there was no evidence of cracking. Because of some flooding of the column and a drop in the readings of the differential refractometer on the last few fractions, the distillation was stopped when 22 fractions had been separated. These last fractions, 17 to 22, were returned to the still, the distillation resumed, and 8 more fractions separated.

The freezing points of the Reference Fuel Cetane before and after silica-gel treatment, and of certain of the fractions, were determined and the purity of the samples calculated [2, 3]. The kinematic viscosities of these samples and of NBS standard sample No. 568–5S (99.94 ± 0.04-mole-percent *n*-hexadecane) were determined at 20° C. Freezing point, viscosity, and density determinations were made on a composite of fractions 6 to 16, inclusive, and on a second, more recent (1957) lot of ASTM Reference Fuel Cetane (after silica-gel treatment). This lot was from the same supplier as the first lot used for the distillation. The appreciably higher purity of this material is understood to be the result of improvements in the production process. The densities of the composite sample and of the second lot of reference fuel (after treatment with silica gel) were determined at 20°

[1] Figures in brackets indicate the literature references at the end of this paper.

and 25° C with a dilatometer (capacity about 50 cm^3). The densities of the NBS standard sample, and of the composite sample also, were determined at room temperature with two small dilatometers of approximately 2-cm^3 and 1-cm^3 capacities. The values thus obtained were corrected to 20° C using the average coefficient of thermal expansion derived from the measurements at 20° and 25° with the large dilatometer.

Kinematic viscosity measurements were made with four Cannon master type U-tube viscometers, the same instruments used in determining the viscosities of the calibrating liquids supplied by NBS. Calibration of the instruments has been described elsewhere [4]. The instruments were used in pairs, and measurements were made with each instrument on each sample, except that only two instruments were used for the NBS standard sample. Also, after measuring three of the samples, one of the instruments was found to contain a small obstruction in the capillary, e. g., a lint fiber apparently introduced when charging the instrument. Observations in these three instances were discarded. The values reported for each sample and each instrument represent the average of at least two observations of the flow time. The estimates of the standard deviations are based on the individual determined values, not the averages for each instrument.

The temperature of the viscometer thermostat was measured with a platinum-resistance thermometer and a Mueller G–2 bridge which were calibrated prior to start of the viscosity measurements. The viscosity work was carried on somewhat intermittently over a period of 16 months. To detect any significant changes in the instruments or conditions, the instruments were thoroughly cleaned with chromic acid solution and the flow time for freshly distilled water at 20° C was determined for each instrument before the first measurements were made and before resuming measurements after an interruption. These tests did not reveal any significant changes.

Times of flow were measured with electric stopclocks operating on a crystal-controlled 60-cps current.

3. Results

The results of the viscosity measurements together with data on freezing points and estimated purity are presented in table 1. This table also includes results of the density determinations and estimates of the standard deviations of the viscosity measurements for each sample.

Considering only the samples of purity greater than 99.3-mole percent, the average value for kinematic viscosity at 20° C was found to be 4.4620 centistokes (cs) with a standard deviation of 0.0022 cs which is equivalent to ±0.1 percent at the 95-percent confidence level.

The kinematic viscosity at 20° C of the sample of highest purity, i. e., the NBS sample with purity of 99.94 ± 0.04-mole percent, was found to be 4.4642 cs with a standard deviation of 0.00099 cs which is equivalent to ±0.04 of 1 percent at the 95-percent confidence level. It is believed that the true value for *n*-hexadecane of absolute purity would fall within these limits. Using the value 0.77370 g/cm^3 for the density at 20° C, the absolute viscosity of *n*-hexadecane was found to be 3.4540 centipoises (cp).

4. Discussion

A plot of purity versus kinematic viscosity is shown in figure 1. Obviously for these samples there is no simple relation between kinematic viscosity and mole-percent purity as estimated from the freezing point. The failure to effect suitable purification by

TABLE 1. *Results of measurements*

Material	Freezing point	Purity [b]	Density	Kinematic viscosity						Absolute viscosity
				Instr. 1	Instr. 2	Instr. 3	Instr. 4	Mean	s	
				Determinations at 20° C						
	°C	Mole %	g/cm^3	cs	cs	cs	cs	cs	cs	cp
Reference fuel, lot 1	17.262	93.65	.....	4.4636	4.4635	4.4644	4.4626	4.4635	8.2×10^{-4}	.....
Reference fuel, lot 1 [a]	17.398	94.59	.....	4.4619	4.4614	4.4615	4.4606	4.4614	5.3	.....
Distillate fraction 3	17.377	94.44	.....	4.4578	4.4574	4.4570	4.4564	4.4572	5.8	.....
Distillate fraction 5	17.856	97.83	.....	.....	.....	.....	.....	.....	.....	.....
Distillate fraction 6	.....	.....	.....	.....	4.4595	4.4591	4.4585	4.4590	5.2	.....
Distillate fraction 13	18.090	99.52	.....	4.4598	4.4596	4.4594	4.4586	4.4593	5.3	.....
Distillate fraction 16	18.076	99.42	.....	4.4599	4.4595	.....	4.4584	4.4592	7.1	.....
Distillate fraction 21	18.104	99.63	.....	4.4636	4.4636	3.4633	.....	4.4635	1.9	.....
Distillate fraction 23	18.100	99.60	.....	4.4632	4.4634	4.4634	4.4628	4.4632	2.9	.....
Distillate fraction 24	18.074	99.41	.....	4.4625	4.4627	4.4625	4.4622	4.4625	2.1	.....
Composite of fraction 6 to 16, inclusive	18.048	99.22	0.77370	4.4610	4.4606	4.4601	4.4595	4.4602	8.1	3.4509
Reference fuel, lot 2 [a]	17.837	97.69	.77355	4.4598	4.4592	4.4599	4.4602	4.4598	7.1	3.4499
NBS standard sample 568–58 [c]	(18.147)	99.94	.7737	.....	.....	4.4651	4.4634	4.4642	9.9	3.4540
				Determinations at 25° C						
Composite of fraction 6 to 16, inclusive	18.048	99.22	0.77021	3.9724	3.9722	3.9723	3.9717	3.9721	3.8	3.0594
Reference fuel, lot 2 [a]	17.837	97.69	.77013	3.9719	3.9715	3.9718	3.9710	3.9716	3.4	3.0586

[a] Percolated through silica gel.
[b] Calculated from freezing points and cryoscopic data given in reference [3].
[c] NBS standard sample is the same as the API standard. Freezing point from reference [3].

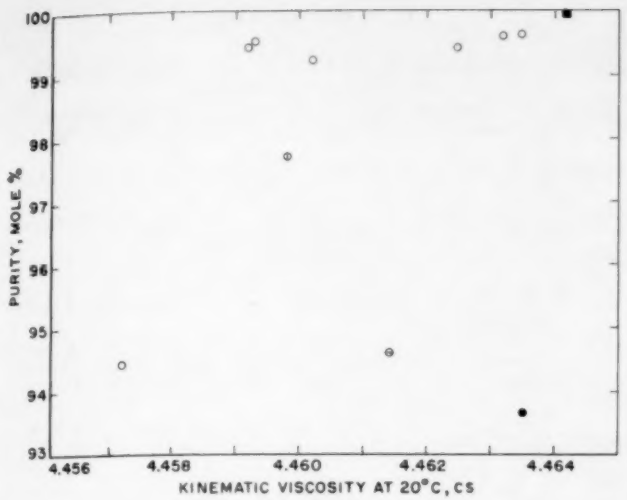

FIGURE 1. *Kinematic viscosity versus purity.*

■, NBS Standard Sample; ●, lot 1 of Reference Fuel; ⊖, lot 1 of Reference Fuel after silica gel treatment; ⊕, lot 2 of Reference Fuel after silica gel treatment, ○, distillate fractions.

recrystallization suggests the formation of solid solutions during the freezing. If this be true, the calculations of purity from the freezing points may be expected to be in error, particularly if substantial amounts of impurities are present. Explanation of the scatter of the points in figure 1 probably is to be found in this and the possibility that two or more impurities are present in different proportions in the different samples.

TABLE 2. *Absolute viscosity* [a] *of n-hexadecane at 20° C*

Observer	Viscosity	Density	Reference
	cp	*g/cm³*	
Ubbelohde and Agtha	3.322	-------	5
Evans, E. B.	3.499 determined	0.7752	6
	3.493 smoothed		
Nederbragt and Boelhouwer	[b](3.44)	.77385	7
API Project 44	3.474	.77342	8
Schiessler et al	3.453	.7737	9
This work	3.454	.7737	---

[a] Viscosity values reduced to basis consistent with the value 1.002 cp for water at 20° C.

[b] Extrapolated from 25° C. Unreduced value. The basis of their calibration is not given.

Values for the viscosity of *n*-hexadecane at 20° C reported in the literature are presented in table 2. Various instruments were used, but, with one exception, all were of the kinematic type and all were calibrated with water. Evans [6] used mercury also as a calibrating liquid. The values in table 2 have been reduced to the common basis of 1.002 cp for the viscosity of water at 20° C insofar as information is available. Nederbragt and Boelhouwer [7] did not indicate the calibration temperature or the value they used for the viscosity of water. The API Project 44 [8] selected value is based on the work of Ubbelohde and Agtha (as reported by Engler and Höfer) [5], of Evans [6], and of Nederbragt and Boelhouwer [7], together with information from API Research Projects 42 and 44. This selected value appears to be high, but within its estimated uncertainty, i. e., 0.003 to 0.030 cp, it agrees with the value reported here and the value reported by Schiessler and co-workers [9].

In every instance, the value used for the density of the sample was a factor affecting the value found for the absolute viscosity. Thus uncertainties in the density of the sample, though small, do contribute to the uncertainty of the value found for absolute viscosity. In the present work, with the two small dilatometers, the densities of the NBS standard sample and of the composite sample were found to be 0.77344 g/cm³, which agrees with the API Project 44 [8] selected value of 0.77342 g/cm³. With the large dilatometer, the density of the composite sample was found to be 0.77370 g/cm³ which agrees with the value 0.7737 g/cm³ reported by Schiessler and co-workers [9]. The values obtained with the small instruments were interpreted as indicating that the densities of the two samples were essentially the same. However the value obtained with the large instrument was believed to be more accurate and was considered to apply to both samples.

It may be noted that the values found for the kinematic viscosity of the original material and of several other samples are included in the range of values ascribed to samples of purity greater than 99.3-mole percent. In fact, the average value for all the samples examined is 4.4611 cs with a standard deviation of 0.00227 cs and the total spread of values determined with the four instruments is only 0.18 of a percent. These figures cover material ranging in purity from 93.6- to 99.94-mole percent. However, since only two lots of ASTM Reference Fuel Cetane from the same source are involved, the data do not warrant the assumption that they could be applied to any sample of *n*-hexadecane of purity in this range.

5. Conclusions

Under present conditions, cetane or *n*-hexadecane is not satisfactory as a calibration standard for viscometry because of the difficulty of purification. Although many laboratories are equipped for purification work of this type, it is not to be expected that most laboratories interested in viscosity determinations would care to use a standard requiring such extensive preliminary treatment and testing. To attempt to overcome these difficulties by arrangements to supply certified samples of *n*-hexadecane from a central source would appear to have little if any practical advantage over the present system of supplying calibration oils by NBS and API.

It is desirable that a calibration standard should be a material that can be purified by common laboratory techniques with a high degree of assurance that the purified material will have a definite viscosity. Also, it would be desirable, if not absolutely necessary, that the purity be verifiable by some test that is at least as sensitive as viscosity. At present, water seems unique in the ease with which these requirements are met.

The objections to the use of water as a calibration standard are that its viscosity is low and its surface

tension is high, both in comparison with many organic liquids, such as lubricating oils. Corrections can be made for the difference in surface tension between water used as a calibration standard and a liquid whose viscosity is to be measured, the uncertainty in such corrections being well under 0.1 of a percent, when properly calculated [10] or determined experimentally. Thus, if *n*-hexadecane were used as a calibration standard, the uncertainty that would arise due to the uncertain purity, and hence viscosity, of a given sample would be greater than that presently resulting from the use of water as a calibrating liquid and evaluation of a surface-tension correction. Similar difficulties probably would be encountered in purifying other hydrocarbon liquids with viscosities equivalent to or higher than that of *n*-hexadecane.

The author acknowledges the advice and cooperation of other members of the staff, and in particular the work of A. B. Bestul and Vera Belcher in attempting purification by recrystallization; of Thomas W. Mears and George S. Saines (present address Pennsylvania State University) for determinations of freezing points, silica-gel treatments, and experiments with the hydrocarbon-urea clathrate complex; the work of Robert Leslie in conducting the distillations; and the assistance of Walter E. Shipp with viscosity and density determinations.

6. References

[1] J. F. Swindells, J. R. Coe, Jr., and T. B. Godfrey, J. Research NBS **48,** 1 (1952) RP2279.
[2] A. R. Glasgow, Jr., A. J. Streiff, and F. D. Rossini, J. Research NBS **35,** 355 (1945) RP1676; ASTM D1015–55.
[3] A. J. Streiff, A. R. Hulme, P. A. Cowie, N. C. Krouskop, and F. D. Rossini, Anal. Chem. **27,** 411 (1955).
[4] J. F. Swindells, R. C. Hardy, and R. L. Cottington, J. Research NBS **52,** 105 (1954) RP2479.
[5] Engler and Höfer, Das Erdöl **1,** 53 (1913).
[6] E. B. Evans, Inst. Pet. Tech. **24,** 38 (1938).
[7] G. W. Nederbragt and J. W. M. Boelhouwer, Physica **13,** 305 (1947).
[8] API Project 44, Selected values of physical and thermodynamic properties of hydrocarbons and related compounds, Table 20c (1955), Table 20a (1956).
[9] R. W. Schiessler and F. C. Whitmore, Ind. and Eng. Chem. **47,** 1660 (1955) and private communication.
[10] G. Barr, Proc. Phys. Soc., London, **58,** 575 (1946).

Washington, May 5, 1958.

Journal of Research of the National Bureau of Standards Vol. 61, No. 5, November 1958 Research Paper 2913

Revision of the Phase Equilibrium Diagram of the Binary System Calcia-Titania, Showing the Compound $Ca_4Ti_3O_{10}$

Robert S. Roth

The compound $Ca_4Ti_3O_{10}$ has been found to be a stable phase in the system CaO-TiO_2. It melts incongruently at about $1755 \pm 10°$ C, presumably to $CaTiO_3$ plus liquid. This compound is shown in a revision of the phase diagram for the system CaO-TiO_2.

1. Introduction

Phase equilibrium diagrams for the system CaO-TiO_2 were published almost simultaneously by Coughanour, Roth, and DeProsse [1][1] and by DeVries, Roy, and Osborn [2]. The diagrams are very similar, both showing the existence of two compounds, $CaTiO_3$ and $Ca_3Ti_2O_7$. DeVries et al. [2], discussed the reactions between the two compounds and, on the basis of some changes in the X-ray patterns of the mixtures, concluded that a small amount of solid solution existed in both compounds. They published an X-ray pattern of $Ca_3Ti_2O_7$ which was quite similar to that reported by Fisk [3] for the same compound. Coughanour, Roth, and DeProsse [1] did not find solid solution between the two compounds but reported an X-ray pattern for $Ca_3Ti_2O_7$ which contained many more lines than those of the other publications.

Ruddlesden and Popper [4] studied the compound $Sr_3Ti_2O_7$ and have indicated it to be body centered tetragonal with $a=3.90$ A and $c=20.38$ A. They have also found a compound Sr_2TiO_4 [5] which contains alternate layers of perovskite and SrO, and have proposed that $Sr_3Ti_2O_7$ contains double perovskite layers interleaved with one SrO layer.

2. X-Ray Diffraction Data

The X-ray pattern previously published by Coughanour, Roth, and DeProsse [1] for $Ca_3Ti_2O_7$ can be partially accounted for on the basis of a body centered tetragonal cell with $a=3.832$ A and $c=19.505$ A. The pattern published by DeVries, Roy, and Osborn [2], which contains fewer lines, can be almost completely accounted for by a body centered tetragonal unit cell with $a=3.8$ A and $c=19.5$ A. These values correspond to double perovskite layers interleaved with CaO layers.

In the SrO-TiO_2 system Ruddlesden and Popper [4] predicted the possible existence of phases with triple or quadruple perovskite layers interleaved with SrO layers. They found some evidence for a compound $Sr_4Ti_3O_{10}$, which is also body centered tetragonal, with $a=3.90$ A and $c=28.1$ A, and contains triple perovskite layers.

Many of the extra lines in the pattern of Coughanour, Roth, and DeProsse [1][2] can be accounted for by assuming a mixture of two body centered tetragonal compounds, $Ca_3Ti_2O_7$ and $Ca_4Ti_3O_{10}$, the latter having a c-axis of 27.147 A. In the present study the two compounds have been isolated and the partially indexed X-ray patterns of both compounds are shown in tables 1 and 2. Although these two

TABLE 1. *X-ray diffraction powder pattern for the compound* $Ca_3Ti_2O_7$ ($CuK_{\alpha 1}$ *radiation*)

Fisk	DeVries, Roy, Osborn	Present work				*hkl*
d	d	d_{obs}	I/I_0	$1/d^2_{obs}$	$1/d^2_{cal}$ [a]	
------	9.77	9.73	[b] 100	0.0106	0.0105	002
(4.88)	4.887	4.873	[b] 100	.0421	.0421	004
------	3.762	3.762	8	.0707	.0707	101
------	------	3.302	3	.0907	.0918	103
------	------	------	------	------	.0946	006
------	2.730	2.733	100	.1339	.1338	105
2.70	2.710	2.708	66	.1364	.1362	110
------	------	------	------	------	.1467	112
2.51	2.481	2.478	7	.1629	------	------
------	------	2.439	[b] 5	.1681	.1682	008
------	------	------	------	------	.1783	114
2.19	2.254	2.255	11	.1967	.1969	107
	2.080	2.081	23	.2308	.2308	116
1.93	1.9509	1.9505	[b] 100	.2629	.2629	0·0·10
1.91	1.9141	1.9159	27	.2724	.2724	200
------	1.8860	1.8871	14	.2808	.2810	109
------	------	------	------	------	.2829	202
------	------	------	------	------	.3044	118
------	------	1.7836	6	.3143	.3145	204
------	------	1.7363	3	.3317	------	------
------	------	1.7080	3	.3428	.3432	211
------	------	1.6581	4	.3637	.3642	213
------	------	------	------	------	.3671	206
------	------	1.6258	[b] 37	.3783	.3785	0·0·12
------	------	------	------	------	.3862	1·0·11
1.57	1.5826	1.5831	38	.3990	.3991	1·1·10
	1.5679	1.5690	27	.4062	.4062	215
------	------	------	------	------	0.4406	208
------	------	1.4598	4	0.4693	.4693	217
------	------	------	------	------	.5123	1·0·13
------	------	------	------	------	.5147	1·1·12
------	1.3912	1.3933	[b] 32	.5151	.5152	0·0·14
1.358	1.3662	1.3667	14	.5354	.5353	2·0·10
------	------	1.3539	10	.5455	.5448	220
------	1.3423	1.3444	5	.5533	.5534	219
------	------	------	------	------	.5554	222
------	------	------	------	------	.5869	224
------	------	------	------	------	.6156	301
------	------	------	------	------	.6366	303
------	------	------	------	------	.6395	226
------	------	1.2394	5	.6510	.6509	2·0·12
------	------	------	------	------	.6514	1·1·14
------	1.2303	1.2318	5	.6591	.6586	2·1·11
					.6595	1·0·15
------	------	1.2191	[b] 15	.6729	.6729	0·0·16
------	------	------	------	------	.6787	305
1.210	1.2119	1.2109	4	.6819	.6811	310
------	------	------	------	------	.6916	312
------	------	------	------	------	.7131	228
------	------	------	------	------	.7231	314
------	------	------	------	------	.7417	307
------	------	------	------	------	.7757	316
------	------	------	------	------	.7847	2·1·13

See footnotes at end of table.

[1] Figures in brackets indicate literature references at the end of this paper.

[2] This pattern is represented in the ASTM index of X-ray diffraction powder patterns by card No. 6-0698. As this pattern is a mixture of two compounds it should be eliminated and replaced by the two patterns listed in this paper.

TABLE 1. *X-ray diffraction powder pattern for the compound* $Ca_5Ti_2O_7$ (CuK$_{\alpha 1}$ *radiation*)—Continued

Fisk	DeVries, Roy, Osborn	Present work				*hkl*
d	*d*	d_{obs}	I/I_0	$1/d^2_{obs}$	$1/d^2_{cal}$ [a]	
------	------	------	------	------	.7876	2·0·14
------	------	1.1234	2	.7924	------	------
------	------	1.1124	4	.8081	.8077	2·2·10
------	------	------	------	------	0.8091	1·1·16
------	------	------	------	------	.8259	309
------	------	1.0995	4	.8272	.8277	1·0·17
------	------	------	------	------	.8493	318
------	------	------	------	------	.8516	0·0·18
------	------	------	------	------	.8880	321
------	------	1.0559	9	.8969	------	------
------	------	------	------	------	.9090	323
------	------	------	------	------	.9233	2·2·12
------	------	------	------	------	.9310	3·0·11
------	------	------	------	------	.9319	2·1·15
------	------	1.0292	6	.9441	.9439	3·1·10
------	------	------	------	------	.9453	2·0·16
1.021	------	1.0251	4	.9516	.9511	325
------	------	------	------	------	.9878	1·1·18
------	------	------	------	------	1.0142	327
------	------	0.99168	10	1.0168	1.0170	1·0·19
------	------	.97534	[b] 71	1.0512	1.0514	0·0·20
------	------	------	------	------	1.0572	3·0·13
------	------	------	------	------	1.0596	3·1·12
------	------	------	------	------	1.0600	2·2·14
------	------	.95764	2	1.0904	1.0897	400
------	------	.95359	3	1.0997	1.0983	329
					1.1002	2·1·17
					1.1002	402
------	------	------	------	------	1.1241	2·0·18
------	------	------	------	------	1.1317	404
------	------	------	------	------	1.1604	411
------	------	------	------	------	1.1814	413
------	------	------	------	------	1.1843	406
------	------	0.91768	7	1.1875	1.1876	1·1·20
------	------	------	------	------	1.1962	3·1·14
------	------	------	------	------	1.2034	3·2·11
------	------	.91125	5	1.2043	1.2044	·0·15
------	------	------	------	------	1.2177	2·2·16
------	------	------	------	------	1.2235	415
------	------	.90346	6	1.2251	1.2259	330
------	------	.90236	11	1.2281	1.2273	1·0·21
------	------	------	------	------	1.2364	332
------	------	------	------	------	1.2579	408
------	------	------	------	------	1.2680	334
------	------	.88673	[b] 43	1.2718	1.2722	0·0·22
------	------	------	------	------	1.2866	417
------	------	.88058	8	1.2896	1.2894	2·1·19
------	------	------	------	------	1.3205	336
------	------	.86915	4	1.3238	1.3238	2·0·20
------	------	------	------	------	1.3296	3·2·13
------	------	.85982	5	1.3526	1.3525	4·0·10
------	------	------	------	------	1.3540	3·1·16
------	------	------	------	------	1.3621	420
------	------	.85388	4	1.3715	1.3707	419
					1.3726	3·0·17
					1.3726	422
------	------	------	------	------	1.3919	2·1·20
------	------	------	------	------	1.3941	338
------	------	------	------	------	1.3965	2·2·18
------	------	------	------	------	1.4042	424
------	------	.84268	5	1.4082	1.4084	1·1·22
------	------	------	------	------	1.4567	426
------	------	------	------	------	1.4586	1·0·23
------	------	------	------	------	1.4682	4·0·12
------	------	------	------	------	1.4758	4·1·11
------	------	------	------	------	1.4768	3·2·15
------	------	0.81968	4	1.4884	1.4887	3·3·10
------	------	.81272	[b] 22	1.5140	1.5140	0·0·24
------	------	------	------	------	1.5303	428
------	------	------	------	------	1.5327	3·1·18
------	------	.80463	5	1.5446	1.5446	2·0·22
------	------	------	------	------	1.5618	3·0·19
------	------	------	------	------	1.5962	2·2·20

[a] The $1/d^2$ values have been calculated on the basis of a tetragonal unit cell with $a=3.832$A, $c=19.505$A.
[b] These (00l) peaks are probably abnormally strong due to preferred orientation.

TABLE 2. *X-ray diffraction powder pattern for the compound* $Ca_4Ti_3O_{10}$ (CuKα_1 *radiation*)

d_{obs}	I/I_0	$1/d^2_{obs}$	$1/d^2_{cal}$ [a]	*hkl*
13.5	6	0.0055	0.0054	002
6.78	7	.0217	.0217	004
4.525	11	.0488	.0489	006
3.795	9	.0694	.0696	101
------	------	------	.0805	103
------	------	------	.0868	008
3.337	5	.0898	------	------
------	------	------	.1022	105
2.725	100	.1347	.1348	107
2.718	100	.1353	.1357	0·0·10
2.706	46	.1365	.1365	110
------	------	------	.1420	112
------	------	------	.1582	114
2.422	8	.1705	------	------
2.367	4	.1785	.1782	109
------	------	------	.1854	116
2.283	3	.1919	------	------
------	------	------	.1954	0·0·12
2.212	4	.2044	------	------
2.116	10	.2234	.2234	118
2.075	3	.2323	.2325	1·0·11
1.939	33	.2660	.2660	0·0·14
1.915	65	.2726	.2722	1·1·10
------	------	------	.2731	200
------	------	------	.2785	202
1.874	3	.2848	------	------
------	------	------	.2948	204
1.832	7	.2979	.2976	1·0·13
1.764	6	.3214	.3219	206
------	------	------	0.3319	1·1·12
1.713	4	0.3409	.3427	211
------	------	------	.3474	0·0·16
------	------	------	.3535	213
1.664	5	.3612	.3599	208
------	------	------	.3736	1·0·15
------	------	------	.3753	215
1.576	15	.4028	.4025	1·1·14
------	------	------	.4078	217
1.565	40	.4085	.4088	2·0·10
------	------	------	.4396	0·0·18
------	------	------	.4512	219
------	------	------	.4604	1·0·17
------	------	------	.4685	2·0·12
------	------	------	.4839	1·1·16
1.405	4	.5067	.5055	2·1·11
1.362	21	.5388	.5390	2·0·14
------	------	------	.5428	0·0·20
1.351	9	.5477	.5461	220
1.326	4	(b)	(b)	
1.323	5	(b)	(b)	
1.256	4	(b)	(b)	
1.224	4	(b)	(b)	
1.213	12	(b)	(b)	
1.109	7	(b)	(b)	
1.087	3	(b)	(b)	
1.052	3	(b)	(b)	
1.044	3	(b)	(b)	
1.028	8	(b)	(b)	
1.026	9	(b)	(b)	
1.023	10	(b)	(b)	

[a] The $1/d^2$ values have been calculated on the basis of a tetragonal unit cell with $a=3.827$A and $c=27.147$A.
[b] Due to the very large unit cell, no attempt was made to index the rest of this pattern.

patterns can be almost completely accounted for on the basis of two tetragonal unit cells, there are still some very small peaks which cannot be indexed on this basis. It seems possible that these calcia-titania compounds are not completely isostructural with the corresponding strontia-titania compounds. It is possible that these compounds have lower symmetry, just as $CaTiO_3$ has a lower symmetry than $SrTiO_3$.

DeVries, Roy, and Osborn [2] have published parts of X-ray diffraction patterns of a series of mixtures

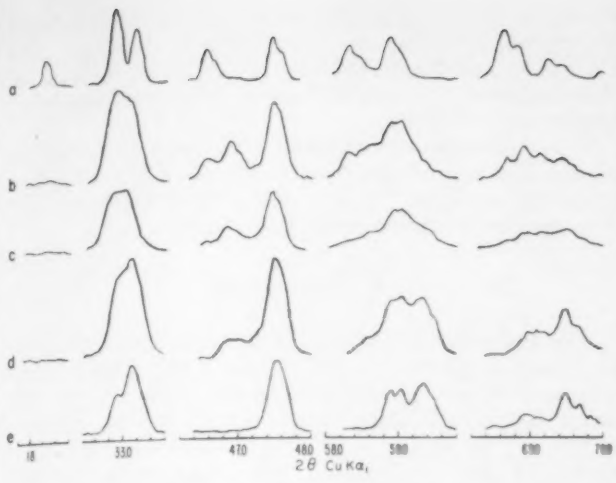

FIGURE 1. *X-ray diffractometer patterns of a series of mixtures from* $Ca_3Ti_2O_7$ *to* $CaTiO_3$ *(after melting and quenching).*

Taken from DeVries, Roy, and Osborn [2].

a=51.29/48.71 wt. % CaO/TiO_2 ($Ca_3Ti_2O_7$)
b=48.65/51.35 wt. % CaO/TiO_2
c=46.00/54.00 wt. % CaO/TiO_2
d=48.60/56.40 wt. % CaO/TiO_2
e=41.24/58.76 wt. % CaO/TiO_2 ($CaTiO_3$)

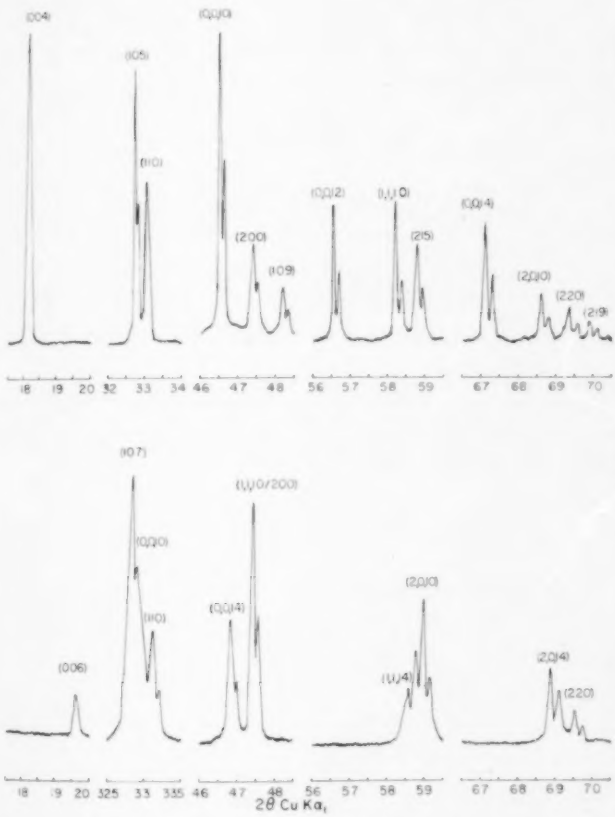

FIGURE 2. *X-ray diffraction patterns, from the present work, of the two compounds* $Ca_3Ti_2O_7$ *(above) and* $Ca_4Ti_3O_{10}$ *(below) covering essentially the same part of the diffraction spectra as figure 1.*

from $Ca_3Ti_2O_7$ to $CaTiO_3$ after melting and quenching. Part *a* (of fig. 3, ref. [2] reproduced here as fig. 1) represents a portion of the pattern of $Ca_3Ti_2O_7$ and part *e* that of $CaTiO_3$. Figure 2 shows essentially the same portions of the X-ray patterns of the two compounds $Ca_3Ti_2O_7$ and $Ca_4Ti_3O_{10}$, as found in the present work. Although all of the patterns in figure 1 are very poorly resolved it can be seen in part *b* that there are three peaks in the region of 46 to 48°2θ. The composition of this mixture is very close to $4CaO:3TiO_2$ and this pattern represents the compound $Ca_4Ti_3O_{10}$ with a small amount of $Ca_3Ti_2O_7$. Parts *c* and *d* are mixtures of $CaTiO_3$ and $Ca_4Ti_3O_{10}$ and both show the center of the three peaks at 47° 2θ, while this peak is eliminated in part *a*, $Ca_3Ti_2O_7$. These published X-ray diagrams support the theory of an intermediate compound ($Ca_4Ti_3O_{10}$) much better than the theory of solid solution proposed by the authors of the published patterns.

3. Experimental Procedures

It might be thought possible that $Ca_4Ti_3O_{10}$ is only a metastable compound having no true equilibrium position in the CaO-TiO_2 phase diagram. If such were the case, an equi-molar mixture of preformed $CaTiO_3$ and $Ca_3Ti_2O_7$ would not form the $Ca_4Ti_3O_{10}$ phase upon heating. Such an equi-molar mixture was prepared, using the same raw materials as in the previous study (Coughanour, Roth, and DeProsse [1]). The specimen was heated in a conventional Pt-wound quench furnace to 1,650° C, held for 2 hr, and quenched in air. The compound $Ca_4Ti_3O_{10}$ was the only product identified in this specimen. It must therefore be concluded that the compound $Ca_4Ti_3O_{10}$ is the equilibrium product of the composition $4CaO:3TiO_2$, at least at 1,650° C.

From the data of Coughanour, Roth, and DeProsse [1] as well as that of DeVries, Roy, and Osborn [2], it can be seen that the compound $Ca_4Ti_3O_{10}$ can not melt congruently. It must either dissociate before melting or else melt incongruently at a temperature somewhat higher than the incongruent melting point of $Ca_3Ti_2O_7$, given in both papers as 1,750° C.

Specimens with a calcia-titania ratio of 4 : 3 were pressed into pellets, calcined in a conventional Pt-wound furnace at 1,250° C, ground, repressed, and reheated to 1,600° C and slow-cooled. They showed only the compound $Ca_4Ti_3O_{10}$. Specimens were then ground and placed in a Pt envelope, heated in the Pt-wound quench furnace, and quenched into water from temperatures of 1,500° C, 1,550° C, 1,600° C and 1,650° C. All of these quenched specimens still showed only the compound $Ca_4Ti_3O_{10}$. Specimens were then heated and quenched in a graphite susceptor induction furnace, from temperatures of 1,700° C and 1,725° C. These two specimens also showed only the compound $Ca_4Ti_3O_{10}$. One more specimen was placed in a smooth Pt tube, so that the temperature could be read more precisely with an optical pyrometer, heated to 1,745° C and quenched. This specimen still showed only $Ca_4Ti_3O_{10}$. As the reported solidus for $Ca_3Ti_2O_7$ is 1,750°

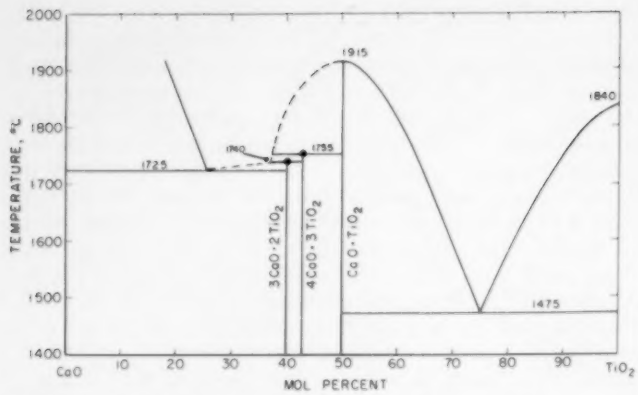

FIGURE 3. *Revised phase equilibrium diagram of the system* CaO-TiO_2, *showing the compound* $Ca_3Ti_2O_7$ *melting incongruently at 1,740° C and the compound* $Ca_4Ti_3O_{10}$ *melting incongruently at 1,755° C.*

(After Coughanour, Roth, and DeProsse [1]).

● Solidus temperatures determined in the present study.

C, it must be assumed that $Ca_4Ti_3O_{10}$ either does not dissociate to two solids, or that such dissociation cannot be quenched.

In order to check the solidus temperatures of the two compounds $Ca_3Ti_2O_7$ and $Ca_4Ti_3O_{10}$, fragments of the two materials, previously heated to 1,650° C for 2 hr, were set side by side on an iridium button in the graphite induction furnace. The $Ca_3Ti_2O_7$ specimen definitely began melting before the $Ca_4Ti_3O_{10}$ specimen. However, the fluid liquid quickly spread over the iridium button, obscuring the results of melting of the second specimen. As it appeared that the iridium button was hotter than the inside of the graphite crucible, a new experiment was performed utilizing only an iridium crucible with an iridium button inside. Using a flat button and a cover on the crucible and sighting through a hole in the cover, perfect black-body conditions were obtained and the specimen could not be seen. By utilizing a concave button and no cover, the specimen could be watched during the whole experiment. The temperature of the solid specimen at beginning of melting appeared 25° to 30° C cooler than the true temperature, but the liquid formed appeared to show the true temperature. The solidus temperature for $Ca_3Ti_2O_7$ was found to be 1,740° C and that of $Ca_4Ti_3O_{10}$ was 1,755° C. These results were rechecked by again heating fragments in the iridium crucible using a flat button and the crucible cover. The $Ca_3Ti_2O_7$ specimen when heated to 1,740° C showed a rounding of the corners and a small amount of crystal growth on the iridium button. The $Ca_4Ti_3O_{10}$ specimen showed no sign of melting at this temperature but did show some melting when heated to 1,755° C.

These measurements have been used to revise the phase diagram of the binary system CaO–TiO_2 first proposed by Coughanour, Roth, and DeProsse [1].[3] The revised diagram is shown in figure 3.

4. Summary

The compound $Ca_4Ti_3O_{10}$ has been shown to exist as a stable phase in the system CaO–TiO_2. Both compounds are pseudo-tetragonal with only a few weak lines indicating a departure from tetragonality. The c–axis = 19.505 A for $Ca_3Ti_2O_7$ and 27.147 A for $Ca_4Ti_3O_{10}$. The dimensions indicate that $Ca_3Ti_2O_7$ has double perovskite layers interleaved with CaO, while $Ca_4Ti_3O_{10}$ has triple perovskite layers interleaved with CaO. The new compound, $Ca_4Ti_3O_{10}$, has been found to melt incongruently at about 1,755° C, while the incongruent melting point of $Ca_3Ti_2O_7$ has been shown to be about 1,740° C. The revised phase diagram for the system CaO–TiO_2 is presented.

The assistance of Charles R. Drew in preparing and heating the specimens and of Sylvanus F. Holley for operating the induction furnace is gratefully acknowledged.

5. References

[1] L. W. Coughanour, R. S. Roth, and V. A. DeProsse, J. Research NBS **52,** 37 (1954) RP2470.
[2] R. C. DeVries, R. Roy, and E. F. Osborn, J. Phys. Chem. **58,** 1069 (1954).
[3] H. G. Fisk, Jr., J. Am. Ceram. Soc. **34,** 9 (1951).
[4] S. N. Ruddlesden and P. Popper, Acta Cryst. **11,** 54 (1958).
[5] S. N. Ruddlesden and P. Popper, Acta Cryst. **10,** 538 (1957).

---

[3] The two previously published diagrams of Coughanour et al. [1] and DeVries et al. [2] disagree on the temperatures of the melting point of $CaTiO_3$ (1,915° C and 1,970° C) and on the temperature of the eutectic between CaO and $Ca_4Ti_3O_7$ (1,725° C and 1,695° C). No attempt has been made in the present study to reconcile these two discrepancies.

WASHINGTON, August 4, 1958.

U. S. GOVERNMENT PRINTING OFFICE: 1958

THE NATIONAL BUREAU OF STANDARDS

The scope of activities of the National Bureau of Standards at its headquarters in Washington, D. C., and its major laboratories in Boulder, Colorado, is suggested in the following listing of the divisions and sections engaged in technical work. In general, each section carries out specialized research, development, and engineering in the field indicated by its title. A brief description of the activities, and of the resultant publications, appears on the inside of the front cover.

WASHINGTON, D. C.

Electricity and Electronics. Resistance and Reactance. Electron Devices. Electrical Instruments. Magnetic Measurements. Dielectrics. Engineering Electronics. Electronic Instrumentation. Electrochemistry.

Optics and Metrology. Photometry and Colorimetry. Optical Instruments. Photographic Technology. Length. Engineering Metrology.

Heat. Temperature Physics. Thermodynamics. Cryogenic Physics. Rheology. Engine Fuels. Free Radicals Research.

Atomic and Radiation Physics. Spectroscopy. Radiometry. Mass Spectrometry. Solid State Physics. Electron Physics. Atomic Physics. Neutron Physics. Radiation Theory. Radioactivity. X-rays. High Energy Radiation. Nucleonic Instrumentation. Radiological Equipment.

Chemistry. Organic Coatings. Surface Chemistry. Organic Chemistry. Analytical Chemistry. Inorganic Chemistry. Electrodeposition. Molecular Structure and Properties of Gases. Physical Chemistry. Thermochemistry. Spectrochemistry. Pure Substances.

Mechanics. Sound. Mechanical Instruments. Fluid Mechanics. Engineering Mechanics. Mass and Scale. Capacity, Density, and Fluid Meters. Combustion Controls.

Organic and Fibrous Materials. Rubber. Textiles. Paper. Leather. Testing and Specifications. Polymer Structure. Plastics. Dental Research.

Metallurgy. Thermal Metallurgy. Chemical Metallurgy. Mechanical Metallurgy. Corrosion. Metal Physics.

Mineral Products. Engineering Ceramics. Glass. Refractories. Enameled Metals. Concreting Materials. Constitution and Microstructure.

Building Technology. Structural Engineering. Fire Protection. Air Conditioning, Heating, and Refrigeration. Floor, Roof, and Wall Coverings. Codes and Safety Standards. Heat Transfer.

Applied Mathematics. Numerical Analysis. Computation. Statistical Engineering. Mathematical Physics.

Data Processing Systems. SEAC Engineering Group. Components and Techniques. Digital Circuitry. Digital Systems. Analog Systems. Application Engineering.

• Office of Basic Instrumentation.

• Office of Weights and Measures.

BOULDER, COLORADO

Cryogenic Engineering. Cryogenic Equipment. Cryogenic Processes. Properties of Materials. Gas Liquefaction.

Radio Propagation Physics. Upper Atmosphere Research. Ionospheric Research. Regular Propagation Services. Sun-Earth Relationships. VHF Research. Ionospheric Communication Systems.

Radio Propagation Engineering. Data Reduction Instrumentation. Modulation Systems. Navigation Systems. Radio Noise. Tropospheric Measurements. Tropospheric Analysis. Radio Systems Application Engineering. Radio Meteorology.

Radio Standards. High Frequency Electrical Standards. Radio Broadcast Service. High Frequency Impedance Standards. Electronic Calibration Center. Microwave Physics. Microwave Circuit Standards.

Recent Publications of the National Bureau of Standards

Periodicals

Journal of Research of the National Bureau of Standards, Volume 61, No. 3, September 1958 (RP2894 to RP2899 incl.). 60 cents. Annual subscription $5.00. $1.75 additional for foreign mailing.

Technical News Bulletin, Volume 42, No. 9, September 1958. 15 cents. Annual subscription $1.50. 75 cents additional for foreign mailing.

Basic Radio Propagation Predictions for December 1958. Three months in advance. CRPL-D 169. Issued September 1958. 10 cents. Annual subscription $1.00. 50 cents additional for foreign mailing.

Available from the Superintendent of Documents, U. S. Government Printing Office, Washington 25, D. C. The three NBS periodicals are available on a 1-, 2-, or 3-year subscription basis, although no reduction in rates can be made.

UNITED
GOVERNMENT
DIVISION OF PUBLIC DOCUMENTS
WASHINGTON 25, D. C.
OFFICIAL BUSINESS

PENALTY FOR PRIVATE USE TO
PAYMENT OF POSTAGE,
(GPO)

ITY OF MICHIGAN
LIBRARY
LABORATORY
MICH

Journal of Research of the National Bureau of Standards Vol. 61, No. 5 November

Contents

		Page
On the diffraction and reflection of waves and pulses by wedges and corners. F. Oberhettinger.	RP2906	343
A liquid-helium cold cell for use with an X-ray diffractometer. Igor A. Black, Leonard H. Bolz, Frank P. Brooks, Floyd A. Mauer, and H. Steffen Peiser.	RP2907	367
The second spectrum of ruthenium (Ru II). Allen G. Shenstone and William F. Meggers.	RP2908	373
Self-ignition temperatures of materials from kinetic-reaction data. Daniel Gross and A. F. Robertson.	RP2909	413
Some studies of atmospheric transmittance on Mauna Loa. Ralph Stair and Russell G. Johnston.	RP2910	419
Central notations for the revised ISCC–NBS color-name blocks. Kenneth L. Kelly.	RP2911	427
Viscosity of n-hexadecane. Robert C. Hardy.	RP2912	433
Revision of the phase equilibrium diagram of the binary system calcia-titania, showing the compound $Ca_4Ti_3O_{10}$. Robert S. Roth.	RP2913	437

[A list of recent NBS publications is given on page 3 of the cover.]

For sale by the Superintendent of Documents, U. S. Government Printing Office, Washington 25, D. C. Price 60 cents (single copy)
Subscription price: $5.00 a year; $1.75 additional for foreign mailing.
UNITED STATES GOVERNMENT PRINTING OFFICE, WASHINGTON : 1958